Universidade do Porto

FEUP Faculdade de Engenharia

STRUCTURAL CHARACTERIZATION AND MONITORING OF HERITAGE CONSTRUCTIONS

by

ESEQUIEL FERNANDES TEIXEIRA MESQUITA

A Thesis presented to the Faculty of Engineering of University of Porto
for the Degree of Doctor in Civil Engineering.

Advisors:
Professor Humberto Salazar Amorim Varum,
Professor António José Coelho Dias Arêde
Doctor Paulo Fernando da Costa Antunes

JULY 2017

Universidade do Porto

FEUP Faculdade de Engenharia

STRUCTURAL CHARACTERIZATION AND MONITORING OF HERITAGE CONSTRUCTIONS

ESEQUIEL FERNANDES TEIXEIRA MESQUITA

The present thesis was submitted to Faculty of Engineering of University of Porto as partial fulfillment of the requirements for the Degree of Philosophy Doctor in Civil Engineering, under main scientific supervision of Professor Humberto Salazar Amorim Varum, Chair in Structural Engineering at Faculty of Engineering of University of Porto and co-supervision of Professor António José Dias Arêde, Associate Professor at Faculty of Engineering of University of Porto, and Doctor Paulo Fernando da Costa Antunes, Post-Doctoral Research at Institute of Telecommunications and at University of Aveiro.

Financial support by CAPES foundation, Ministry of Education of Brazil, fellowship number 10023/13-5.

JULY 2017

The jury:

President: Doctor Rui Artur Bártolo Calçada
Full Professor at Faculty of Engineering of University of Porto

Members: Doctor Francisco Carvalho de Arruda Coelho
Adjunct Professor at Universidade Estadual Vale do Acaraú

Doctor Paulo Sérgio de Brito André
Associated Professor at Technical University of Lisbon

Doctor Patrício António de Almeida Rocha
Adjunct Professor at Polytechnic Institute of Viana do Castelo

Doctor Celeste Maria Nunes Vieira de Almeida
Assistant Professor at University Fernando Pessoa

Doctor Humberto Salazar Amorim Varum
Full Professor at Faculty of Engineering of University of Porto

Doctor João Paulo Sousa Costa de Miranda Guedes
Assistant Professor at Faculty of Engineering of University of Porto

To my dears parents, Xavier and Valméria and my two brothers Silas and Davi.

"Every person must work for his own improvement, and at the same time he must share a general responsibility for all humanity"

Marie Curie

ACKNOWLEDGEMENTS

Initially, I would like to thank immensely my family for their unconditional love, support and encouragement during my entire life, in special form to my loved parents Xavier and Valméria, and my two brothers Silas and Davi.

I would like to express my sincere gratitude to my main advisor, Professor Humberto Varum, for his constant support, patience, guidance and permanent motivation, daily expressed during my PhD course, as well for his professional and personal example that motivated me to improve myself.

To my co-advisors, Doctor Paulo Antunes, for all moments of scientific support, patience and by opportunity to take part in other activities in his scientific group, and most important, for his friendship, and to Professor António Arêde, for the constant incentive, assistance and exciting conversations about SHM, and for the immense support for the realization of this work.

To Eng. Esmeralda Paupério for all appreciable considerations and incentives, for sharing with me her skills on heritage construction preservation and make me sensible to this subject.

To Professor Francisco Carvalho for introducing me in the scientific world, for all years of encouragement, since my graduate studies, for motivation and friendship, my deep acknowledgment.

To Professor Paulo S. André, Doctor Nélia Alberto, Doctor José Melo, M.Sc. Jorge Fonseca and Doctor Carlos Marques, my sincere acknowledgements for your collaboration during the stage of sensors development at University of Aveiro.

To all LESE team, especially to Nuno Pinto, Valdemar Luis, Guilherme Nogueira, for appreciate collaboration during all experimental works, and to Doctor Hugo Rodrigues, for his friendship and important contributions along of this work.

Also, to my dear friends from University of Aveiro for the reception, friendship and support during my period of adaptation in Portugal, in the first phase of this work,

specially Eng. Pedro Narra, Eng. Maria João, Doctor Regina Modolo, Doctor Thiago Silva. To Professor Fernanda Rodrigues and Professor Romeu Vicente.

Special thanks to my dear friends (and PhD-partners) Rachel Martini, Claudio Horas, Ana Mafalda Matos, Despoina Skoulidou, Tuba Tatar, Ana Ramos, Guilherme Alencar, Iviane Cunha, Cassio Gaspar, Jovana Borozan and Doctor Aralya Mosleh for all lovely moments lived in Porto.

To my dear friends, Eng. Leandro Souza, Daniele Albuquerque Eng. Natália Gomes, Eng. Karisa Marques, Eng. Felipe Martins, Eng. Alexsandro Melo and Eng. Almircélio Marques for all support, encouragement and long friendship.

To Instituto do Patrimônio Histórico e Artístico Nacional do Brasil, Direção Regional do Patrimônio do Norte de Portugal, University of Aveiro and Institute of Telecommunications of Aveiro, for appreciable collaboration for development of this work.

To all friends and colleagues that I had meet along of these years.

Finally, to CAPES by financial support through the Doctoral fellowship number 10023/13-5.

ABSTRACT

Due to their high cultural value, variability and complexity of the structural systems, heritage constructions had become an interesting and challenge field for development of new techniques for characterization and structural assessment, and most recently to Structural Health Monitoring (SHM), as well. In fact, since 1980s the number of applications of continuous monitoring systems in civil engineering structures had grown considerably, however these applications had occurred essentially in large structures, as for example bridges, tunnels and offshore platforms, and few cases of heritage constructions monitoring are reported in the literature. This way, the present Thesis has as main aim the development of tools for support of characterization and structural assessment of heritage construction through employment of SHM techniques. Thus, in order to contribute for implementation of the state-of-the-art on SHM, this work introduces two new optic sensors based on fiber Bragg grating, namely: a groundwater level sensor and a bond-slip sensor. It is important to highlight that these sensors were designed considering its applications for heritage constructions monitoring. In addition, methodologies for SHM of heritage constructions were developed and its respective strategies are deeply discussed. Finally, for validation of the concepts developed in this work three HC case studies were selected, in Portugal and Brazil. The present work presents relevant contribution for the field of SHM of heritage constructions, as well to conservation and rehabilitation of these structures, and, potentially, for decreasing of the failure risk and implementation of the maintenance techniques.

KEYWORDS: Structural health monitoring, heritage constructions; safety assessment, dynamic characterization, optical sensors.

RESUMO

Devido ao elevado valor cultural, variabilidade e complexidade dos sistemas estruturais, construções históricas tornaram-se um interessante e desafiador campo para o desenvolvimento de novas técnicas para caracterização e avaliação estrutural, e mais recentemente para o campo da monitorização estrutural. De fato, desde 1980, o número de aplicações de sistemas de monitorização em estruturas de engenharia civil tem crescido consideravelmente, entretanto estas aplicações têm ocorrido, essencialmente, em estruturas de grande porte, como pontes, tuneis e estruturas *offshore*, por exemplo, e poucos são os casos relacionados com construções históricas reportados na literatura. Nesse contexto, este trabalho tem como principal objetivo o desenvolvimento de ferramentas de suporte a caracterização e avaliação estrutural de construções históricas através de técnicas de monitorização. Assim, de modo a contribuir com a implementação do estado-da-arte no campo da monitorização, este trabalho introduz dois novos sensores óticos baseados em redes de Bragg, nomeadamente: um sensor de nível freático e um sensor de deslizamento aço-concreto. É importante destacar que estes sensores foram projetados de modo a considerar sua aplicação para a monitorização de construções históricas. Adicionalmente, foram desenvolvidas metodologias para monitorização estrutural de construções histórica, bem como suas respetivas estratégias são descritas. Finalmente, para validação dos conceitos desenvolvidos neste trabalho, três casos de estudos relacionados ao patrimônio histórico foram selecionados, em Portugal e no Brasil. Este trabalho apresenta relevantes contribuições para o avanço no âmbito da monitorização de construções históricas, bem como para a conservação e reabilitação destas estruturas e, potencialmente, para a diminuição do risco estrutural e para a implementação de técnicas de manutenção.

PALAVRAS-CHAVE: Monitorização estrutural, construções históricas, avaliação da segurança estrutural, caracterização dinâmica, sensores óticos.

RESUMEN

Debido al elevado valor cultural, variabilidad y complexidad de los sistemas estructurales, las construcciones patrimoniales tornaran-se un interesante y desafiador campo para el desarrollo de nuevas técnicas para la caracterización y evaluación estructural, y últimamente para el campo del monitoreo de las estructuras. De hecho, desde 1980, el número de aplicaciones de sistemas de monitoreo continuo en estructuras de ingeniería civil ha aumentado considerablemente, aunque estos casos de aplicación han ocurrido esencialmente en grandes estructuras, como por ejemplo puentes, viaductos, o plataformas offshore, y solo están reportados en la literatura un escaso número de casos de monitoreo de construcciones patrimoniales. En este contexto, este trabajo tiene como principal objetivo el desarrollo de herramientas de suporte a la caracterización y evaluación estructural de construcciones patrimoniales con uso de técnicas de monitoreo. De este modo, como contribución a la implementación del estado-del-arte en el campo del monitoreo estructúrale, este trabajo hace la introducción de dos nuevos sensores ópticos basados en redes de Bragg: sensor de nivel de agua subterránea y sensor de deslizamiento acero-hormigón. Es importante señalar que estos sensores fueron diseñados considerando las construcciones patrimoniales, y por lo tanto se buscó una alternativa menos intrusiva para las construcciones patrimoniales. Además, se fueran desarrolladas metodologías para monitorización de las construcciones patrimoniales, así como se fueran descriptas las respectivas estrategias adoptadas. Finalmente, para la validación de los conceptos desarrollados en este trabajo tres casos de estudio relacionados con el patrimonio fueran seleccionados en Portugal e Brasil. Este trabajo presenta relevantes contribuciones para el avanzo en el área del monitoreo estructúrale de construcciones patrimoniales, como también para la conservación y rehabilitación de estas estructuras e, potencialmente, para la diminución del risco estructúrale y para la implementación de técnicas de manutención

PALABRAS-CHAVE: Monitorización estructural, construcciones patrimoniales, evaluación de la seguridad estructural, caracterización dinámica, sensores ópticos.

SOMMARIO

Per il loro alto valore culturale, varietà e complessità dei sistemi strutturali, le costruzioni storiche sono diventate un interessante e stimolante campo per lo sviluppo di nuove tecniche per la caratterizzazione e la valutazione strutturale e, più recentemente, anche per il monitoraggio strutturale. In realtà, dagli anni '80 il numero di applicazioni di sistemi di monitoraggio continui in strutture di ingegneria civile sono cresciute considerevolmente, anche se queste applicazioni hanno riguardato essenzialmente grandi strutture come, per esempio, ponti, viadotti e piattaforme *offshore*, invece solo pochi casi di monitoraggio di costruzioni storiche sono riportati in letteratura. Per questo, la presente Tesi ha lo scopo principale di sviluppare degli strumenti per il supporto alla caratterizzazione e alla valutazione strutturale delle costruzioni storiche attraverso l'impiego delle tecniche di monitoraggio strutturale. Quindi, con lo scopo di contribuire allo stato dell'arte sul monitoraggio strutturale, questo lavoro presenta due sensori a fibre ottiche innovativi basati sul reticolo di Bragg, ovvero: un sensore per il livello dell'acqua di falda e un sensore per l'aderenza. È importante evidenziare che questi sensori sono stati progettati considerando la loro specifica applicazione per il monitoraggio delle costruzioni storiche. Inoltre, si sono sviluppate metodologie per il monitoraggio strutturale delle costruzioni storiche e si sono discusse nel dettaglio le loro rispettive strategie. Infine, come validazione dei concetti sviluppati in questo lavoro, si sono selezionati tre casi studio di edifici storici in Portogallo e Brasile. Il presente lavoro offre un rilevante contributo nel campo del monitoraggio strutturale di costruzioni storiche, come anche per la conservazione e recupero di queste strutture e, potenzialmente, per la diminuzione del rischio di collasso e l'implementazione di tecniche per manutenzione delle stesse.

PAROLE-CHIAVE: Monitoraggio strutturale, costruzioni storiche, valutazione della sicurezza, caratterizzazione dinamica, sensori ottici.

TABLE OF CONTENTS

1. Introduction 1
1.1. Motivation 1
1.2 Aims 6
1.2.1. Main aims 6
1.2.2. Specifics aims 6
1.3. Originality and relevance 6
1.4. Work organization 8
2. Global overview on advances in SHM 11
2.1. Introduction 12
2.1.1. From construction to retrofitting: the change of focus. 12
2.1.2. Importance of SHM for structural safety maintenance 13
2.2. Short history and recent advances on SHM 17
2.2.1 The initial history 17
2.2.2. Recent advances on SHM 22
2.3. Level responses of the SHM platforms 26
2.3.1. Level 1 27
2.3.2. Level 2 28
2.3.3. Level 3 29
2.3.4. Level 4 30
2.3.5. Level 5 31
2.4. Heritage constructions: a special case study for SHM 32
2.5. New perspectives for SHM 36
2.6. Final comments 38
3. New optical sensors for heritage construction monitoring 41
3.1. Groundwater level sensing for SHM 42
3.1.1 Introduction 42
3.1.2 Sensor, setup and experimental program 44
3.1.3 Results 48
3.1.4 Final comments 53
3.2. Optical sensors for bond-slip characterization and monitoring of old RC structures 54
3.2.1. Introduction 54

3.2.2. Fiber Bragg grating 57
3.2.3. Sensors description and manufacturing 59
3.2.4. Specimens detailing and experimental setup 62
3.2.6. Results 64
3.2.7. Final comments 68
4. Strategies for SHM design 71
4.1. A proposal for São Lourenço Church monitoring through wireless sensor network 72
4.1.1 Introduction 72
4.1.2. Procedures for HC assessment through SHM system 73
4.1.3. Historical remarks of the São Lourenço Church 75
4.1.4. Damage assessment of the internal and external area of the São Lourenço Church 80
4.1.5. Dynamic characterization and long-term SHM proposals 86
4.1.6. Final comments 89
4.2. Monitoring plan for Nossa Senhora das Dores Church 90
4.2.1. Introduction 90
4.2.2. The Nossa Senhora das Dores Church 95
4.2.3. Experimental setup and natural frequencies identification 98
4.2.4. Optimized SHM proposal 101
4.2.5. Final comments 104
5. Long-term monitoring of the Foz Côa Church 105
5.1. Introduction 106
5.2. The Vila Nova de Foz Côa Church 108
5.3. Real-time monitoring system implemented at Foz Côa Church 111
5.4. Influence of the temperature on structural displacements 114
5.5. Combined effect of the temperature and relative humidity on structural displacements monitored 120
5.6. Final comments 123
6. Structural monitoring of the retrofitting process, characterization and reliability analysis of the Santo António Church 125
6.1. Introduction 126
6.2. Guidelines for heritage construction assessment 128
6.2.1. Area of application 128
6.2.2. Criteria 129

6.2.3. SHM system definition 129
6.2.4. Step-by-step of the guidelines for HC assessment 130
6.3. Santo António Church: case study 136
6.4. Structural health monitoring of the Santo António Church retrofitting 140
6.4.1. SHM system 140
6.4.2. Setups of monitoring 141
6.4.3. Retrofitting monitoring of the Santo António Church 144
6.5. Structural characterization of the Santo António de Viana Church 148
6.5.1. Pressuremeter testing 149
6.5.2. Operational modal characterization 152
6.6. Reliability analysis of the Santo António Church 157
6.7. Final comments 160
7. Conclusions and future work 163
References 173
Annex: Scientific publications resulted from the work developed 187
Patent 187
Technical Reports 187
Articles in international journals with referee 188
Articles in conference proceedings 189

LIST OF FIGURES

Figure 1. Examples of ancient buildings damaged by past earthquakes occurrences in Italy, where Mw is moment magnitude [2]. 2

Figure 2. Example of a relative displacement optical sensor: a) illustrative view and b) sensor implemented [15]. 5

Figure 3. New and renovation ration on residential buildings in Europe in 2014[17]. .. 13

Figure 4. Natural hazards occurrence since 1980: a) number of events and b) monetary losses [30]. 14

Figure 5. Material degradation by environmental action. 15

Figure 6. Illustrative scheme of a SHM system with decentralized distribution and remote access. 16

Figure 7. Summarized view of the Lifshitz & Rotem's work: a) samples (Polyester) used on the experimental (a' – unfilled, b' – 40% filled before reaching dewetting and c' – 40% filled after reaching dewetting), b) experimental setup and c) and d) the results of the dynamic changes detected by vibrational testing [47]. 18

Figure 8. Patents register classification in sensor, methods, systems and platforms. 23

Figure 9. ASCE benchmark steel frame structure [80]. 25

Figure 10. SHM of a T-beam bridge: a) profile of the beam and its sectional reinforcement (cm) and b) configuration of the SHM system [102]. 31

Figure 11. Canton Tower monitoring scheme [42]. 32

Figure 12. Examples of important HC: a) Porto historic downtown and b) Coliseum, Rome, Italy. 33

Figure 13. Characterization of the HC analyzed: a) construction age, b) main assessment methods c) main buildings components affected by damages e d) main damage founded. 34

Figure 14. Brass mold employed to create the grooves in the POF, below the mold a detail of the POF with the grooves is shown. 45

Figure 15. Data acquisition system. 46

Figure 16. Computational management system 46

Figure 17. Experimental setup: a) details of the experimental work and its components; b) detail of the groove in the fiber during the optical signal processing, and c) soil test box without sand and with sand. 47

Figure 18. Grain size distribution of the sand used to experimental tests. 48

Figure 19.Variation of the transmitted optical power with the water level for the two sensors produced, during the water level increasing. 49

Figure 20. Variation of the transmitted optical power with the water level for the two sensors produced, during the water level decreasing. 50

Figure 21. Variation of the transmitted optical power with the groundwater level increase, for sensors S050 and S025. 51

Figure 22. Residual analysis of the optical power measurements to S050 and S025 to groundwater rising, water rising and water decreasing. 53

Figure 23. Fortaleza's Cathedral. 54

Figure 24. FBG structure and detail of the spectral responses. 58

Figure 25. Details of the sensor FBG01: (a) front and (b) bottom views. 60

Figure 26. Details of the two components of the sensor FBG01 (a and b) and aspect of the sensor after PU spray fulfillment without surfaces regularization. 60

Figure 27. Setup of the bond-slip optical sensor FBG01. 61

Figure 28. Details of the implemented bond-slip optical sensors FBG02 (a) and FBG03 (b). 62

Figure 29. Disposition of the bond-slip FBG sensors inside the specimen. 63

Figure 30. RC specimen before a) concrete fulfillment and after b) concrete fulfillment process. 63

Figure 31. Experimental setup of the pull-out testing: a) details of the pull-out testing equipment and b) photography of the testing carrying-out. 64

Figure 32. Experimental data from pull-out testing: a) Trial 1 and b) Trial 2 collected by FBG01 sensor at position SM. 65

Figure 33. Experimental results from the Trial 1, where a) correspond to Force vs. Time and b) presents Force vs. Relative displacement, both collected by LVDT, and c) and d) show the data collected by the FBG02 (positions S2, S7 and S9) and FBG03 (positions S1, S5, S6, S8 and S10) sensors. 66

Figure 34. Experimental results from the Trial 2, where a) correspond to Force vs. Time and b) presents Force vs. Relative displacement, both collected by LVDT, and c) and d) show the data collected by the FBG02 (positions S2, S7 and S9) and FBG03 (positions S1, S5, S6, S8 and S10) sensors. 67

Figure 35. Maximums reinforcing bar displacements at 600 seconds (Trial 1) and 200 seconds (Trial 2) measured during the experimental setups each 5 cm. 68

Figure 36. Reinforcing bar displacement each monitored point at 100 kN of pull-out force. 68

Figure 37. Case studies analyzed by IC-FEUP since 2000 [148]. 72

Figure 38. Flowchart of the procedures for designing system monitoring of HC. 74

Figure 39. São Lourenço Church: a) Main façade and b) interior view. 75

Figure 40. View in plant of the São Lourenço Church. 76

Figure 41. Buttresses at the West zone of the São Lourenço Church. 79

Figure 42. Positioning of the relative displacement sensors provided by LNEC. 79

Figure 43. Mapping of soil classification for construction according with Porto Geotechnical Report and location of the São Lourenço Church. 80

Figure 44. General scheme of the displacement mechanism at São Lourenço Church.. 81

Figure 45. Cracks occurrence at the exterior zone of the São Lourenço Church. 82

Figure 46. General view of the cracks location at the interior of the São Lourenço Church. 82

Figure 47. Crack mapping of the lateral chapels of the São Lourenço Church: a) Santas Mães Chapel, b) Santa Quitéria Chapel, c) São José Chapel, d) Santa Rita de Cássia Chapel, e) Nossa Senhora da Soledade Chapel and f) Nossa Senhora da Conceição Chapel. 83

Figure 49. Damage occurrences on Santíssimo chapel: a) vault, b) cracks on the vaults, c) and d) present the cracks occurrence on the chapel walls. 84

Figure 50. Nossa Senhora da Conceição Chapel: a) vault and b) location of the main crack. 84

Figure 51. Altar-Mor of the São Lourenço Church: a) general view and b) main cracks occurrences. 85

Figure 52. Examples of the thermographies collected at interior of the São Lourenços' Church. 85

Figure 53. Experimental scheme proposed for dynamic characterization of the São Lourenço church. 86

Figure 54. Optical system proposed for implementation in the São Lourenço Church: a) global longitudinal central section view of the church, b) detail of the FBG sensors' layout and São José Chapel. 87

Figure 55. Distribution of the linear displacements, tilts, accelerations and temperatures sensors along of the São Lourenço Church. 88

Figure 56. Detailing of the components of the SHM system for be implemented at São Lourenço Church. 89

Figure 57. Relation between the effective modal mass and the natural frequencies of the main modal shapes of different structures geometry [9]. 93

Figure 58. Ambient vibration procedure selected for Nossa Senhora das Dores Church characterization. 94

Figure 59. Distribution of the number of seismic occurrences at Ceará State since 2008 till 2016, and its respective maximum magnitudes. 95

Figure 60. Nossa Senhora das Dores Church: a) main façade and b) lateral view of the church. 96

Figure 61. Schematic cut of the Nossa Senhora das Dores Church geometry, where 1 is the Central Nave, 2 is the Altar-Mor, 3 is the lateral Nave, 4- is the Coro-Alto, 5 is the bell-tower and 6 is the office. 96

Figure 62. Interior of the Nossa Senhora do Rosário Church: a) Altar-Mor, b) Central Nave and Coro Alto, c) columns and arches and d) lateral Nave. 97

Figure 63. Damage mapping of Nossa Senhora das Dores Church. 97

Figure 64. Examples of the damages found during the inspection on Nossa Senhora das Dores Church: a) degradation by biological action, b) cracks in the arches and c) humidity presence in the roof slab. 98

Figure 65. Accelerometers positioning and data collecting. 99

Figure 66. Firsts 16s of the acceleration registered on Nossa Senhora das Dores Church: a) acceleration collected in X direction and b) acceleration collected in Y direction. ... 99

Figure 67. Frequencies spectra obtained, thought the FFT, by OMA of the Nossa Senhora das Dores Church. 99

Figure 68. Scheme of accelerometers positioning. 101

Figure 69. SHM proposal: linear displacement sensors positioning. 102

Figure 70. Scheme of the optical sensors placement: a) general view of the optical sensors positioning on the Southeast façade and b) detail of the sensors. 103

Figure 71. General scheme of the SHM proposal for Nossa Senhora das Dores Church. 103

Figure 72. Foz Côa Church: a) main façade, b) geographic location, and c) interior view of the Foz Côa Church. 108

Figure 73. Photograph of column 2, evidencing its inclination. 109

Figure 74. Main façade of the Foz Côa's Church in 1960, undamaged (a), and b) in 1996 with damages [170]. 110

Figure 75. Main interventions carried out on Foz Côa Church in the 1970s: a) bracing of the Main Arch and columns, b) details of the columns bracing and c) details of the main arch bracing; d) inspection performed on foundations elements and e) detail of project of the reinforced concrete roof slab built[170]. 110

Figure 76. Geometric view of the Foz Côa Church (a) where 1- is the main façade, 2- is the Central Nave, 3- is the Altar-Mor and 4- is an office; the transversal view of the detail AA is presented in (b) and the sensors positioning are shown by (c). 111

Figure 77. Setup of the SHM system implemented at Foz Côa Church. 112

Figure 78. Schematic view of the movements and orientations monitored through sensors C1A and P1. 113

Figure 79. Schematic view of the movements and orientations monitored through sensors F7 and F8. 114

Figure 80. Schematic view of the movements and orientations monitored through sensor F4. 114

Figure 81. Time evolution of the internal and external temperatures and relative humidity monitored at Foz Côa Church. 115

Figure 82. Time evolution of the inclination measured by sensor C1A on column 2 with and without the temperature effect. 116

Figure 83. Time evolution of the displacements measured by sensor P1 on the bottom of the column 2 with and without the temperature effect of T1. 117

Figure 84. Time evolution of the temperature and displacements measured on the bottom of column 2 in July and August 2015. 118

Figure 85. Time evolution of the displacements measured by sensor F8 on the top of the internal side of the main façade with effect of the temperature and without temperature effect of T1. 119

Figure 86. Time evolution of the displacements measured through sensor F4 on the top of the tower and sensor F8 on the internal side of the main façade (transversal movements) with the temperature effect. 120

Figure 87. Influence of the combined effect of the internal temperature and relative humidity on the inclination movements, measured through sensor C1A at column 2. 121

Figure 88. Influence of the combined effect of the internal temperature and relative humidity on the displacement measured at the bottom of column 2, by sensor P1. 122

Figure 89. Influence of the combined effect of the internal temperature and relative humidity on the movements at internal side of the main façade collected by sensor F8. 122

Figure 90. Structural health monitoring platform for heritage construction safety assessment. 131

Figure 91. Santo António Church: (a) view in plant, (b) section AA and (c) main façade. 137

Figure 92. Details of the chapel walls: (a) wall without mortar layer and (b) detail of the wall after the retrofitting. 139

Figure 93. Main cracks observed on Santo António Church during the visual inspections. 139

Figure 94. Superior view of the vaults with some cracks retrofitted through a steel structure. 139

Figure 95. General setup of the SHM system implement on the Santo António de Viana Church. 141

Figure 96. Columns 1, 2 and 3 and arches 1, 2 and 3. 142

Figure 97. Monitoring steps of the Santo António de Viana's Church, and correspondent sensors location. 143

Figure 98. Time evolution of the temperatures collected by sensors T1 and T2. 144

Figure 99. Time evolution of the inclination measured through (a) sensor C1A and (b)sensor C1B. 145

Figure 100. Time evolution of the relative displacements measured by sensors (a)F2 and (b)F3. 146

Figure 101. Time evolution of the relative displacements collected by sensors (a)F4, (b) F5 and (c)F6. 147

Figure 102. Time evolution of the relative displacements collected by sensors (a)L1, (b)L2 and (c)L3. 148

Figure 103. Experimental setup of the Pressuremeter testing and measurements location. 149

Figure 104. Experimental results of the Pressuremeter testing. a, b, c, d, e and f correspond to openings P1, P2, P3, P4, P5 and P6, respectively. 150

Figure 105. Pressure curves versus deformation, measured during the Pressuremeter testing, where (a), (b), (c), (d), (e) and (f) correspond to P1, P2, P3 P4, P5 and P6 positions, respectively. 152

Figure 106. Experimental setup of the ambient vibrational characterization of the Santo Antonio's Church, where (a) testing area, (b) and (c) are trial 1 and 2 respectively, (d) transversal detail of the accelerometer positioning and (e) and (f) are details of the of the accelerometers placed on the columns and roof. 154

Figure 107. Visual aspect of the Labview® data acquisition system implemented, during the first trial. 155

Figure 108. a) test setup and measurement points and b) corresponding geometry in Artemis. 155

Figure 109. Enhance Frequency Domain Decomposition of the measured acceleration data collected by vibrational ambient characterization. 156

Figure 110. First six modal shapes of the Santo António Church. 157

Figure 111. Acceleration data measured during the first trial. 158

Figure 112. Maximum displacement histograms, on the X and Y directions for a) and b), respectively. 158

Figure 113. Reliability indexes of the Santo Antonio's Church from current state till next 100 years. 160

LIST OF TABLES

Table 1. Damage identification methods classification proposed by Rytter (1993). 20

Table 2. Method of classification for SHM platforms 27

Table 3. Historical remarks of the São Lourenço Church 76

Table 4. Natural frequencies identified through ambient vibration testing of the Nossa Senhora das Dores Church. 100

Table 5. Determination coefficient (R2) between temperature T1 and T2 and the displacement monitored at sensors C1A, P1 and F8. 116

Table 6. Main contents of the technical reports performed on Santo António de Viana's Church. 138

Table 7. Average values of the GPMT and EPMT obtained from the Pressuremeter tests. 151

1

Introduction

1.1. Motivation

Heritage constructions (HC) comprise a special group of structures that due to their high cultural value, variability and the lack of knowledge on its structural behavior, have become an interesting and challenging topic for the technical-scientific community. The large time of exposition to environmental influences changes the structural system over time and, in some cases, the absence of adequate maintenance or retrofitting measures, are examples of factors that can contribute to the fragile behavior and consequently a high failure risk under dramatic environmental scenarios, such as earthquakes, typhoons and floods occurrence, among others [1].

The past experiences of seismic occurrences in Italy (Figure 1) demonstrates how fragile ancient buildings can be, especially because most of them comprise masonries structures (with low resistance under tension). In recent years, the earthquakes that have occurred in L'Aquila (2009), Christchurch (2010-2011) and Emilia Romagna (2012), highlighted the current necessity to keep HC safe. The occurrence of L'Aquila earthquake, for example, left 410 cases of HC with critical damages [2]. The previous information and performance evaluation of the structural systems of these structures could have been useful for the adoption of retrofitting measures and to minimize the damage scenarios [2].

Early maintenance is important to minimize the structural risk. However, the performance assessment of HC can be a complex activity, especially due to the lack of information about materials characteristics (material composition and performance under service

work), loading history [3], as well as the fact that HC requires specific approaches that consider their cultural value, structural system variability and application of non-destructive testing (NDT) [4].

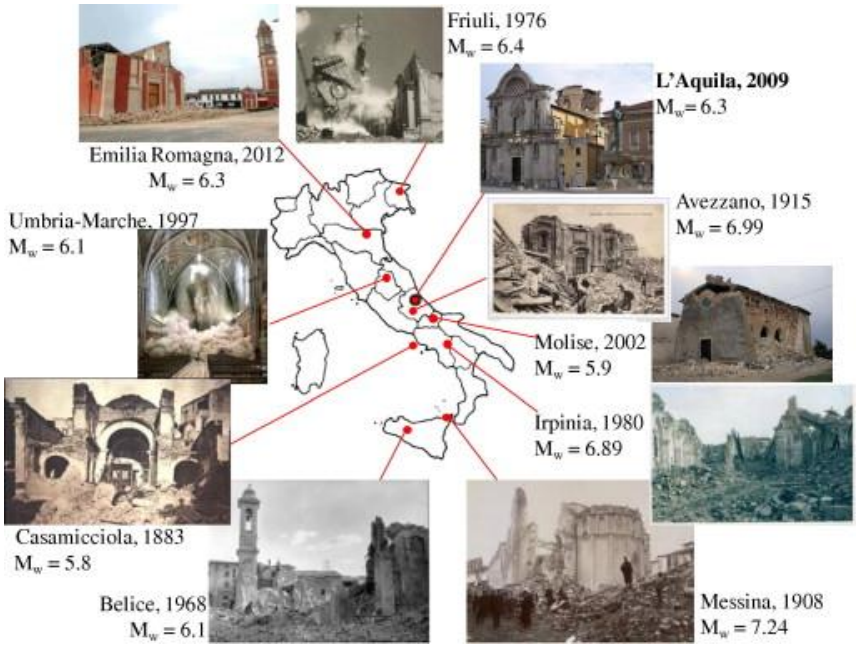

Figure 1. Examples of ancient buildings damaged by past earthquakes occurrences in Italy, where *Mw* is moment magnitude [2].

According to Venice Chart (1964) cited in CIB (International Council for Research and Innovation in Building Construction) publication 335 – *Guide for the structural rehabilitation of heritage construction* [4], the assurance of the structural safety, acceptance of the cultural value of the HC, guarantee of minimum intervention, reversibility of the intervention carried out, integration and compatibility between geometry and materials of the structural components, and also the minimum cost, are the main principles that all interventions on HC should comply to. Nevertheless, technical reports on HC maintenance can present different approaches, considering the variation between countries and its own regions, according to level of interest in the maintenance and preservation of HC (for instance, the recent *Norme tecniche per le costruzioni* - NTC of 14th of January of 2008 [5] and Bulletin 11 of ALCONPAT [6]), making it difficult to establish international codes that combine the fulfillments and interests of different societies. This issue, however, highlights the necessity of implementation of different strategies and methodologies for characterization and structural assessment of HC a way for overcoming technical issues.

In this way, SHM (Structural Health Monitoring) can be a relevant and modern tool to support the characterization and structural assessment of HC, especially because it can combine non-destructive approaches with real time data acquisition. The possibility to use data processing systems, combined with safety assessment methodologies in real time, can also contribute for the early identification of changes on structural behavior. Moreover, the data acquisition cost decreases and the high number of sensor devices implemented in the literature have contributed for the spread of SHM application on civil constructions [7]. Some factors still are pointed as issues to be overcome by technical community, for instance, the design step and early procedures often request large periods of time because tasks as the sensors selection, details of the data acquisition system and even the choice where the sensors will be positioned need to be supported by a comprehensive view of the assessed HC and its damage mechanism, as well the increase in the time of monitoring can demand the employment of large data storage systems, making that a high cost strategy.

In fact, the employment of SHM for HC monitoring can be interesting because usually HC presents a dense history of changes in its materials properties and their structural systems, especially motivated by environmental actions and the large number of interventions carried out during their service life. These changes, on its material properties and/or structural systems, can provoke different structural responses along the time, making SHM an adequate approach for investigating the time-evolution responses of these structures, as well to collect reliable information on its safety state. Additionally, only few cases regarding SHM of HC can be found in the literature, as also mentioned by [8, 9], and the existing cases are mainly related with description of strategies for dynamic monitoring, highlighting the need of contributions on this topic, especially related with:

- Development of new sensors focused on HC necessities;
- Implementation and systematization of strategies and news methodologies for SHM of HC;
- Advances on data processing and strategies for real-time monitoring of HC;
- Employment of technological tools, as smartphones and video cameras, for instance, as part of the monitoring system.

In fact, SHM is commonly designed as way to measure dynamic effects than static ones [10, 11], because dynamics phenomenon observation requires a high frequency of data acquisition, and, in this case the structural responses under dynamic effects can be minimally observed and analyzed. However, there are other phenomenon's that can slowly affect the structural parameters and also need attention, especially in the cases of HC, as for instance the environmental influence on relative displacements of the structural system. While these slow mechanisms do not need a high frequency data acquisition, they request long-term monitoring for an accuracy investigation of the environmental influence on structural performance, and can be used for local identification of structural changes. Moreover, SHM can be an alternative technique to support retrofitting processes, allowing to quantify the impact of the retrofitting on the structural system, making possible to change early the repair strategy if the structural response does not correspond to the structural answer previously idealized in the design stage. It is worth of notice that, in this research perspective, in 2000, IC/FEUP was one of the first research groups to start working in the area of HC monitoring, when the data acquisition systems were still limited and the communication between the SHM system components needed to be made through cables.

For a good and adequate level of responses, SHM systems should comprise measurement devices compatible with the building requirements and monitored parameters, with adequate data collecting frequency, proper measurement range, high durability and low interference on the signal processing. For the case of HC, depending of the constructive typology, the sensorial system can present special needs, as for instance the ability to record small displacements with a high level of accuracy (specially for structures with high rigidity level) and to be visually less intrusive as possible. In this case, optical sensors can be an assertive choice for SHM of HC, because they present high sensibility, small dimensions (see Figure 2), immunity to electromagnetic field influences and different sensors can be multiplexed in the same optical fiber, moreover with the recent advances its production cost decreased [12]. Nonetheless, no reports on optical sensors specifically designed for HC applications were found in the literature (see [13, 14]) making that a good contribution opportunity on the SHM development.

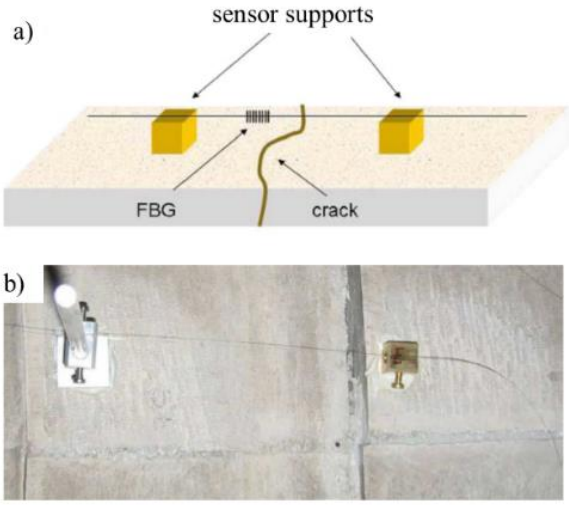

Figure 2. Example of a relative displacement optical sensor: a) illustrative view and b) sensor implemented [15].

Considering the above mentioned, the present thesis aims to contribute for overcoming the lack in the techno-scientific field through development of new optical sensors focused on HC necessities, as well as the development of methodologies for the HC characterization and monitoring with recurrence to real case studies, especially churches, namely São Lourenço Church, Nossa Senhora das Dores Church, Foz Côa Church and Santo António de Viana Church.

The SHM cases are approached in different stages and presented according to the SHM stage evolution, essentially due to the large time period comprised between the design of the SHM system, its installation, data collection and processing. In the cases of the São Lourenço and Nossa Senhora das Dores Church, for instance, this work contributes through the damage characterization and design of a monitoring proposal, while in the cases of Foz Côa and Santo António de Viana Church, this work contributes through data processing.

1.2 Aims

1.2.1. Main aims

The present work intents to contribute for the advance on conservation and rehabilitation techniques by the development of support tools for the characterization, monitoring and structural assessment of heritage constructions.

1.2.2. Specifics aims

- To develop, implement and validate SHM methodologies for characterization and assessment of HC;
- To report the conception and strategies employed for characterization and long-term monitoring of HC based on wireless sensor networks;
- To study the effect of the environmental effects, namely temperature and relative humidity on structural displacements of HC through long-term monitoring systems;
- To develop a new approach for HC construction safety assessment based on reliability analysis with recurrence to monitoring of vibrational measurements;
- To develop and to implement new optical sensors based on fiber Bragg grating (FBG) technology focused on HC applications, specifically to groundwater level and bond-slip monitoring.

1.3. Originality and relevance

This work present original and relevant contributions for civil engineering development, specifically in the employment of SHM techniques for characterization and monitoring of HC. The contributions are listed according to work timeline order, as following:

i) In complementary way to overviews reported in the literature, in this work a global review on SHM advances, mainly focused between 1993 and 2015, are presented and the main works developed in this field are described in a summarized form. A patent survey is showed as form to provide a global

perspective about the state of development on SHM techniques, and new opportunities for advances on SHM, introducing HC related topics.

ii) A method for SHM platform classification, divided in 5 levels is presented. The main aim of this methodology is to provide orientation for owners and technicians about the level of performance that the SHM system should present under work, optimizing the design phase;

iii) The groundwater level monitoring sensor introduces an innovative liquid level monitoring concept as well a simplified system. In fact, the sensor developed provides a lower-cost device for SHM, employing POF (Plastic Optical Fiber), that do not demand a complex data acquisition system. The sensor was designed considering the problems related with foundations settlement reported in the literature, developed to work under hostile environments, and can be applied for the foundation elements monitoring, for instance;

iv) The relative displacement optical sensor introduces a new measurement device for SHM application, essentially focused for linear relative displacements monitoring between two points. The employment of FGB technology in this application, and the sensor design configuration provides a simplified system that allow to measure relative micrometer displacements between two superficies in real time, really useful for structures with high rigidity, as stone structures for instance. In this work, the sensor was tested and validated through the monitoring of a reinforced concrete sample.

v) Considering that SHM is not an easy task and require time for an adequate evaluation of the structural condition, an optimized proposal for a SHM system design is presented, recurring to the real case studies, such as the São Lourenço Church (Porto, Portugal) and Nossa Senhora das Dores Church, built in XIX century (Sobral, Brazil). Concerning the Nossa Senhora das Dores Church, this contribution represents a fundamental effort towards the development of SHM of HC in Brazil, especially to study of the structural behavior under environmental influence.

vi) Moreover, the effects of the temperature and relative humidity on relative displacements of structural stone elements are studied in this Thesis, with recurrence to case study of Foz Côa Church, a Portuguese HC from XVI

century. The conception and strategy of long-term monitoring through a wireless sensor network is also presented in this work.

vii) A new methodology for HC assessment based on reliability analysis is also presented in this thesis, and its application is demonstrated through a Portuguese case study from XVIII century, namely Santo António Church. Furthermore, the conception of the monitoring system, as well the structural characterization and the retrofitting monitoring results are discussed.

viii) This work presents relevant contribution for the field of HC monitoring because it reports monitoring strategies employed for different situations and in different case studies. The application of the concepts developed in the present work allow different SHM employment approaches for HC, namely for structural characterization, study of the environmental effects on structural elements and safety analysis.

In a general form, this work presents some relevant contributions for the SHM field advances, summarized by the development of two innovative sensors, implementation of a new methodology for HC safety assessment, by the description of the conception strategies and results, by monitoring of the cases studies already described. Thereby, these contributions fill an existing gap in the techno-scientific field on the development of SHM platforms and studies, especially dedicated to HC safety assessment.

1.4. Work organization

This work was organized in seven chapters. In Chapter 1 the initial considerations about the motivation, main goals and relevance of the present work are presented. Chapter 2 is dedicated to literature review about the scope of the Thesis. Chapter 3 is devoted to the presentation of the optical sensors developed in this work, while the Chapters 4, 5 and 6 are dedicated to description of the cases studies carried out in this work. Chapter 7 presents the main conclusions found throughout the development of this work, a critical analysis followed by suggestions for future developments on SHM of HC, identified during this work evolution. The annex includes further information not presented in the main text but relevant for the global understanding of this work.

Chapter 2 provides a literature review on advances on SHM. The basic concepts are shown and the main contributions reported in the literature are mentioned. The result of a survey realized in the main patent register banks is presented, and a system of SHM platform classification is proposed. In addition, some cases of SHM of HC are mentioned and comments about the future development of SHM performed.

Chapter 3 unveils the optical sensors developed in this work considering the implementation of SHM systems for HC. Namely, two optical sensors were developed and experimentally tested, a groundwater level sensor and a relative displacement sensor.

Chapter 4 describes the early procedures for SHM, presenting as well the monitoring proposals for São Lourenço and Nossa Senhora das Dores Churches. An historic survey is presented followed by structural damage characterization those HC. Concerning to the São Lourenço Church, based on the damage mapping, a damage mechanism hypothesis is proposed, as well as a detailed SHM system. Regarding to the Nossa Senhora das Dores Church, an ambient vibrational characterization was carried out in order to identify the first fundamental frequencies, and a monitoring proposal is also presented. Despite the absence of significant damage scenarios at the Nossa Senhora das Dores Church, its selection as a case study in this work is related with the necessity of boosting developments on structural behavior studies and characterization techniques for ancient Brazilian structures under environmental influence.

In Chapter 5, the long-term monitoring of the Foz Côa Church through a wireless sensor network is presented. In this chapter, a study on the influences of the temperature and relative humidity on the relative displacements of the structural elements of the Church is performed.

In Chapter 6, the structural monitoring of the retrofitting process, characterization and monitoring results of the Santo António Church are presented. Specifically, a methodology for HC assessment is described, as well a new approach for safety assessment based on reliability analysis. Moreover, the dynamic characterization was performed trough OMA (Operational Modal Analysis), and potentiometer tests were carried out in order to characterize the mechanical properties of the columns in the retrofitted area.

In Chapter 7, the main conclusions, through the development of this Thesis, are described, and a critical analysis on SHM is performed. Additionally, suggestions for further developments on the SHM of HC field are presented.

2

Global overview on advances in SHM

Summary

Advances in the development of sensors, data processing systems and numerical models have motivated the implementation of SHM, specially focused on the assessment of structural safety. Thus, this chapter presents a literature review about SHM platforms, especially from 1993 to 2014. In this way, a short history review about the recent advances on SHM, mainly related with dynamic monitoring, was summarized, and a benchmark and the main guidelines related with SHM platforms were also included in this review. Some case studies are also described here. Special attention was given to SHM platforms, and a method for their classification (an extension of Rytter's method) is presented. Additionally, experiences related with heritage constructions, specially focused on maintenance were included in this work. In the final section, some observations are made about the new prospects for SHM. The recent advances on SHM platforms contributed to the development of adaptive systems and to the cost reduction of the monitoring systems implementation, allowing the increase of its application in real structures. However, the monitoring systems should be implemented optimizing all the available sensing technologies.

Keywords: Structural health monitoring, platforms for structural monitoring, heritage construction, damage assessment, smart structures.

2.1. Introduction

2.1.1. From construction to retrofitting: the change of focus.

Currently, the worldwide population is around 7 billion people and the predictions are that by 2100 this number be of 11.2 billion [16]. In fact, the population growth will cause an increase in the need for housing. Nevertheless, considering the actual scenario of the climate conditions and its influence on the increasing probability of occurrence of natural hazards, this growth will be conditioned by the need for lower environmental impact new buildings and also by the recovery of heritage buildings, adapting them to the owners' needs. Consequently, new materials will be developed and introduced in the construction industry and maintenance approaches, new repair interventions methods for structural assessment will be implemented.

In emerging economies, the association between the development and introduction of new materials and the increase in the search of structural retrofitting, also motivated by compulsion for more competitive costs, tends to present a higher impact than in stabilized economies, with direct repercussions on building materials and constructive methods. Nowadays reinforced concrete is the most employed material in the construction industry, but the forecast on worldwide concrete consumption points towards a decrease in its employment by 2100 [16]. If the concrete consumption decreases, especially in emergent countries like Brazil and South Africa, the number of new constructions also will decrease and the need for maintenance of the current structures will grow. This change of focus from "design of new structures" to "maintenance of the current constructions" in the construction industry is starting to be observed nowadays in the European community (see Figure 3).

Therefore, the main issue is: how does the civil engineering sector intend to maintain the existing buildings safe and in good habitability conditions for the future generations? This question has motivated, essentially since the 1960 decade, the development of reinforcement techniques with lower impact for existing buildings and new methods of nondestructive assessment specially focused on the detection of damages in real time, the so-called structural health monitoring (SHM). In this context, the development of systems for the control, gathering and management of data on structural safety parameters aimed

at SHM is a new opportunity for researchers, builders and construction companies to contribute to the development of "smart structures".

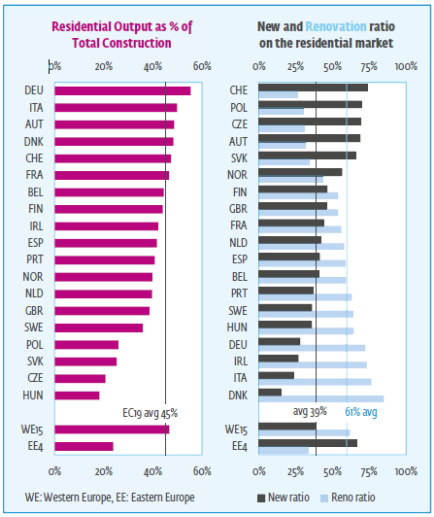

Figure 3. New and renovation ration on residential buildings in Europe in 2014[17].

2.1.2. Importance of SHM for structural safety maintenance

Often the structures are subjected to natural actions, and can also be subjected to the occurrence of environmental hazards and excessive loadings that were not considered during the design phase, compromising its structural safety. Nevertheless, the structural lifetime also depends on a series of other requisites, namely: materials quality, adequate design approach, adequate construction methods, execution and existence of maintenance phases [18]. However, if the emergence of damage had been diagnosed early and if safety measures had been adopted, dramatic consequences such as the resulting from the recent seismic events in Loma Prieta (1989), Northridge (1994), Kobe (1995), Chi-Chi (1999) and Emilia-Romagna (2012) could have been avoided or minimized [19]. Thus, it is correct to consider that after the construction stage the structural lifetime is principally conditioned by the adoption of maintenance measures and the intensity of environmental actions. This way, the SHM could be applied in the detection and diagnostic of damage in early stages and in the prediction of structural risk.

Case studies on SHM [20–23], specially focused on damage identification and structural safety maintenance, for application on large infrastructures as well as on residential and commercial buildings, have become increasingly narrated in the literature. Examples of the decentralized systems and advances on the development of sensors are frequently

introduced in the structural monitoring area [24–26]. Essentially the innovation on SHM was initially motivated by the increase in the number of occurrences of natural disasters, like earthquakes, hurricanes, cyclones, floods and typhoons, that according to Munich RE [27] survey has grown since 1980. In fact, the occurrence of a natural hazard in populated zones tends to present more dramatic losses, and this effect should be most intense if the affected zone presents a low economic development index [28, 29].

Annually the worldwide monetary losses related to the occurrence of natural hazards are in the order of billions of dollars (Figure 4.a), and are deeply linked with structural and infrastructural damages. A survey report presented by Munich RE about global economic losses caused by natural disasters occurred between years 2010 and 2015 relates that in this short time the losses were of US$ 1 075 billions (Figure 4.b), and it is expected that until 2020 the losses will be the highest ever recorded in world history [30].

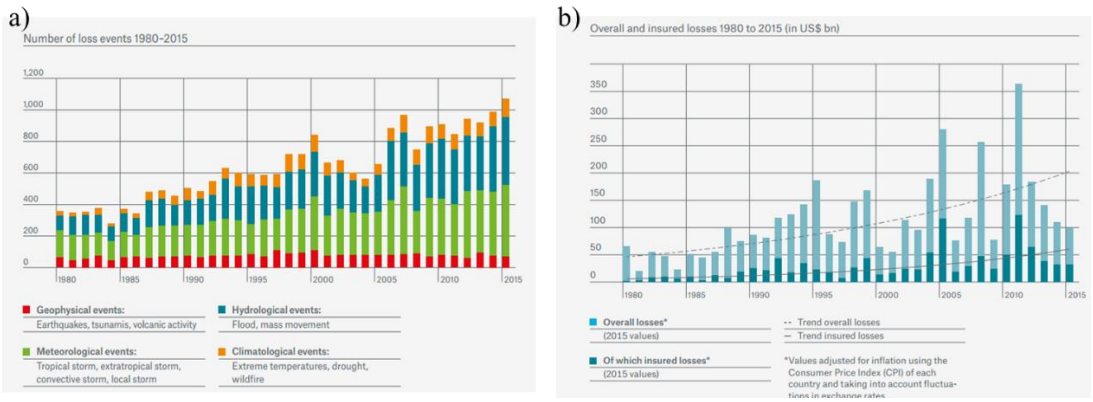

Figure 4. Natural hazards occurrence since 1980: a) number of events and b) monetary losses [30].

In fact, the economic crises all around the world have often been initially motivated by the occurrence of environmental disasters [31] in opposition to economic and industrial development. Thus, considering that the rise in the number of natural hazards on vulnerable zones are centered in the global climate changes, global policies have been developed in order to raise sensibility to natural disasters, the Conference on Sustainable Development – Rio +20 [32], organized by the United Nations in June of 2012 in Brazil, being a prime example, and this endorses the relevance and need for innovative developments in structural safety maintenance.

Beyond natural hazard occurrences, the structures are subjected to other natural phenomena due to exposition to environmental conditions, like corrosion, carbonation,

and alkali-silica reaction, which also have an influence on accelerating material degradation (Figure 5), and consequently decreasing their lifetime. From these, corrosion may possibly be the most evident phenomenon of material degradation in steel and reinforced concrete structures being accelerated essentially by the formation of chlorides or another inorganic salt. Hence, corrosion constitutes a global problem [33] that has mobilized the academic community to study its mechanisms of occurrence, catalytic agents, and methods of prevention (especially mixtures to concrete) and repair [34–37]. A survey performed by the Federal Highway Administration in the United States demonstrated that there are 134000 bridges requiring immediate repair measures and 226000 bridges presenting corrosion problems, resulting from environmental actions combined with a low frequency of repair proceedings [18]. Indeed, the structural assessment should not only include the structural parameters but also consider durability parameters, for a most effective evaluation with the purpose of offering data to a better structural characterization.

Figure 5. Material degradation by environmental action.

Actually, structural assessment is based on two distinct groups of data: 1) the information from visual inspection and, 2) the data from experimental testing. Essentially the visual inspection has been the initial step for the start of structural assessment, and the alert on damage emergence should be firstly noted by the own owners' observations. For structural behavior characterization, the employment of destructive test (DT) can be essentials, however the new perspectives in SHM introduce the concept of "non-intrusive assessment" in the structural evaluation. Along this line, the number of the nondestructive tests (NDT), especially for *in situ* applications, have presented an expressive rise [38–40]

motivated primarily by need of lower impact to construction, more competitive cost and time reduction for data acquisition during the assessment process. In truth, the advances on NDT for structural assessment allowed the expansion of information about special constructions, namely HC, especially due to the fact that these constructions present a large cultural value and their original characteristics should be preserved.

In complementary way, the advances on the sensing field allowed for the use of sensors in SHM applications with the multifunction of measuring, collecting and transferring data. Today the sensing systems present a decentralized distribution and their configurations can be framed according to the construction's needs in order to provide information for global structural characterization [25], as the illustrative scheme provided by Figure 6. In fact, some working sensing systems could also be optimized for the information to be available in a virtual platform, allowing the remote access to the data [41]. This practice has been implemented with the aim of optimizing technical work for the structural assessment in real time [42]. However, the technological advances on SHM do not have as a goal to eliminate the human role in the structural assessment [43], but to offer a high performance tool for the evaluation of structures.

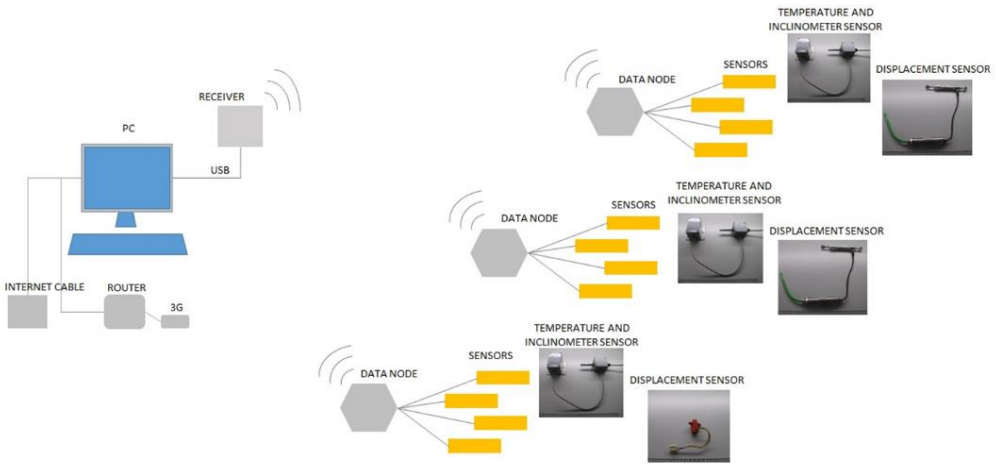

Figure 6. Illustrative scheme of a SHM system with decentralized distribution and remote access.

Differently from other works on SHM state-of-the-art (see [44, 45]) the present chapter approach is focused on issues related with HC maintenance, providing suggestions for ancient constructions preservation. This work provides a global overview on SHM latest advances, especially concerning the systems and platforms. An introductory section about the main historical advances is presented in order to offer a global perspective about the

aims of SHM. Recent case studies related with heritage constructions and SHM were also included in this review. Moreover, the present review contemplates a literature analysis from 1993 to 2014, and the information was organized in six sections, namely: 1) Introduction, 2) Short history and recent advances on SHM, 3) Classification of the SHM systems, 4) Heritage constructions: a special case for SHM, 5) New perspectives for SHM and finally section 6) Final comments.

Thus, this literature review is expected to provide high quality information for future advances on SHM and, especially, to contribute to the multiplication of cases studies on SHM considering HC.

2.2. Short history and recent advances on SHM

2.2.1 The initial history

In the initial step of civilization, the human necessity of keeping in safety motivated the development of civil construction. However, due to the materials' own characteristics, environmental actions and excessive loads, the construction degradation, evidenced by damage along the structure, made the need for structural assessment methods to emerge. In fact, the structural assessment is based on damage detection and its consequences for structural safety. Nevertheless, considering the various changes that can occur on a structure along its service life, it is necessary to delimit the comprehension about damages. Therefore, damages should be understood as the product of the harmful alterations in the material properties, due to physical, chemical, biological or human interference, that can reverberate in changes on geometry and modal responses, affecting negatively the durability and structural safety [44, 46].

Damage can affect the structures in two ways, namely: producing linear or nonlinear alterations on the structural behavior. The damages effects are characterized as linear when the structure presents a linear-elastic behavior and after the damage emergence this behavior is not altered and the predictions about the behavior should be determined based on the previous behavior. Examples of these types of damages can be the effects from material degradation processes like rebar depassivation and concrete disaggregation. Nevertheless, when modifications occur in the structural behavior, namely from linear to

nonlinear, after the damage emergence, this effect can be classified as nonlinear damage. Fissures and cracks are common cases of nonlinear damages, for instance [44].

The implementation of the NDT occurred in largest scale since the 60s, with the development of the new methods of testing and its application in real structures, was fundamental for the structural assessment evolution. In the 60s decades, the modal parameters were introduced as a way of analyzing the structural state. But the implementation of the structural monitoring was limited by the numerical models. One of the initial studies performed, which can be cited as a precursor of the SHM, was developed by Lifshitz & Rotem in 1969 [47] (see Figure 7). In the Lifshitz & Rotem's [47] studies vibrational techniques were employed in structural characterization by modal parameters, namely changes in the natural frequencies were used for identify damages emergence [48].

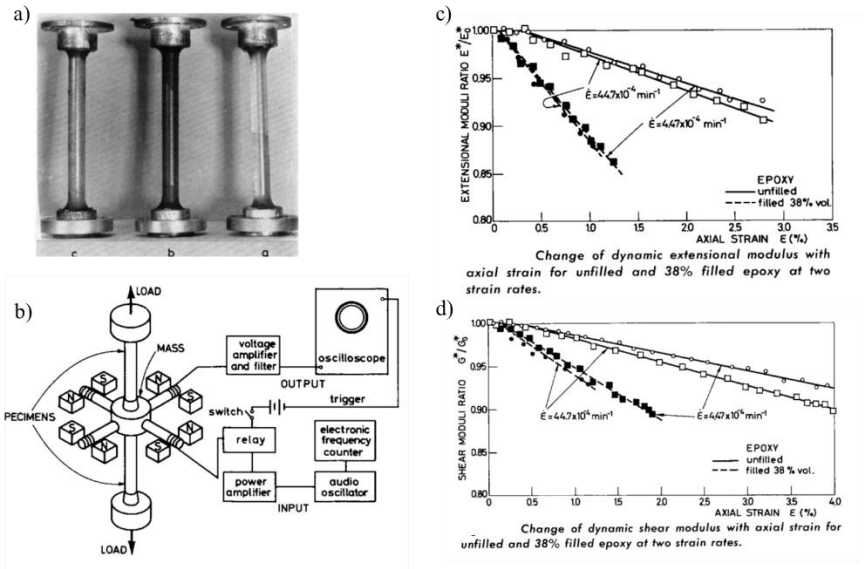

Figure 7. Summarized view of the Lifshitz & Rotem's work: a) samples (Polyester) used on the experimental (a' – unfilled, b' – 40% filled before reaching dewetting and c' – 40% filled after reaching dewetting), b) experimental setup and c) and d) the results of the dynamic changes detected by vibrational testing [47].

In this way, the employment of a time-history is of interest for the structural analysis because it can provide data for a long-time period considering different environmental conditions, variable loading situations and damage evolution. To implement the monitoring, devices which do not introduce new damages on the assessed structure (non-destructive methods) were developed, as well static methods and its applications [49], [50], especially after 1970 [48]. But, the most innovative works were developed focused

on to damage detection and assessment based on vibration analysis, especially based on changes in the natural frequency [51–53]. However, the employment of dynamic analysis also can give unspecific answers on structure behavior, this way the adoption of static method can contribute for a most complete understanding on the current situation of the structure.

The basic principle for damage detection using the vibrational analysis is that the modal parameters of the structure (frequency, modal shape and modal damping) can be defined through physical parameters (mass, damping and stiffness), and any alteration in these physical parameters results in variations in the modal properties. Thus, the relations between material degradation and its influences on physical structural parameters allowed the development of a large quantity of studies and, as a result, some methodologies for damage detection based on vibration analyses were developed [48]. However, other non-destructive methods can also be used for damage characterization such as the acoustic, magnet, radiograph, Eddy-current, thermic [46, 54] and more recently, the optical methods [13].

The analysis of the natural frequencies has been intensively studied in order to provide information about the initial moment of the damage emergence [46]. The initial advance for the use of frequencies changes for structural damage detection was given when was observed that, in structural elements, the occurrence of variations in the physical properties induced changes in the natural frequencies spectrum. However, the application of natural frequency analysis for damage detection has presented some limitations, especially to detection of the small cracks and fissures and the difficulty to differentiate the damages nature. Often, such methods provide a global analysis of the structures integrity, but do not give the location of the damage. Other recognized limitation is the environmental effect as the temperature or winds, for example, they cause changes in the structural frequencies and may result in incorrect interpretation about the damage occurrence. It's clear that this problem tends to be proportionally lower if the number of the monitored points is greater and the structural complexity is lower too [55, 56].

In fact, it's not totally understood yet what is the minimum magnitude of changes in the natural frequencies for the damage identification, but the most daring issue that has been motivating the studies development is: how does a specific damage can be identified

based in the natural frequencies changes? In order to answer this question, basically, the works realized between the years 1975 and 1996 were developed around the phenomenal of natural frequencies changes as result of the damage emergence in structures. Nonetheless, it is not yet possible to establish a relation with this phenomenon and its influence on the modal parameters, but these works present a series of data about the structural behavior on different situations, namely: variable environmental actions, structural complexity, variable work ability, and different experimental programs. Nevertheless, the introduction of numerical methods and models for analysis of the damage emergence and the employment of the information available by the previous works has contributed for advances on the damage identification methods, being a step forward in the damage characterization, localization and geometrical aspects and also to the prediction about the lifetime and structural behavior [44, 54].

The growth of the assessment methods focused in the damage characterization and its variability, has brought to light the emergence of the necessity for a classification system. Considering this question, in 1993, Rytter [48] proposed a classification to damage identification methods. The methods were organized according to the answer level, essentially centered in the damage existence, location, characterization and prediction. The classification proposed by Rytter is presented in the Table 1, as following.

Table 1. Damage identification methods classification proposed by Rytter (1993).

Graduation	**Objective**
Level 1	Damage detection (just provide information that the damage is present);
Level 2	Damage location (information about the geometrical damage configuration and the specifically occurrence location);
Level 3	Damage characterization (provide information about the intensity of the damage effects to structure)
Level 4	Lifetime prediction

Since the 70s, the development and application of the vibrational techniques based on natural frequencies changes were applied in the damage detection field, mainly in bridges and offshore structures. The methods of the structural assessment developed were based in linear behavior, due to the limitation imposed by the lack of numerical models. The results found through these methods in real structures provided information about the damage presence, the location and the damage characterization. Starting in the 80s and 90s the numerical models were implemented, primarily related with non-linear behavior,

but the damage detection methods presented a low sensibility. The first sensors, focused in the detection of parameters for modal analyses, were developed and applied in the field, the processing system was also implemented. For other types of structures, such as highways and buildings, the first SHM systems were introduced and tested [46, 54, 57]. The development of methods and devices focused on damage detection, and the integration between these devices with data processing systems and advances in the numerical analysis modified the practice of the structural assessment. As a result of this advance, the initial concepts of the SHM emerged in the 90s [56].

Hence, structural health monitoring can be defined as a structural assessment process based on measurements of structural responses, along of a determined time period, by use of non-destructive methods, essentially implemented with sensorial systems connected to a data central, capable of offering information in real time about damage emergence and characterization, in the most early ages, and to be able to collect information about the structural integrity during structure service life [7, 43, 44, 56]. In general terms, SHM is different from other structural assessment methods by the adoption of the NDT, comprising a monitoring system (sensors and data processing), possibility of the remote access, management of the regularity and the duration of data acquisition [43].

The advent of SHM systems makes possible the data collecting in real time and its integration with structural analysis models and systems for prediction of the structural performance in uncommon situations, specifically when structures are subjected to unexpected loads, as natural hazard occurrences, and it should provide information about the necessity of a building evacuation [58, 59]. Also, SHM may be applied both for local as for global damage detection, according to system complexity but for this option, the circumstances of the materials degradation must be taken under consideration [56]. For a simpler global damage detection, commonly the changes in structural behavior can be associated with development of fissures and therefore with changes in the modal parameters [60].

In 1996 Doebling *et al.* [54] presented the survey overview about the modal parameters used for detection, identification, damage characterization and structural monitoring. Essentially, the authors showed experimental proceeds of SHM based on modal parameters changes for damage detection and pointed that the implementation of the

algorithms should be made in order to minimize the dependence of the damage assessment process of the data set from the undamaged structure. Additionally, it was observed the necessity for the development of methods that consider non-linear damage and studies about sensors quantity and measuring location should be performed in field for a most accurate analysis about the design of SHM systems.

In complement to the work presented by Doebling *et al.* [54], in 2004 a survey presented by Sohn *et al.* [44] reported a review about SHM between 1996 and 2004. In this survey it was demonstrated the initial implementations proposed by Doebling *et al.* [54], in the field of the numerical modeling and sensitivity of the damage detection methods. The gradual decreasing of artificial excitation used in the modal analysis experiments, the widening of the field of application in engineering structures and the development of integrated systems for structural assessment were the main justifications of the advances verified. However, this review highlights the need for the development of comparative studies employing different methods of structural assessment and the implementation of the SHM systems in field, using decentralized systems in real time [54].

2.2.2. Recent advances on SHM

Essentially from the years 2000, the implementation of systems and sensors employing optical technologies presented a new sort of advantages [61–66]. The optical fiber sensing techniques make possible the measurement of a high number of parameters with only one fiber cable, through the sensors multiplexing techniques [67]. Such sensors are also immune to electromagnetic interference, work at high temperatures, no electric power is needed at the measuring point, and have low size and weight, among other advantages. A search in the World Intellectual Property Organization – WIPO [68] in February of 2014, using the expression “optical fiber sensor” shows the existence of 473 registered applications focused on SHM.

Recently, some SHM monitoring platforms were implemented with devices to collect and control, and data processing systems working together, in the same framework, focused in the structural assessment. The necessity of platform development can be associated with the reduction of the time of assessment and global costs. This way, some platforms were developed and implemented centered to modal parameters monitoring [26, 59, 69,

70]. One of the first patents related to SHM application was developed by the Hughes Aircraft Company, in 1993, with the register number US 518516. This patent reported an integrated system, composed by strain gauges and a device based on acoustic emission to detect crack.

When a search is realized employed the term “structural health monitoring” in WIPO [68], EPO [71] and United States Patents Trademark Office (USPTO) [72] 1707 patents can be found registered, namely: 1077 registers were founded in WIPO database, 177 registers in EPO database and 453 in USPTO database. Those registers were analyzed and classified in 4 different groups: i) sensors, namely measurement devices; ii) methods, specifically numerical methods; iii) systems, that is integrated devices of sensors and data processing able to provide measurements and data processing around a specific monitored parameter and iv) platforms, to be precise more complex systems of assessment composed by association between systems of different parameter monitoring that aims the management of the data and an output about the structural safety. The results of this survey are presented in Figure 8, where for WIPO, USPTO and EPO, 48%, 52% and 51% of the patent register correspond to sensors, respectively, while 28%, 27% and 22% correspond to methods. For systems, the percentage of patent registers are 20% (WIPO), 22% (USPTO) and 25% (EPO), being only 2% (WIPO), 1% (USPTO) and 2% (EPO) of the registers found related with platforms.

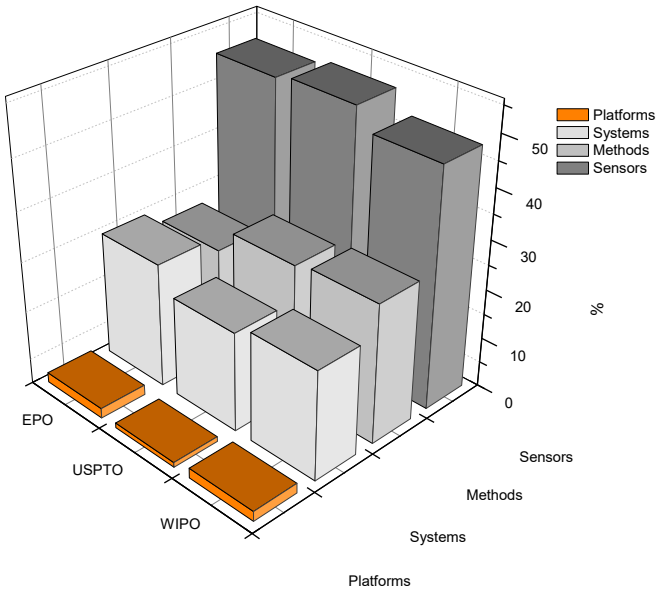

Figure 8. Patents register classification in sensor, methods, systems and platforms.

The survey showed that the United States of America presents 67% of patent registers related with SHM in the World Intellectual Property Office (WIPO) and 48% in the European Patent Office (EPO). Nevertheless, the percentage of patents related with platforms is considerably lower than the number of the registers related with measurement devices, methods and processing systems.

Among the SHM platform registers, the patents US 20130132032 [73] , US 20120123981 [74], CN 102034021 [75], US 20110035187 [76], US 20090083004 [77], US 20090048721 [78] and US 20070223003 were founded [79]. In general, terms those patents presented structural monitoring platforms composed by integrated systems, collecting and data processing systems, focused to answer about the presence or not of specifics damages, namely considering modal parameters. Highlighting that the platform's component systems are active and the interaction between the owner and the system is limited to predefined parameters. Also, it should be considered that the answer about structural behavior is focused around a specific point of measurement, and not by correlation between the modal and durability parameters. Additionally, the answer level provided by the platforms can vary according to structure complexity and the owners' requests. This aspect is explored in section 3 with recurrence to case studies available on literature.

One of the most innovative and recent patent register about structural heath monitoring platforms is the one with the reference US 20130132032 [73], providing a system able to employ a system of multiplexed sensors, for modal analyses, employing devices based on sonic, magneto elastic, electrical induction, piezoelectric, fiber optical and nanotubes technologies, in order to provide data about the current structural safety. In this patent, the communication system was implemented using a wireless connection between the elements of the platform (sensors, storing system, processing system, and output). The sensors provide information about changes in parameters such as strain, temperature, vibration, torque, angular rotation, bending, tension and compression. The current structural behavior is presented by direct comparison between the values for predefined parameters and the measured ones.

Consequentially, the advances in SHM systems have imposed the emerging need for standardization methods aiming to compare the different methods of evaluation

developed. Recently, Zhou *et al.* [80] presented a work about benchmarks and guidelines related with SHM methods. In this work the authors present a "*good practices guide*" from the American Society of Civil Engineering (ASCE), and guidelines for testing methods standardization from the experiments combining numerical modeling in a steel structure, performed by [81], for damage detection on a full-scale structure. Linear analysis and posterior non-linear analysis were carried out, focused to global characterization by modal response.

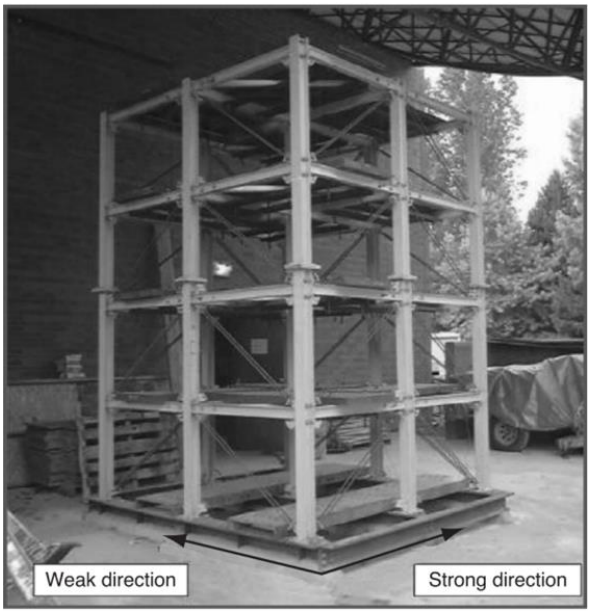

Figure 9. ASCE benchmark steel frame structure [80].

The guidelines reported by Zhou *et al.* [80], including SHM benchmarks are:

- Guidelines for structural health monitoring, reported by ISIS Canada in 2001[82];
- Monitoring and safety evaluation of existing concrete structures, presented by Bergmeister *et al.*, in 2002 [83];
- Development of a model health monitoring guide for major bridges, presented by Aktan *et al.*, in 2002 [84];
- Mechanical vibration-evaluation of measurement results from dynamic tests and investigations on bridges, ISO, in 2004 [85];
- Guideline for Structural Health Monitoring, introduced by SAMCO, and reported by Rucker *et al.*, in 2006 [86];
- Guideline for the Assessment of Existing Structures, presented by SAMCO, and reported by Rucker *et al.*, in 2006 [87];

Most recently Daum *et al.* [88] presented the Guideline for Structural Monitoring. In this work beyond the stat-of-the-art review about SHM, some benchmarks are presented specially related with SHM systems implementation.

In monetary terms, SHM systems implementation still represents a high cost of investment, however it can produce a significant return in terms of the maintenance optimization, structural failures detection in early ages, equipment and structure losses, and most important avoiding human injuries or fatalities [89]. Nevertheless, the SHM systems cost has been decreasing, especially by the constant development of lower cost sensors and techniques [90], [91].

Another important advance for SHM application, especially on full-scale analysis, was the development of minimization of environmental effect to data collected, as OMA techniques for instance (see [92–94]).

2.3. Level responses of the SHM platforms

Taking into account that a wide diversity of methods and measurement devices for SHM have been developed, especially linked with SHM platforms, it is recommended that the owners, as well as the design and installation personnel, take some time to consider the answer level necessary for that SHM system to be efficient and cost effective.

In fact, the sensing system configuration of the SHM platforms can change according to each construction, but it was observed that the level of damage detection monitoring required by the owners did not present deep changes. Therefore, platforms can be organized according with the specificity level of the answer provided. So, the present work introduces a method of classification for SHM platforms (Table 2), that can be understood as an extension of Rytter's method [48].
In subsections 2.3.1 to 2.3.5, and considering the classification method previously mentioned, some already reported studies were re-organized. The reference to the platforms application in the survey performed in this work had the sole propose of illustrating the current knowledge, therefore only the main registers was discussed. Moreover, the systems' configuration and the results are also summarized and included.

The objective of these subsections is to provide an exemplification on the employment of the classification method introduced by this work.

Table 2. Method of classification for SHM platforms

Level	Aims	Provide information about:
1	Damage emergence	damage identification;
2	Damage location	damage emergence and location.
3	Damage characterization	damage characteristics, as type, intensity and geometry, in addition to the information descripted in the above-mentioned levels.
4	Structural risk characterization	the structural risk in the current state, as well the information described in the previous levels.
5	Structural lifetime prediction	the structural lifetime taking in account the current structural state, in addition to the information related in the above-mentioned levels.

2.3.1. Level 1

The first step of the damage detection methods is to recognize changes in the active forces as an indication of the damage presence. A large quantity of studies were developed such as in [55, 56], and references therein. However, in order to provide a recent case study about damage detection, Razi, Esmaeel and Taheri [95] improved a vibrational method employing piezoelectric sensors to monitor a steel pipe. The results showed that the vibrational method can be successfully employed for damage detection and that the employment of wireless monitoring system in real time can be a good alternative for damage detection in the most early age.

Sequentially, a study developed by Bandara *et al.* [96] aiming nonlinear damage detection using natural frequencies change was presented. In this study, the authors introduce a neural network method for damage detection and employ data from a three-story bookshelf structure at Los Alamos Laboratory for validating the new damage detection method. Beyond the detection of damage, the method also allowed the assessment of the damage level. So, this method can be an important tool for nonlinear and light damage detection.

While both SHM platforms presented by Razi *et al.* [95] and Bandara *et al.* [96] were built focused to solve the same problem, they differs in terms of the technology used. The first introduces a concept based on vibration analysis monitoring and its data analysis depends on a technical group experiences. In the second case, the SHM platform employs an artificial neural network for the data processing, collected by SHM platform. However, other data processing methods can also be successfully used, such as wavelet, proper orthogonal decomposition and auto-regression. Essentially, both technologies can be applied in the same problem solving, namely damage detection in the early age, however, the field application is directly related with the level of automation required by monitoring system.

2.3.2. Level 2

Naturally, Level 1 platforms evolution is likely towards the damage location. Nie *et al.* [97] introduced a new parameter for damage detection based on changes on the phase of the vibration signal and the damage location is determined using a derivative from vibration time-history. The sensing system was composed essentially by strain gauges. Numerical modeling and experimental tests were carried out on an arch structure for demonstration, the method described can be applied for single or multi damage location. The results showed that this method provides information about the damage emergence and location, even when the damage emergence is far away from the measurement point. Beyond the damage detection, the data processed allowed to follow and monitor the damage progression.

A suitable method for local damage detection in large polymeric structures is presented by Naghashpour and Van Hoa [98]. In this work, an epoxy resin is modified by dispersion of multiwalled carbon nanotubes (95% of purity, diameter between 2-20 nm, and length from 1 to 10 μm). For large composites plates, with incorporated nanotubes, the electric properties are unique and those can be used as sensing devices. The damage detection was based on electrical measurements, specifically the four-probe method. The advances on the platform included an increased performance, allowing minimal damage detection and real time monitoring. In the same line of work, recently D'Alessandro *et al.* [99] presented a smart cement for structural health monitoring based on nanosensors (carbon

nanotubes), providing information about the mechanical deformations through changes in the electrical resistivity.

The SHM platforms presented by Naghashpour and Van Hoa [98] and D'Alessandro *et al.* [99] present some advantages relatively to the one developed by Nie *et al.* [97], as, for example, a most distributed and lower intrusive sensing system. However, the use of devices that can notice changes in the materials electrical properties can be less interesting, if the material durability is taken into account, as for example on materials exposed to corrosive environments. Therefore, this technology is more restrictive than the SHM platform developed by Naghashpour and Van Hoa [98]. Nonetheless, if used in a combined form in the same global monitoring system for all the building components, the probability of early damage occurrence detection in a large area of the material surface will be high.

2.3.3. Level 3

The evolution and continuous implementation of monitoring devices and methods allowed Hosser, Klinzmann and Schnetgöke [100] to correlate SHM data with a probabilistic model in a pre-stressed bridge element. The authors demonstrated, and described, the complete process of integration of sensors and probabilistic models, and the use of SHM data for damage characterization.

Rodrigues *et al.* [58] implemented and tested a monitoring system in a concrete bridge, Lezíria Bridge (Portugal), using optical fiber sensors . In this study, several sensors located in the structure surface and embedded in the structure were used. Two new transducers based in Fiber Bragg Grating (FBG) technology were introduced and all the sensors implementation steps are described. They demonstrated that, it is possible to use measurements in normal traffic conditions as excitation, and to establish an accurate prediction model around the deformed shape evolution.

The main difference between the two SHM platforms presented above is related with the implementation of the sensing system. The work presented by Rodrigues *et al.* [58] can be more attractive if a large number of sensors are needed to be used, due to the fact that the optical sensors can be multiplexed into the same fiber cable, adding to the fact that

they are not susceptible to electromagnetic interferences. These two characteristics can be of particular interest when a complete structural characterization is required, due to cost reduction of sensor multiplexing. However, the system presented by Hosser, Klinzmann and Schnetgöke [100] provided information about the interaction between the sensorial and data processing systems, also considering a reliability method for structural characterization.

2.3.4. Level 4

In 2010, Yi *et al.* used the dynamic response of the Dalian BeiDa Bridge (China) with frequency vibration measurements within a SHM system with the employment of a real time kinematic (RTK) global positioning system (GPS) [101]. The ambient vibration measured by the accelerometers was used to improve the numerical model proposed in the work. The authors concluded that this system is an alternative for conventional methods of structural monitoring, providing indicators that can be used for structural risk prediction.

With a similar method, Zhang *et al.* [102] reported a case study using optical fiber sensors for SHM on a simply supported reinforced concrete T-beam bridge (Figure 10), during dynamic and static loads aiming to identify the better moment for rehabilitation. The optical sensors employed were based in FBGs and Brillouin Optical Time Domain Reflectometry (BOTDR). The structure was submitted to dynamic and static testing and the collected data was used for numerical simulation and model calibration, finally the proposed model was tested. The failure prediction evaluation results from the proposed numerical model showed a suitable degree of precision, however the stiffness and non-linear analysis parameters should be improved.

SHM platforms included in level 4 present efficient communication systems, essentially based on wireless communication. In addition, the structural risk assessment considering the structural behavior under environmental and service conditions are a tendency for this type of platform, as can be seen in Yi *et al*. [101] and Ni and Wong [103]. However, the concepts developed by Yi *et al*. [101] combine technologies aiming to decrease the number of sensors used, such as GPS technologies, and for this reason, it might be more attractive for large structures or when a high number of sensors is need.

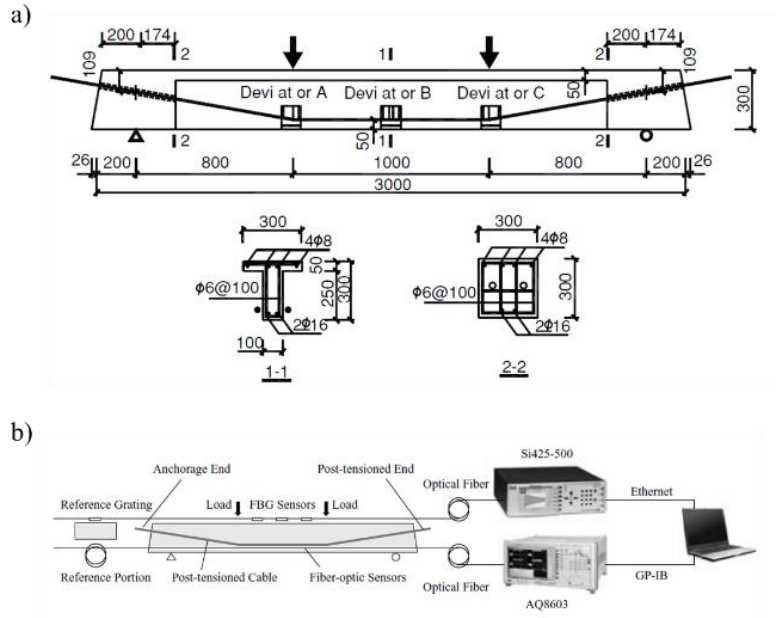

Figure 10. SHM of a T-beam bridge: a) profile of the beam and its sectional reinforcement (cm) and b) configuration of the SHM system [102].

2.3.5. Level 5

In Runyang Suspension Bridge (China) the effect of the ambient temperature and the increase of vehicular traffic (loading) for fatigue was studied by Guo, Li & Wang [104]. The structure structural safety and fatigue, were predicted by numerical analysis (finite element model) based on the data collect by field application.

Other example of SHM platforms, that can be included in the level 5, was demonstrated in the Canton Tower (Figure 11), situated in Guangdong, China. Canton Tower is constituted by a concrete-steel structure with a main 456 m tall tower. The sensorial system was composed by 800 sensors for 16 types of different parameters analysis. The results have shown that the implemented system provides accurate data (with GPS measurements and synchronization) about the horizontal displacement and consequently can be used as an alternative method for this type of assessment. In addition, the temperature influence in the tower horizontal displacement and the collected values were also used to predict the structural behavior until failure. The error analysis of the sensors system implemented were also verified to be higher than the error values checked by GPS measurements. So, in this work, the authors had demonstrated the use of a large number of synchronized sensors working for SHM, but highlighting the necessity of a data processing implementation for lifetime prediction [42].

Currently, the reliability analysis is an important tool for structural safety assessment, especially for employment on areas with high environmental hazard incidence or probability of occurrence. SHM platforms combining a lower, as possible, number of sensors, and allowing the prediction about the structural risk based on dramatic natural scenarios, are the most attractive, as related in Xia, et al [42].

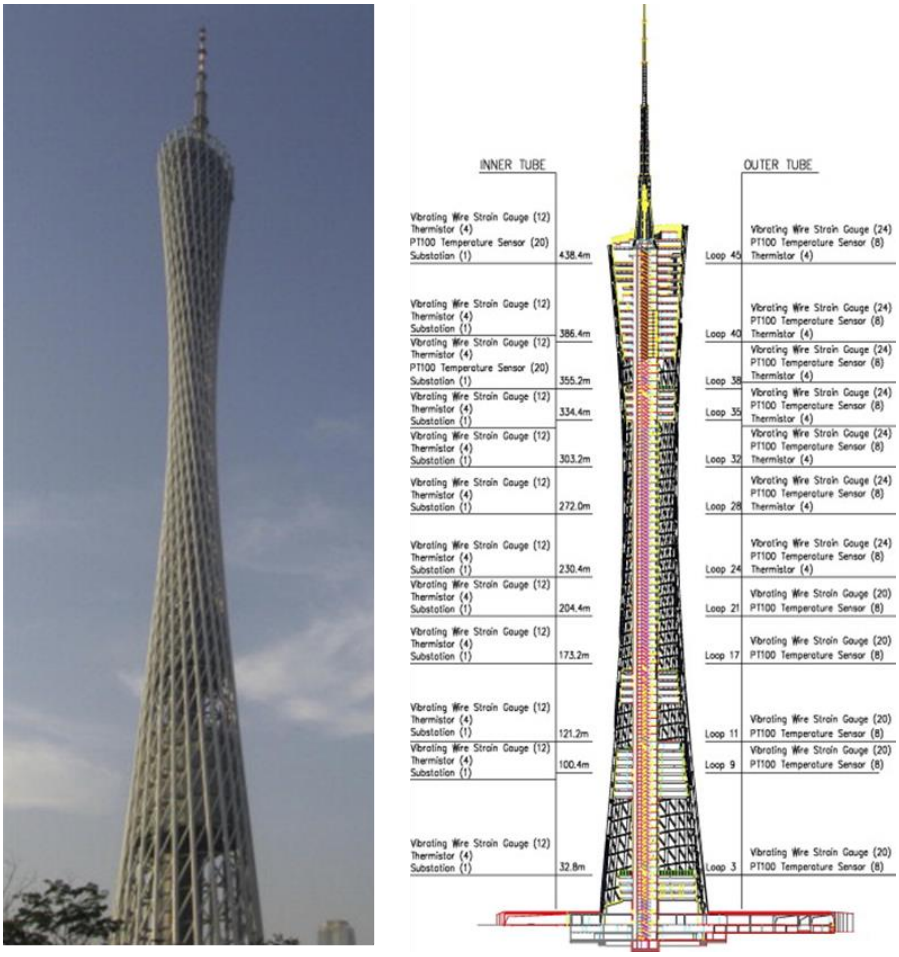

Figure 11. Canton Tower monitoring scheme [42].

2.4. Heritage constructions: a special case study for SHM

Considering the SHM above mentioned studies, the HC special case had not been addressed with the same often, dissimilar from other large structures, such as bridges and tall buildings. Consequently, this lack existence, discloses the development necessity of specific studies on HC structural behavior, improving the knowledge on this special and very important group of structures. Consequently, adding the need to develop new adequate assessment methodologies, tools and devices for the real-time safety analysis.

HC can be assigned as a special case, because they are structural systems different from the current ones, with complex behavior that often cannot be assessed or understood through the current codes, standards, techniques or devices.

The International Council for Research and Innovation in Building and Construction (CIB) in its publication number 335 define HC as any existing civil engineering construction that presents an elevated cultural value to the community around it. Cases of application of SHM in HC are especially interesting, from the techno-scientific perspective, due to the importance of this type of structures for the community (Figure 12). Essentially, evaluating a HC is a difficult task due to the need for classification of the cultural value and comprehension about the important occurrences (natural or human) that the structure is submitted during its lifetime, especially how time-expressions should be conserved and how restoration should occur. For such cases, it is important to highlight the limitation around the assessment method that in most HC cases are limited to use of non-destructives techniques. The CIB publication 335 recognizes the necessity of collecting information about the structural time-history of HC, highlighting that often no information is available [4].

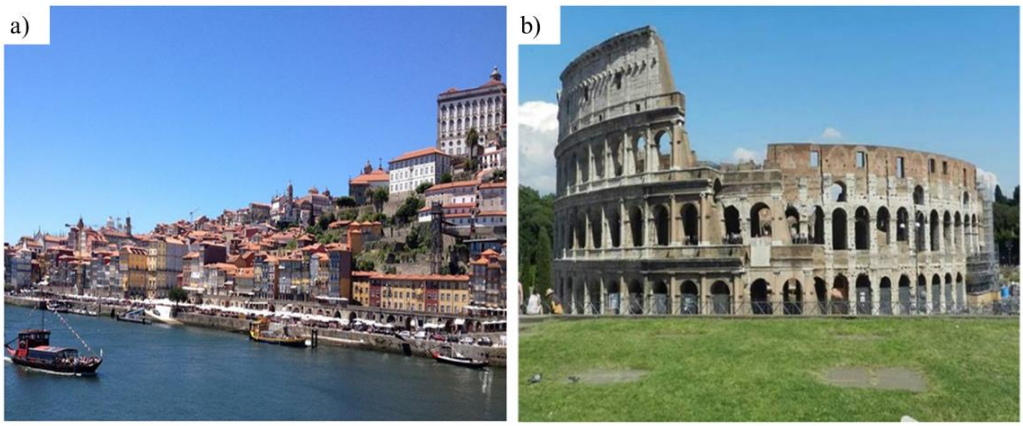

Figure 12. Examples of important HC: a) Porto historic downtown and b) Coliseum, Rome, Italy.

The structural time-history objective is to offer information about the construction materials, safety parameters, natural actions, human interference, damage emergences, pathologies, structural parameters and any type of constructive modification, in order to take action on preventive measures to maintain the structural safety. Additionally, data from numerical modeling can be included in such reports as a method to improve the time-history.

An analysis of 50 reports executed between 2000 and 2015 by the *Instituto da Construção* (Civil Engineering Faculty of the University of Porto) on HC built in the time period comprised between the XVI and XX centuries (32% between X and XV centuries, 64% between XVI and XVIII centuries and 4% between XIX and XX centuries) showed that a visual inspection was included in 100% of the assessment processes and only 58% of the HC presented any document with constructive information about the HC. The reports also showed that experimental tests were performed in 12% of the HC, and in only 8% of the assessment was performed with recurrence to SHM techniques. Concerning to damage analysis, walls and arches are the most affected elements, essentially 80% and 58%, respectively. Additionally, the presence of damage on floors and columns was observed in 20% and 10% of the cases, respectively. It was also perceived the presence of cracks in 85% of the cases and in 70% of the buildings some displacements were noticed. Humidity related damages were observed in 60% of the HC assessed. The complete information on this analysis can be seen in Figure 13.

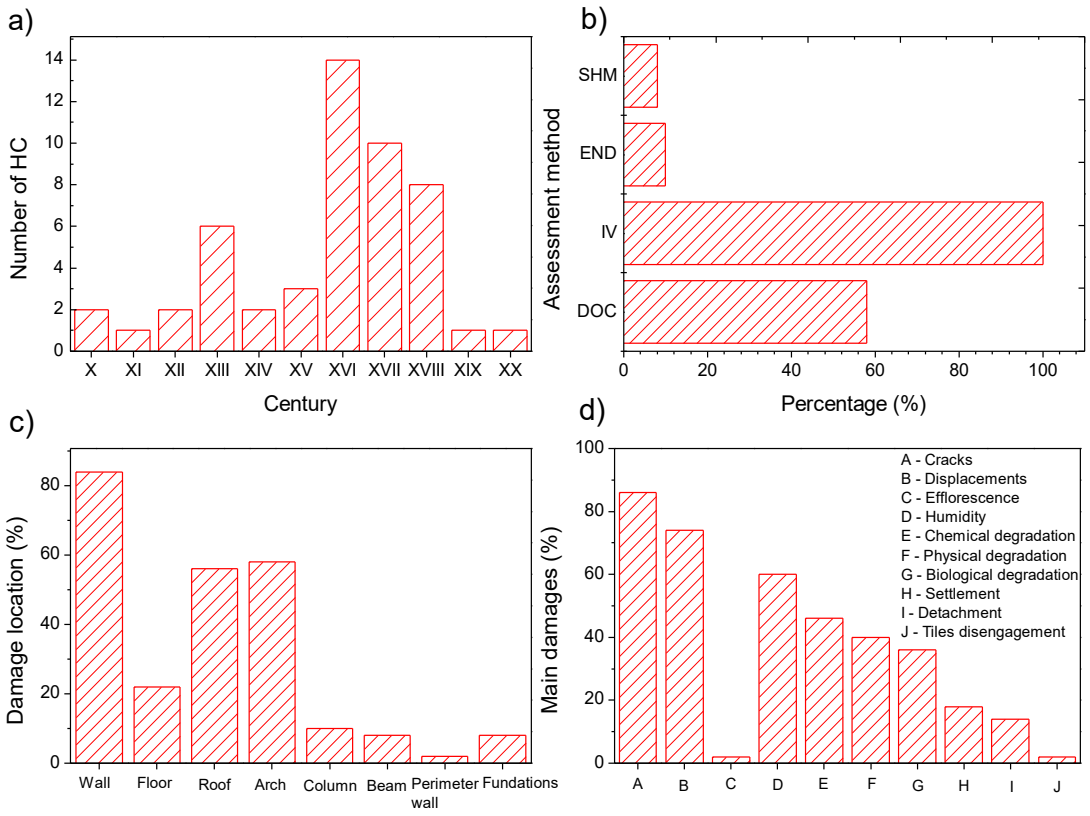

Figure 13. Characterization of the HC analyzed: a) construction age, b) main assessment methods (SHM, non-destructive tests, visual inspection and document analysis), c) main buildings components affected by damages and d) main damage founded.

Considering the necessity for organized information regarding the inspections on HC and the structural time-history, recently a maintenance guide focused to HC was presented by Tavares, Costa and Varum [105]. In this work, the authors present a check-list of the main activities that should be realized during the inspections organized by aim of the inspection, measurements, inspections regularity and persons responsible by each listed action.

Most of the HC monitoring experiences reported in the literature are related with modal parameters analyses, essentially by changes in natural frequencies. Abruzzese *et al.*, in [106], presented a wireless system focused on the management of the structural safety when a structure is succumbed to a natural disaster, like an earthquake. The dynamic characterization of an historical tower was done and the data were used in a computational simulation. The data acquisition system was essentially composed by accelerometers linked wirelessly to a signal processing module central station. In fact, in a real disaster the changes in the natural frequency showed similar values to the ones originated by the computational simulation. An alarm was implemented, that can alert the owners about the structural collapse eminence. Similar works were also presented in [107] and in [108].

Another important case of heritage construction monitoring was presented in [15]. In this work, a construction built between the centuries XVI and XVII also was monitored. For assessment process, initially a visual inspection was carried out and the main damages were identified. The authors agree that a preliminary inspection is necessary to an initial evaluation about the structural risk assessment and to the definition of the monitoring system. In order to provide information about the best location to the sensors installation, a numerical modeling was done and the high-risk zones were identified. Essentially, the monitoring system measured displacements (crack evolution) by transductors placed along the structure, temperature variation, and vibration to estimate the natural frequencies evolution due the damage presence. The considerations about the proceedings of HC assessment, above mentioned by [4] and [105], have been followed by the technical and academic community.

Nevertheless, beyond the modal parameters analyses in the structural safety assessment, especially in HC, the material degradation should be also considered in the measurements [4] in order to provide predictions about the life expectancy and local damage emergence,

for reinforcing measures adoption. It was shown in [44] that the structural analysis only based in modal parameters chances does not allow a significant identification about the zone affected by the damage. Nevertheless, the ideal location for sensors positioning will have a better performance if based in a preliminary modeling, focused into the identification of the fragile zones.

Recently, 30 case studies on rehabilitation of HC developed between 2003 and 2012 by *Instituto da Construção* and Faculty of Civil Engineering of University of Porto were organized and presented by Costa, *et al.* [109]. In fact, the importance of structural monitoring systems for structural assessment is highlighted along the related cases, where special attention is given for non-destructives techniques. In addition, this work demonstrated the University of Porto experience on SHM methods for safety assessment, contributing for knowledge dissemination about the good practices on HC assessment.

2.5. New perspectives for SHM

The recent advances on SHM show that the monitoring systems can be functional for different circumstances of structural assessment. The sensors development and monitoring techniques had been improved and the inclusion of the durability parameters have been an upgrade, in order to promote a better damage characterization and an accurate structural lifetime prediction [110]. A significantly quantity of optical sensors has been developed and implemented, motivated by the better signal to noise ratio, good sensitivity, electromagnetic interference immunity, multiplexing possibility, low size and weight, robustness, low attenuation on remote monitoring, no electrical power needed at the measuring point, among other advantages [67, 111, 112]. Thus, such sensors can potentially provide an optimized sensing system with higher performance. However, the emergent sensing systems should be able to collect data and interact with the available and older installed technologies, for example video cameras, electronic sensors and environmental or climatic predictions available from web platforms. Additionally, the owners should also be included as part of the sensing system due to the fact that they can contribute for the structural time-history composition over photos register and observations about a damage emergence or human interference.

Thus, the new data processing systems should be able to store and organize all the collected information and process it. In other words, further than the numerical analysis tools improvement, computational systems and data collecting systems implementation, it is necessary to define the information circle and optimization, till the platform's outputs, providing a more interactive and user friendly platform for the owners or end users. Nevertheless, the technician's role during the structural assessment process should be sustained and adjusted. On most recent platforms design and implementation, the wireless communication has been used [25, 106, 107] aiming at most "clean" and flexible monitoring system without cabling.

For HC monitoring, special care and attention should be given during the monitoring plan design and implementation. In fact, the less intrusive techniques should be employed to preserve the historical characteristics [113]. Thus, the durability parameters monitoring might be included in order to provide information about the damage emergences in the earliest age and, consequently the maintenance measures can be minimized. Though, for most real assessment, the building should be modeled considering its current state, including the damages already found. Beyond structural monitoring, the data collected should be correlated with data from visual inspection, photo and video and information about human interference on HC. In any predefined limit overpassing, the responsible offices must be immediately contacted such as including a specific alarm based on natural frequency changes. An automated monitoring system would perform periodic measurements of the natural frequencies, and in case of a change greater than a pre-established value, a signal alarm will be sent. Additionally, reliability methods should be considered in order to provide most accurate answer about the structural safety.

The increasing advances on SHM has contributed for the broadening of the assessment process in a wide variety of structures [22, 52, 114]. With lower-cost systems development, SHM systems tend to be popularized [115] and integrated with other management systems, as security and comfort system for instance. In this way, the current and future systems must be implemented optimizing the sensing system and the interaction with the available technologies, including older ones [116].

2.6. Final comments

This chapter intended to review the employment of SHM systems for structural assessment, essentially related with dynamic monitoring. A short historical review on structural monitoring advances from 1993 to 2014, including the recent advances on sensors for SHM systems and some field implementation cases, was performed. Additionally, recent damage detection methods based on modal responses, especially focused on nonlinear damages effects characterization, also were reported.

The state-of-the-art of the data processing systems were shown and its imminent necessity for implementation in this area, essentially systems and methods that offer an objective answer to owners on the structural safety should be developed. In addition, the construction material properties should also be reflected in the structural parameters.

A special consideration was given for SHM platforms. A benchmark report was carried out aiming to illustrate the current state-of-the-art, and was showed the necessity of development focused on methods of data processing and platforms for structural assessment. Case studies reported in the literature were described and organized according with the method of classification for SHM platforms proposed in this work (an extension of the method developed by Rytter). The classification for SHM systems based in the answer level aims to provide a most objective orientation to owners, promoting the adequate selection of the monitoring system to install.

Sequentially, SHM case studies on HC were introduced and the important system configurations were pointed. For HC monitoring, the systems should be very low intrusive (mechanically and visually) and the employment of the current technologies available (digital cameras, smartphones or tablets, for instance) can introduce an additional advantage to SHM: the possibility of recording and monitoring the human interference on the construction degradation. In addition, it was shown the necessity of implementation of studies including full-scale structures and real structures, and especially the development and application of SHM techniques focused on HC.

Finally, “New perspectives for SHM” has shown that some areas should be most explored, namely: the optimization of the sensing systems with technological tools

available, the interaction of the owners in the assessment process as an informative source about the day-by-day occurrences, in the integration of the SHM systems with other systems (smartphones, cameras, etc.).

The present state-of-the-art shown that the new sensors development is responsible by half of all innovation related with SHM field, and points to the necessity of SHM systems and platforms implementation. Additionally, no SHM system or platforms is specifically addressed to HC issues, making it a great opportunity for development of studies and innovation on SHM field, taking into account the high cultural, social and economic importance of HC for human societies.

In fact, HC are an interesting case for SHM development, because they impose the necessity of flexible and open SHM systems and platforms, allowing the possibility of performing changes on the sensorial system along time, all with very low intrusion. The development of tools for the safety maintenance support, in real time, can be an effective way to avoid dramatic losses, especially for monuments and constructions with visitors.

3

New optical sensors for heritage construction monitoring

Summary

The first criteria for SHM implementation is the existence of a sensing system. The sensors network can be composite by measure devices positioned in a specific place, as accelerometers, or distributed into material, as nanosensors for instance. However, a large number of measurements devices addressed for structural monitoring can be found in the literature, especially electronic sensors and this has motivated the development of optical sensors as technologic alternative for this type of application. In the current chapter two innovative optical sensors for SHM will be implemented, namely: groundwater level monitoring sensor and a relative displacement sensor. It is important to highlight that these sensors were designed considering the most common parameters monitored on heritage constructions and a previous research performed in order to identify the main damages occurrences on HC. Considering their good performance under work during the experimental testing, the two optical sensors implemented in this work can be used as sensing systems for structural monitoring of HC.

Keywords: Groundwater level sensor, relative displacement sensor, optical fiber sensors, fiber Bragg grating, structural health monitoring.

3.1. Groundwater level sensing for SHM

3.1.1 Introduction

A high number of sensors for structural monitoring has been developed [98], especially after the turn of the millennium, such as strain measuring, acceleration, temperature, displacement, evolution of cracks and corrosion. Motivating a high number of application cases, where different sensors has been employed for structural assessment in real structures [54]. Usually these case studies mention SHM in bridges, highways, pipelines, turbines and offshore platforms [13].

Comparative performance assessment studies between electrical sensors and fiber sensors, for structural monitoring, made on different types of structures (adobe wall, steel footbridge and a reinforced concrete water reservoir), showed that the optical sensor has similar performance in dynamic and static tests to his electric counterpart [62].

During the construction of a reinforced concrete building, optical fiber sensors, based in fiber Bragg grating (FBG) were employed for structural monitoring of the strain evolution and the concrete temperature [117]. This case-study yield the following conclusions: i) the adoption of especial protection is necessary to improve the performance of the sensors; and ii) temperature changes and strain data might be used for the understanding of the structural behavior and for the prediction of structural risk [118]. It is important to highlight that the optical fiber sensors were introduced in SHM due to their advantages when compared with other measurement devices, such as: no interference from external electromagnetic fields, electric isolation (passive operation with no electrical power needed at the measuring point), possibility to use a high number of sensors in the same fiber (multiplexing), and reduction of the implementation and maintenance costs.

In the literature, a large number of the structural monitoring applications, using optical fibers have already been described, as reported in Kostecki, et al [110], Laing, et al [119], and Antunes, et al [120], and in the references therein. Beyond the application in structural assessment, the optical fibers have been used to evaluate material performance, as well as to monitor the concrete curing process [117]. However, in order to provide high durability sensor systems and to ensure good performance, it is recommendable that the

sensors are designed to resist aggressive environmental conditions [118], for example the presence of salts and water pressure.

The water level is an important topic for SHM in civil engineering applications and geotechnical studies, due to the variety of applications, such as water reservoir level and groundwater level monitoring. Especially in reinforced concrete structures, the foundation elements are exposed to the humidity effect, and this might accelerate the occurrence of damage like corrosion. Other than the durability aspect, the water level monitoring is important in the observation of soil characteristics with direct impact on the engineering project, and this can be done during the design phase, before any works have commenced. Moreover, natural hazards like typhoons and floods can increase the water level in the soil mass, reducing the soil strength and influencing the stability of slopes and structures; for these cases, special maintenance procedures are needed to preserve a safe condition. As previously presented by Figure 13, in the chapter 2, the soil settlement corresponds directly to 20% of the damages found on HC, provoking cracks emergency and structural displacements, the most usual damages identified on HC, present in 88% and 75% of the cases analyzed.

Traditionally, water level measurements in real time are implemented using pressure transducers inside sealed piezometric tubes, however, recent developments in the sensors technology have enabled the use of optical fibers for water level measurement. Some recent examples of the application of optical sensors, based on fiber Bragg grating, are a sensorial systems for sea level prediction, where this system measures changes in the optical spectral properties, as reported in Ferreira et al [121]. Another application is for the prediction of a liquid level through of a distributed sensing system based in temperature measurements, as mentioned by Peng, at al [122]. In Lin. et al [91] a group of plastic optical fiber (POF) segments, aligned and equally spaced was proposed as a low-cost water level sensor, taking into account the different transmission coefficients between water and air. In fact, POF presents a higher optical loss than silica fiber, nonetheless, such sensing systems are designed for the interrogation unit to be a few meters away from the sensor head, not for remote monitoring at bigger distances. For example for short-distance applications [123], other fiber properties also should be taken in account, as can be cited the low-cost, high flexibility, large diameter and easy

manipulation [124], and this characteristics have motivated the employment of POF for sensors development, as can be noted in Golbani and Azimi [125], Lin et al [91], and Antunes et al [61].

In the literature, some optical sensors for water level monitoring had been described [124–126], but the present chapter introduces a simplified alternative water level sensing system, based on plastic optical fibers, focused on water and groundwater level monitoring, offering an easy application and low cost of production and implementation.

3.1.2 Sensor, setup and experimental program

The implemented sensors, here designated S025 and S050, have a total length of 5.00 m of optical plastic fiber, essentially composed by polymethylmethacrylate. The sensing portion starts on one end of the fiber and has 2.00 m in length, with groves spaced at every 0.20 m. The diameter of the fiber employed was 1 mm (Avago Technologies HFBR-RUS100Z) and the grooves had a depth of 0.25 mm in sensor S025 and 0.50 mm in sensor S050. The opposite extremity of the fiber (without grooves) was connected to the data acquisition system. The decision about the sensor design was based in the main idea of to provide a most simplified sensing system for water level monitoring. This same direction has been defended by others works [108, 127].

A standard plastic optical fiber is composed of three concentric layers, named: the protective layer, the cladding layer and the core. The protective layer and the cladding layer provide physical and chemical isolation of the core fiber from the environmental action, while the core of the fiber is responsible for signal passage. When grooves are introduced, along the fiber and the core is exposed, each groove is responsible for provoking a signal loss, due to the local change in refractive index between the fiber core and the environment. If the grooves are filed by a material that presents a refractive index similar to the fiber core, like water, the signal losses will decrease according to the number of grooves being progressively filled or vice-versa.

The principle applied in this experimental work is based on the fact that the contact between the water and the fiber grooves promotes a decrease in signal dissipation when

compared with air. A similar application of this principle was used on a case of concrete curing monitoring [117].

The grooves were made manually, with a sharp knife and a brass mold, that allow the grooves to be made with a minimum spacing of 1 cm and depths of half and/or one quarter of the diameter of the fiber (Figure 14). The presence of a groove in an optical fiber disturbs the propagation of the optical signal to the external region, interacting with the surrounding environment and inducing an additional optical signal attenuation. When the space on the groove is filled with a substance with a refractive index closer to the refractive index of the fiber core, the amount of light propagated increases, therefore the optical signal measured will increase.

Figure 14. Brass mold employed to create the grooves in the POF, below the mold a detail of the POF with the grooves is shown.

Considering the sensor disposition in the soil test column and the simulation of the water level increase, the liquid fulfilling the grooves refractive index is different from the POF core index, changing the propagation of the optical power. Therefore, the optical signal power transmitted depends on the refractive index of the fluid. If the fluid's refractive index does not change during the acquisition, for each fulfilled groove, the transmitted optical power increases. A plastic fiber with several grooves, placed perpendicularly to the liquid surface, can act as a sensor. When the liquid rises, it will sequentially fulfill each groove, increasing the transmitted optical power.

The data acquisition system (Figure 15) used is composed of four identical channels, each one with a LEDs emitting at 670 nm (IF-E96, Industrial Fiber Optics Inc, USA) and four

photodetectors channels (FB120-ND, Industrial Fiber Optics Inc, USA). The control module comprises of a 16-bit microcontroller (model PIC24FJ256DA206 from Microchip Technologies) with a 16-bit ADC, operating within a 2.5V range and resulting in a resolution of 38.15 µV. It can be controlled remotely, paired with a computer via a wireless system (module MiWiTM - P2P from Microchip Technologies), or through a USB cable connection, with the data acquisition and the analysis performed in real time. In this work, the data acquisition was done using the USB connection to collect the optical signal power.

Figure 15. Data acquisition system.

For field monitoring, the system has a battery and the capability of recording data on an SD card. The optical signal is received and processed through a computational management system developed on *Labview*® (Figure 16).

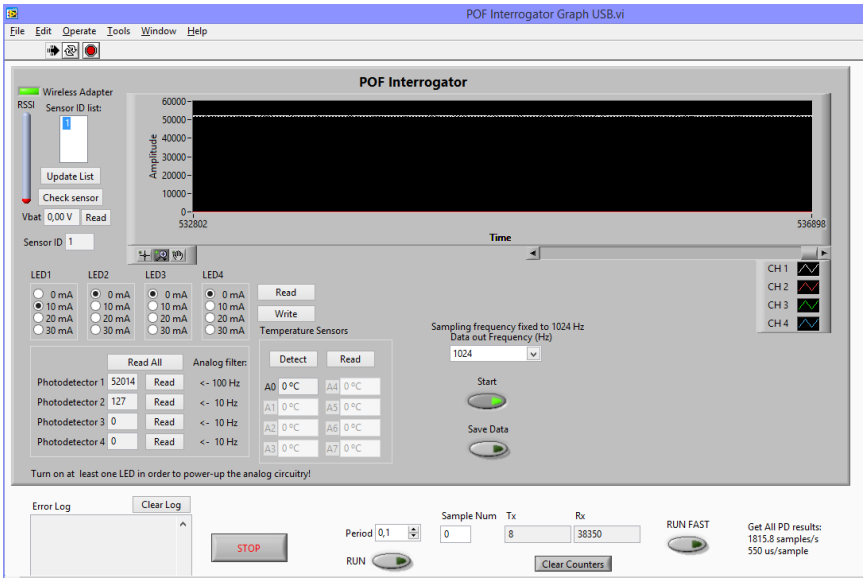

Figure 16. Computational management system

Initially the two sensors (S025 and S050) were attached along a rebar using adhesive tape (sensor detail in Figure 17.b). The rebar with the sensors was then installed in the center of the test column, leaving the fiber extremities outside, to be connected to the control module; a baseline or an initial reading was taken immediately after installation. Following the installation, the water level was raised in steps of 0.20 m until the final height of 2.00 m. The reading corresponding to each step was taken once the optical signal was stable, with the stabilization time varying depending on the time test type. After this, the reverse procedure was carried out, in order to check and analyze the changes in the optical signal due to the reduction of the water level. The experimental tests, were performed twice for each situation, namely water increase, water decreasing and groundwater increase (test A and test B), in order to demonstrate the repeatability and accuracy of the results.

The column used in this experiment was made of an external steel frame, holding 3 side panels made of glass and one made of steel with 8 channels for water input. The internal dimensions are 0.40 m x 0.40 m x 2.00 m (Figure 17.a). The aim of this test was to assess the changes in the optical power by varying the water level.

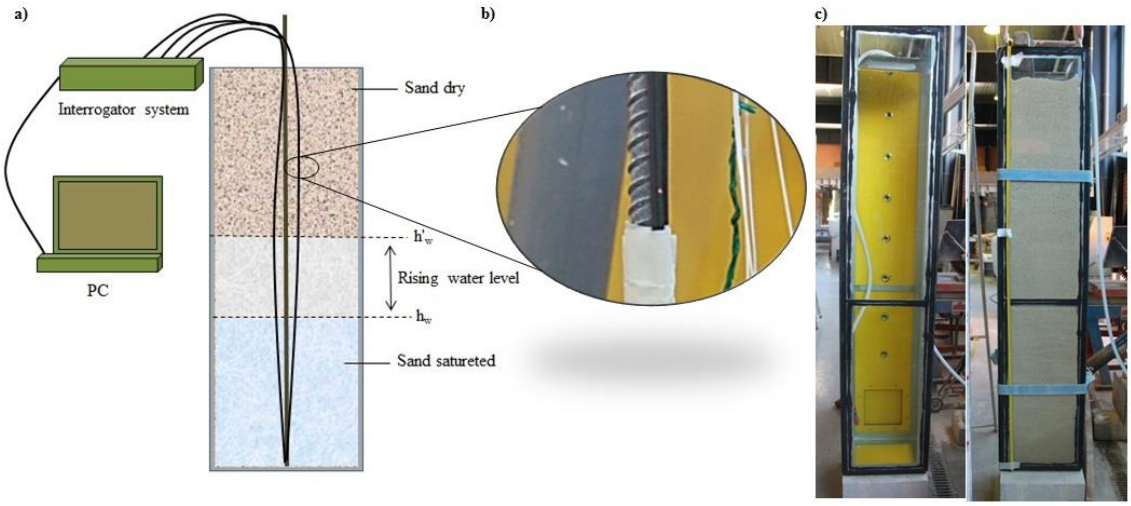

Figure 17. Experimental setup: a) details of the experimental work and its components; b) detail of the groove in the fiber during the optical signal processing, and c) soil test box without sand and with sand.

In order to simulate the groundwater variation, the column (Figure 17.c) was filled with sand up to the top. The sand used had an initial moisture content of 1.90% and its grain size distribution is shown in Figure 18. As in the previous test, once the sensor and soil

were in place, the baseline readings were taken and the water level raised and lowered following the same procedure explained previously.

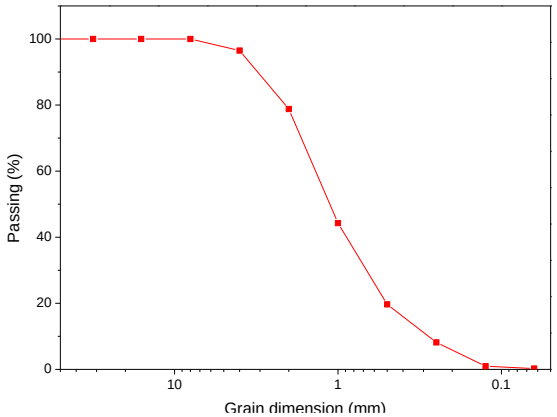

Figure 18. Grain size distribution of the sand used to experimental tests.

3.1.3 Results

Both sensors (S050 and S025) were initially tested without soil and later with soil. For every step (either raising or lowering the water level by 0.20 m) a measurement of the optical power passing through the fiber was performed, typically after a 15min stabilization period. After the water was raised to its maximum level a 30mins resting period was used before starting to lower the water level. The test results are shown in Figure 19 and Figure 20.

As expected, an increase of the optical signal power occurred with the rise of the water level and the opposite occurred when the water level decreased. In fact, changes in the optical power presented a proportional relationship with the water level increase or decrease. Essentially, this phenomenon occurs due to the fact that the water refraction index is higher than the air refraction index and, as the grooves are submerged and the air is expelled from the grooves by the water, the local refraction index change and more optical power is required. However, the optical power measurements in the two sensors also can be affected by several factors, as the characteristics of the LED emission, photodetector accuracy, POF length and the number and deep of the grooves carved along of the optical fiber.

Temperature changes can also influence the measurements. This way, compensation measures should be adopted, one possibility is to place a similar POF fiber, without

grooves, close to the one acting as a sensor. Such fiber with serve as a reference, and the signal changes on that fiber will be due to temperature effects (or other, such as emission LED optical power fluctuation) and can be compensated on the sensing fiber.

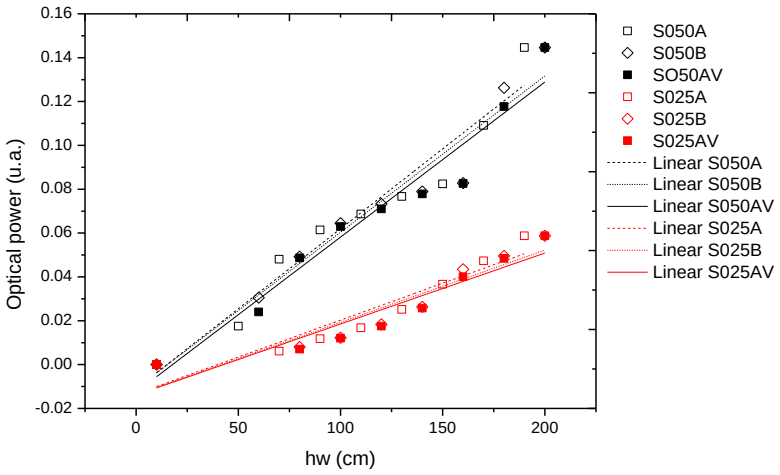

Figure 19.Variation of the transmitted optical power with the water level for the two sensors produced, during the water level increasing.

The average optical power change per groove observed during the water level increase was of 0.0717 u.a. for S050 and 0.0306 u.a. for S025. Now, in relation to the water level decrease, the average changes in the optical power presented values in order of 0.0385 u.a. and 0.0380 u.a. for S050 and S025 respectively.

It was also noted that, during the water level increase (Figure 19), the optical power presented the highest variability in values when compared to the values collected during the water level decrease. If the values of the optical power measurements of S050 and S025 were compared between them, the average variation per groove will be of 0.0407 u.a. for the water increase simulation and 0.005 u.a. for the water level decrease test.

Considering that when the decreasing water level test was done (Figure 20), after the water level increase test, and based in the linear variation of the optical power measured, it is correct to say that the stabilization time has an influence on the optical signal calibration. During the experimental it was observed that sensor S050 required around 20 min less time for the stabilization of the optical signal than sensor S025, while the water level was being raised. In fact, this characteristic can be related to the difficulty offered by the grooves to the penetration of the water (e.g. the bigger the size of the grooves, the

easier it is for the water to occupy this space, requiring, therefore, a lower stabilization time; another important consideration is how the surface tension influences the flow of the water in and out of the grooves.

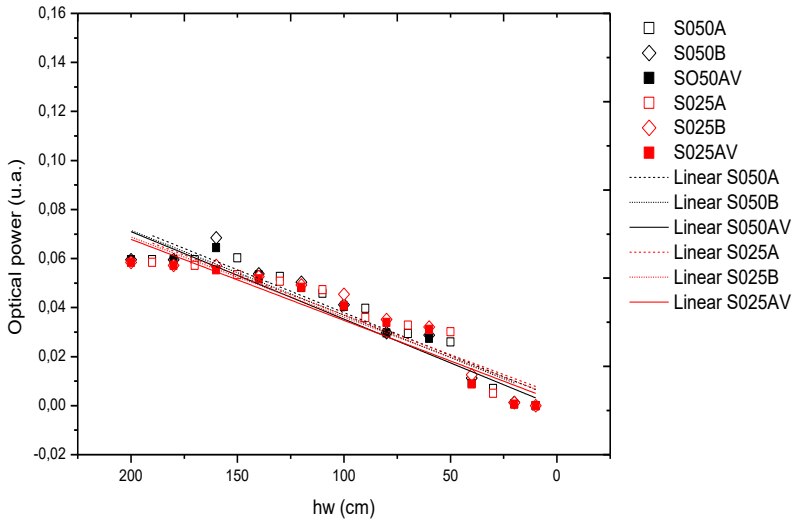

Figure 20. Variation of the transmitted optical power with the water level for the two sensors produced, during the water level decreasing.

Additionally, the results showed that the optical power readings of sensor S025 are more sensible to water variation than the readings from sensor S025. This is also due to the greater depth of the grooves, which allow a higher amount of optical radiation to be lost to the outside of the fiber. The optical power changes, observed during the water level increase simulation, in the column test, showed variations of the order of 0.1461 for sensor S050 and of 0.0675 for sensor S025. The level of confidence of the linear fit applied to the results obtained for the water increase test, is of 95% for sensor S050 and 96% for sensor S025.

The second part of this experimental program was dedicated to simulating the groundwater level in the soil. During the test in a soil column, the optical power presented a similar linear behavior like the one observed in the tests without soil. The time needed for signal stabilization was around 1h for each measured point. The results from this experimental setup are presented in Figure 21.

Measurements with sensor S050 presented a smaller change between the water level points due to the biggest groove depth. This can be explained by the influence of the initial moisture content of the sand on the measurements of the optical signal. The size of

the grooves on S025 present a higher resistance to the penetration of water due to its smaller size, therefore, given its area, it's easier for water entering into the sensor S050 groves. Also, the sand humidity should be considered because it can affect the signal amplitude variation, as observed in the results water rising in the soil column test.

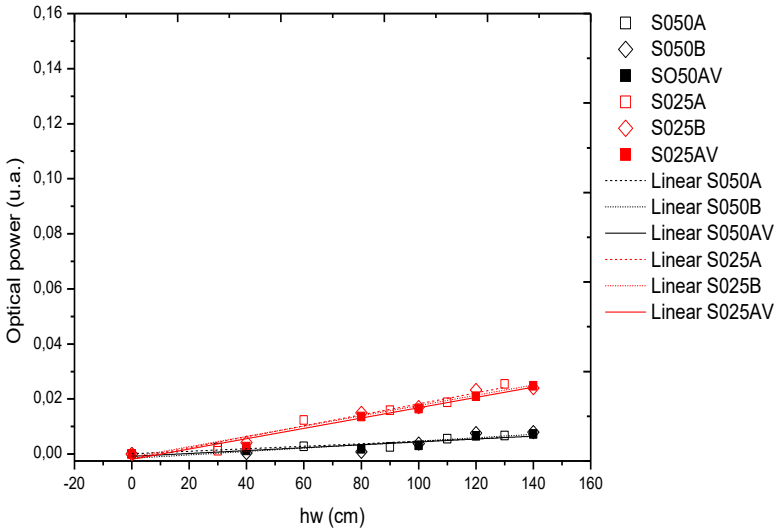

Figure 21. Variation of the transmitted optical power with the groundwater level increase, for sensors S050 and S025.

Initially, the sand humidity did not promote any changes in the optical signal transmitted by S025, but during the experiment, when the water rises on the optical fiber, fulfilling the grooves, a signal increase was noticed, as expected.

However, the sand humidity can influence the optical signal attenuation according with the groove area. Before the water rising started, the optical signal of S050 was influenced by sand humidity and when the experiment was carried out the signal transmitted by S050 showed lesser changes than the signal transmitted by S025. Additionally, due to optical fibers composition, namely polymethylmethacrylate, which is a hydrophobic material, the water pressure effect on the groove fulfillment must be considered. For smaller area grooves, the needed water pressure for a full contact between the water and the hydrophobic material (to fully fulfill the groove) must be superior than for higher area grooves [128]. Such explanation, justifies the difference between signal amplitude changes of sensors S050 and S025, when submitted to the soil column text.

The calculus of the pressure necessary for the water penetration in the optical fibers grooves of sensors S050 and S025 can be gathered through Expression 1 [128], where γ is the surface tension and θ is the contact angle, and r is the radius of the groove.

$$P = -2.\gamma.cos\theta/r \quad \text{(Expression 1)}$$

Considering γ = 0.072 N.m^{-1} (for water), θ = 120º (for polymeric materials), r_{S050} = 0.0025 m and r_{S025} = 0.00125 m, the necessary water pressure for penetration in the fibers grooves is 57.6 N.m^{-2} and 28.8 N.m^{-2}, for sensors S025 and S050, respectively. Nonetheless, the opposing phenomenon, the pressure force required for water to exit the grooves, was also observed.

Indeed, the average between the changes in the optical power during the water level increase test, by comparative analysis between the values of the optical power, collected when the water level was at the base (or 0.00 m) and when it was at the top (or 2.00 m), were of 0.0035 and 0.0131 for S050 and S025. In this experiment, the sensor S025 presented higher sensitivity and a better linear behavior than the results by the sensor S050. The confidence level of the linear results, measured during the water level increase simulation, in the soil column, were of 96% for S025 and 81% for S050. It was also observed that the sensor S025 needed 20 min longer for the signal stabilization than S050.

If the measurement points of the optical power were compared between S050 and S025, namely 0.0073 u.a. and 0.0247 u.a., one can perceive that the optical signal of sensor S025 is 3.37 times more powerful than the optical signal of sensor S050. This observation about the optical signal is particularly important because it shows that potentially sensor S025 will present a better performance at greater depths than sensor S050, considering that the same signal power is used for both sensors.

Additionally, the dispersions between all results collected in the test column and all the linear fits were plotted in Figure 22. It can be seen that the results showed a low dispersion between them. In fact, this endorses the linearity behavior of the optical power when submitted to changes in the water level both in the presence or absence of soil.

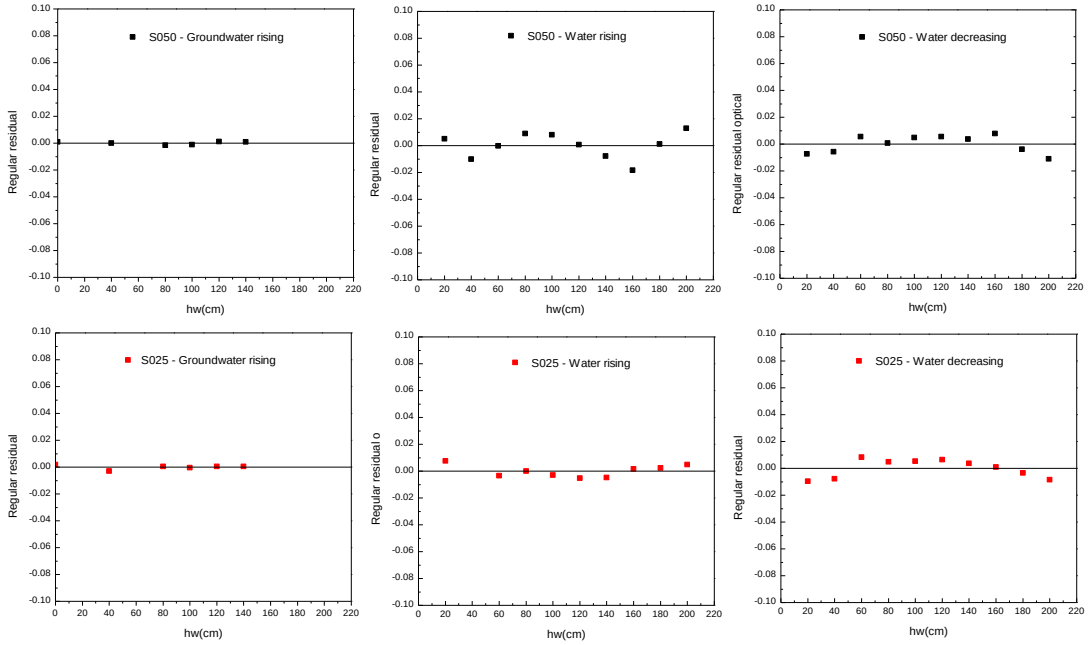

Figure 22. Residual analysis of the optical power measurements to S050 and S025 to groundwater rising, water rising and water decreasing.

3.1.4 Final comments

In this section, new optical sensors were implemented, namely by grooves made along of the optical fiber length, with depth of 0.50 mm (sensor S050) and 0.25 mm (sensor S025) and experimentally tested. The plastic optical fiber sensors developed in this work provide a simplified sensing system for liquid level monitoring based on changes on the optical power.

The proposed water level sensors, presented a suitable performance for measurement of variations on water level, with an adequate sensitivity, based on changes on the optical power. The two proposed sensors can be used for *in situ* applications of water level monitoring. However, the sensor S025 presented better signal performance than S050.

The advantages of employing such sensors, in structural health monitoring systems, to monitor groundwater levels, are the simplicity of the measurement system and a suitable sensitivity, added to the low manufacturing, interrogation and maintenance costs.

3.2. Optical sensors for bond-slip characterization and monitoring of old RC structures

3.2.1. Introduction

Some features as workability, high durability and low cost of production have contributed for the concrete be the building material most consumed in the world, namely around 12 billion of tones per year [18]. Essentially in emerging economies, as Brazil and South Africa for example, reinforced concrete (RC) structures correspond a large part of the existing structures, that in no rare cases they also present cultural value as Metropolitan Fortaleza's Cathedral (Figure 23), a neo-gothic building, built in the final of the XX century, placed in Fortaleza, Brazil.

Figure 23. Fortaleza's Cathedral.

Fundamentally in recent nations, as the found in the American continent, the age of heritage constructions (HC) are shortest than the historical buildings found in Europe, and sometimes, can give the wrong idea that the employment of modern build materials, as cement, can disfigure the cultural value of a HC. However, this fact does not mean that the cultural value of the recent HC can be less than another one.

In truth, historical RC structures had its values recognized by Madrid's Letter, where is evident that the cultural value is not related with the building age or the material employed, but with the importance of the building for the community development [129]. Due to that, the development of studies related with safety maintenance of recent HC are

relevant, motivating the development of the present work, devoted to development of optical sensors for characterization and monitoring of bond-slip mechanism in old RC structures. However, the sensors presented in this section have not its applicability limited to RC structures, they can be applied for relative displacement monitoring in other typologies, as masonries structures, for instance.

In fact, the adherence between concrete and reinforcing bars is the essential characteristic to existence of RC. Nonetheless, this adherence is not a simply mechanical phenomenon, but can be understanding and described, in general terms, by chemical adhesion, mechanical adhesion and adhesion by friction, that in zones of tensions presents two considerable aspect of work to bond control, namely, mechanism of tensions transference between the reinforcing bar and concrete and the RC resistance to pull-out solicitations [130]. In the same line, to Daoud, Maurel & Laborderie [131] the bond existent in the reinforcement bars and the surrounding concrete is indicate as the fundamental factor for RC performance, being its existences conditioned by factors as steel bars performance, concrete resistance to loads, and by mechanism process of tension transfer between reinforcing bars and the surrounding concrete.

According to Silva et. al. [132] the study of the RC adherence is important to definition of the structure safety, and can be used to estimating the concrete axial strength, reducing the time wait necessary to realize the compressive tests, across the traditional methods (see [133]). However, the authors highlight that this method of test present restriction, when realized in laboratory or by specimens collected in field due to length and loads actions restrictions.

Another way to analyze the adherence zone between the reinforcing bars and the concrete is by crack analysis that based in the opening and cracks spacing, numerical and experimental proceedings can be used to predict the bond state of reinforcement bars with the concrete [134]. The crack evolution is influenced by tension distributions on the surrounding area between reinforcing bars and concrete, age, material, geometrical and loading and can be used to analys the steel-concrete adhesion through the bond stress-slip evolution obtained, often, by pull-out test. In this testing method, the crack emergence on the specimen is influenced by the pulling of the reinforcing bars and the crakes on the specimen surface are not visible. Although the results of the pull-out test the limit

maximum bond stress (also called by bond strength) can be obtained. The maximum strength is found although the division of the applied force necessary to promote the slip of the reinforcing bars inside the concrete by the lateral surface area of the bars [135]. Examples of this testing application can be seen in [132, 134, 135].

Studies considering the effect of the corrosion process in different levels using 3D chemo-hydro-thermo-mechanical model on emergence of cracks in the adherence zone of rebar-concrete were recently developed by Ožbolt, Oršanić and Balabanić [136]. Basically, the model built by the authors considered the physical and electrochemical characteristics of the corrosion process with the concrete properties. The modeling was based on finite element method (FEM) and the modeling of the RC adherence was characterized according to results come from standardized test carried-out in RC specimens [131]. However, the authors highlight that the recurrence to pull-out tests is the simplest way to collect accuracy data on adherence zone, but its performance on real structure is really complicated. In fact, the recurrence to pull-out tests is a good way to characterize the mechanical adherence of the RC. But, especially in RC heritage constructions, to collect specimens for characterize the adherence zone between reinforcing bars and concrete is not always possible, and the adoption of less intrusive techniques for this proposes can be a better alternative way for perform it.

Although the interest in application of optical fiber sensors (OFS) in RC structures monitoring only emerged in 1980s[137], several kinds of OFS has been developed since them. Davis, Bellemore and Kersey [138] reported a FBG sensor focused to RC strain measures in RC beams and decks tested till failure, that were bonded to the rebar, embedded in the concrete and embedded in composite matrix. The results show that FBG sensors can be used to measure the strain level inside concrete. However, this technique is limited to RC failure analysis because consider only the concrete strain level for failure monitoring, and does not includes the essential property for RC existence, namely adherence rebar-concrete.

Recent sensors advances had been performed in order to provide alternative techniques for RC bond-slip monitoring. In Qin et. al. [139], smart aggregates, composed by a fragile piezoceramic patch, were used for RC bond-slip monitoring. The results demonstrated that the smart aggregates can be used for monitoring the initiation and bond-slip

development. Nonetheless, the smart aggregates sensors can be its measures affected by electromagnetic field due to piezoelectric properties, and in this way the data accuracy compromised.

In order to provide a less intrusive method for old RC bond-slip characterization and monitoring the present section details three OFS based on FBG and discuss on the experimental results founded.

The main advantages of the optical sensors presented in this section are the high accuracy for monitoring micro-displacements and the fact that it is a less intrusive characterization technique, allowing its application on HC. In addition, the principle of work of the sensors is really the displacement and not the stress level, making the collected results an assembly of the current physical and mechanical properties of the adherence zone. Also, the implemented acquisition system can be used for long distance monitoring when connected to internet, allowing real monitoring of the relative displacements of the contact zone between the concrete and reinforcing bars.

3.2.2. Fiber Bragg grating

Essentially, FBG sensors are based on fiber core refractive index modulation, by exposition of a photosensitive optical fiber to an intense ultraviolet periodic radiation, along the fiber longitudinal axis. In the detail of the Figure 24, the optical signal is emitted and transmitted by the core, with a reflective index knowledge, and when this signal pass by the Bragg grating a specific wavelength is filtered and reflected to contraire direction of the normal signal way and a resultant spectrum is transmitted. Thus, by the observation of the change in the spectrum of response is possible to identify variation in the monitored parameter. Additionally, is important to say that the reflective index of the fiber nucleus is variable according to temperature and tension. Thus, for most accuracy applications is necessary a preliminary study to knowledge the effect of the influence of this two physical parameters in form to minimize measurement errors [1-2].

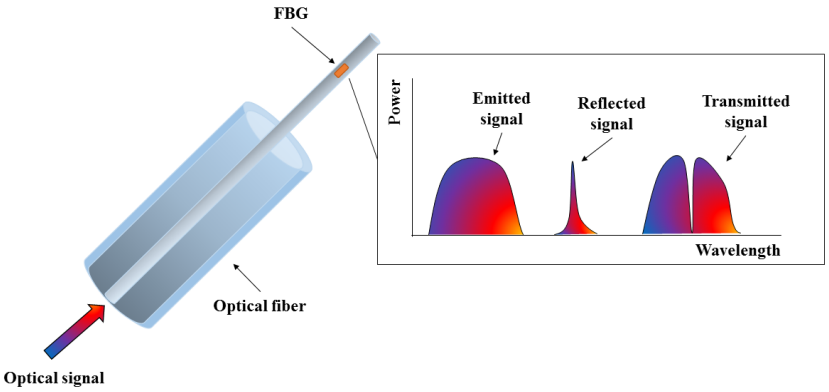

Figure 24. FBG structure and detail of the spectral responses.

The FBG presents high sensibility, high capability of multiplexing, no magnetic interference and low signal losses over others optical fiber. This characteristics has been contributed to popularizations of this optical technology, especially in the sensors industry [141]. The basic principle of the FBG consist in the wavelength reflected modulation of the optical signal emitted, express by Fresnel reflection, so-called Bragg wavelength (Expression 2), where λ_B is a Bragg wavelength, $2n_{eff}$ is the optical signal without Bragg effect and Λ is the period of the grating. However, if were known the number of the perturbation derivate of the grating period N, and the reflectivity index, s, and the quantity of the refractive will be possible to identify, by Expression 3, the pick of the spectrum reflected [1, 3].

$$\lambda B = 2n\text{eff}\Lambda \qquad \text{(Expression 2)}$$

$$\lambda rm = \lambda Bs\sqrt{\left(\frac{\Delta n}{2n}\right)^2 + \left(\frac{1}{N}\right)^2} \qquad \text{(Expression 3)}$$

Basically, the process of to print a Bragg grating in a fiber core consist in the exposition of the core in ultraviolet ray, however is important to certificate that the fiber is sensible of the ray that the core will be submitted. Currently, exist a variable numerous of the techniques to Bragg gratings print in the optical fiber, as should be cited the optical fiber hydrogenation method, based in the oxygen diffusion in the interior of the fiber and the consequent elevation of the photosensibility; the Hill method, based in the incidence of an argon ray in the optical core, and the phase mask method, based in the superposition of the of two signals at the optical core. The last method, namely phase mask, was implement by Institute of the Telecommunication of Aveiro and used in this work, that

consist in laser signal that is reflected by a system of four mirrors in the direction of a phase mask previously positioned and that make possible adjust the reflected signal at the specific point at the fiber core [12].

Nonetheless, the optical signal reflected by FBG is sensible to physical parameters, as deformations and temperature changes. This dependence between FBG, temperature changes and deformations can be represented by Expression 4, where n_{eff} is the optical fiber refractive index, l is the optical fiber deformation and T is the temperature.

$$\Delta\lambda B = 2\left(\Lambda\frac{\delta neff}{\delta l} + neff\frac{\delta\Lambda}{\delta l}\right)\Delta l + 2\left(\Lambda\frac{\delta neff}{\delta T} + neff\frac{\delta\Lambda}{\delta T}\right)\Delta T \quad \text{(Expression4)}$$

3.2.3. Sensors description and manufacturing

Three prototypes of FBG optical sensors for bond-slip characterization of RC elements were developed and assigned as FBG01, FBG02 and FBG03. The FBG01 (Figure 25) was composed by two metallic components, namely copper, according to specifications presented by Figure 27, with 32.00 mm of total height, 5.00 mm of thickness and 41.00 mm of total length. The superior component presents an "L" form with a hook placed at the center of the total length while the inferior component presents an "F" form and a curvature (R= 5.00 mm) on the bottom surface. Along of the total length of the FGB01 sensor, the inferior and superior surfaces are not in direct contact, the minimum spacing between them is of 1.00 mm in the extremities. A polyurethane spray layer was employed as fulfillment of the space between the two metallic surfaces (Figure 25), and in the left and right lateral a layer of 16.00 mm x 10.00 mm x 5.00 mm and 5.00 mm x 10.00 mm x 5.00 mm, respectively, were performed in order to guarantee the FBG01 sensor movements in the left and right direction till a maximum displacement of 10.00 mm. In the Figure 26.a and b is showed the details of the spacing between the two surfaces of the FBG01 sensor, and the Figure 26.c show the aspect of the FBG01 sensor during the polyurethane fulfillment process.

In fact, the inferior metallic component of the FBG01 sensor was designed to be accomplished along of the reinforcement rebar, while the superior component was designed to be hooked by concrete (Figure 25). Thus, once that the superior component of the FBG01 sensor is fixed in the concrete and the inferior component is fixed on the

reinforcement rebar, any movements reinforcement rebar will provoke deformation (by tension) on the FBG's, and consequently will provokes changes in the transmitted wavelength.

For manufacturing of the FBG01 bond-slip sensor one optical fiber with two FBG printed on the core fiber, namely FBG-D and FBG-T, the first one dedicated to performing displacement measures and the second dedicated to temperature measurements, was positioned at 2.50 mm of the stickiness and the FBG extremities connected to superior and inferior sensor's components, at 13.00 mm of height. The temperature sensor, FBG-T, was printed in the same OFS in order to reduce the temperature effect on the displacements measures.

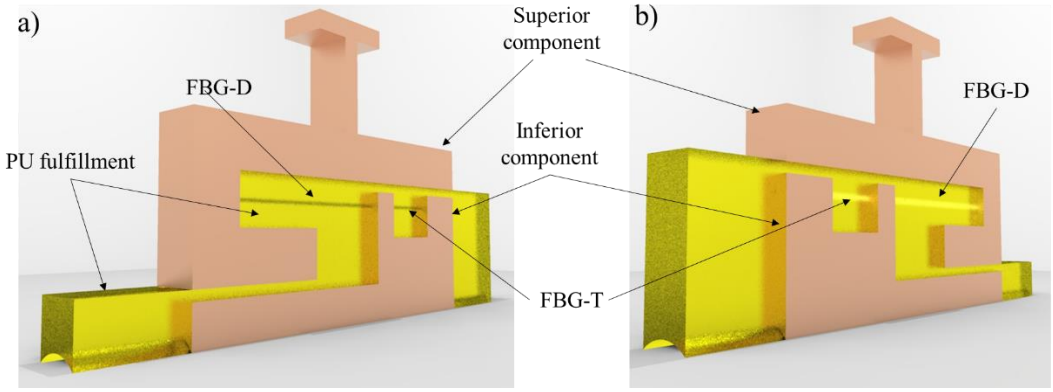

Figure 25. Details of the sensor FBG01: (a) front and (b) bottom views.

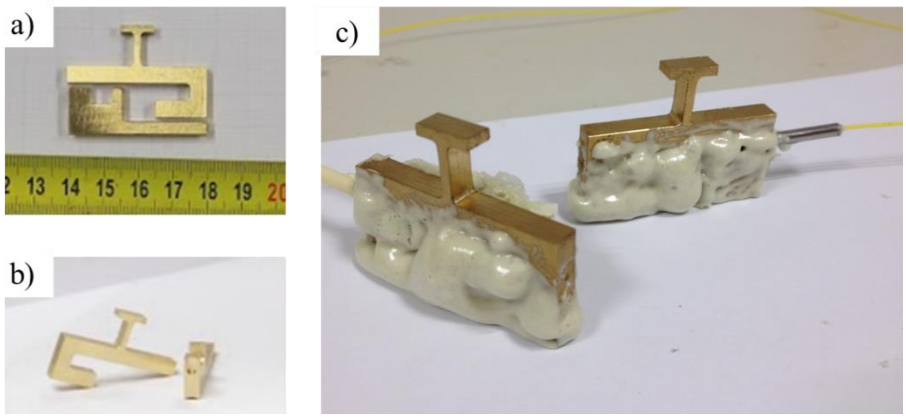

Figure 26. Details of the two components of the sensor FBG01 (a and b) and aspect of the sensor after PU spray fulfillment without surfaces regularization.

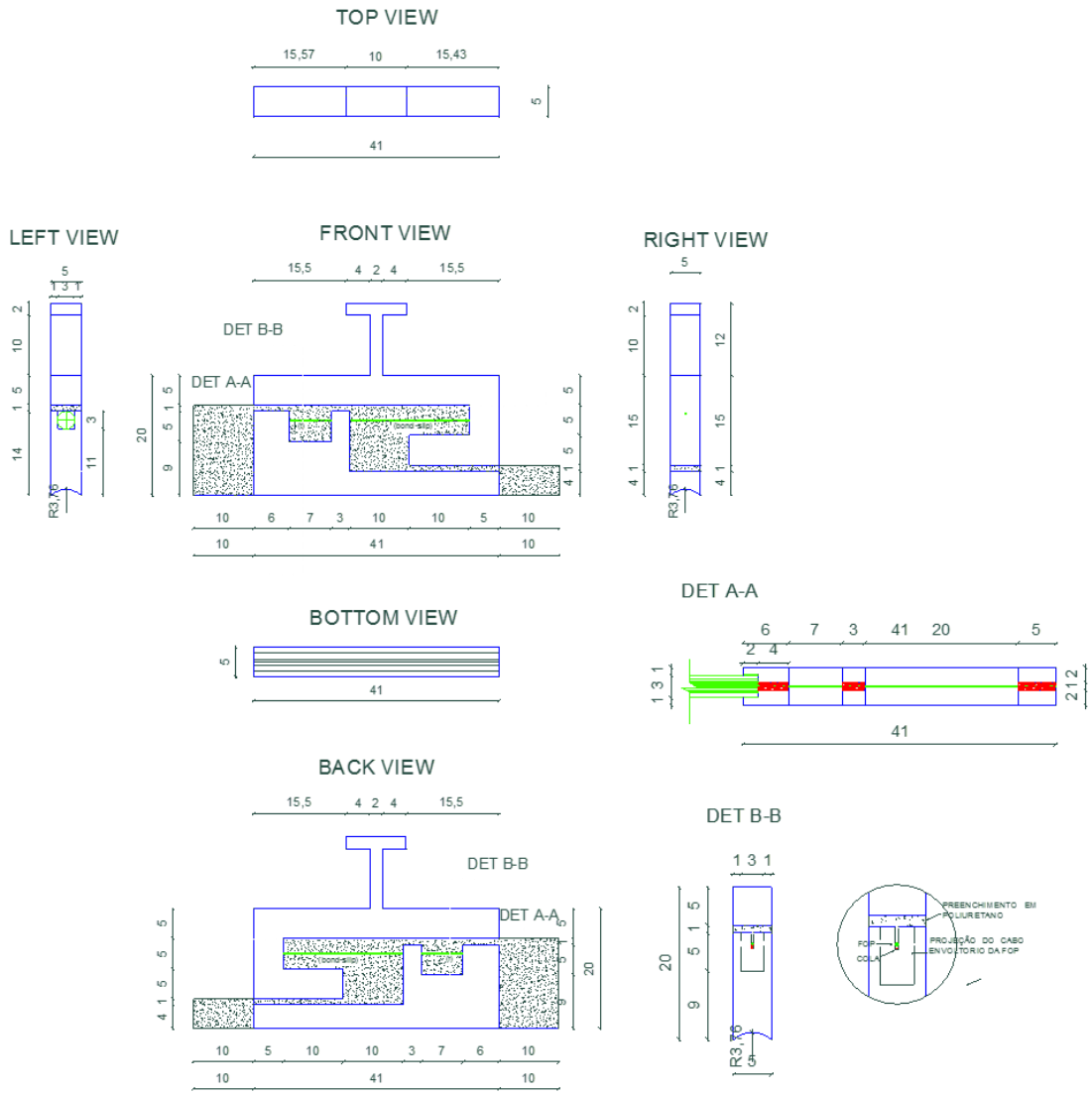

Figure 27. Setup of the bond-slip optical sensor FBG01.

The FBG01 was implemented in monomode photosensitive plastic optical fiber (POF), with a cladding diameter of 125.00 µm, a core diameter of 10 µm and a signal attenuation over around of 0.2 dB/m. A KrF excimer laser was used for printing the FBG on the POF by technique of phase mask.

The FBG02 and FBG03 (Figure 28) presents a simplest configuration, characterized by a FBG printed in one of the extremities of the OF and placed on the surface of the reinforcement rebar by silicon glue, as can be seen by Figure 29. For the FBG02 sensor manufacturing a POF with a cladding diameter of 125.00 µm and a core diameter of 10 µm and a signal attenuation over around of 0.2 dB/m was used, while for FBG03

implementation a POF (POF specifications) essentially composed by polymethil-metacrylate with a cladding diameter over around 10.00 µm, a core diameter over around 1.00 mm and a signal attenuation over 60 dB/km was employed. The same FBG printing technique employed in the FBG01 was used in the FBG02 and FBG03 sensors.

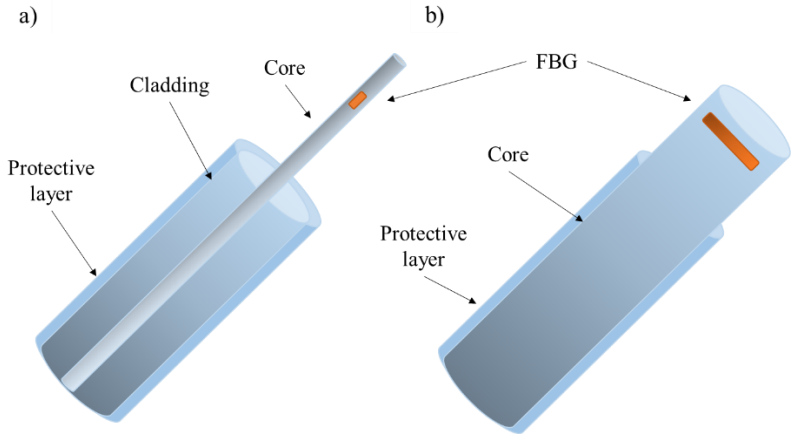

Figure 28. Details of the implemented bond-slip optical sensors FBG02 (a) and FBG03 (b).

3.2.4. Specimens detailing and experimental setup

For the experimental all three implemented prototypes of the FBG sensors for RC bond-slip characterization, namely FBG01, FBG02 and FBG03, were tested twice, in two RC specimens prepared according to Annex D of the EN 10080 [143]. For the experimental setup two concrete block with dimensions of 0.20 m x 0.20 m x 0.30 m and a centralized rebar embedded with diameter of 16.00 mm was manufactured. According to proceedings specified in EN 12390-3 [133] the mean compressive strength value of the concrete employed in the manufacturing of the specimens of test was 17.6 MPa.

For each experimental testing were employed one prototype of the FBG01 sensor, four prototypes of the FBG02 sensor and six prototypes of the FBG03 sensor. The FBG01 sensor was positioned centralized on the rebar surface at 75.00 mm of the right extremity of the RC specimen. Two prototypes of the FBG02 sensor were positioned with 100.00 mm and 200 mm of the right extremity of the RC specimen distant of the right extremity, in opposite direction each other. Also, two prototypes of the FBG03 sensors were positioned with 50.00 mm, 150.00 mm and 250.00 mm of the right extremity of the RC specimen, aligned in opposite sides. The Figure 29.a show all the bond-slip sensors

positioning inside the RC specimen, and Figure 29.b show the detail of the sensors arrangement during the specimen preparation step.

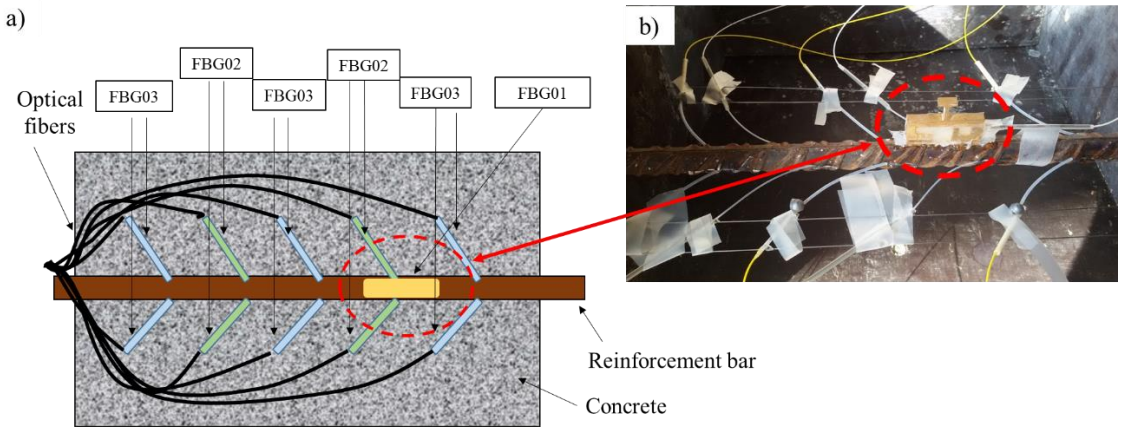

Figure 29. Disposition of the bond-slip FBG sensors inside the specimen.

Following the specimen preparation step, all the sensors were connected to data acquisition system by optical fibers and the RC specimen was concreting (see Figure 30). During the first 24 hours, all implemented sensors were monitored in order to identify sensors damage occurrences and signal losses provoked during the concreting step. After this period, all sensors were disconnected from the data acquisition system, and the RC specimen was submitted to concrete cure process by 28 days, in a humidity chamber (relative humidity of 95% and 20ºC of temperature), till the pull-out testing.

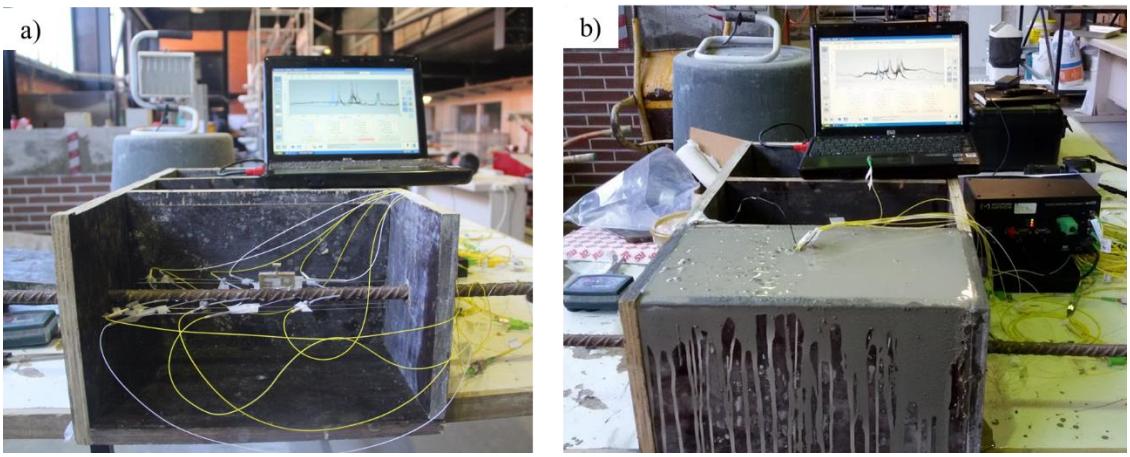

Figure 30. RC specimen before a) concrete fulfillment and after b) concrete fulfillment process.

The pull-out testing was performed according to descriptions of the Annex D of the EN 10080[143], and the details of the equipment used are shown in the Figure 31. For this testing the RC specimen was positioned in centralized form and the vertical specimen

displacement was restricted by employment of two metallic plans, fixed in the inferior beam of the steel-frame. The rebar was fixed to an actuator, and one LVDT (*Linear Variable Differential Transformer*) was positioned at the inferior surface of the RC specimen. Following, the optical sensors were connected to data acquisition system and the optical signal record started, and the pull-out testing was carried-out with velocity of displacement of 1.00 mm/s.

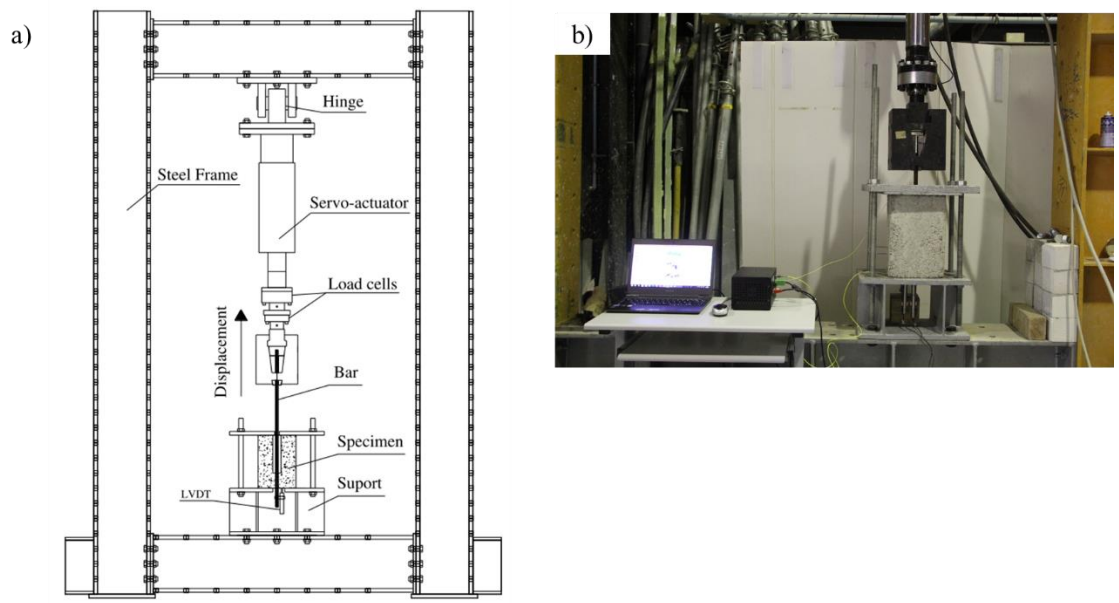

Figure 31. Experimental setup of the pull-out testing: a) details of the pull-out testing equipment and b) photography of the testing carrying-out.

3.2.6. Results

Pull-out tests were carried out on the concrete samples with optical sensors embed and all the collected curves presents a linear elastic part with different levels of displacement. The Figure 32 shows the results of relative displacement versus time collected by FBG01 sensors. In the Trial 1 the displacement curve is composed by a linear elastic phase, which moves up to the maximum relative displacements, 208.88 μm, followed by a continuous curve and an abrupt decline.

During the Trial 2 (Figure 32.b), the FBG01 sensor collected partial measure data on linear elastic curve up to the maximum of 172.52 μm, followed by unexpected broken of the FBG01. In fact, the silica optical fiber (SOP) does not present high levels of elasticity. If mechanical perturbation is applying on an optical fiber, the deformation will be

proportional to applied force, as predicted by Hooke's law (Expression 5), where K is the elastic constant and Δl is the relative deformation imposed by perturbation force, F.

$$K = \frac{|F|}{|\Delta l|} \quad \text{(Expression 5)}$$

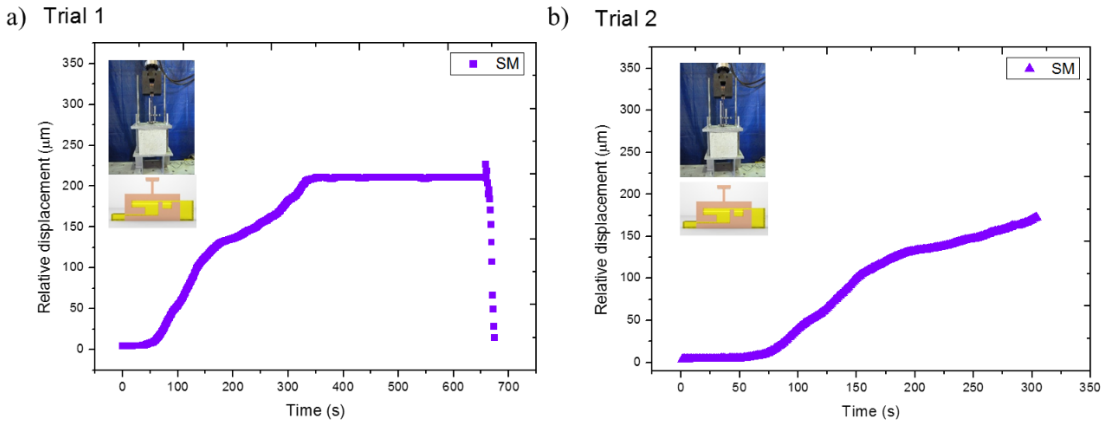

Figure 32. Experimental data from pull-out testing: a) Trial 1 and b) Trial 2 collected by FBG01 sensor at position SM.

Considering that the fiber Young's modulus, E_f, is proportional to perturbation force, F, and given by Equation 6, where A is the area and l is the length of optical fiber under perturbation, the constant elastic K can be rewrite by Expression 5 and 6 in the presented form given by Expression 7.

$$F = E_f . A . \frac{\Delta l}{l} \quad \text{(Expression 6)}$$

$$|K| = \frac{E_f . A}{l} \quad \text{(Expression 7)}$$

Taking into account the sensors FBG01 characteristics and the experimental results founded by Trial 1 and 2, were considered the average perturbation force F of 156.00 kN and the average relative deformation of the SOP, Δl, of 190.70 µm, and were founded the E_f and K values of 2.74 GPa and 821.05 kN/mm. According to [144], the average Young's modulus of a photosensitive optical fiber without cladding is 69.05 GPa, really high than the E_f founded in this experimental work. In fact, the E_f founded does not correspond to optical fiber properties, but should be related with sensor configuration properties. The FBG01 presents zones of low resistance to pull-out test, as the adherence

zone between the optical fiber and the metallic support by the polymeric resin (at extremities of the fiber inside the metallic support), that contribute for attenuation of the values of E_f and K.

The Figure 33.a and b presents the results Force versus Time and Force versus Relative displacements, from LVDT placed outside of the sample at opposite way of the loading cell. Concerning to sensors FBG02 and FBG03, the Figure 33.c and d show the results of the Trial 1 pull-out test, where the sensors placed near of the loading cell presented the main displacements, corresponding to rebar movements. The maximums rebar displacements of the FBG03 were collected at positions S5 and S10, respectively 305.32 µm and 288.93 µm. While the minimum rebar displacements were founded at S1 and S6 positions, corresponding to 2.94 µm and 2.86 µm. Now, in relation to sensors FBG02, the maximum displacement was collected at S9 position, namely 80 µm, and the minimum displacement collected occurred at position S7, corresponding to 6.14 µm. One each sensors model placed at S3(FBG03) and S4(FBG02) position does not work.

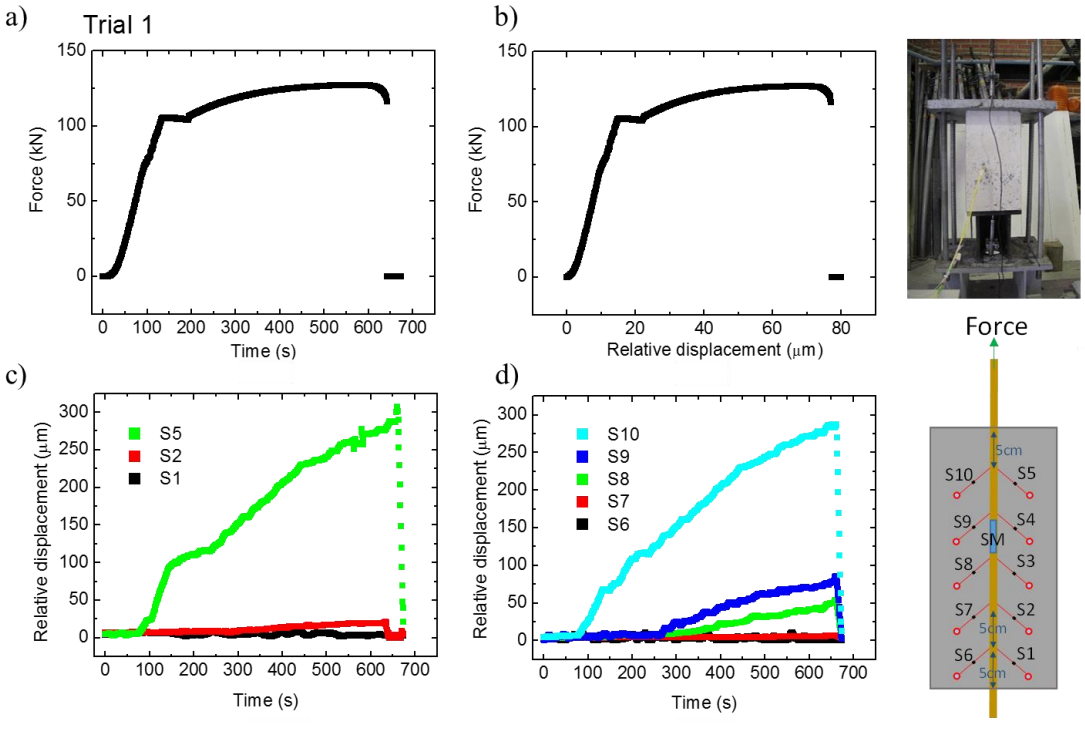

Figure 33. Experimental results from the Trial 1, where a) correspond to Force vs. Time and b) presents Force vs. Relative displacement, both collected by LVDT, and c) and d) show the data collected by the FBG02 (positions S2, S7 and S9) and FBG03 (positions S1, S5, S6, S8 and S10) sensors.

The Figure 34 presents the results obtained by Trial 2, where the maximum displacement observed for FBG02 was obtained at position S9, namely 127.22 µm, while the maximum observed to FBG03 was 462.66 µm, at S5 position. Supposedly, the displacement value at position S10 should be near of the value founded at S5 position by FBG03, as occurred at first trial. However due to the loss fiber-concrete adherence, the sensor FBG03 at position S10 was not able to collect displacements data. At positions S2 and S7, the maximums displacements measured by FBG02 were 27.81 µm and 18.71 µm, while at positions S1 and S6 the FBG03 collected 3.70 µm and 8.53 µm of displacement respectively.

Considering the maximum displacements collected at 600 s in the Trial 1 and at 200 s in the Trial 2 (Figure 35), it is possible to observe the reinforcing bar flowing. As mentioned above, during the second pull-out test the reinforcing bar suffer abrupt rupture does not allowing to obtain all the phases of the curve force versus displacement. Another way of to visualize the reinforcing bar flowing is by Figure 36, where the force was fixed at 100 kN and is possible to see the correspondent displacements for each point.

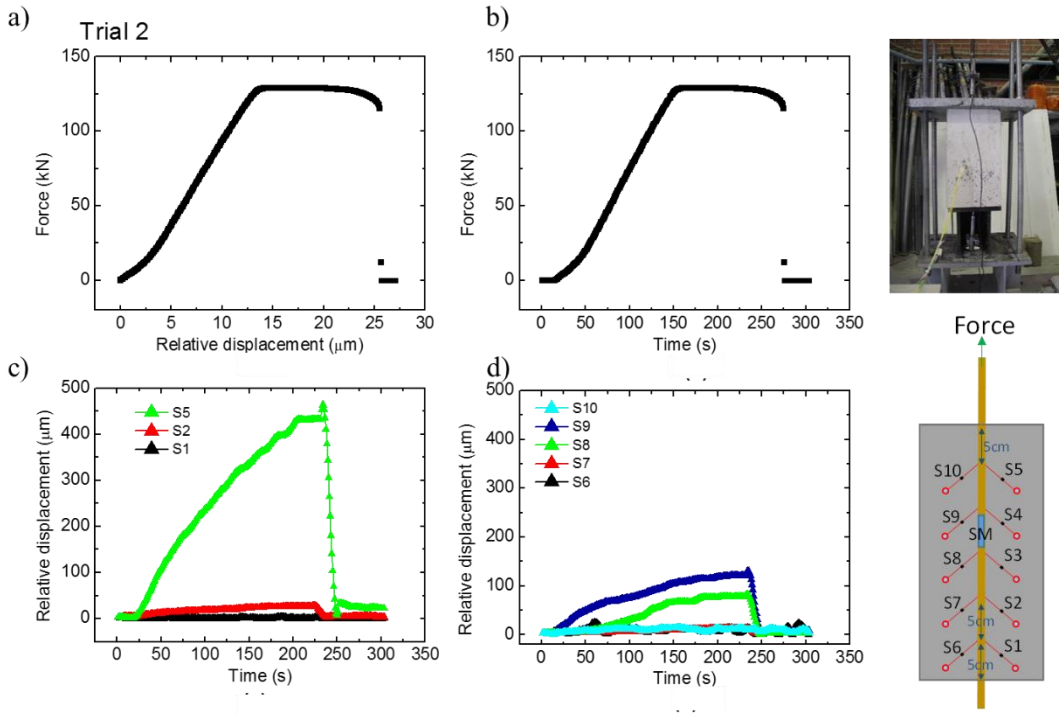

Figure 34. Experimental results from the Trial 2, where a) correspond to Force vs. Time and b) presents Force vs. Relative displacement, both collected by LVDT, and c) and d) show the data collected by the FBG02 (positions S2, S7 and S9) and FBG03 (positions S1, S5, S6, S8 and S10) sensors.

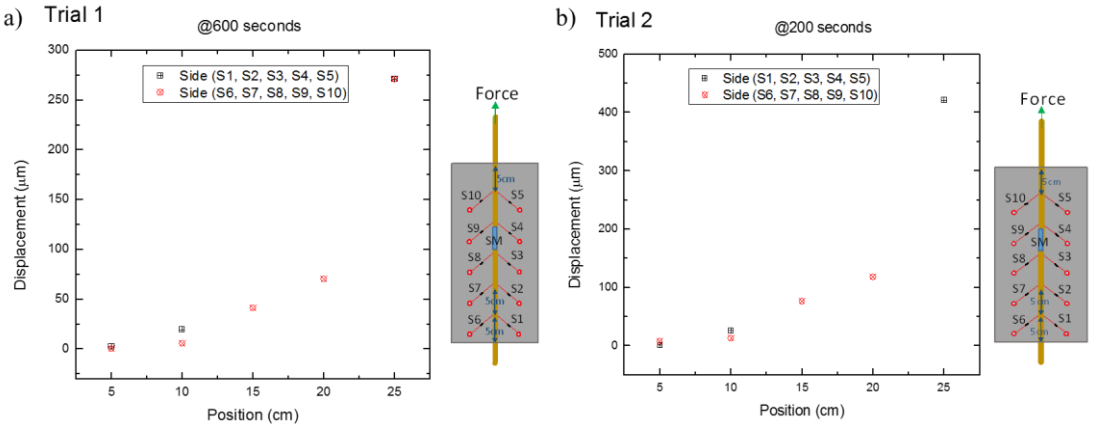

Figure 35. Maximums reinforcing bar displacements at 600 seconds (Trial 1) and 200 seconds (Trial 2) measured during the experimental setups each 5 cm.

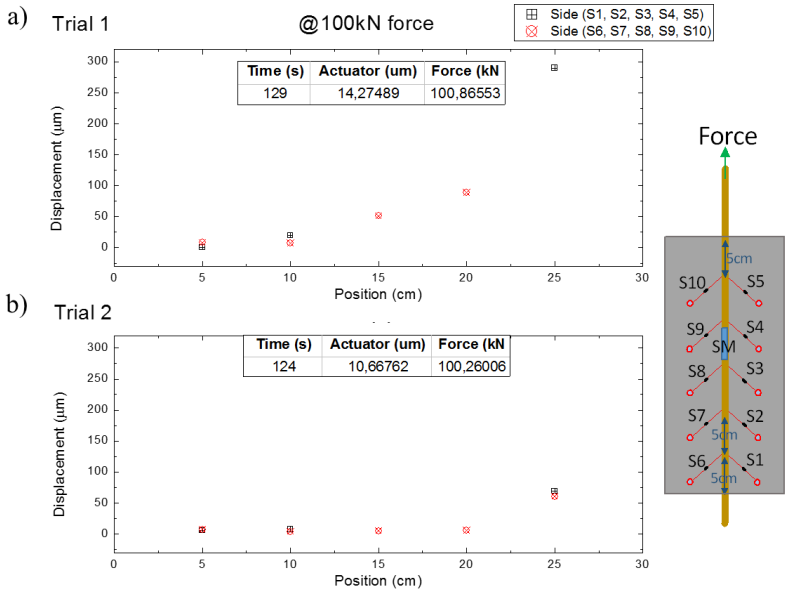

Figure 36. Reinforcing bar displacement each monitored point at 100 kN of pull-out force.

3.2.7. Final comments

In this section, three optical fibers sensors based on FBG for bond-slip monitoring of old RC structures, namely FBG01, FBG01 and FBG03 were described and tested. The FBG01 is constituted by a FBG connected to a metallic support, while FBG02 and FBG03 are composed only by plastic optical fiber and a simple fixing support, while another two prototypes presents a simplest configuration.

The results found showed that all the three implemented sensors were able to characterize the bond-slip displacements in the samples tested in the order of micrometers. As well a high level of sensibility to micro-displacements. The positioning of the sensors FBG02 and FBG03 along of the rebar allowed the characterization of the pull-out displacement along of the reinforcing bar.

The system for bond-slip monitoring proposed in this work is a technique that can be applied on existing RC structures characterized for be less intrusive without the necessity of removal of samples from the structure, keeping it potential application on structure with cultural values. Also, the possibility of to connect this monitoring system to internet for remote monitoring can be an assertive tool for support the risk management of heritage constructions in real time.

4

Strategies for SHM design

Summary

The development of strategies for structural monitoring is important for optimization of the available sources. Indeed, an adequate SHM planning, indicating the sensors characteristics and its distribution on the structure components, the architecture of the monitoring system and the way how the sensing system, data acquisition system and data management system will communicate between them, present relevant influence for reliability of the data collected by SHM system. In the case of heritage constructions (HC) monitoring, essentially, there are several factors which should be considered such as the time-retrofitting history, current state of the structure, its damage characteristics and behavior of its structural components to understand the historical remarks of the assessed structure, for a proper SHM planning. In order to contribute for implementation of the knowledge on the field of SHM of HC, this work presents a proposal for SHM of the São Lourenço Church, a stone masonry structure built in the XVII century, located at Porto, Portugal, as well a proposal for monitoring of the Nossa Senhora das Dores Church, from XIX century, located in Sobral, Brazil. Concerning São Lourenço Church, the monitoring proposal comprises a wireless sensor network, an optical system, focused on monitoring of the environment influence on relative displacements of stone masonries; an electrical sensorial system designated to measure cracks evolution; and a sensorial dynamic system, devoted to record acceleration data, while the monitoring proposal addressed to Nossa Senhora das Dores Church is focused on characterization of the environmental influences on structural behavior. Both SHM proposals can be classified as Level 4, according to levels of classification of SHM system proposed in this work

Keywords: Strategies for SHM, heritage constructions, sensing network, long-term monitoring, São Lourenço Church, Nossa Senhora das Dores Church.

4.1. A proposal for São Lourenço Church monitoring through wireless sensor network

4.1.1 Introduction

The integration between smart technologies, as wireless sensing systems, with structural assessment can be a great opportunity for optimization of the investigation procedures, especially considering the high number of heritage constructions (HC) present in the cultural centers of the cities and its variability. In fact, the understanding of the damages mechanisms in ancient structures, request not only that experimental tests be carried out in selected structural elements, but also a time-evolution analysis of structural intervention and maintenance measures, along with a comprehensive view of the building history [145, 146]. This way, the development of strategies and methodologies for real-time assessment can be an important contribution on the safety maintenance of HC.

Since the beginning of this century, the Institute of Construction (IC-FEUP) has been developing strategies for the assessment and monitoring of HC (Figure 37), especially with recurrence to case studies placed at the north of Portugal. Moreover, based on the advances on the field of system communications, the monitoring strategies had evolved and wireless data acquisition had been integrated with the traditional assessment techniques. Additional information on the case studies performed by IC-FEUP can be found in [109, 147]

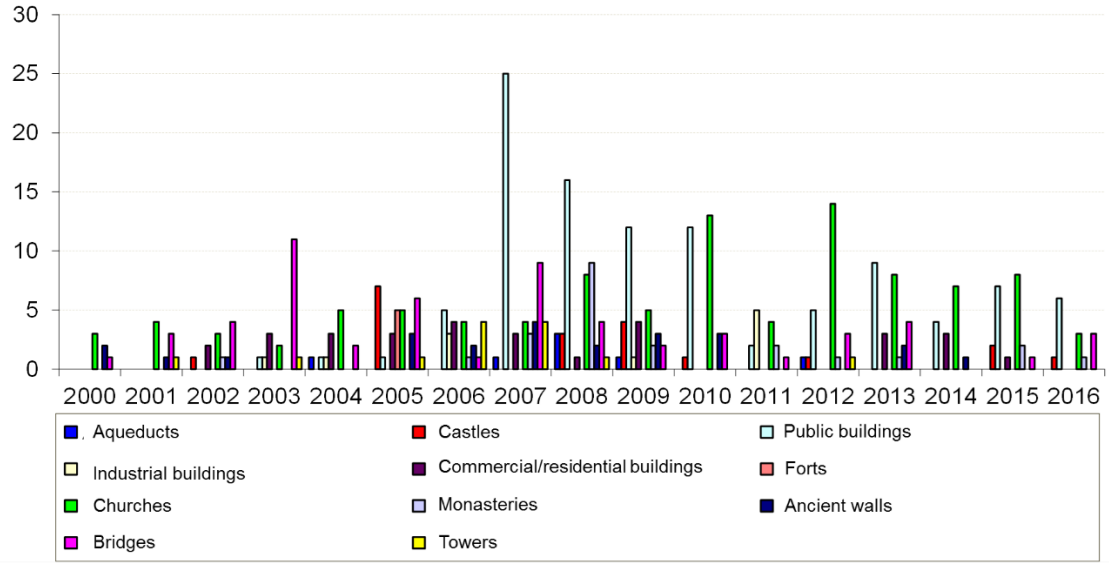

Figure 37. Case studies analyzed by IC-FEUP since 2000 [148].

The employment of wireless monitoring systems can be an interesting support tool for the safety management of heritage constructions, basically because it can allow long-term and real-time data records, as well the remote access for the simultaneous assessment of different HC placed in different zones occur from the same location [149, 150]. Nevertheless, description of the procedures for implementation of monitoring systems based on wireless communication are missing in the support literature [8, 9], making evident the necessity of contributions in this topic.

This way, the principal motivation for the present work development was the existence of a lack in the techno-scientific field about specific tools to support the characterization, monitoring and structural assessment of heritage construction, especially considering the environmental effects (as evidenced by [44, 151, 152]. The present work describes the necessary steps for an optimized design of SHM system based on IC-FEUP experience. In order to clarify and provide a practical view, the methodologies described in this work will be made by referring real case studies, namely the São Lourenço Church.

4.1.2. Procedures for HC assessment through SHM system

The most adequate configuration of a SHM system focused to HC assessment depends not only on the technical specifications of the data acquisition system, but also on the sensorial system correct positioning relative to the most critical zones and on the technical team experience; the latter, in particular, has a strong influence for the monitoring system be optimized or not. In addition, in the case of HC assessment the cultural value also includes additional issues to be taken into account for the SHM system design, as for instance, how to provide an adequate system with the least visual intrusion possible.

The number of sensors should also be optimized in order to achieve a monitoring system as cheap as possible, without neglecting performance. In this particular issue the sensors multiplexing possibility, particularly in optical fiber based sensor systems [153], has been contributing for decreasing costs.

With the HC SHM optimization in mind, Figure 38 presents a flowchart with general designing procedures.

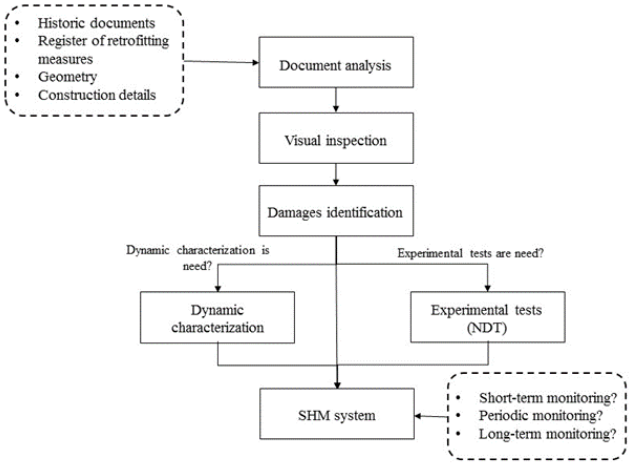

Figure 38. Flowchart of the procedures for designing system monitoring of HC.

All available information, as historic records, construction details and retrofitting measures carried-out, need to be collected in order to provide sufficient planning information before proceeding with the visual inspection, minimizing its time duration and increasing its efficiency. Early information allows the technical team to disregard some unimportant aspects and define some hypothesis that will be soon confronted with evidences collected during visual inspection. The later basically aims confirming the information collected by document analysis, namely structural geometry data, and also to identify the main evidences or damages present on the HC under study.

Subsequently, depending on the damages found and the uncertainties related with the structural behavior, dynamic characterization and experimental test can be required. The tests' nature will depend on the type of damages or evidences found during the visual inspection and on the assessment objective. However, non-destructive tests (NDT) are the first candidates to be carried-out, since the main guidelines for HC construction assessment (see [1, 4, 154]) state that it needs to be the least intrusive possible.

Once the structural information details are collected the type of SHM must be selected concerning duration issues, namely: short-term, periodic or long-term monitoring. Essentially, the system type depends on the structure damages and on the owner's needs. For instance, the short-term monitoring is mostly employed for the identification of structural parameters and the assessment of retrofitting measures, while the cases reported on the literature on periodic and long-term monitoring are focused on damage detection or damage progression assessment [56, 155].

4.1.3. Historical remarks of the São Lourenço Church

The São Lourenço Church (Figure 39), also called Grilos Church, is a stone masonry structure built in the XVII century placed at the Paço Episcopal (Bishop Palace) in Porto downtown. The presence of Jesuits architectural marks can be found in the whole church, namely an essentially educative and religious architecture, jesuitic-baroque and neoclassic. In 1982, the São Lourenço Church was classified as part of the Portuguese Nacional Heritage and, in 1998, the Porto's Historic Center was classified by UNESCO as world heritage.

The main façade of the São Lourenço Church (Figure 39.a), with 29.48 m of high, has two levels composed by continuous walls of large stone blocks, essentially granite, while the main door is constituted by two columns placed under pedestals. In the laterals of the main façade, two secondary doors exist with triangular pediments. In the church interior, as shown by Figure 39.b, a granitic vault with 20.24 m of high, with Jesuits marks, extends its self all long the Central Nave, the latter adjacent to the Main-Altar Chapel and the two secondary Chapels all covered by granitic vaults as well; the central dome joins all the four vaults.

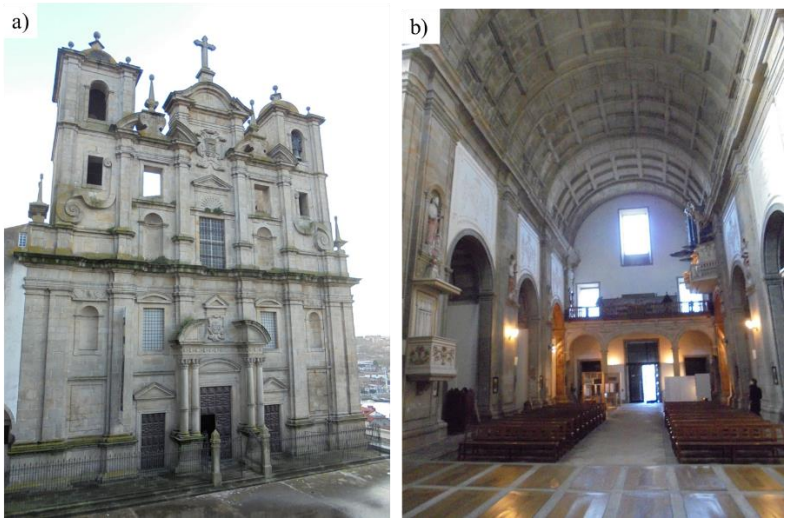

Figure 39. São Lourenço Church: a) Main façade and b) interior view.

The church has 50.48 m of length and 26.44 m of width, and presents a longitudinal plant characterized by the Central Nave with three chapels placed at each side, the Main-Altar and two secondary chapels, namely the "Nossa Senhora da Purificação Chapel" and "Santíssimo Chapel", as presented in Figure 40.

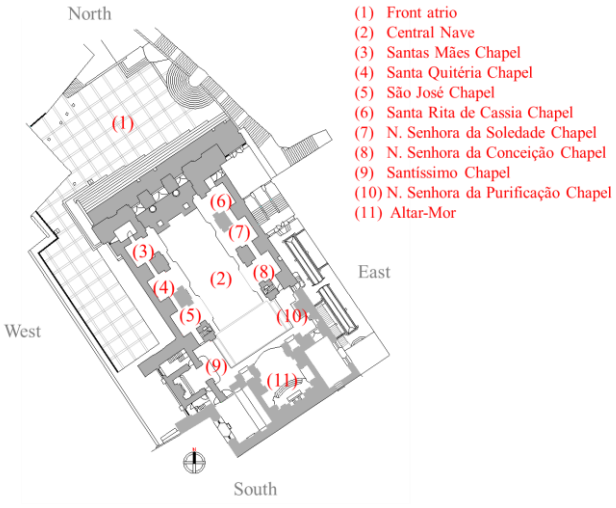

Figure 40. View in plant of the São Lourenço Church.

According to [156], and to a search in the historical documents of São Lourenço Church the construction chronology and some important historical remarks of the São Lourenço Church are presented at Table 3.

Table 3. Historical remarks of the São Lourenço Church

Year	Area	Description
1573	Major seminary	The fundamental stone of the "Colégio do Seminário Maior do Porto" was released on August 20th;
1574	Major seminary	The construction work at the foundations level began on January, 31th;
1575	Major seminary	Interruption of the construction work due to financial issues, on January, 21th;
1577	Church	Beginning of the foundations construction of the São Lourenço Church construction;
1579	Major seminary	The construction of the "Seminário Maior do Porto" is restarted, on January 28th. The construction of the rooms and balconies of South zone is started;
1589	Fountain	Acquisition of the entitlement of to conduct water from "Fonte das Fontainhas" and its uses;
1595	Exterior stairs	Construction of a stair flight between "Largo do Agouçe" and "Largo do Colégio";
1603	Major seminary	Conclusion of eight rooms at South zone dedicated to 3rd year seminarians;
1613	Major seminary and the church	Conclusion of the East zone of the Major seminary and the living area near of the eight rooms at South zone;
1614	Church	Beginning of construction of the Central-Nave, properly;

1625	Church	Conclusion of the Church body and roofs, and beginning of the ornamental work at interior and exterior zone of the Church;
1642-1669	Church	Construction of the Capela-Mor, as well ornamental works on Sacristia, Claustro, Capela-Mor and Retabulo da Imaculada Conceição;
1675	Church	Beginning of the construction work of the Portaria and Patio das confições;
1690	Major seminary and the church	Construction of a frame with five class rooms and to Officine, in the seminary, and beginning of the work at Main façade of the church;
1694	Church	Conclusion of the first level of the Main façade of the church, and construction of storage rooms;
1700	Church	Beginning of the second level of the Main façade of the church;
1704	Church	Construction of the retable de São Francisco Xavier";
1709	Church	Conclusion of the Main façade of the Church, Coro-Alto; opening of windows at transept and constructions of the church' floor;
1715-1737	Church	Construction of Santa Quitéria and Santa Ana altarpieces; constructions of an external wall and some work at the main Largo;
1784-1785	Major seminary	Adaptation of the class rooms to Porto Senate;
1795	Church	Conclusion of the Retable-Mor;
1800	Church	Santíssimo Chapel construction;
1853-1854	Major seminary	Construction work at seminary roofs;
1862	Major seminary	Opening of the Major seminary;
1873	Major seminary and the Church	Construction of additional rooms, kitchen unit and bathrooms, as well the enlargement of the Coro-Alto;
1899	Major seminary	The period of building enlargement is over;
1906	Major seminary	Construction of the library and additional rooms;

1907	Church	Maintenance procedures at Santíssimo Chapel and Altar-Mor;
1908	Church	Maintenance procedures at Altar-Mor;
1909	Church	Altar-Mor adornment;
1910	Major seminar and the Church	Ornament of the Arch-cruise and of the Alta-Mor; installation of chairs at Coro-Alto and beginning of the library installation;
1949	Major seminary and the Church	Retrofitting focused on reduction of the loading on Ribeira Tunnel, namely through construction of a balcony, ring and arches at exterior zone of the Seminary; Construction of the Suez channel, rooms and a gym;
1962	Major seminary	Enlargement and renovation of the Interior Chapel, kitchen and its storage rooms;
1988-1989	Church	Renovation of the North tower and general maintenance procedures at the roofs; These works were conducted by General Direction of Buildings and National Monuments (DGEMN).
1990-1991	Major seminary and the Church	Damage occurrences on the walls, especially at the Santíssimo Chapel zone were identified, namely cracks provoked by foundation settlement. A structural retrofitting proposal for São Lourenço Church stabilization was presented by LNEC;
1994	Major seminary	Renovation and general maintenance procedures were performed at Art Sacra Museu;
1994	Major seminary and the Church	A geometric levelling of the Seminary and Church area was carried out;
1997	Church	Renovation of the floors and roofs of the Church and positioning of the lateral Altars according to original position;
1998	Church	Conclusion of the renovation works at the Museu;

Over the last decades, some interventions were performed on São Lourenço Church, essentially focused on the building stabilization. In the West of the Church, for instance, buttresses (Figure 41) were built, possibly after 1949, in order of to avoid drastic structural movements.

Figure 41. Buttresses at the West zone of the São Lourenço Church.

In 2008, the observation of cracks at church exterior side (stairs zone) led to the adoption of retrofitting measures. One decade before, between 1994-1997, short-term monitoring was performed by LNEC in order to collect data about the damage progression.

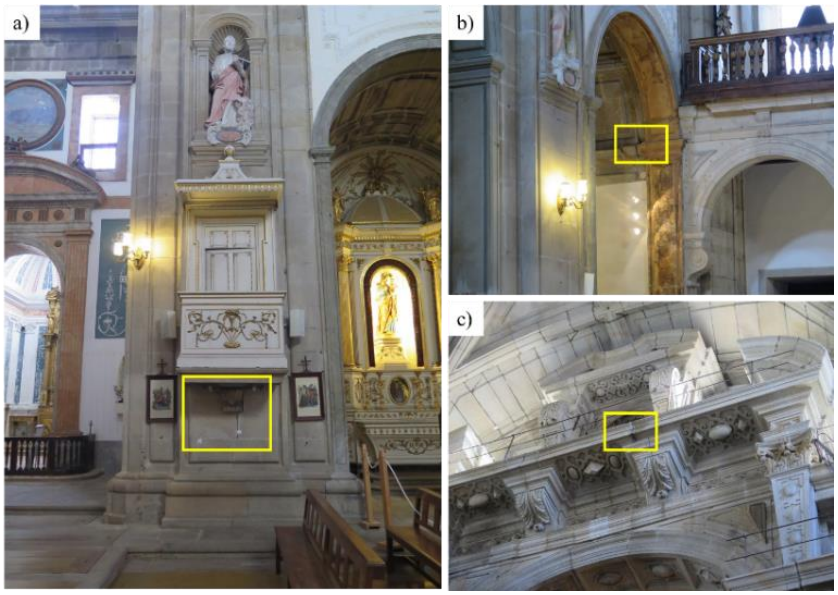

Figure 42. Positioning of the relative displacement sensors provided by LNEC.

The monitoring results collected by LNEC team were centered in the measurements of linear displacements of the walls' cracks and foothills' movements; the maximum recorded crack opening was 0.8 mm, but the monitoring procedures did not take into account the temperature influence on the crack opening-closure mechanism. Finally, in 2010, an official report of the *Cultural Heritage Department of the São Lourenço Church* called the attention for the "dramatic structural damages observed on the church and the real need to proceed with urgent intervention."

4.1.4. Damage assessment of the internal and external area of the São Lourenço Church

In the recent years, progression of cracks and structural displacements has been observed, mainly at the West side of the church, as notice by a survey for damage mapping carried out both in the external and internal zones of the São Lourenço Church. Indeed, the structural movements of the Church can be not exclusively related with the Ribeira Tunnel construction, in 1949, because soil properties changes would be noticed, as well. According to [156], problems related with soil characteristics during the foundations execution of the Major seminary where notice in the *Annuis Litteris*[1], still in 1573. Most recently, an experimental study performed by the Geology Department of University of Porto presented a mapping of the areas indicated for construction, according to soil properties, shown by Figure 43, confirming that the São Lourenço Church is placed in an area with soil with different properties, where the north and south zones of the church are not properly indicated to construction.

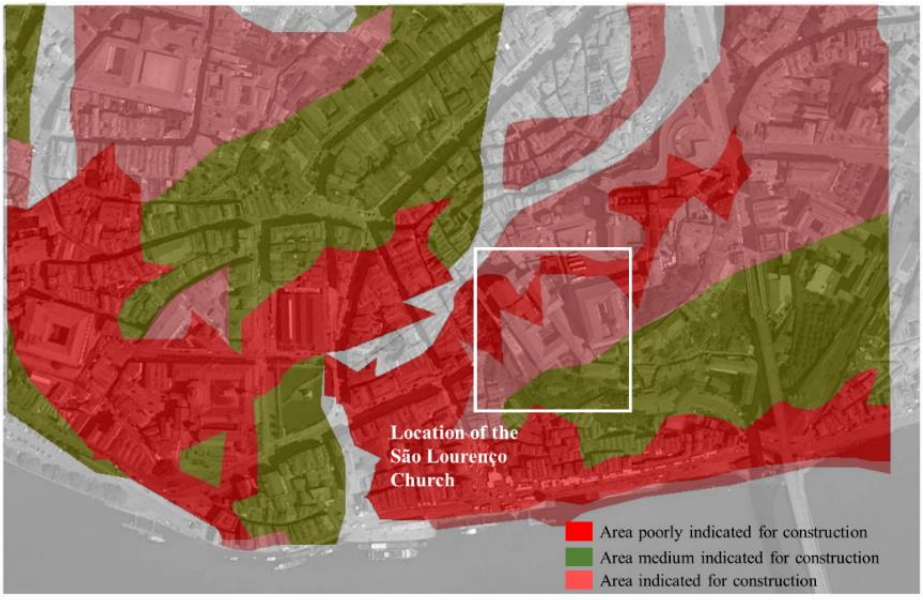

Figure 43. Mapping of soil classification for construction according with Porto Geotechnical Report and location of the São Lourenço Church.

From the information collected in the documental analysis and by visual inspection, it was possible to infer a global frame for the damage occurrences in the church, as shown

[1] Annual report from the Porto Diocese, destined to the Vatican, including the main occurrences along the years.

in Figure 44. Essentially, the observed damage is considered to have been caused by vertical and horizontal soil settlement in the region where a tunnel was built, that has induced rotation of the foundation elements and lateral displacements of the right-side walls of the church. To date, it is not yet possible to know whether these displacements were or are being accelerated by road traffic in the tunnel, i.e. if they are stabilized, for which the installation of a SHM system on the church was decided to be undertaken.

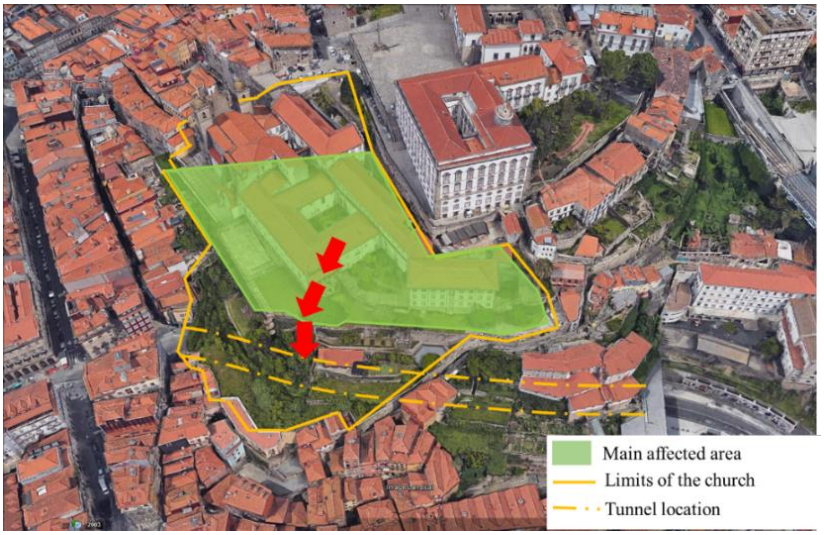

Figure 44. General scheme of the displacement mechanism at São Lourenço Church.

Figure 45 shows the damage found during the visual inspection in the church external zone, where the most expressive cracks can be seen mainly at the church west side. Inside the church, most cracks were found mainly in the lateral chapels' vaults, columns and walls, as illustrated in Figure 46. As shown in Figure 45 and Figure 46, the area most affected by the ground displacements, illustrated by Figure 44, is coherent with cracking location, which suggests rotation of the church west side. However, this rotation did not only affect the left side, because some cracks (less opened) were also found in the right-side chapels' vaults.

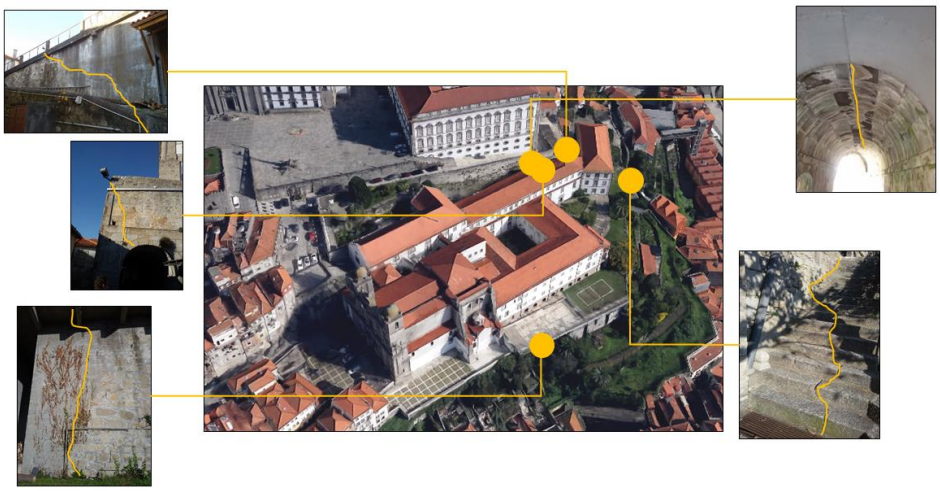

Figure 45. Cracks occurrence at the exterior zone of the São Lourenço Church.

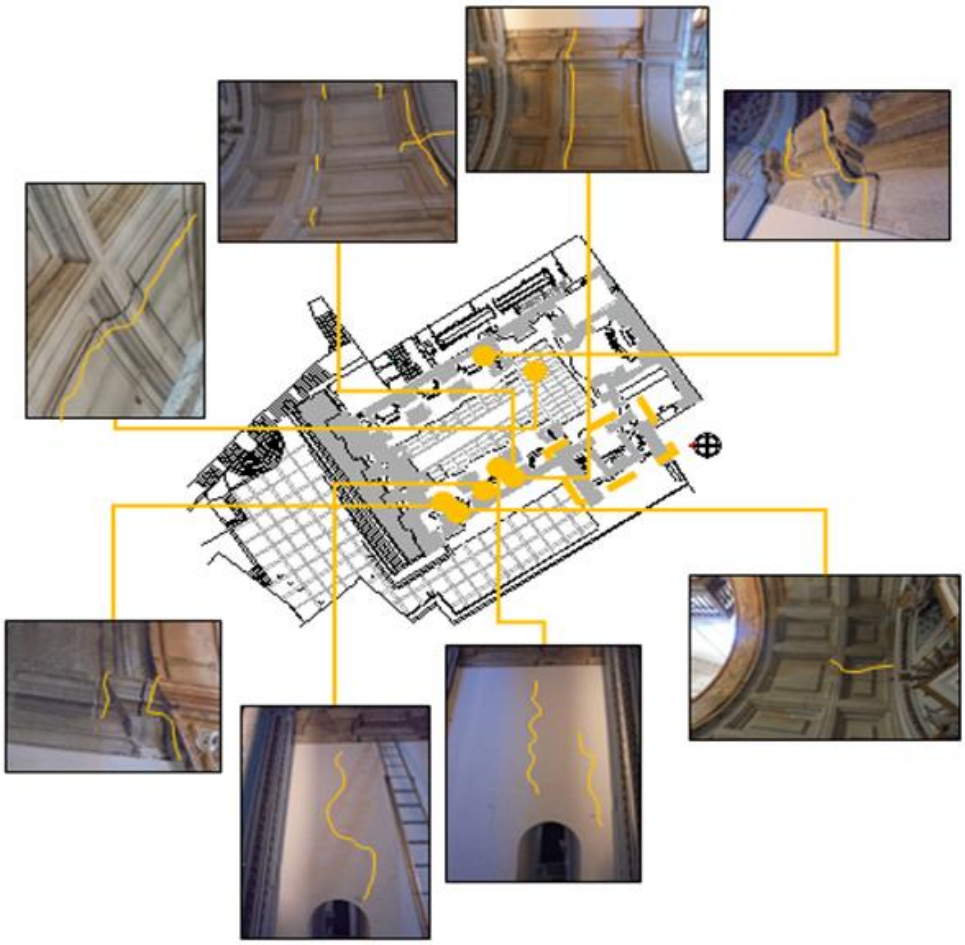

Figure 46. General view of the cracks location at the interior of the São Lourenço Church.

A detailed view of the cracks on the lateral chapels is presented by Figure 47, where the Figure 47.a, b and c refers to chapels placed at west of the church, while the Figure 47.d,

e and f shows the chapels placed at east zone. The chapels positioning along the Church can be seen in Figure 40.

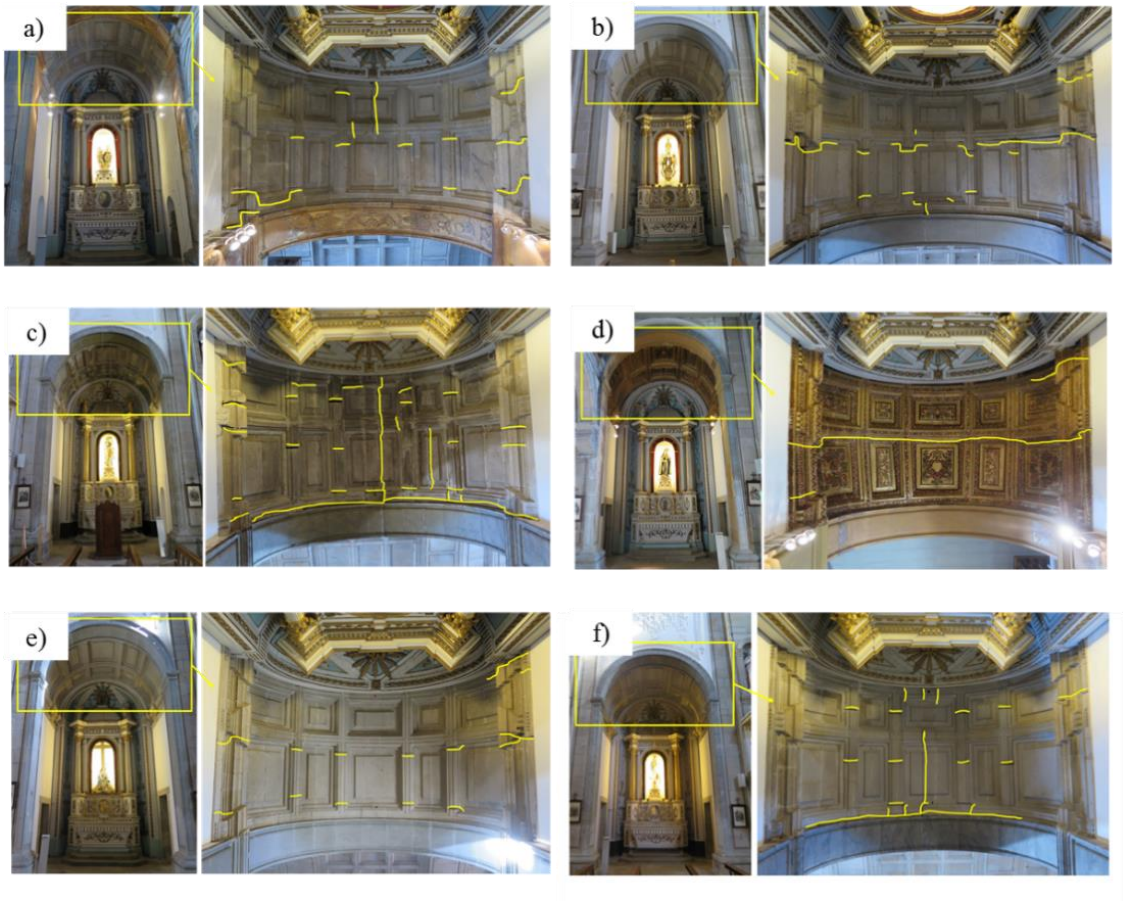

Figure 47. Crack mapping of the lateral chapels of the São Lourenço Church: a) Santas Mães Chapel, b) Santa Quitéria Chapel, c) São José Chapel, d) Santa Rita de Cássia Chapel, e) Nossa Senhora da Soledade Chapel and f) Nossa Senhora da Conceição Chapel.

Basically, through Figure 47, it can be noticed that the chapels placed at the west side of the church are most damaged than the others, presenting evidences of structural displacements, namely crack openings on the chapels arches, mainly oriented with longitudinal direction of the church. Whereas, the chapels located at southwest presents significantly more damages, as observed at São José Chapel, (Figure 47.c), a reduced number of cracks opening were noticed on the chapels positioned at the northeast zone, as observed at Santa Rita de Cássia Chapel, shown by Figure 47.d. Similar damage critical situation, was detected at Santas Mães, Santa Quitéria and São José Chapels, and also observed at Santíssimo Chapel, shown by Figure 48. Beyond the damages identified on the chapels at the Central-Nave, both lateral chapels of the Altar-Mor also present cracks occurrence, despite they are mainly located in the vaults connections. Figure 48 shows the crack occurrence on the vaults and walls of the Santíssimo chapel, while the main damages occurrence on Nossa Senhora da Conceição Chapel are shown by Figure 49.

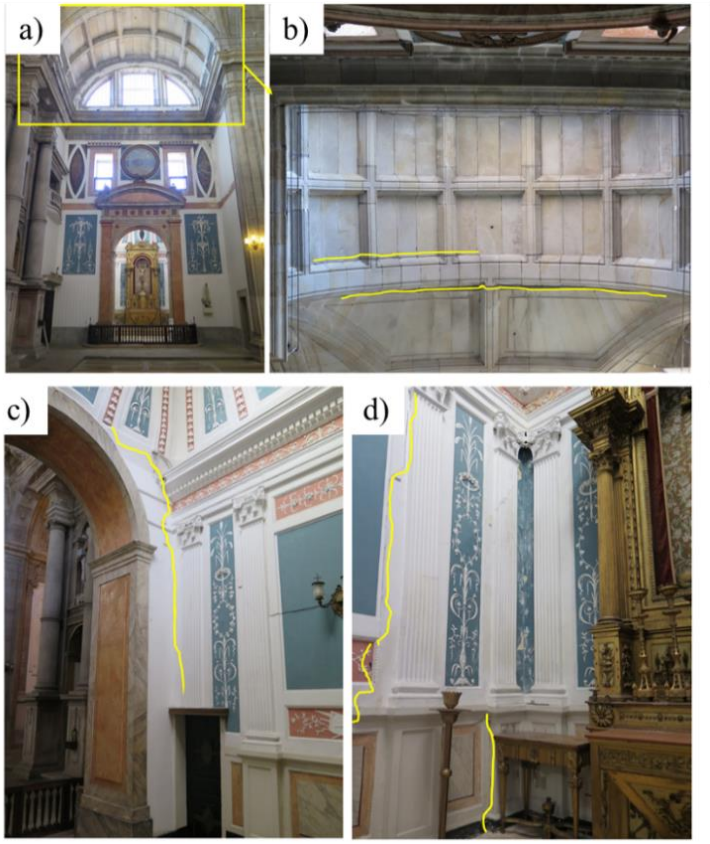

Figure 48. Damage occurrences on Santíssimo chapel: a) vault, b) cracks on the vaults, c) and d) present the cracks occurrence on the chapel walls.

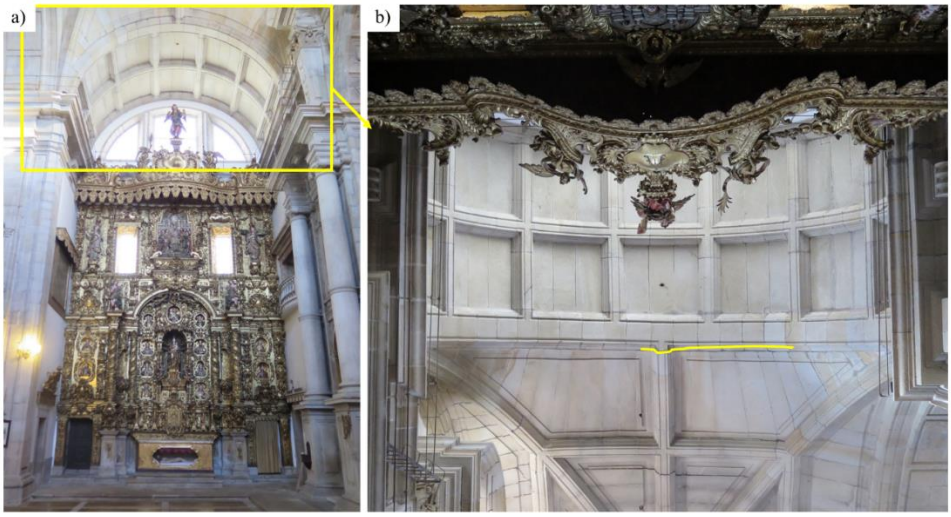

Figure 49. Nossa Senhora da Conceição Chapel: a) vault and b) location of the main crack.

The Santíssimo chapel presents some cracks along of the walls high, as well as on the floor and dome, that globally can be characterized as a rotation movement in the southwest, evidencing displacements occurrence at the foundation level, also confirming the damage scenario hypothesis previously shown in Figure 44.

Regarding the Altar-Mor, Figure 50, the cracks are principally located on the vault, along the transversal direction of the Central-Nave, however cracks at the longitudinal section also can be found.

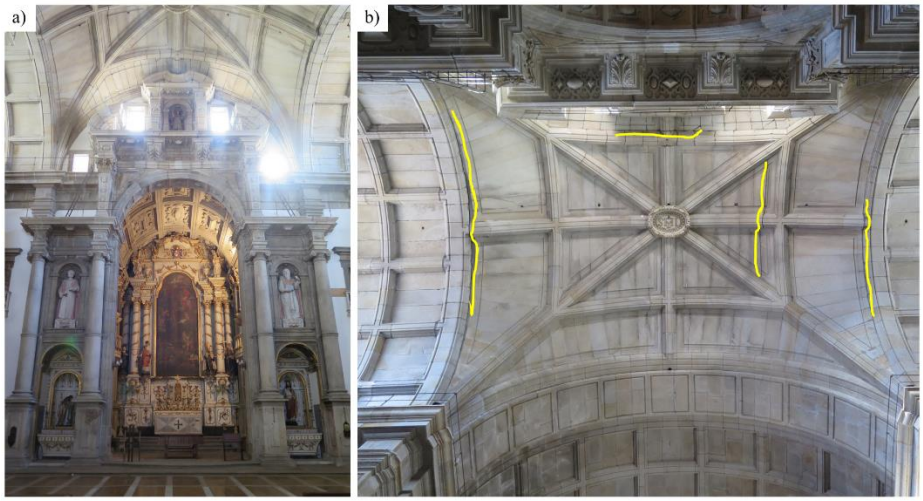

Figure 50. Altar-Mor of the São Lourenço Church: a) general view and b) main cracks occurrences.

The inspection included also thermography recordings in order to examine the existence of moisture zones, suggested by the presence of dark spots in the vaults-walls. However, no significant moisture was found in the walls, for which the dark areas were assumed as the result of water infiltration before the roof rehabilitation. Examples of thermography records taken in the church interior, at the Central-Nave, are shown through Figure 51.

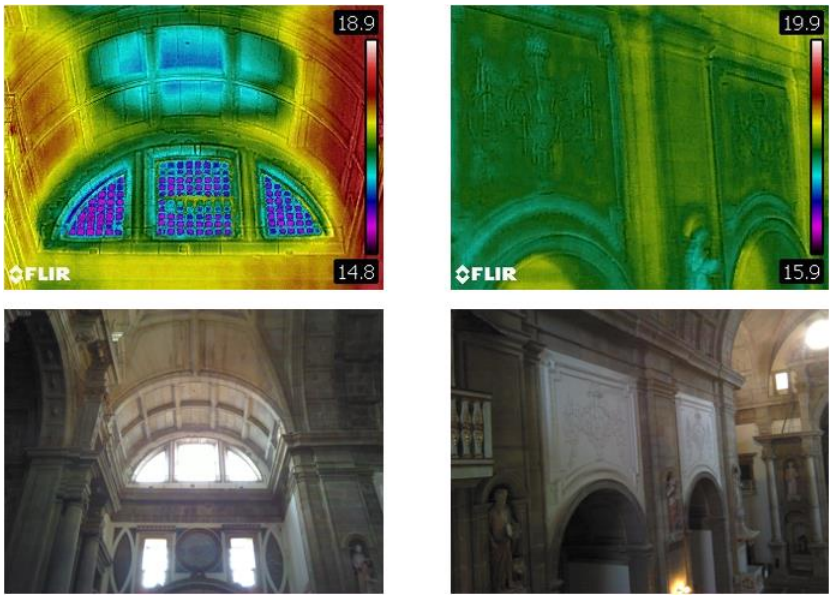

Figure 51. Examples of the thermographies collected at interior of the São Lourenços' Church.

4.1.5. Dynamic characterization and long-term SHM proposals

The dynamic characterization constitutes a useful tool for the structural behavior understanding, as well can be used for numerical modeling optimization. This way, an experimental testing scheme proposal for dynamic characterization of the São Lourenço Church is presented in Figure 52, where 10 triaxial accelerometers are considered along of the church, allowing recording acceleration in the transversal, longitudinal and vertical directions, due to ambient vibration, of which 2 will be placed in the main façade. This experimental setup design was prepared based on the CONSTRUCT-LESE team experience and also on relevant literature (see [9]).

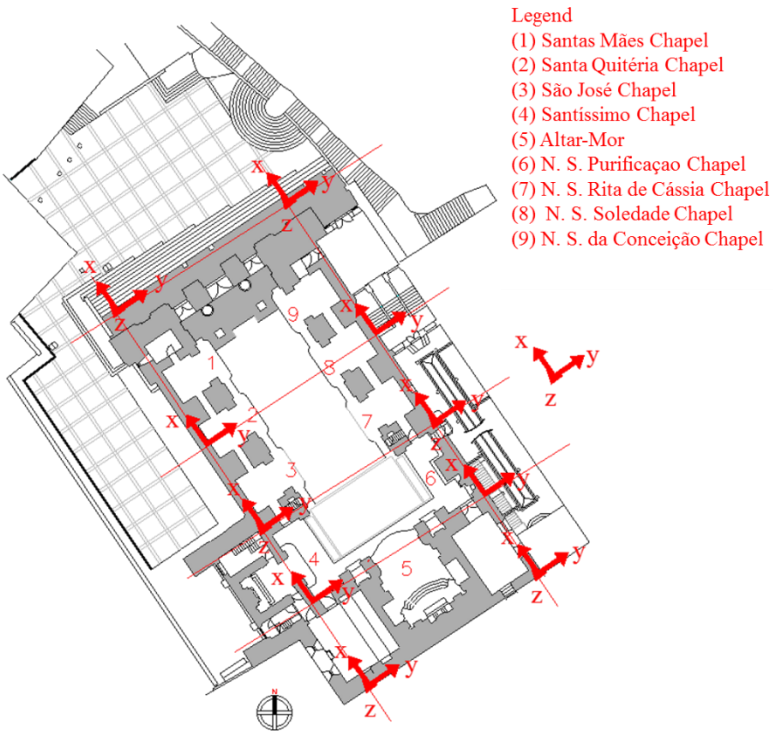

Figure 52. Experimental scheme proposed for dynamic characterization of the São Lourenço church.

In order to characterize the effect of the temperature on the stone masonry displacements, the long-term monitoring proposal of the São Lourenço Church structure, includes an optical system based on FBG. The proposed optical system relies on six optical FBG sensors to measure relative displacements and temperature, according to scheme presented by Figure 53. Similar framed optical sensors distribution was used by [157]. This simplified SHM system aims to monitor the crack opening-closing taking advantage of the high accuracy level of FBG sensors for displacement measurement (bellow 1 µm).

In addition, both optical sensors developed and presented in the Chapter 3, namely the groundwater level monitoring sensor and the bond-slip monitoring sensor can be used to complement the monitoring of the São Lourenço Church, to monitor the soil characteristics, and the RC elements introduced in the church vaults after it retrofits, in 1987, respectively.

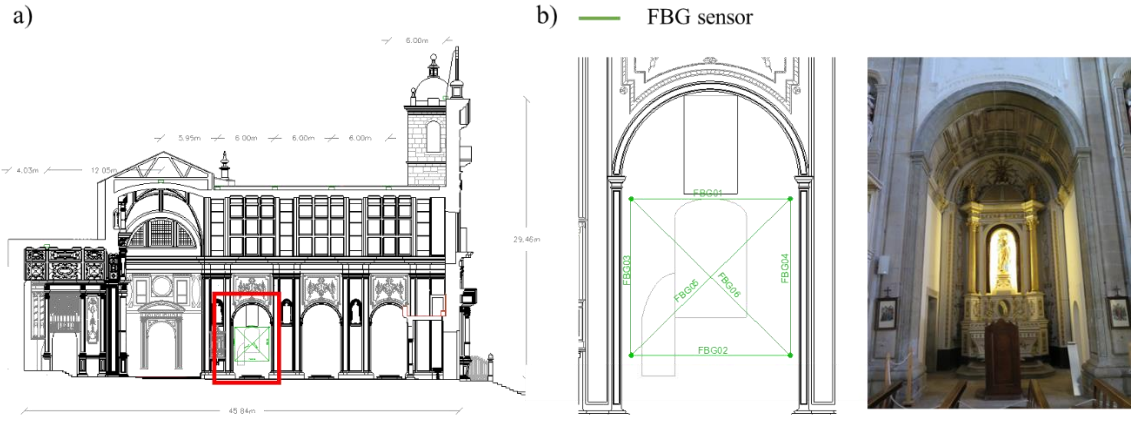

Figure 53. Optical system proposed for implementation in the São Lourenço Church: a) global longitudinal central section view of the church, b) detail of the FBG sensors' layout and São José Chapel.

Complementary, Figure 54 shows the 14 electric linear displacement sensors distribution along of the church, the positioning of 2 temperature sensors, 2 inclination sensors and 2 accelerometers. Take into account the damage scenarios discussed in the previous section, the sensors are mainly addressed to west and south zone of the church. On the chapels at the west side, relative displacements sensors for monitoring longitudinal and transversal movements, were considered, while in the chapels with less damage occurrence only its transversal displacements are monitored. In addition, as the damages found in the southwest zone of the church, specifically where Santíssimo Chapel is placed, indicates the existence of settlement movements, inclinometer sensors also were selected. Temperature in the interior of the church will be also monitored by a sensor placed at Altar-Mor and another one placed inside of the Santa Quitéria Chapel.

As the Santas Mães, Santa Quitéria and São José chapels present damages characterized by linear cracks along of the longitudinal and transversal section of the vaults chapels, the employment of two linear relative displacement sensors in each chapel for monitoring the movements into the cracks propagation direction can be justified. In another hand, three relative displacement sensors (one in each chapel) are proposed to be placed directed to measure the crack propagation/evolution along of the transversal section of the Santa Rita de Cassia, Nossa Senhora da Soledade and Nossa Senhora da Conceição Chapel. The

main cracks observed on these chapels propagate along of the longitudinal section of the chapels vaults, requesting the sensors to be longitudinally oriented.

As the Santíssimo Chapel presents an elevated number of cracks, and evidences of displacements out-of-plane, the employment of relative linear sensors aligned to transversal and longitudinal section of the chapel, combined with inclination sensors is proposed in this monitoring plan. Additionally, the employment of temperature sensors will be helpful to understand the effect of the temperature on structural displacements of the São Lourenço church.

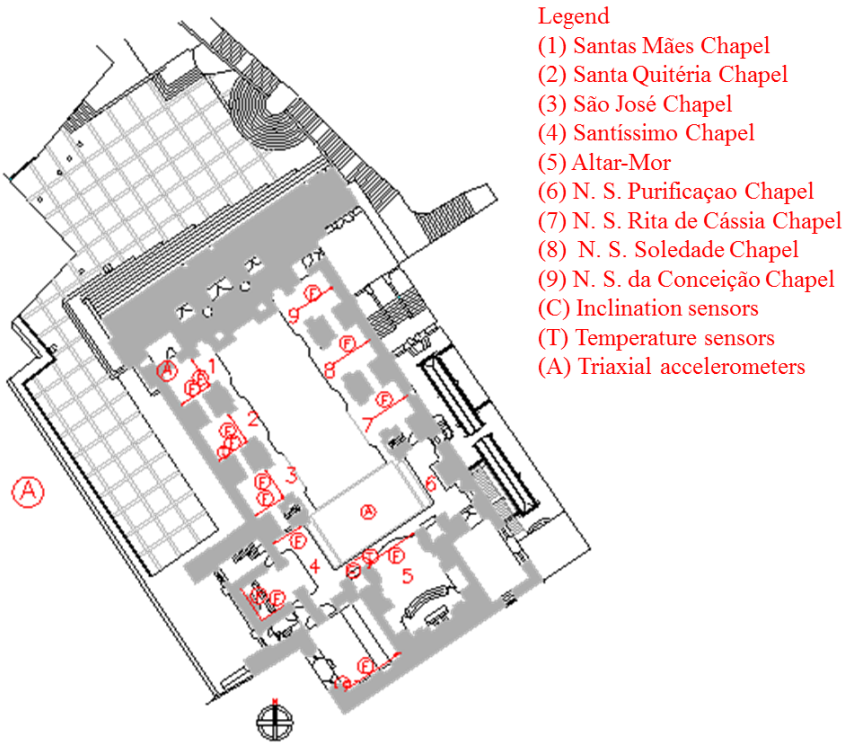

Figure 54. Distribution of the linear displacements, tilts, accelerations and temperatures sensors along of the São Lourenço Church.

One of the hypothesis on the damage mechanisms on the São Lourenço Church include the combined effect of the poor soil characteristics with vibration induced by road traffic. In order of to investigate the influence of the vibration induced by traffic at Ribeira Tunnel to structural behavior of the São Lourenço Church, 2 accelerometers were included in this proposal, the first one placed on the top of the Main façade, while the another one should be installed in the soil, as assigned by Figure 54. It is expected that the vibration measurement over the time allows the understanding on the effect of the road traffic on the damages emerged on the church. Moreover, a combined analysis of the temperature

and natural frequencies changes can be performed, for instance, and the dynamic properties of the church characterized under environmental influences.

The SHM system architecture (prepared for remote access) is presented in Figure 55, where the different components and their interaction are illustrated. The sensing system comprises three independent units, namely FBG sensing system, electric displacement and acceleration sensors, each one connect to a specific input module. The data acquisition system comprises the input modules linked to a Real-time controller with remote communication. This data acquisition system will communicate the collected data to a PC with internet access, by wireless connection, allowing the real-time access from the technical staff and owners. The architecture design of the SHM proposed is based on the previous experiences of the IC-FEUP team, where a most simplified and clean architecture communication of the system was prioritized.

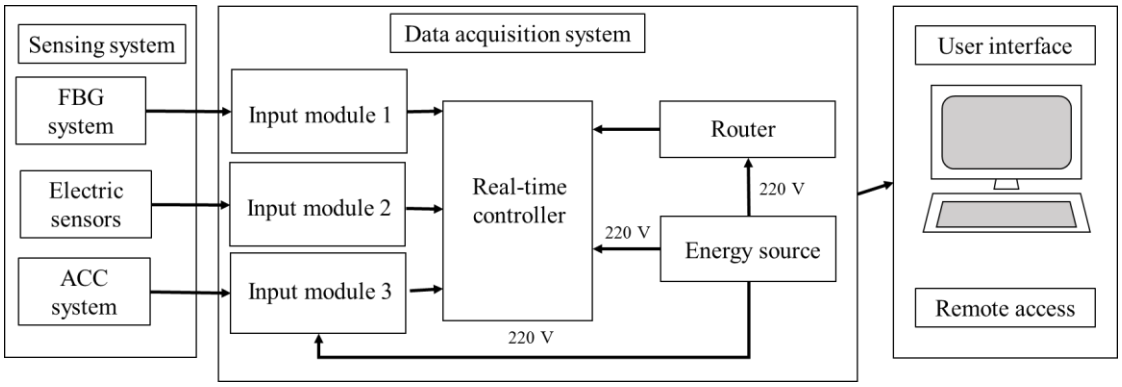

Figure 55. Detailing of the components of the SHM system for be implemented at São Lourenço Church.

The SHM proposed in this section can be classified as Level 4, according to system of classification presented in Chapter 2. Here the main goal of the SHM is to collect reliable data for the damage characterization, including the investigation on its progression and impact to the global behavior of the church. Furthermore, the strategies here presented and discussed can be used as support for further monitoring applications in other types of HC.

4.1.6. Final comments

Considering the relevant necessity on development of strategies for support heritage construction assessment, this chapter presented the procedures for a SHM system design, making use of a real case study, namely the São Lourenço Church, located at Porto, Portugal.

The presented procedure described a simplified work scheme, require unavoidable adaptations to each specific HC, yet providing important contribution for HC assessment, that can be used as tool for the intervention planning stage. The methodology was described concerning the early assessment stages for the SHM, namely, historical analysis, current damage state evaluation and SHM system design.

Concerning the SHM system proposal for the São Lourenço Church, the historic analysis and visual inspection allowed to obtain relevant information about the damage scenarios, while the thermography records allowed the clarification about the non-existence of humidity inside the church. The damage mapping was essential for understanding on damage mechanism, as well to identify the main affected zones.

The SHM proposal main aim was to characterize the cracks behavior, especially located in the chapels vaults, monitoring the inclination movements around Santíssimo Chapel, and to characterize the effect of the temperature on the stone masonry displacements, as well as to study the influence of the vibration induced by traffic, at the Ribeira Tunnel, on the structural behavior. For that, the SHM plan include 14 linear displacement sensors, 2 temperature sensors, 2 inclination sensors, 6 optical sensors based on FBGs and 2 accelerometers, connected to a data acquisition system with remote access.

Finally, the present work is deemed to provide a positive contribution to HC SHM field by describing procedures for designing and implementing optimized remote monitoring systems, and will likely yield reliable information to be used as support of structural risk management in heritage constructions.

4.2. Monitoring plan for Nossa Senhora das Dores Church

4.2.1. Introduction

Heritage constructions had become an interesting and challenge field for engineering advances due to high variability and complexity of its structural systems and the current necessity of to implement news techniques for non-destructive assessment opened to be integrate with structural monitoring systems. In this way, vibrational methods are one of the most employed techniques for non-destructive assessment reported in the literature [9, 48].

In fact, vibrational testing had been applied in different types of structures in order to collect data for dynamic characterization [93, 94, 158], especially due to possibility of to characterize globally the structures, and in the case of ambient vibration characterization because they allow the structural characterization without no excitation equipment [159]. The recent developments on sensors devices, data processing tools, and its application on buildings and infrastructures allowed overcoming several technical issues on this field [160–163], however cases involving vibration characterization of HC had been rarely reported in the literature, especially out of European zone [152].

Ambient vibration measurements were obtained and analyzed by [10] to characterize and monitor the Basilica di Santa Maria Collemaggio, in Italy. The partial collapse of the church after L'Aquila earthquake in 2009, increased the uncertainties on its structural behavior, motivating the necessity of characterization and monitoring of this historical construction from Italian Romanesque period. The church was instrumented with accelerometers and the data collected allowed the dynamic characterization of the church. The contributions of this work can be summarized in terms of the dynamic behavior identification of the church, as well by description of the strategies employed for the vibrational testing.

Essentially, the identification of the structural dynamic properties are an useful tool for safety analysis, making possible the investigation of damages influence on global behavior of structures, as previously demonstrated [10]. Moreover, this tool can also provide useful information to be used in support of structural risk reduction, as for instance in accordance with proceedings described in [5] and [4].

In [159], an ambient vibration testing was carried out in order to provide complementary information on the bell-tower of the Cathedral of Monza, Italy. This work presented a simplified methodology for the dynamic characterization based on data from Operational Modal Analysis (OMA), and the results allowed optimizing a 3D finite element model to be used in the support of the safety analysis of the tower under different loading conditions. The authors highlight that this approach seems a promising way of assess HC globally, especially to analyze the impact of hypothetic scenarios of damage to structural safety.

Optimized procedures for dynamic identification of heritage constructions are described in [9]. In this work, the authors provided reliable information for ambient vibration characterization of churches, towers and palaces, as for instance the general range of fundamental frequencies found experimentally, namely ranging from 2.5 Hz to 7 Hz, while the frequencies around 1.50 Hz are mostly related with domes and façades (see the complete survey in Figure 56). Furthermore, the authors highlight the existence of a lack of knowledge on structural behavior of heritage construction, demanding further efforts by technical-scientific community, to overpass this issue.

Beyond the current necessity of characterize the dynamic behavior of heritage constructions, the understanding of the environmental influence, namely the effect of the temperature and relative humidity on structural behavior is also needed. Fundamentally, the thermic cycles can affect the modal properties, as well as promote structural displacements. Founding how the temperature can influence these displacements is relevant to define if the damage mechanisms are related with real structural issues, and to state a correct understanding on the data collected by SHM system over the time, properly. A methodology for analysis of the effect of the temperature on dynamic properties can be found deeply discussed in [93] and [94]. Although these experimental studies are not addressed to HC, the implemented methodology can be used in HC cases. In addition, a study presented by [164] discuss briefly the effects of the temperature on historic structures.

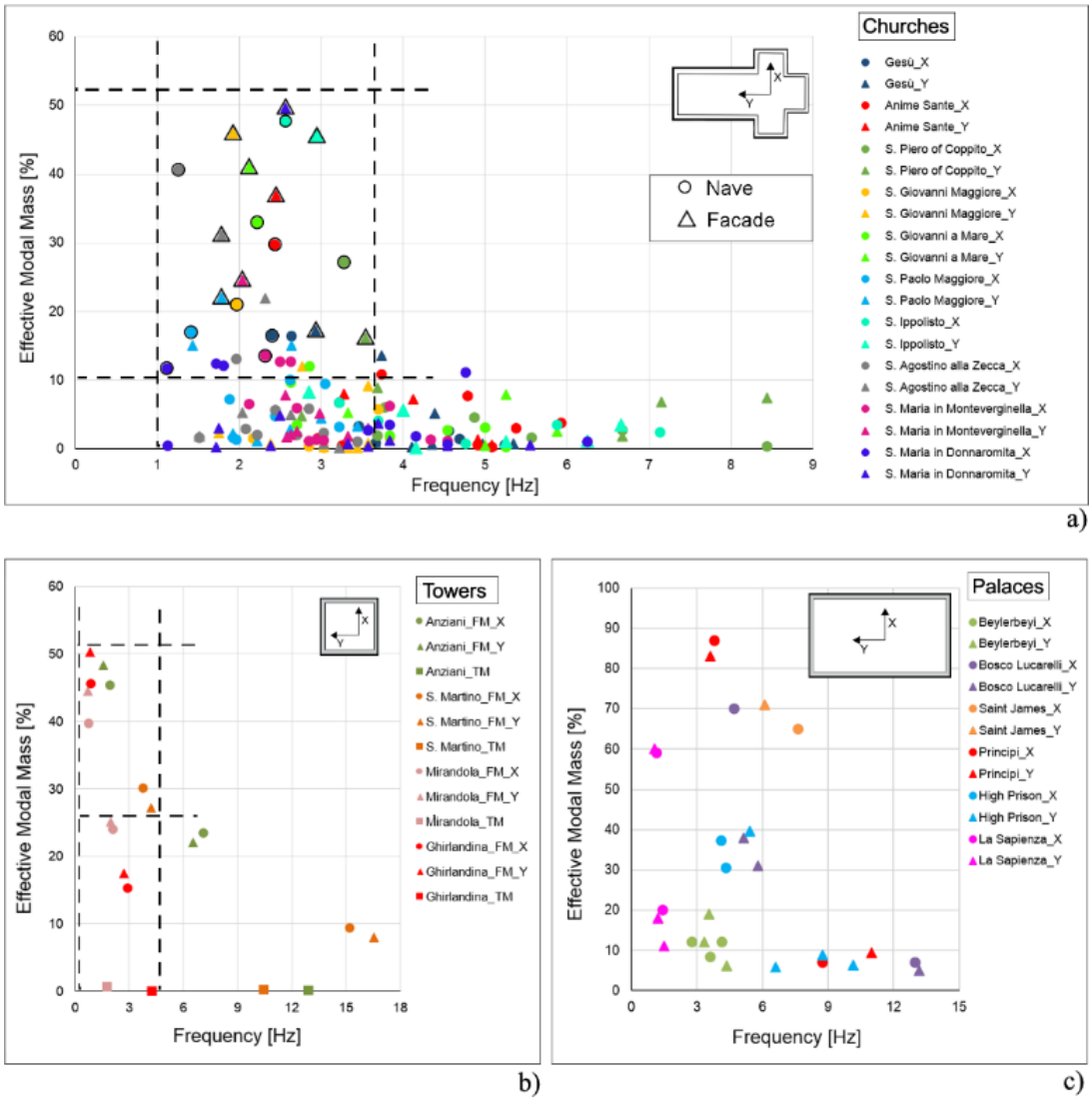

Figure 56. Relation between the effective modal mass and the natural frequencies of the main modal shapes of different structures geometry [9].

As an initial step to study the Brazilian ancient structures, the present chapter was developed with the main aim of identifying the dynamic properties of the Nossa Senhora das Dores Church, located in Sobral, Brazil, through a theoretical-experimental based strategy, and to present a monitoring proposal focused to study of the temperature on structural displacements. This way, in this chapter, an ambient vibration procedure was carried out to identify the natural frequencies of the Nossa Senhora das Dores Church (see Figure 57).

The ambient vibration procedure selected to this work includes the steps bellow mentioned. However, only the steps ii and iii were included in this chapter, because

further experimental tests will be carried out in order to collect reliable information on modal shapes for an adequate numerical model updating.

i. Finite Element Analysis (FEA);

ii. Ambient vibration testing;

iii. Operational modal analysis;

iv. Numerical model updating;

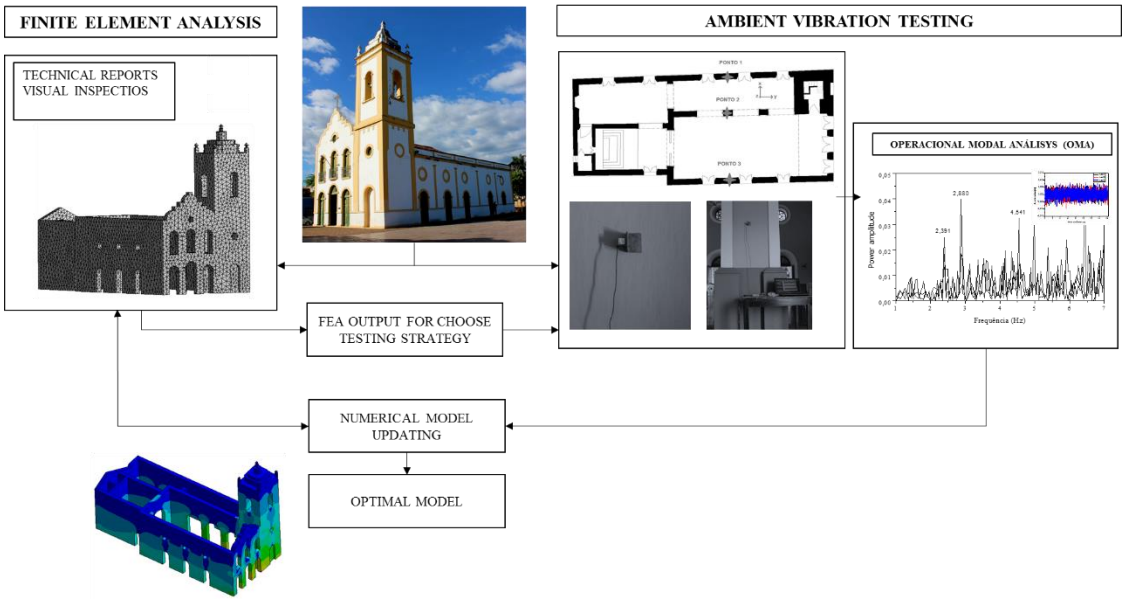

Figure 57. Ambient vibration procedure selected for Nossa Senhora das Dores Church characterization.

The selection of the present case study can be justified by necessity of development of studies on structural behavior of Brazilian heritage structures, especially on the influence of temperature changes to masonry displacements. Even the present chapter being limited to the design of a monitoring proposal, the strategies here discussed can be used to support furthers studies. Furthermore, no report was identified in the technical literature concerning ambient vibration characterization of Brazilians HC by OMA or related with SHM of Brazilian HC, making this work an important contribution for study and understanding of the structural behavior of Brazilian ancient structures.

4.2.2. The Nossa Senhora das Dores Church

The Nossa Senhora das Dores Church (Figure 59) is a clay brick historical structure, built on 1880s, placed at Sobral downtown, near of the Acaraú river. Sobral is located at north of Ceará State, in Brazil, 230 Km away from Fortaleza. The city was founded on XVII century, and presents one of the biggest historical centers of Brazil, with over around 1200 buildings classified since 2009 by *Instituto do Patrimônio Histórico e Artístico Nacional (IPHAN).* Since 2008, some seismic events had been registered at Sobral region, with a maximum event of 4.9 and the continuous monitoring had confirmed that its occurrence is getting more frequent (Figure 58). In the past, a seismic event with 5.1 degrees occurred in the Brazilian Northeast, namely at João Câmara city, damaging 4.000 buildings, highlight the necessity of maintenance and retrofitting measures.

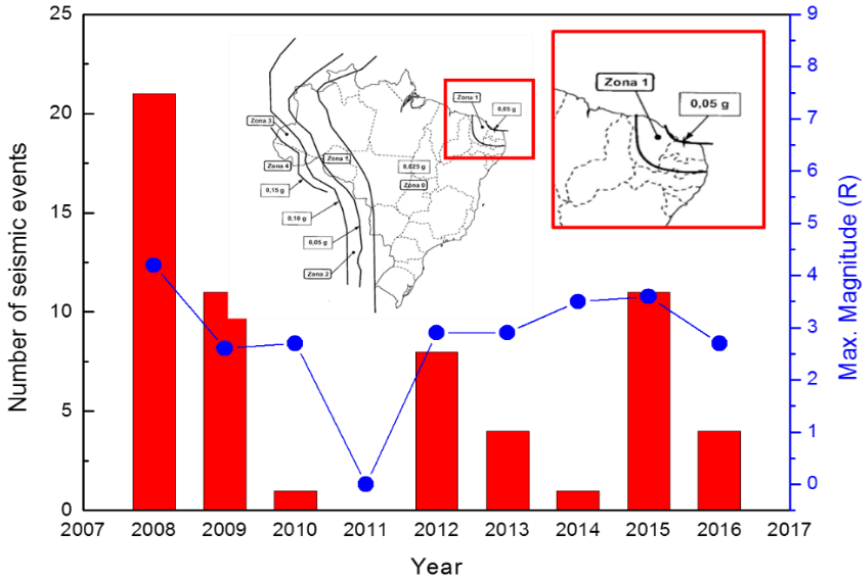

Figure 58. Distribution of the number of seismic occurrences at Ceará State since 2008 till 2016, and its respective maximum magnitudes.

The church façade presents two levels of doors, the first with three arched doors, and the second level with the arched windows aligned with the doors of the first level. The façade can be characterized as architectural neoclassic style, however the lateral bell-tower (Figure 59.b) does not follow the same architectural style, because its construction just was finished in 1924.

Figure 59. Nossa Senhora das Dores Church: a) main façade and b) lateral view of the church.

The Nossa Senhora das Dores church geometry is regular, with 26.17 m of length and 11.87 m of width, and a maximum high of 20.50 m (the tower), and it is divided in a Central Nave separated from a Lateral Nave by two columns and three arches, the Coro-Alto, the lateral bell-tower, the Altar-Mor and an office (in the end of the building). Figure 60 shows a schematic view of the Nossa Senhora das Dores Church geometry, while Figure 61 presents details of the interior of the church.

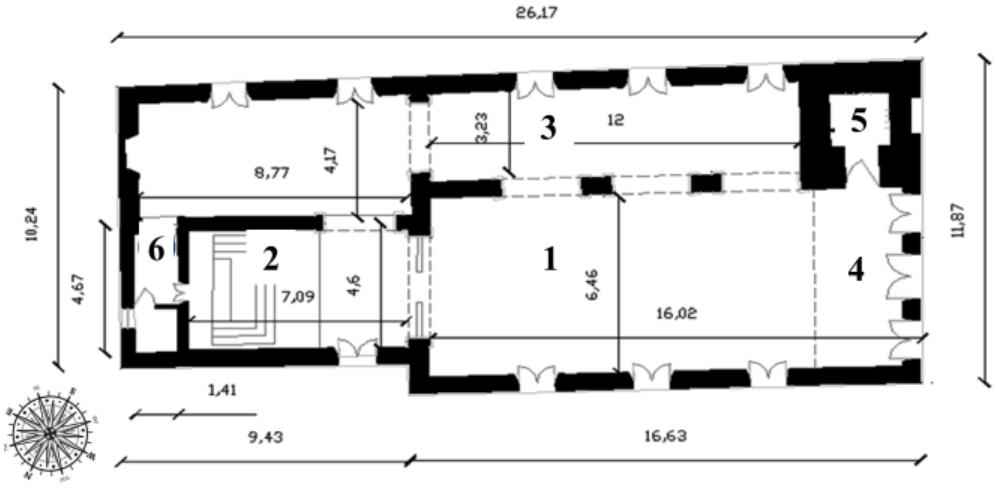

Figure 60. Schematic cut of the Nossa Senhora das Dores Church geometry, where 1 is the Central Nave, 2 is the Altar-Mor, 3 is the lateral Nave, 4- is the Coro-Alto, 5 is the bell-tower and 6 is the office.

Figure 61. Interior of the Nossa Senhora do Rosário Church: a) Altar-Mor, b) Central Nave and Coro Alto, c) columns and arches and d) lateral Nave.

A visual inspection carried out, on the Nossa Senhora das Dores Church, allowed the identification of the main damages present on the façades and to build a damage map, showed in Figure 62.

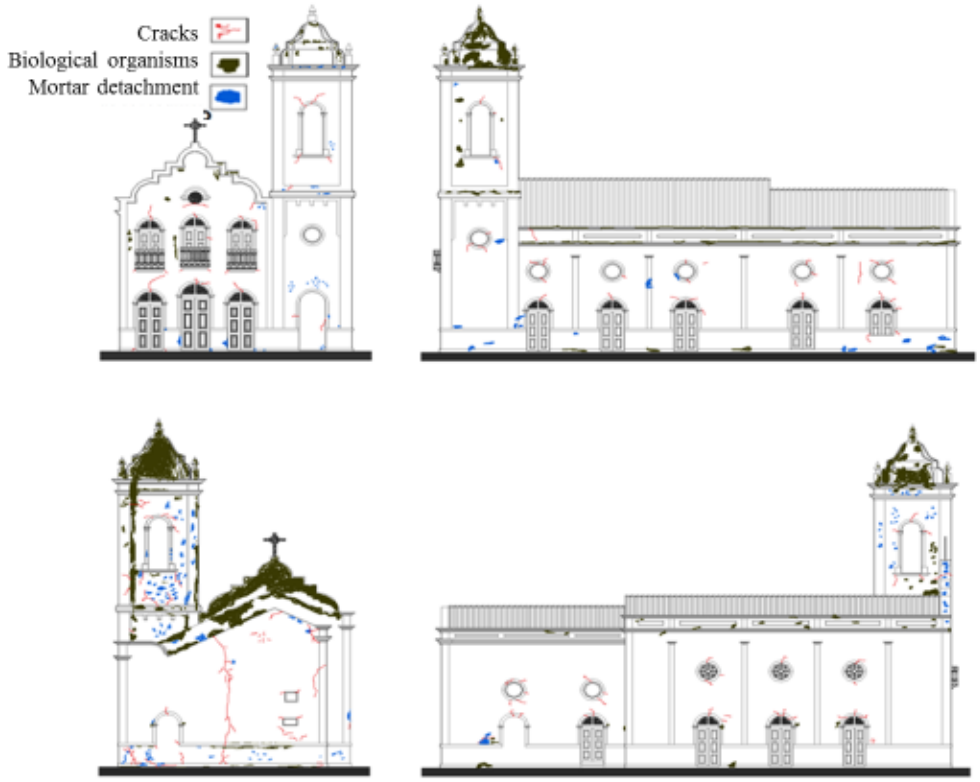

Figure 62. Damage mapping of Nossa Senhora das Dores Church.

Firstly, the damages will be not considered in the FEA, however the damage mapping will be used as support for interpretation of the numerical model results. The main damages identified on the church are cracks (surrounding the opened areas), biological attacks and mortar detachment. In general, these damages are related with material decaying, and does not present risk to structural safety of the church. Figure 63 illustrates the type of damages found on the church.

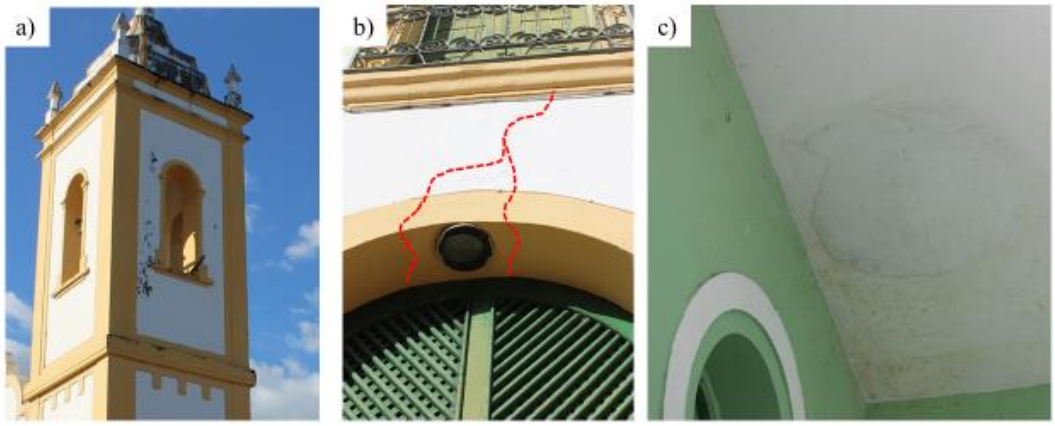

Figure 63. Examples of the damages found during the inspection on Nossa Senhora das Dores Church: a) degradation by biological action, b) cracks in the arches and c) humidity presence in the roof slab.

4.2.3. Experimental setup and natural frequencies identification

The experimental testing was carried out according to experimental setup shown in Figure 64 in April 28th 2016. The accelerometers positioning was defined based on previous numerical results through FEA, where the initial configurations of the modal shapes of the church were obtained. For data collecting, a triaxial accelerometer (Summit, model 34201A), with a frequency working range higher than 100 Hz, controlled through a LabView® software developed by Institute of Telecommunications and the Physics Department of the Aveiro University, was used. The accelerometers were placed at a high of 2.00 m from the footing of the church, and details of the sensors positioning and data collecting can be observed in Figure 64.

Acceleration in 3 directions were recorded during 600 seconds in each measuring point as assigned by Figure 64. The X direction was considered as out-of-plane of the walls (transversal direction), and Y direction was stated as in the plane of the walls (longitudinal direction), while Z was considered as vertical direction.

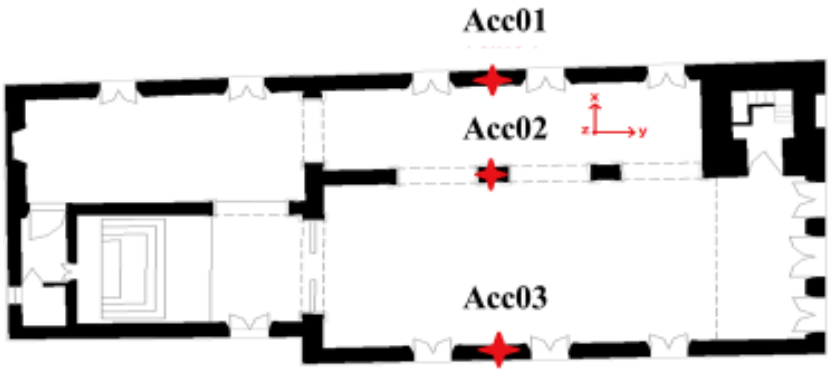

Figure 64. Accelerometers positioning and data collecting.

For OMA, the accelerations registered in the X and Y direction (Figure 65) were processed by Fast Fourier Transform (FFT), with recurrence to commercial software *SeismoSignal*®. For that 16384 points were used, once the FFT function requested samples in the form 2^x, in this case 2^{14}, with a time interval of 0.001 s.

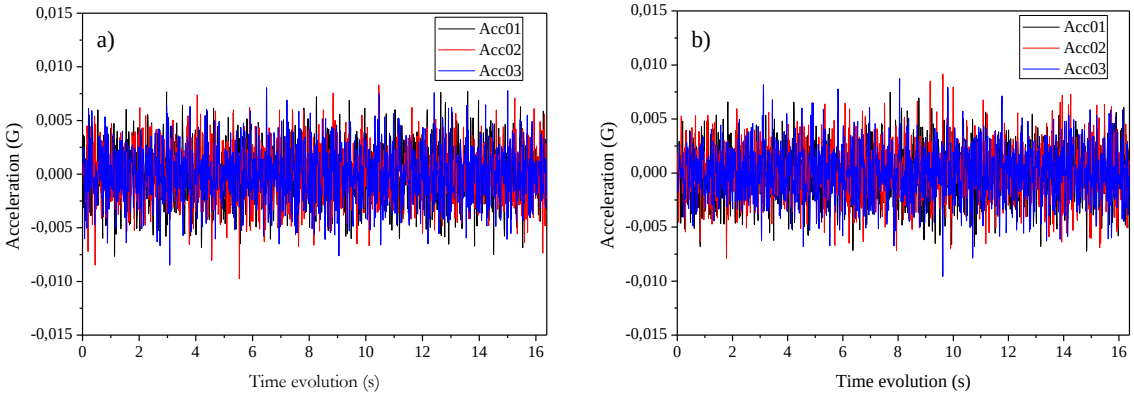

Figure 65. Firsts 16s of the acceleration registered on Nossa Senhora das Dores Church: a) acceleration collected in X direction and b) acceleration collected in Y direction.

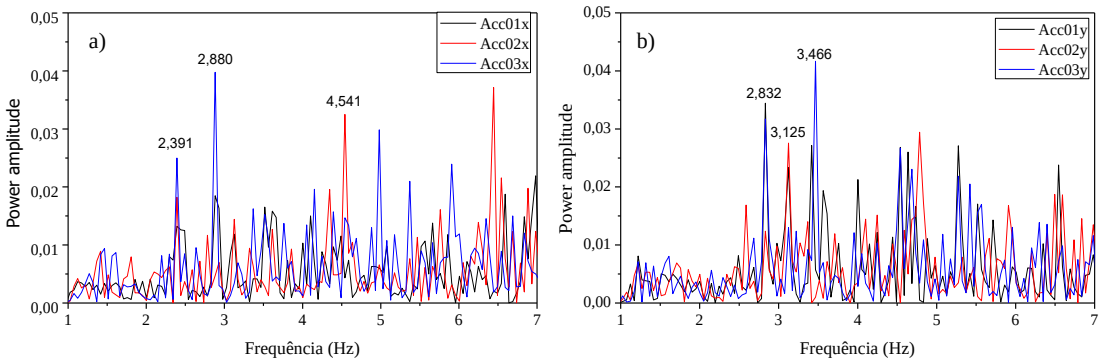

Figure 66. Frequencies spectra obtained, thought the FFT, by OMA of the Nossa Senhora das Dores Church.

The data collecting in the vertical direction (Z) was not considered in the OMA, once based on the preliminary analysis, and as expected, of the signal amplitudes demonstrates that in the vertical direction the church does not present significant values in comparison with signal amplitudes observed in X and Y direction, moreover, the FEA demonstrates that in Y direction the effective modal mass is not expressive. Following, from FEA it was expected to find natural frequencies with values higher than 1.50 Hz, allowing filtering the signal with a *Bandpass* filter, ranging from 1.00 Hz to 30.00 Hz. Furthermore, the amplitude of the frequencies (of the unfiltered signal) between 0 and 1.00 Hz was neglectable, making adequate the employment of the filter on the specified frequency range.

From acceleration recorded, the FFT data processing allowed to plot the frequencies spectra, as can be seen in Figure 66, and the natural frequencies in X and Y were identified through well-known, and simple, Peak Picking method. The fundamental frequencies identified are presented in Table 4.

Table 4. Natural frequencies identified through ambient vibration testing of the Nossa Senhora das Dores Church.

Mode	Frequency (Hz)	Mode type
1	2.391	Transversal bending (X direction)
2	2.880	Possible Torsional mode (X and Y direction)
3	3.125	Longitudinal bending (Y direction)
4	3.466	Longitudinal bending (Y direction)
5	4.541	Transversal bending (X direction)

Analyzing the spectrum of frequencies presented in Figure 66, it can be noticed that the first five frequencies identified by OMA are between 2.00 Hz and 5.00 Hz. The first natural frequency was identified as 2.391 Hz, in transversal mode (X direction), while the second natural frequency was identified in both directions, being admitted as 2.880 Hz, in a possible torsion configuration. The third and fourth frequencies, respectively 3.125 Hz and 3.466 Hz were observed in Y direction, characterized by a longitudinal mode, while the fifth fundamental frequency was characterized as 4.541 Hz, in a transversal mode.

4.2.4. Optimized SHM proposal

The present section is dedicated to description of a SHM proposal for Nossa Senhora das Dores Church. The sensorial system optimization was performed based on recommendations proposed by [9], also considering the principles of ICOMOS letter [165]. The present SHM proposal can be considered optimized because the sensorial system was designed after taking into account the main damages identified during the visual inspection and also presented in the map form (see Figure 62), and the sensors positioning based on the recommendation proposed by [9] aiming the use of the lower number of sensors possible, with the guarantee that reliable data will be collected in order to characterize the global behavior of the church along time. In the total, the proposal includes 8 triaxial accelerometers, 3 linear displacement sensors, 2 temperature sensors and 6 linear displacement optical sensor.

Acceleration acquisitions allow the global characterization of the dynamic structural behavior. Therefore, Figure 67 shows in detailed form where the triaxial accelerometers should be positioned. Namely, 3 accelerometers will be dedicated to the main façade monitoring, while 1 accelerometer was directed to the tower monitoring, and the other 4 should be addressed to the central Nave and Altar-Mor monitoring. The accelerometers ACC01, ACC05 and ACC07, as well ACC04 and ACC06 should be aligned in the same Y axes, at its respective X coordinates. ACC02 and ACC04 should present the same values (in meters) at Z coordinates, while ACC03 will be placed centralized in the top of the main façade. ACC01 should be positioned in the top of the tower.

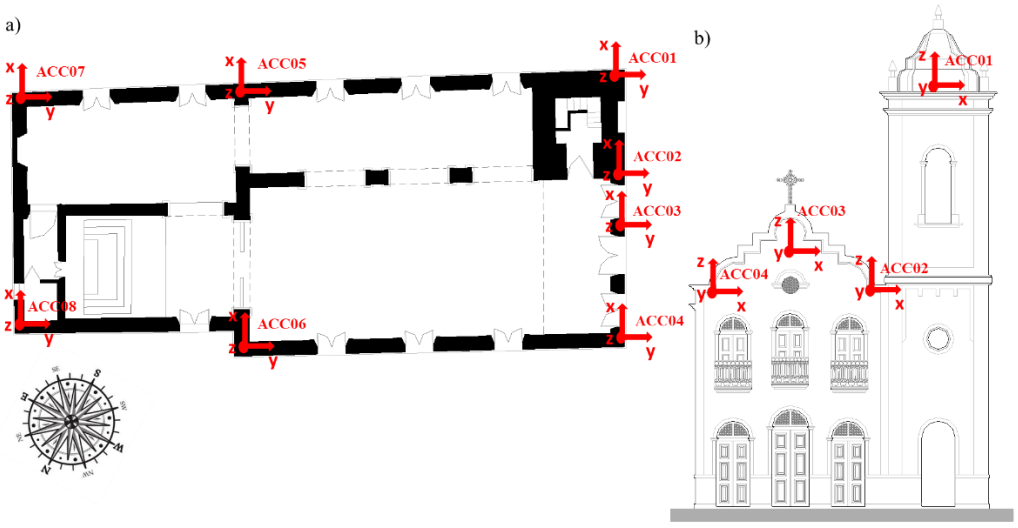

Figure 67. Scheme of accelerometers positioning.

Two linear displacement sensors should be positioned on the internal face of the main façade, as shown by Figure 68, particularly in the Det. A, where the first one should be dedicated to measure relative displacements along the X direction, and the another one should be addressed to measure relive displacements at the Y direction. The main goal of these sensors positioning is to collect data on the façade movements at Y and X direction, and. Temperature data, from internal and external monitoring (T1 and T2, respectively), to characterize the influence of the temperature on the structural displacements should also be included (see details of the temperature sensors in Figure 68, where sensor T1 should be placed in the top of the first column, while T2 sensor is directed to record external temperature, from the top of the tower). Additionally, another linear displacement sensor should be installed at the internal face of the northeast façade, as presented in Figure 68 (Det. B). This sensor aims monitoring the displacements of the most damaged area of the church.

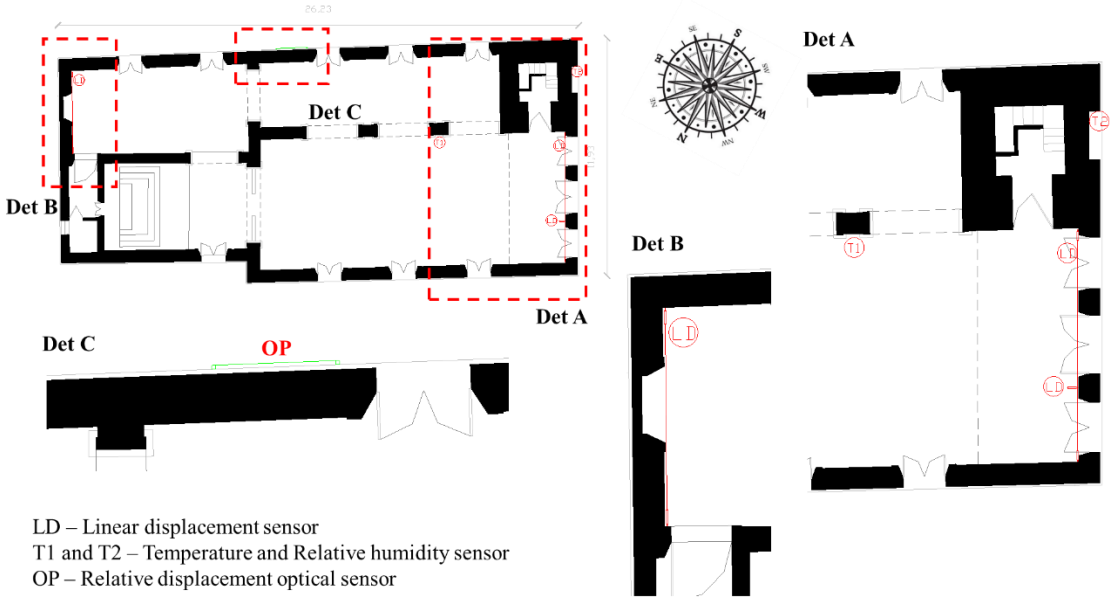

Figure 68. SHM proposal: linear displacement sensors positioning.

Figure 68 also presents, in Det C, the area dedicated to installation of the optical sensorial system. However, Figure 69 provides a most detailed view of the linear displacement optical sensors positioning, following the same setup proposed in [157]. The 6 optical sensors proposed in this monitoring plan, comprises relative displacement optical fiber sensors based on FBGs, with FBG temperature sensors written multiplexed in each one of the optical fibers. By the experimental setup here proposed, 4 optical sensors are addressed to monitoring linear displacements at the vertical and horizontal directions, while 2 sensors are dedicated for the characterization of the linear displacements at diagonal direction. As already discussed at Chapter 3, optical sensors can be used for

relative displacement monitoring, especially when a micrometer level is requested. The main goal of this experimental proposal is to characterize the in-plan relative displacements, as well the environmental effects on structural movements of Nossa Senhora das Dores Church.

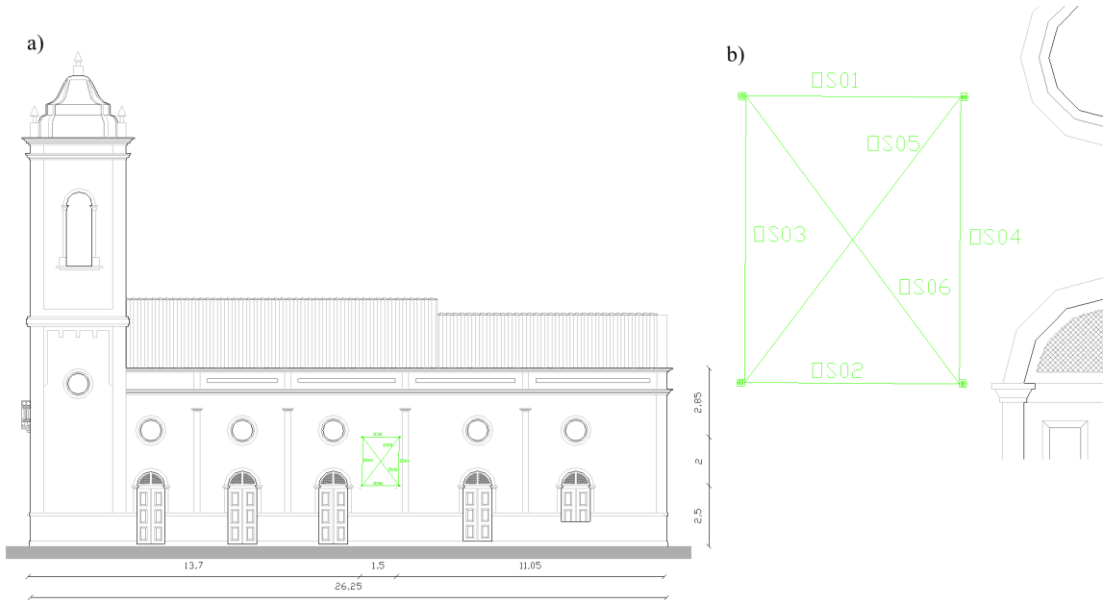

Figure 69. Scheme of the optical sensors placement: a) general view of the optical sensors positioning on the Southeast façade and b) detail of the sensors.

Indeed, the optimization of a SHM system needs to consider the integration between all the devices employed and the way how they communicate between them. This way, Figure 70 presents the architecture communication setup of the SHM system proposal.

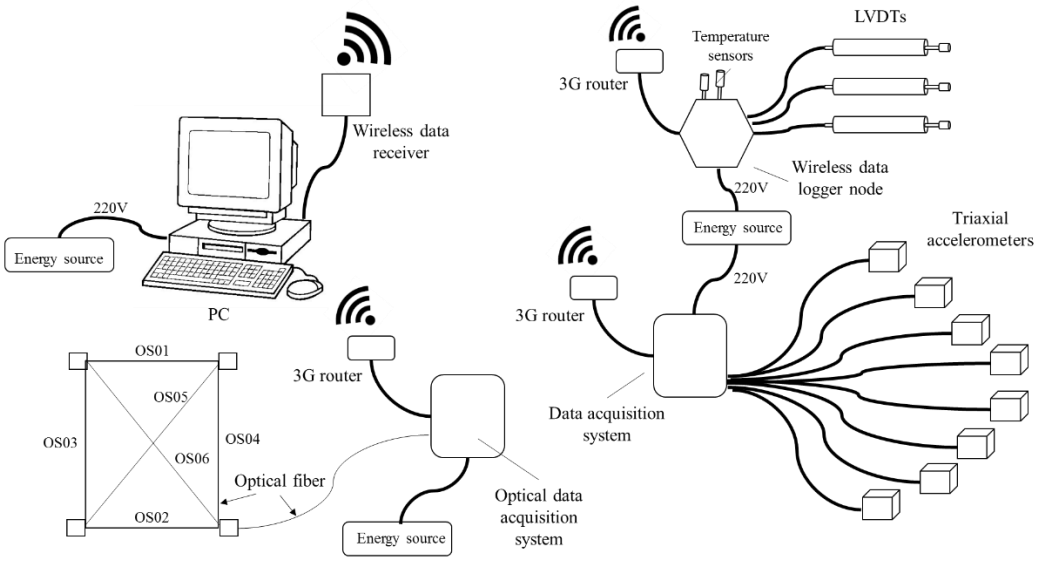

Figure 70. General scheme of the SHM proposal for Nossa Senhora das Dores Church.

The proposed SHM system is composed by 3 wireless data logger's nodes (the first one dedicated to LVDTs, temperature and relative humidity data transmission, while the second and the third can be devoted to accelerometer data transmission, and to optical signal transmission, respectively), 1 wireless data receiver, 1 computer (PC), and a 3G router. Basically, the sensors need to be connected to the data logger nodes, main responsible by signal acquisition and transmission till the data receiver node, connected to the PC, where the storage, management, processing and data display should be done.

4.2.5. Final comments

In this work, the ambient vibration testing of the Nossa Senhora das Dores Church, an important heritage construction for Sobral community, was carried out as way to collect information on its structural properties, as well as its employment in further studies to assess the church degradation over the time.

The experimental dynamic investigation of the Nossa Senhora das Dores Church was performed with OMA, and the strategies employed during the ambient vibration characterization were described, analyzed and the results of the natural frequencies identified were shown. The OMA procedure allowed the identification of the first five fundamental frequencies of the church, that are 2.391 Hz, 2.880 Hz, 3.125 Hz, 3.466 Hz and 4.541 Hz, and to characterize its respective modes.

The SHM proposal provides an optimized monitoring plan focused to structural displacements monitoring, as well as on the analysis of the environment effect on these movements. Additionally, the dynamic monitoring included in the proposal can provide reliable data on global behavior of the Nossa Senhora das Dores Church, and can be useful for the analysis of the structural vulnerability along the time, while the employment of wireless sensor network allow the time assessment optimization, and the real time remote data access.

Finally, the present work contributes for the knowledge onthe structural behavior of Brazilian heritage constructions, through the description of the strategies employed and by the dynamic information collected. The information provided by this study also can be useful for implementing a monitoring system focused to characterize the environmental influence on structural behavior of the church.

5

Long-term monitoring of the Foz Côa Church

Summary

Recent advances on sensing and data communication systems have allowed the optimization of the structural health monitoring systems, as well their employment for long-distance remote monitoring of civil structures. Moreover, structural health monitoring techniques can be particularly interesting for heritage constructions assessment, because they allow a real-time analysis of the structural properties, and the data collected can be used as support of safety maintenance. This work describes the strategies employed for structural health monitoring of a damaged historic structure from the XVI century, namely the Foz Côa Church (Portugal), as well as the results of 1-year monitoring of the displacements observed on the structural elements of the church. Additionally, the influence of the temperature and relative humidity were studied. Removing the environmental influences from the displacements observed in the structural elements allowed to conclude that these are not motived by the damage progression, instead they are related with environmental parameters influence.

Keywords: Long-term monitoring, structural health monitoring, wireless sensor network, heritage construction, environmental effects.

5.1. Introduction

Recent advances on the field of sensorial systems and wireless communications, as well their implementation cost reduction, have contributed significantly to dissemination and employment of structural health monitoring (SHM) in support of the structural characterization and safety assessment [56, 166]. In fact, sensing systems with embedded microprocessors and wireless communication represent a deep change on the way that structures are assessed, monitored and controlled [163], taking into account that these techniques allow the remote access, in real time, to the parameters monitored. In the last two decades, a considerable high number of cases of SHM employment on different typologies civil structures (i.e. bridges, towers and buildings) were described in the literature [44, 155], overcoming several technical issues, while few cases of SHM of heritage constructions (HC) have been reported [167].

In fact, historical structures constitute an interesting challenge for development of SHM due to variability and complexity of its structural components, which demands for advances in the monitoring strategies, as well in the data processing approaches. Additionally, for an assertive and reliable assessment of the HC, the data offered by SHM, that generally are focused in specifics components of the constructions, need to be discussed with information on the current state and global behavior of the structure under service operation. Moreover, it is important to highlight that all strategies employed for characterization and assessment should be conducted with respect to historic value of the construction and without provoking new damage emergence, as stated by [165]. In order to present recent developments on the SHM field, related with HC, some cases reported in the literature will be summarized and discussed following.

In [149], the Torre Aquila, a medieval tower with valuable artworks, was instrumented with accelerometers, relative displacements, as temperature and relative humidity sensors. The sensors were connected to the data acquisition system that send the collected information for a remote platform through wireless communication. Basically, the SHM was focused on to provide information on the vibration and displacements of the tower, as well of the environmental effects on the measurements. The work also demonstrates

how the collected information can be used to predict anomalous situations of the tower behavior under service.

According to [168], the walls inclination of a historic wooden church undergoing rehabilitation was monitored through a simplified wireless sensor network, and even with the low sensitivity of the sensorial modes, they were able of identify long-term trends in the tilt of the church walls. In [15], a sensorial system composed by 19 fiber optical displacement sensors and 5 temperature sensors were employed for monitoring of the damages on Santa Casa de Misericordia de Aveiro, and the data collected was used for updating a finite element model for to assess the damage state of the church.

Following, the long-term dynamic monitoring of the Basilica S. Maria di Collemaggio was reported by [10], where the authors describe the strategies of sensor network design and data processing, focused on seismic assessment. The SHM was focused on the management of the structural safety for situations where the structure can be subjected to natural disasters, such as earthquakes. The dynamic characterization of the church was carried-out, and the data was used in computational simulations. Furthermore, the data acquisition systems were composed by accelerometers connected wirelessly to a signal processing station. The results allowed the clear detection of the interaction between the masonry structures with an existing protective installation, and the modal information identified from different excitation sources (i.e. release tests, seismic events, etc.) was used for updating a finite element model on the church. Further reading on this case study can be found in [11] and [169].

Even that dynamic monitoring of HC constitutes a relevant topic for safety assessment [9], [93], studies establishing a link between the environmental effect with structural behavior are also particularly interesting because they can provide useful information for understand cyclic displacements behavior in stony masonry elements and its damage mechanisms. According to [164], in heterogeneous materials, as stone masonry with low tensile strength, the actuation of small tensions can easily make emerge cracks, mostly first appearing on the connection zones. Even thermal effects can produce sufficient tension to produce a crack, due to the different thermic behavior of the stone and the mortar. Moreover, in historic structures several thermal cyclic over time can provoke plasticization of the structural components, cracks emergence and its progression.

This way, the present work contributes for the SHM implementation through the strategy description and monitoring of the Foz Côa Church (Portugal). Moreover, this work reports the monitoring period between March 13th 2015 to March 29th 2016 and discuss the relative displacements and tilt records in some structural elements of the church, as well analyses the environmental influence on the displacements collected by the wireless sensor network. Additionally, the SHM system implemented in this work can be classified as Level 4, according to classification proposed in this work, namely because the main goal of the system was to collect reliable information for characterize the structural behavior.

5.2. The Vila Nova de Foz Côa Church

The Foz Côa Church (Figure 71) is a stone masonry building from XVI century, located at Vila Nova de Foz Côa, 390 km North from Lisbon, Portugal. The Church presents a *Manuelino* architectural style, with regular geometry, composed by three naves separated between them by columns and arches, as shown in Figure 75. It´s dimensions are 37.00 m of length and 16.00 m of width, with a maximum height at the main façade of 13.30 m.

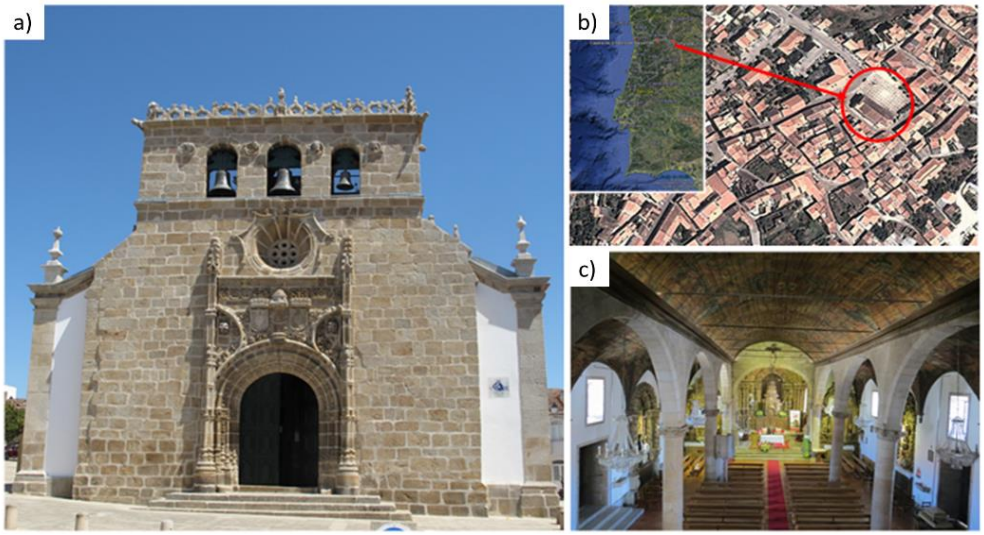

Figure 71. Foz Côa Church: a) main façade, b) geographic location, and c) interior view of the Foz Côa Church.

The main façade is characterized by an exposed granitic stone masonry (Figure 71.a) where the arch on the main door is decorated with *Manuelino* marks, and three bells on

the top. At the interior of the church, two plans of columns and arch does the division between the main nave with the left and right naves. Figure 71.b shows the interior view of the Church.

The church presents some damages, essentially cracks and deformation along the structural elements. The walls and columns on the right side are significantly deformed, especially the columns, as can be observed in the details on Figure 72, as well as some vertical cracks on the main façade, as demonstrated in Figure 73. Fundamentally, the main hypothesis here is that the deformations and cracks are related with two seismic occurrences, namely the earthquakes of 1755 and 1969, being the first one related with the deformation of the structural elements inside of the church, specifically on columns and arches, while the last seismic occurrence has been pointed as the responsible by the emergence of cracks in the main façade (Figure 73).

Figure 72. Photograph of column 2, evidencing its inclination.

Over the years, several inspections and interventions were carried out in order to minimize the damage progression, such as the one performed in the 1970s, characterized essentially through bracing of the columns on the right and left naves (Figure 74.a and b) and main arch (Figure 74.c). Additionally, an inspection on the foundations elements was carried out (Figure 74.d) in order of to investigate the soil properties and its influence on damages progression, however the experimental investigation concluded that the soil

presented good characteristics without settlement risk. The retrofitting process included the arches and columns stabilization through the construction of a pre-stressed concrete slab, shown in Figure 74.e.

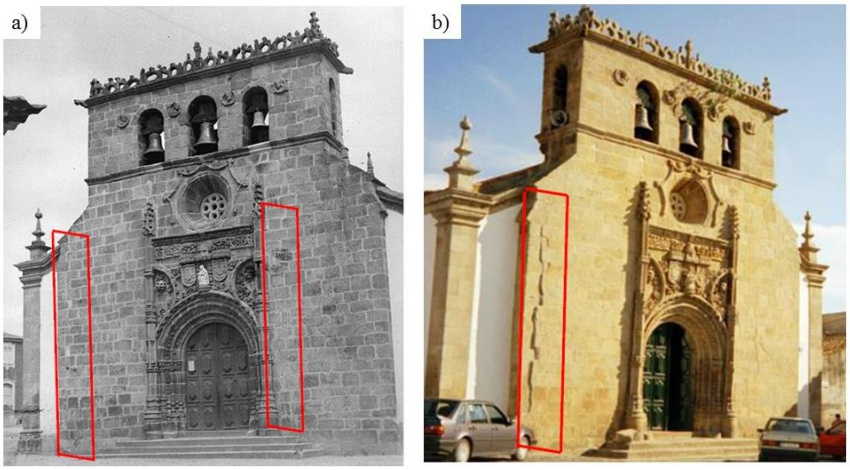

Figure 73. Main façade of the Foz Côa's Church in 1960, undamaged (a), and b) in 1996 with damages [170].

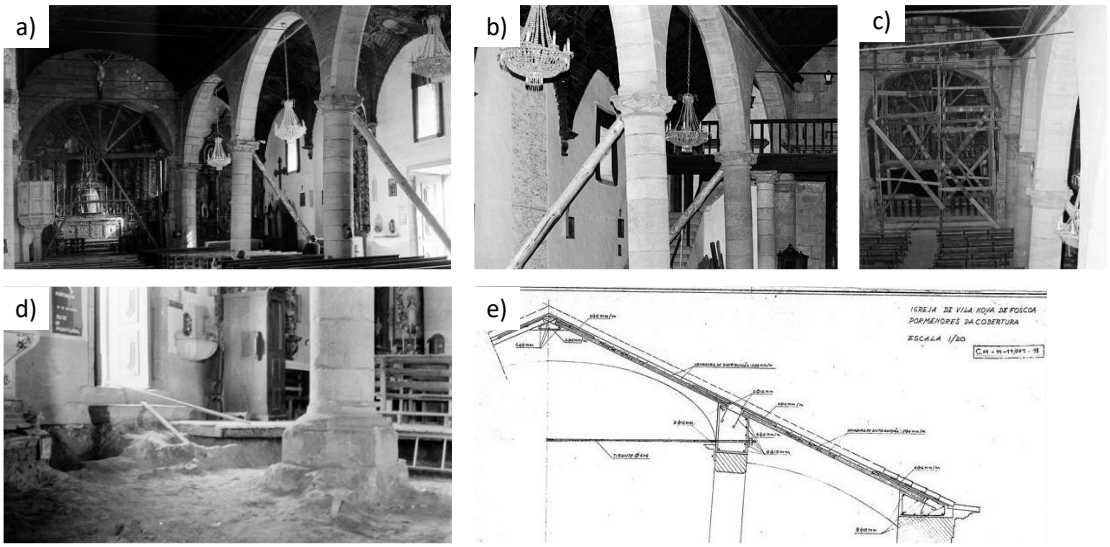

Figure 74. Main interventions carried out on Foz Côa Church in the 1970s: a) bracing of the Main Arch and columns, b) details of the columns bracing and c) details of the main arch bracing; d) inspection performed on foundations elements and e) detail of project of the reinforced concrete roof slab built[170].

Nonetheless, even a retrofitted construction need to be periodically assessed, as way to identify the damage progression mechanisms and to avoid dramatic situations. Therefore, for continuous assessment, in order to identify early stage structural movements, a SHM system was installed at the Foz Côa Church, mainly focused on the columns and arches

of the lateral right, as well on the main façade. The column 2 (Figure 72) was assigned as the region with higher deformations, and hence densely instrumented.

5.3. Real-time monitoring system implemented at Foz Côa Church

For the long term-monitoring of the Foz Côa Church, eight sensors were used in the total, mainly focused on displacements monitoring of the column 2 and main façade, as shown in Figure 75. From those, two temperature sensors, one of them designated as T2, was placed on the top of the main façade while the other one, so-called T1, was positioned on the top of the column 2, close of a relative humidity sensor. An inclination sensor, C1A, was also installed on the top of the same column, while a displacement potentiometer sensor, designated as P1, was placed on the bottom of the same column. Two electric linear displacement sensors, namely F7 and F8, were placed along the internal wall, on the main façade, while another one, assigned as F4, was installed near the T2 temperature sensor, at the top of the façade.

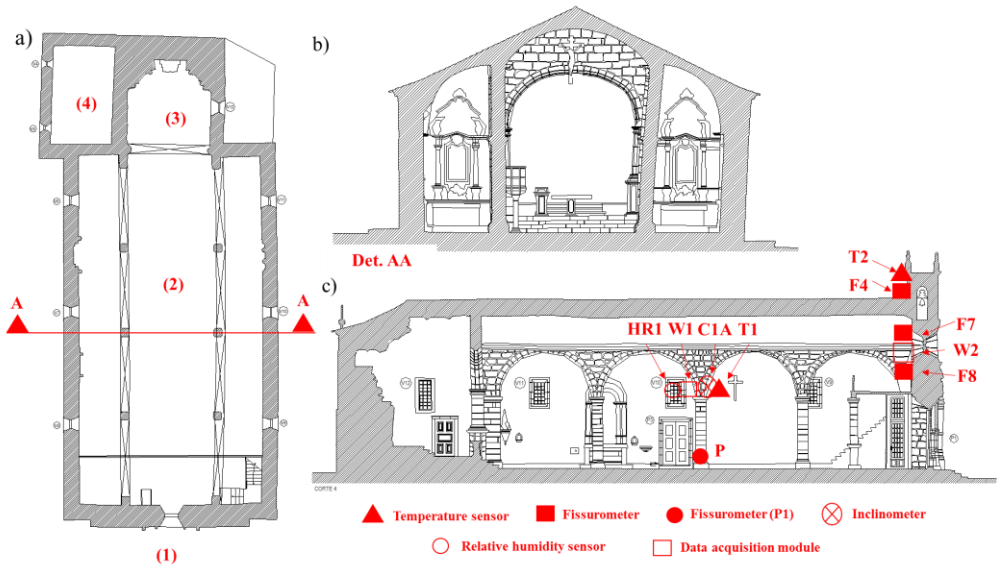

Figure 75. Geometric view of the Foz Côa Church (a) where 1- is the main façade, 2- is the Central Nave, 3- is the Altar-Mor and 4- is an office; the transversal view of the detail AA is presented in (b) and the sensors positioning are shown by (c).

The data acquisition system (W1 and W2) was composed by two HOBO® wireless data logger's node, namely Zw-007 and Zw-006, 1 HOBO® wireless data receive, ZW-RCVR, a 3D router and a desktop computer. An illustrative scheme of the complete SHM system is presented in Figure 76.

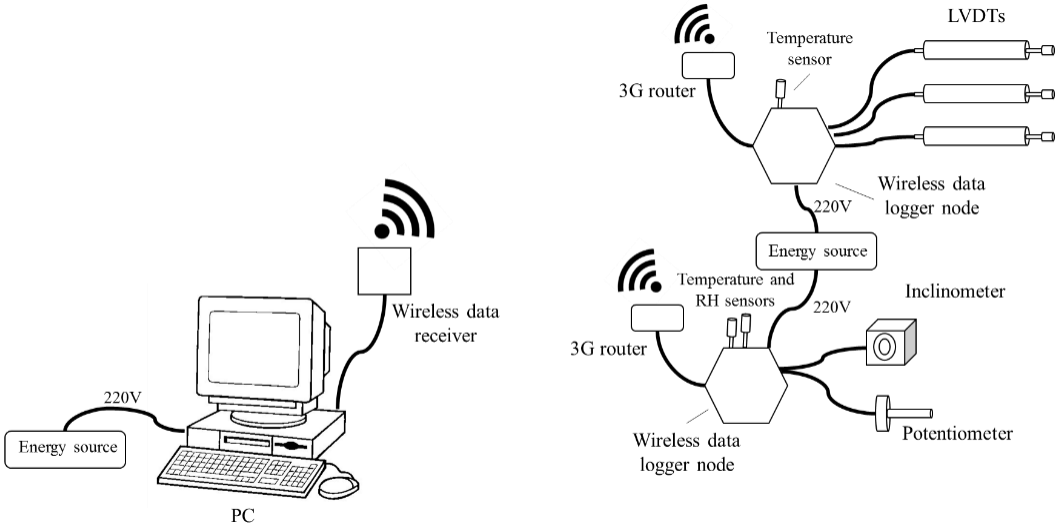

Figure 76. Setup of the SHM system implemented at Foz Côa Church.

All the sensors were connected to the data logger's node, assigned as W1 and W2 in the Figure 75, that provide the data transmission to a data receiver node, connected to a computer, placed at LESE/FEUP, that also allows changing the nodes configuration, the sample rate, transmission node rate, measuring range of the input signals and sensors scaling, for instance, and also can be used for alarm creation with warmings through email, and the data transmission through email and FTP protocol to a remote server. The complete scheme of the sensors distribution along of the Foz Côa Church can be seen in Figure 75.c.

Figure 77 shows in detail the displacement parameters monitored on column 2, one of the most damaged elements inside of the Foz Côa Church. The C1A sensor was positioned to collect displacements concerning inclination along column 2, where the positive values indicate displacement of the column 2 to the interior side of the right lateral Nave, while the negatives values evidence the column 2 inclination in the direction of the Central Nave. Additionally, the P1 sensor was positioned in order to measure the relative vertical displacements on the bottom of the column 2, where the positive values recorded indicate movements in the down direction while the negative values indicate movements in the opposite direction. In other words, the positive values of displacements recorded in the basis of the column 2 can be understood as compression movements, while the negative values can be interpreted as tension.

Concerning the sensors F7 and F8 positioned aligned with the façade stone walls (from interior side of the church), as shown by Figure 78, they measure relative displacements at transversal and longitudinal direction of the façade, respectively. The positive and negative directions indicate movements out-of-plane, where positive displacements can be understood as movements to exterior of the church and the negative displacements indicate that the movements are occurring to the interior of the church. The F4 sensor was placed on the top of the main façade, inside the bell-tower, in order to measure the relative displacements along the transversal direction of the church, as shown in Figure 79, where the positive values correspond to movements to the left while the negative values correspond to movements to the right.

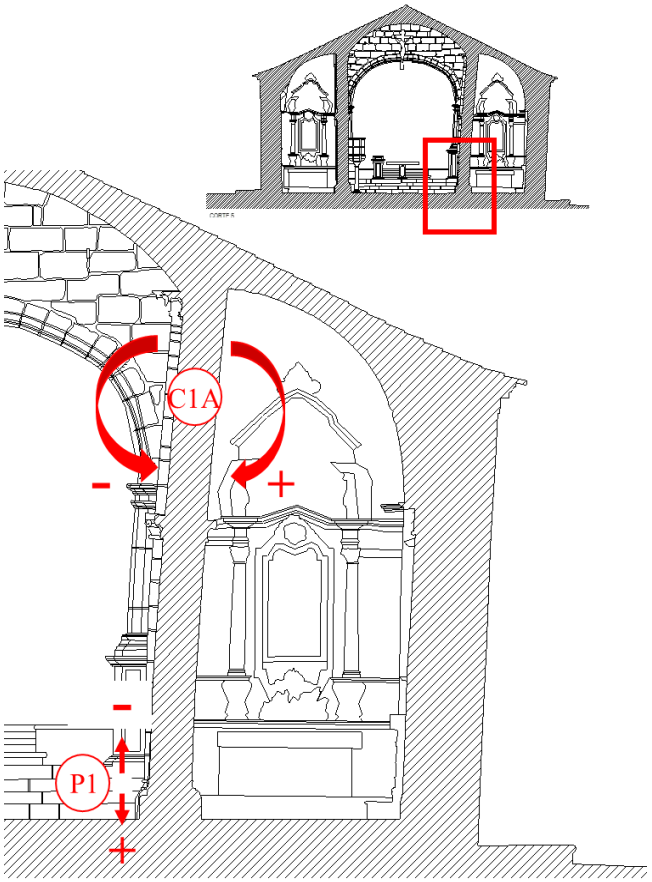

Figure 77. Schematic view of the movements and orientations monitored through sensors C1A and P1.

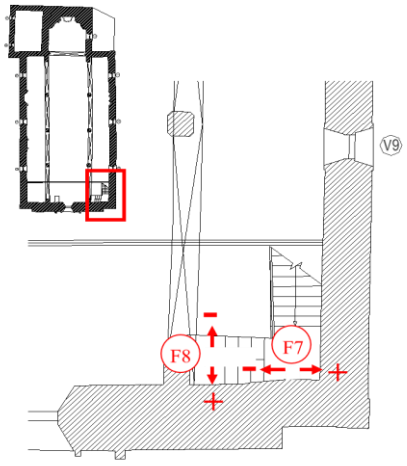

Figure 78. Schematic view of the movements and orientations monitored through sensors F7 and F8.

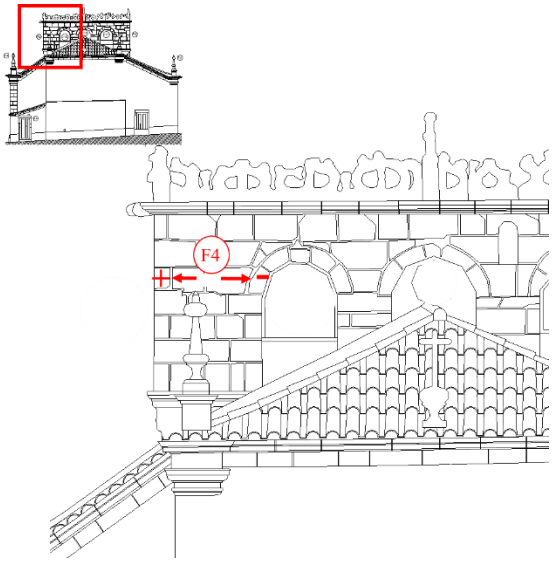

Figure 79. Schematic view of the movements and orientations monitored through sensor F4.

5.4. Influence of the temperature on structural displacements

The time evolution of the internal and external temperatures and the relative humidity recorded by the monitoring system are shown through the data in Figure 80, whereby the maximum and minimum values of temperature measured were over around 39 ºC and 0ºC, respectively, while the maximum and minimum values of relative humidity were of 88% and 25%, respectively. It should be noted that the temperature measurements recorded by the T1C sensor, placed inside the church, present significantly less variation (ranging from 9 ºC to 29 ºC) than the values of temperature collected by sensor T2C, that vary from -1 ºC to 37 ºC, as can be observed in Figure 80.

In order of to investigate the influence of the internal temperature on the displacement parameters monitored in the present work, the values of the temperature collected by sensor T1 were used to estimate a correlation between temperature and relative displacements, and subsequently, the correspondent correlation function was used to remove the thermal effects from the displacement values of originally collected.

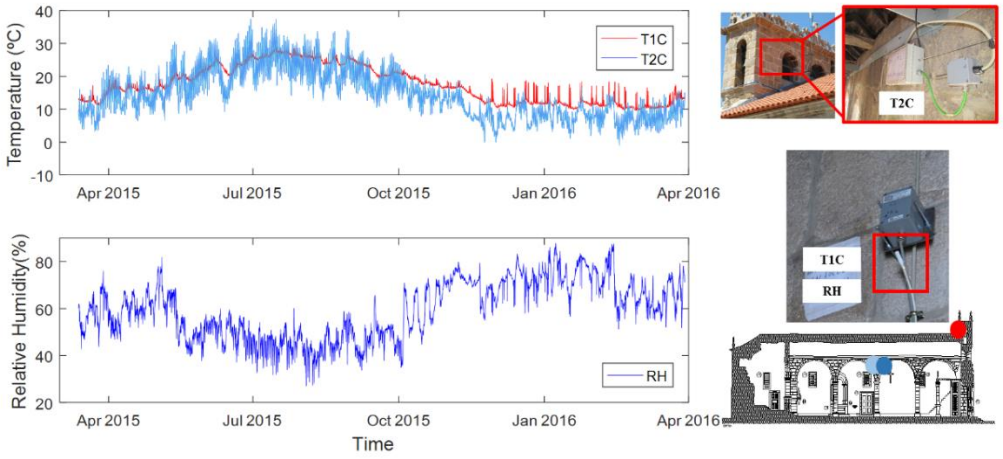

Figure 80. Time evolution of the internal and external temperatures and relative humidity monitored at Foz Côa Church.

From the analyses of the inclination time evolution data, of the column 2, plotted in mm/m, it can be noticed that temperature increases are more influencing than decreases. In general, when the average temperature values are close to 38 ºC, the inclination reach values around 0.320 mm/m. In contrast, during the winter, when the average temperature values are around5 ºC, the inclination measured values are close to 0.100 mm/m, in the opposite direction from the movement observed during the summer (see Figure 81).

Through a correlation between the T1 and T2 temperature values and the displacement acquired by sensor C1A, it was possible to obtain Expression 8, where $D_{C1A}(t1)$ is the displacement as a function of the T1 sensor temperature in [mm/m]/ºC, and x is the temperature in ºC. This way, the thermal influence from the monitored inclination can be removed, as can be seen by the data in Figure 81. The correlation coefficient (R^2) value for the $D_{C1A}(t1)$ function is presented in Table 5.

$$D_{C1A}(t1) = -8.1448\text{x}10^{-4}x^2 + 4.3725\text{x}10^{-2}x - 4.4386\text{x}10^{-1} \qquad \text{(Expression 8)}$$

Removing the temperature effect from the inclination values recorded by sensor C1A allowed to build a linearized curve (see Figure 81). The inclination movements evolution over 1-year monitoring on the Column 2, without the temperature effect compensation shows maximum value of inclination of 0.320 mm/m (ranging from 0.320 mm/m to -0.200 mm/m), and with compensation a maximum value of 0.210 mm/m (in a range between 0.210 mm/m to -0.180 mm/m) was estimated. Therefore, a 34.4 % difference was calculated between the maximum inclination values, estimated with and without compensating the thermal effects.

Table 5. Determination coefficient (R^2) between temperature T1 and the displacement monitored at sensors C1A, P1 and F8.

	C1A	**P1**	**F8**
T1	0.82	0.92	0.84

Essentially, the inclination movements collected over 1-year demonstrate that the increase of the temperature observed between March/2015 and the beginning of August/2015 are influent in the inclination value increase on column 2, to right lateral Nave direction, while between August/2015 to beginning of March/2016, the inclination tends to go in the opposite way, namely to direction of the Main Nave. After the thermal effects removal, it was noticed that the displacements are not related with structural movements, only with annual thermal cycles.

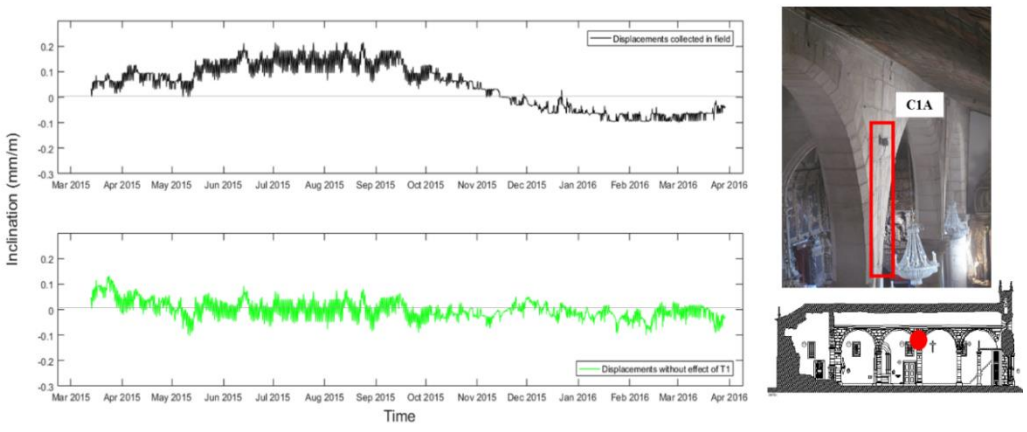

Figure 81. Time evolution of the inclination measured by sensor C1A on column 2 with and without the temperature effect.

Concerning the displacements measured on the bottom of the column 2 by the potentiometer sensor P1, its time evolution is presented in Figure 82. In order of to

identify the thermal effects on the relative displacements collected, a correlation between the displacements and the temperature evolution (T1) was done and the Expression 9 was obtained, where $D_{P1}\,(t1)$ is the relative displacements in function of the temperature T1, in mm, and x represents the temperature value, in ºC. The respective correlation coefficient (R^2) is shown in Table 5.

$$D_{P1}(t1) = -4.0484\text{x}10^{-3}x + 5.6881\text{x}10^{-2} \qquad \text{(Expression 9)}$$

Through the time evolution analysis, while the temperature stimulus induces a displacement, acquired by sensor P1, varying from -0.078 mm to 0.020 mm, the displacement behavior without the thermal effects vary from -0.040 mm to 0.020 mm, evidencing the temperature influence on the basis of column displacements to the up direction, in this case, assigned as the negative values. Essentially, these relative displacements, related with the temperature increase, can be due to the inclination movements, collected by C1A, as well. In fact, the temperature increase can induce the basis of the column 2 to move, aggravating the emergence of tension on it.

Making a comparison between the maximum overall displacement values collected and the maximum displacement estimated removing the effect of the internal temperature (T1), a variation from -0.078 mm to -0.040 mm, was observed, for the maximum displacement with and without the effect of the temperature, respectively. Therefore, a decreasing of -48.7% on the displacement value recorded by sensor P1, was estimated.

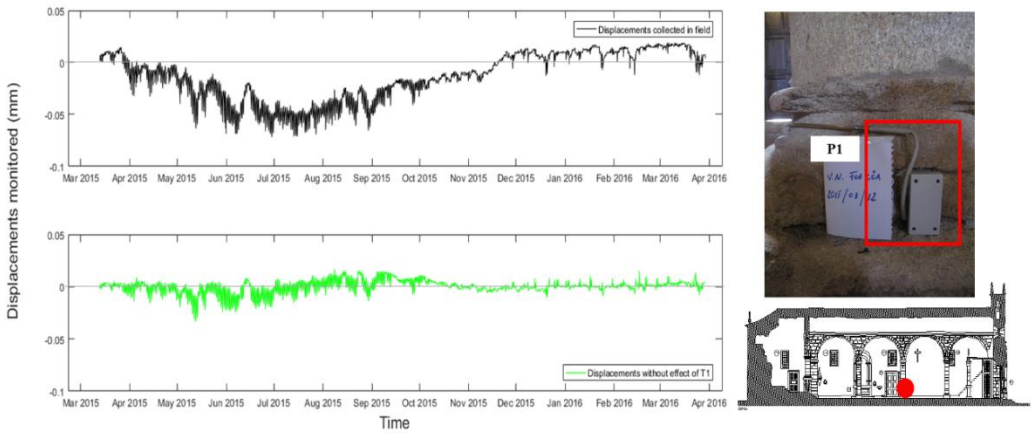

Figure 82. Time evolution of the displacements measured by sensor P1 on the bottom of the column 2 with and without the temperature effect of T1.

Especially during the summer period, the relative displacements recorded through P1 achieved higher values. This way, the temperatures and the relative displacements recorded in July and August of 2015 are presented in Figure 83, allowing to observe the day-by-day thermic cycles, and its correspondent effects on the relative displacements evolution. After removing the temperature effect, the relative displacements tend to stabilize around zero, supporting our finding of absence representative structural movements.

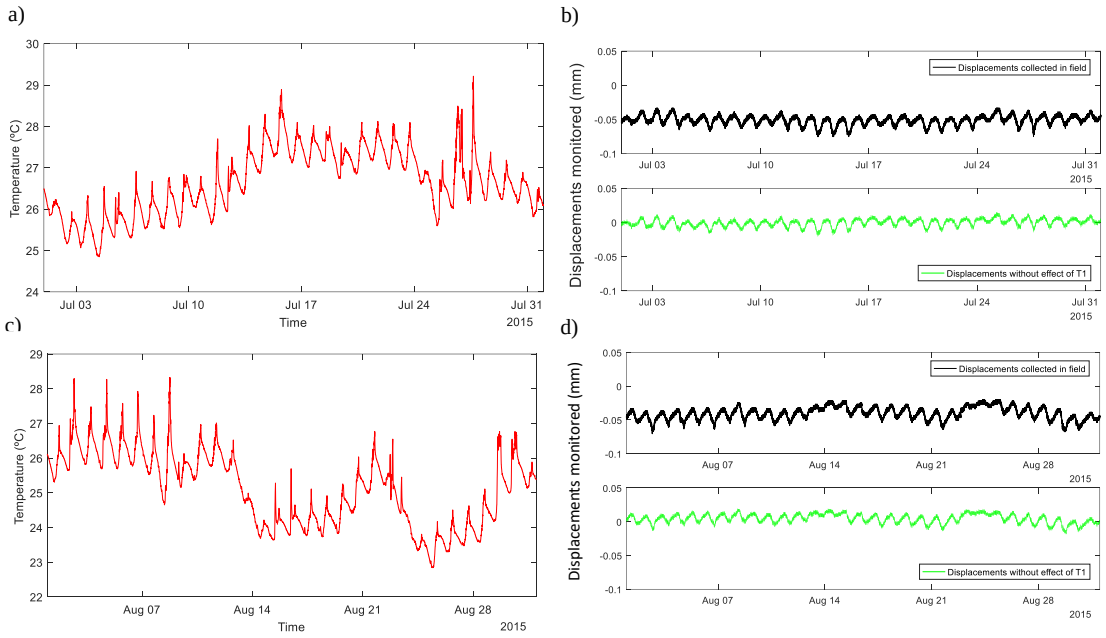

Figure 83. Time evolution of the temperature and displacements measured on the bottom of column 2 in July and August 2015.

The Figure 83 shown the time evolution of the temperature and displacements measured on the bottom of column 2: (a) temperature measured at the sensor T1 location from July 1st to 31th, 2015 and correspondent (b) displacement measured on sensor P1 with and without the temperature effect; (c) temperature measured at sensor T1 location from August 1st to 31th, 2015 and correspondent (d) displacement measured on sensor P1 with and without the temperature.

The linear displacements data, collected by sensor F8, with and without the effect of the temperature T1 is shown in Figure 84. The correlation function between relative displacements and the temperature values was stated based on Expression 10, where

$D_{F8}\,(t1)$ represents the displacement in function of the temperature T1, in mm, and x is the temperature value, in ºC.

$$D_{F8}(t1) = 2.8543\text{x}10^{-3}x - 3.7782\text{x}10^{-2} \qquad \text{(Expression 10)}$$

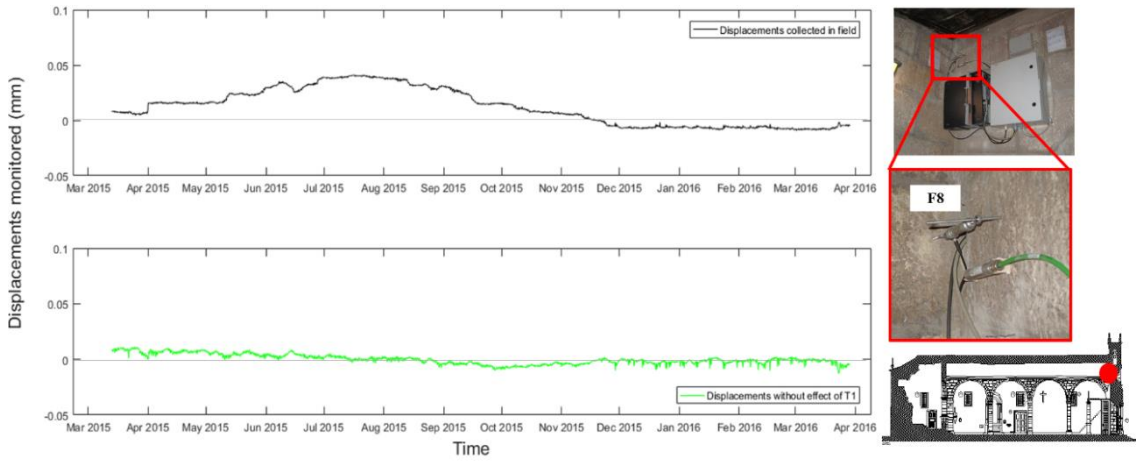

Figure 84. Time evolution of the displacements measured by sensor F8 on the top of the internal side of the main façade with effect of the temperature and without temperature effect of T1.

Based on the evolution of the linear displacements measured at the sensor F8 location, after the removal of the thermal effect (T1), the amplitude of the relative displacement along the longitudinal direction decreased. In July 22, 2015, for instance, the displacement curve with the temperature effect presented a maximum of 0.05 mm, while after the removal of the internal temperature effect (T1), the maximum displacement found was 0.02 mm, in other words, the internal temperature effect virtually increased the displacement up to 250%.

Concerning the transversal displacements on the main façade, monitored through sensors F4 and F7 placed in different points (as assigned in Figure 78 and Figure 79), its time evolution presented in Figure 85 show really small values of relative displacements , always running around 0. The relative displacement average measured by sensor F4 was estimated to be around 0.002 m, during the summer period, where a light influence of the temperature on the displacement curve behavior was noted. However, in both situations, data collected through F4and F7, it was not possible to establish a correlation between the relative displacements and the temperature evolution, due to the small values measured. Additionally, these results also can be understood as a negligible temperature

influence on the stone walls transversal movements, also demonstrating an absence of structural movements in that direction.

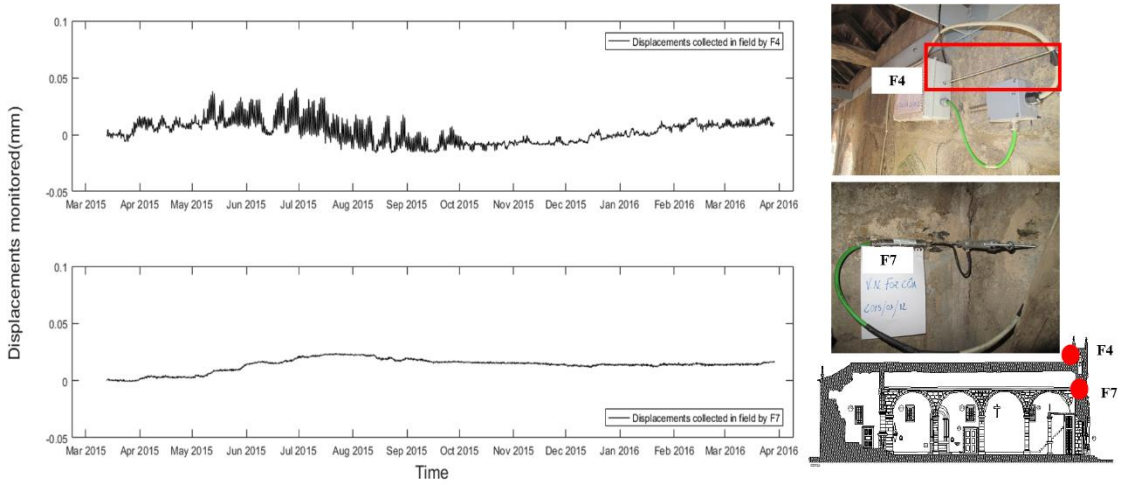

Figure 85. Time evolution of the displacements measured through sensor F4 on the top of the tower and sensor F7 on the internal side of the main façade (transversal movements) with the temperature effect.

5.5. Combined effect of the temperature and relative humidity on structural displacements monitored

The previous section, demonstrates how temperature can affect the structural movements of the monitored elements of the Foz Côa Church. However, the relative humidity (RH) may constitute an amplitude constraint of the observed movements. Therefore, the present section is devoted to the combined effect of the temperature and relative humidity on structural displacements observed on the Column 2, namely inclination and relative displacements at the basis, as well as the relative displacements of the longitudinal section of the main façade, measured through sensor F8, as shown in Figure 78. This study was limited to the data collected through sensors C1A, P1 and F8, excluding the data collected on sensors F4 and F7 due to the fact that their measured relative displacements didn't allow to estimate an adequate correlation coefficient R^2.

The correlation between the temperature (collected through sensor T1) and the relative humidity values and the inclination measured at C1A sensor location, is shown in Figure 86, with an estimated correlation coefficient, R^2, of 0.86.

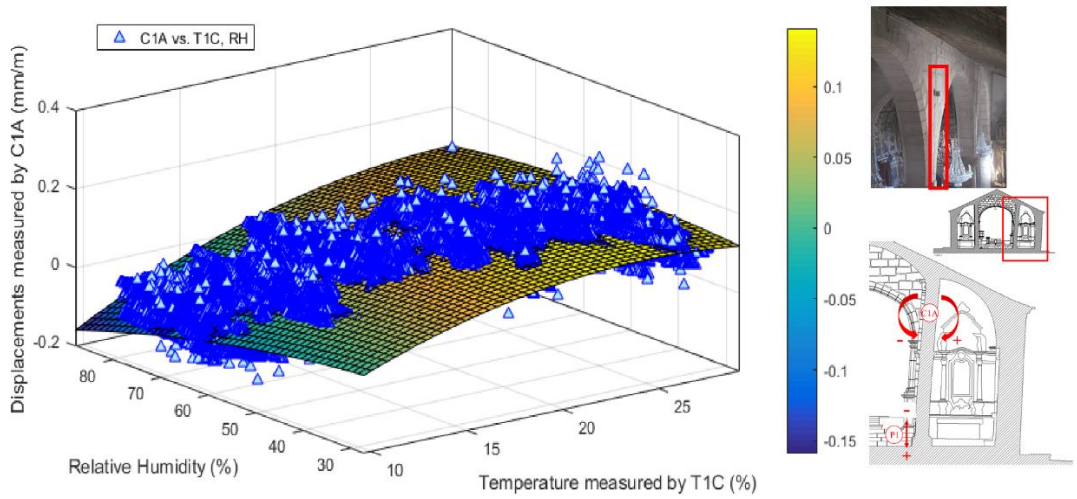

Figure 86. Influence of the combined effect of the internal temperature and relative humidity on the inclination movements, measured through sensor C1A at column 2.

The results confirmed that the combination between a relative humidity (around 80%) and temperature increase (around 10 ºC) can aggravate an inclination movement of the column 2 of roughly 0.150 mm, in the Main Nave direction of the Church. Otherwise, a low relative humidity (between 50% - 60%, for instance) can constrain the column 2 inclination for the same level of temperature variation. The inclination movement in the opposite situation, namely in the direction of the right lateral Nave, occur when the values of temperature are near or higher than 20 ºC for all levels of relative humidity.

Concerning the combined effect of the temperature and relative humidity on the relative displacement observed at the column 2 bases, the results are presented in Figure 87, with an estimated correlation coefficient, R^2, of 0.92.

However, the surface slope, in the Figure 87 data, demonstrate that the relative displacement at the basis of the column 2 are mostly influenced by temperature rather than relative humidity changes. Additionally, inclination along the column 2 also has an impact on the relative displacement observed at the basis, contributing for overlapping the relative humidity effect on the structural movement at the basis of the column 2.

Regarding the relative displacement measured on the stone wall, the combination between the temperature (T1) and the relative humidity effects, in the longitudinal direction, is shown in Figure 88. The correlation coefficient R^2 was identified as 0.84.

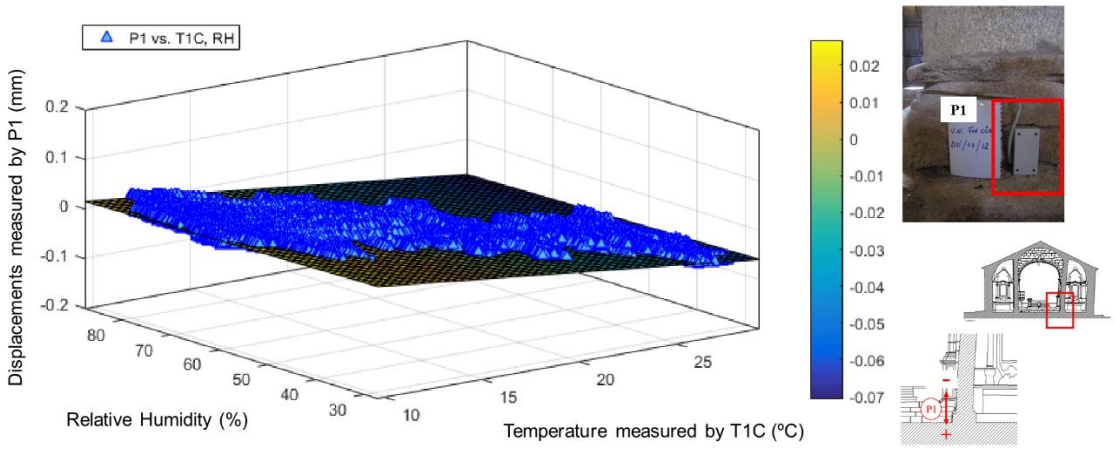

Figure 87. Influence of the combined effect of the internal temperature and relative humidity on the displacement measured at the bottom of column 2, by sensor P1.

The surface represented in the Figure 88 data present a smooth curvature with higher slope, and parallel to the temperature axis. Only in the 60% to 80% RH range, combined with temperature values over 20 ºC, incites the wall movement (on the monitored point) to the interior direction of the Main Nave, otherwise the temperature increase induces a movement in the opposite direction. It was estimated that a ratio of 80% RH combined with a temperature value of 10 ºC produce an average displacement of 0.02 mm to the interior direction of the Main Nave.

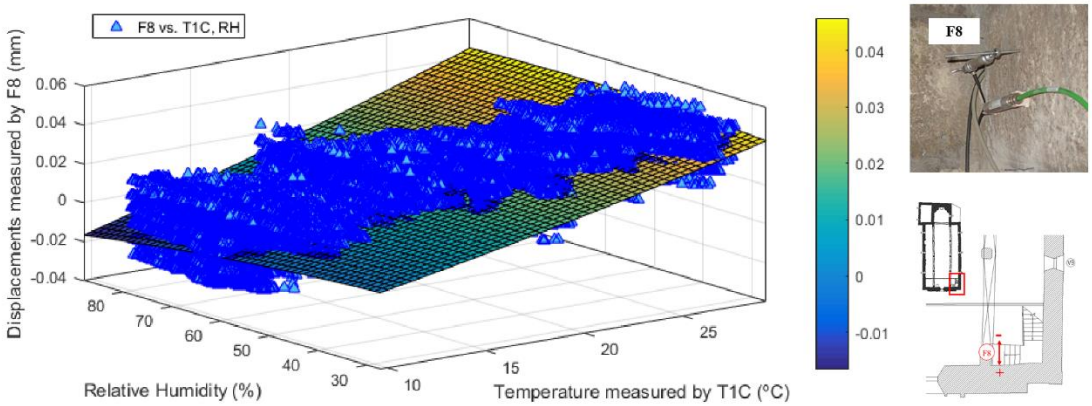

Figure 88. Influence of the combined effect of the internal temperature and relative humidity on the movements at internal side of the main façade collected by sensor F8.

The relative humidity is directly related with the quantity of water inside the material pores of the components, mainly in the mortar, therefore it may induce small movements. Similarly, changes in the ambient temperature can, besides the thermal expansion, to

induce smooth variations on the rigidity of the structural components. To completely understand how the temperature and relative humidity affect the structural movement mechanisms, it is necessary to fully analyze the collected data, to correlate all the known factors, as temperature and humidly changes, and to compensate those in the parameter of interest calculation. That way, it may be used in structural behavior numerical models, and potentially, to identify the damage emergence.

5.6. Final comments

This work described the SHM system implemented on Foz Côa Church (Portugal), as well the main results collected along 1-year monitoring, from 13th March 2015 to 29th March 2016. The sensorial system was composed by temperature, relative humidity and relative displacements sensors.

Four sensors were installed along a pillar (column 2). Temperature, relative humidity and inclination sensors were positioned on the top, and a potentiometer sensor at the basis. Three relative displacements sensors were installed on the main façade, two were placed inside the church to access the displacement in the longitudinal and transversal directions, respectively, and the other was positioned inside the bells-tower, in the top of the main façade, close to another temperature sensor.

The data collected allowed to characterize the structural movements of the column 2, namely the inclination and relative displacements in its basis, as well to relate them with the influence of the ambient temperature, consequently to understand how thermal effects influence the column movement.

Additionally, the relation of thermal effects with the column inclination, and relative displacement, was establish allowing to monitor movements other them the ones provoked by thermal ambient cycles, namely summer and winter. The same data treatment was performed on the data acquired through the displacement sensor on the main facade.

The subtraction of the thermal effect, as well the study of the combined temperature-relative humidity effect, allowed to conclude that the movements observed on the elements monitored are not related with structural issues. Most likely are related with the

temperature and relative humidity influence, the later in lower proportion. Nonetheless, the small displacements values observed, over the time evolution series, does not represent any risk condition to the Foz Côa Church integrity.

Finally, the employment of SHM allowed to collect accurate and reliable data on the displacements of the structural elements of the Foz Côa Church, and the data management employed provided the basis for an adequate interpretation of the results.

6

Structural monitoring of the retrofitting process, characterization and reliability analysis of the Santo António Church

Summary

The employment of SHM and OMA techniques can be worthy alternatives for structural characterization and safety management. However, in the literature few cases of SHM of HC are reported, and guidelines or recommendations specifically for safety assessment of HC is an effort still undergoing. Thus, the present work describes the strategies for SHM and structural characterization of a Portuguese stone heritage construction, namely Santo António Church and introduces a new approach for heritage assessment based on reliability analysis, specifically through vibrational measures, so-called RABVIM. The results showed that SHM allowed to guarantee the efficiency level of the retrofitting measures carried out, while OMA provided useful information on the structure modal parameters, under operational loading actuation, apart from the data for reliability assessment. Finally, this work demonstrates that RABVIM can be an interesting and useful tool to support the safety assessment of HC.

Keywords: Structural health monitoring, Heritage constructions, Vibrational testing, Dynamic characterization, Reliability analysis, Operational modal analysis.

6.1. Introduction

Natural hazards occurrence can seriously affect HC, occasionally provoking the total collapse of the structures or inducing the damage emergence and its progression, as was observed in the recent years. This way, the adoption of preventive measures can be the better practice to reduce the structural risk and to avoid dramatics losses [171]. However, adopting proceedings for preserving HC demand a deeper knowledge on structural behavior due to heterogeneity and complexity of their structural systems. Additionally, while experimental and numerical studies on reinforced-concrete structures were already extensively carried out and had allowed the design of the reinforced concrete characteristics as function of their physical properties, as demonstrated by Eurocode 8 [172]. In the case of HC, its characteristic are mostly provided by case-by-case approaches, often with recurrence to dynamic tests [11, 159, 173] and SHM [8, 168], [174]. Recent reports, see for instance [5] , demonstrate that this is current and significant field, demanding more efforts in the case of HC.

While the dynamic tests can be useful for obtaining global information on the structural seismic response and vulnerabilities, the employment of local testing and SHM can provide a most accurate information on structural characteristics of the HC. Even with the increase in the number of cases reported on literature on HC monitoring in the last 10 years [152], it still remains a lack of knowledge on real time assessment methodologies able to provide the owners objective answers on the current HC condition, particularly to avoid dramatic losses. Therefore, additional efforts by techno-scientific community are essential.

According to [9], SHM of HC is a challenging opportunity at the monitoring field, due to the necessity to understand the structural typology and undergoing through some behavior hypothesis that require deeper attention, during the design and implementation of the monitoring system (and data processing). That will allow to obtain accurate information on global behavior of the HC under analysis. Recent cases of SHM applications on HC, especially motivated by the cost reduction and larger development of the sensors in the last years, demonstrated that SHM technics can be used for structural characterization without introduction of permanent damages to historical construction [8]. Due to the fact that the size of the SHM systems have been reduced, it doesn't affect the visual aspect of

the HC, and can also provide actualization of the monitored parameters in real time [15]. In addition, the implementation of wireless SHM systems, beyond of the above mentioned advances of the regular system, allow the reduction of the communication systems cost and, makes possible to collect data from remote regions [106].

Commonly, the cases of SHM methodologies described in the literature report monitoring systems with similar compositions, essentially composed by a sensing system, a data processing system and a management system [59]. In fact, the main differences among them are the type of implemented sensors and, in some cases, the strategies and its focus [24, 58, 106, 108, 113, 175]. The main guidelines for structural monitoring offer information about the general principles of the SHM techniques, namely, the employment of sensing systems for data collection in real time, the main methods employed and parameters commonly monitored [82, 88], but does not includes specific guidelines for HC. Naturally, the guidelines reported in the literature are based on the most common cases of SHM applications, i.e., bridges, offshore structures, towers and larger buildings [155], and don't consider the special case of the HC.

Considering the heterogeneity and the variability of structural components of HC, the combination between SHM and reliability techniques can be an interesting tool for real time assessment. In the literature, reliability methods have been employed to analyze the performance of modern constructions (e.g. steel structures) [176–178] through analysis of the structural response, in terms of specific parameters, such as displacements, and a safety index stated according with current codes [172].

The present chapter aims aims to contribute to broad the knowledge in the field of characterization and reliability analysis of heritage constructions, throughout the description of the SHM procedures adopted during the retrofitting of a masonry stone heritage construction, namely the Santo António de Viana Church, and proposing and demonstrating a new approach for reliability analysis based on vibrational measurements. However, the reliability approach proposed in this paper, due to the localized measurements of vibrations (that depends of the excitation force, among other aspects), is limited to the analysis of specific structural components. In the present case, the measurements were performed on the vaulted stone ceiling of the church. Therefore, the present methodology required to be combined with experimental tests, according with the

construction needs. Concerning the case study carried out, as it was mainly focused on the columns and the vaulted stone ceiling of the Santo António Church, the experimental campaign included the characterization of the Elastic Modulus of the columns through pressiometer testing and with the modal characterization of the church based on the OMA testing performed. According to levels of response offer by monitoring systems, presented in this work, the SHM system here implemented can be classified as Level 5, once the structural lifetime prediction was taken in account.

6.2. Guidelines for heritage construction assessment

The present section is dedicated to description of the methodology for HC assessment carried out in this work. The main aim of this section is to presents the main guides towards the application of the methodology, and to provide recommendations about it.

Firstly, the general aspects of the assessment methodology will be presented, followed by recommendations on the application criteria, SHM criteria and by the method of data acquisition and update. The main difference between the assessment methodology presented in this work to other methodologies reported in the literature (see [14, 26, 27]) is that this approach is totally focused to HC and includes a reliability analysis based on vibrational measurements aiming to offer the owners an objective answer on the current safety state of the building.

6.2.1. Area of application

In order to consider the variability and vulnerability of the structural systems and the different necessities of adoption of intervention measures for maintenance of the structural safety of HC, the present guide for structural safety assessment based on employment of the SHM techniques can be adopted in the following cases:

- Preventive plans for structural safety maintenance;
- Previous interventions;
- Changes in the structural system;
- Damages emergence;
- Changes in the structural loading;
- Reliability assessment;

- Natural hazards occurrence;

6.2.2. Criteria

Undoubtedly HC comprises different types of structures (houses, monuments, buildings, bridges, among others) having the long service time. This way, the adaptation of the current guide for the specific necessities of each structural group should be made with recurrence to experimental tests, according to the level of assessment, for a most accurate safety analysis. The employment of the present guidelines for HC safety assessment should consider the:

- Case of application;
- Response level 5 required by owners (see Table 2);
- Geometry characteristics;
- Material properties;
- Characteristics of the monitored parameters (data behavior, data frequency, uncertainties, etc.);
- Limit State formulation (Ultimate Limit State or Serviceability Limit State).

6.2.3. SHM system definition

A good SHM system should be practical, functional and durable. Consequently, the implementation of a SHM system on a HC should account for future changes that can occur with the assessed construction, adopting a system that make changes in the sensing system. Also, the design of the SHM system should be built on the current state of the structure, and for this a previous inspection is necessary in order to provide a global vision about the present state of the construction, and to inform if visual damages were found. So, the design of a SHM system should be based on:

- Type of damage found on the construction;
- Level of responses required by owners (see Table 2);
- Level of accuracy of the sensors;
- Open system (that allow future changes or implementation of the sensorial system);
- Sensor optimization (employing the minimum number of sensors possible);

- Energy resources optimization;
- Easy installation and maintenance;
- High durability;
- Low intrusion (especially visual);
- Low cost.

6.2.4. Step-by-step of the guidelines for HC assessment

The present section details the flowchart presented in the Figure 89. Firstly, a historic analysis should be carried out, with the goal of providing information about the building historic importance, repair or structural alterations history, technical reports or any other documental information that can contributes for structural assessment.

It is really important to proceed with the historical investigation on the assessed HC because it offers reliable information about previous events occurrences, as interventions or natural actions, contributes for the technical team understanding about the HC cultural value, and allow the development of a most assertive inspection plan.

During the historic analysis, the technical team can previously identify the different construction techniques and to select appropriated assessment methods for characterize the assessed building. Also, the information collected in this step should be used to estimate the level of intervention needed, in case of necessity of retrofitting measures adoption.

Following, the technical inspection should be carried out in order to collect information on the current state of the HC and identify existing damages and its location, and to validate the previous information collected during the historic analysis. In fact, the main objective of the technical inspection is to collect qualitative data with adequate tables of inspection (for inspection tables see [181]) and to do a photographic register.

The results of the technical inspection should provide data about the damage presence, type of damage, and location, evidence of previous interventions or any change on the operational life or loadings in the HC. In addition, it is during the technical inspection that the necessity of implementation of a SHM system should be defined. However, in the case of the previous existence of a SHM system under work, the information collect

till this moment can be used for an eventual adequacy of the sensing network of the SHM system to current necessities of the HC.

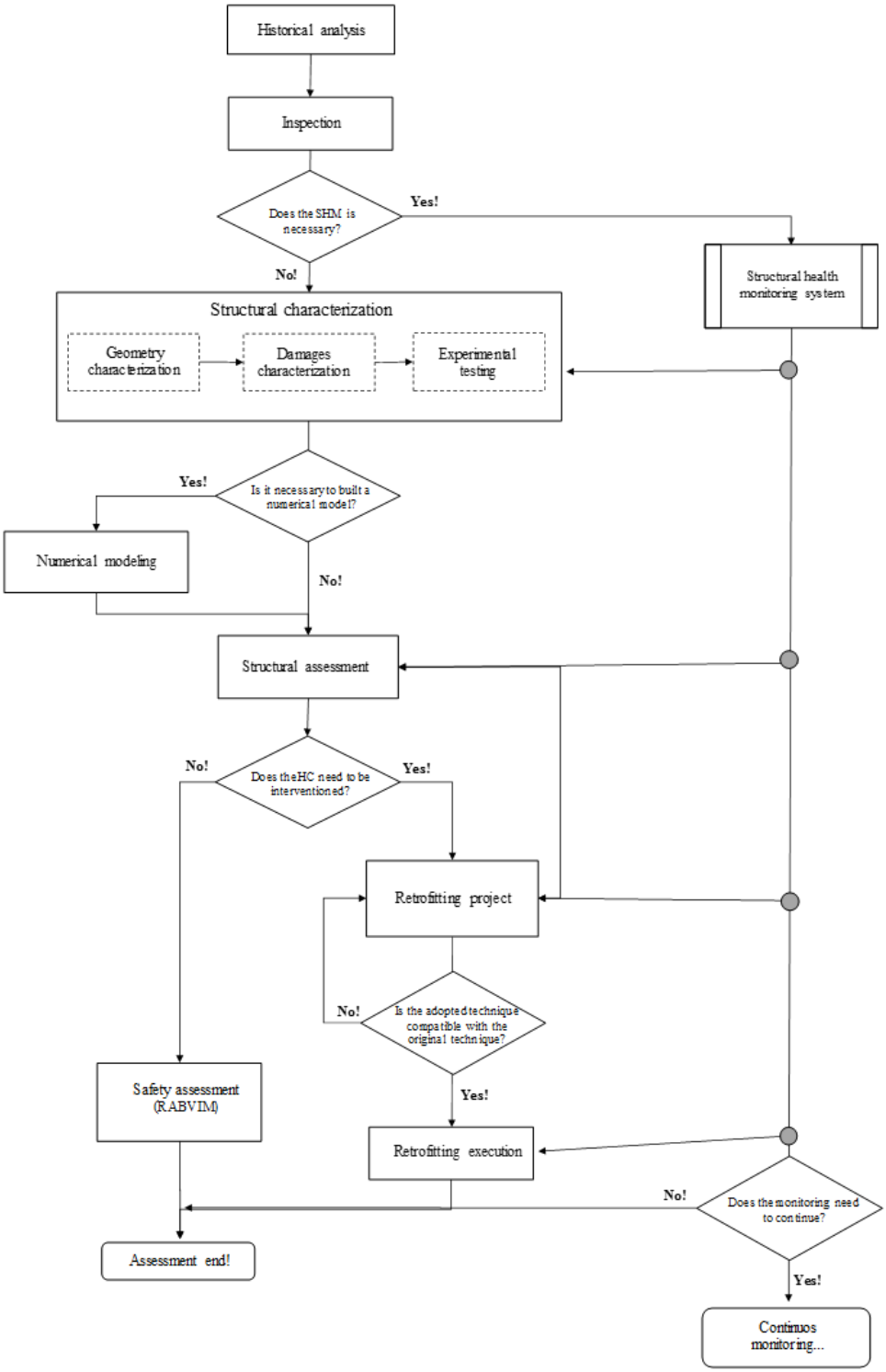

Figure 89. Structural health monitoring platform for heritage construction safety assessment.

Through the analysis of the data collected by the SHM system, it is possible to establish the necessity of experimental testing, to collect reliable data to characterize the current state of the structure, as can be observed by Figure 89.

In the flowchart sequence, present in Figure 89, the structural characterization depends of the scenarios found during the technical inspection and can be divided in three main stages: i) geometric characterization, where the main function is to collect accuracy information about the geometry of the assessed elements, as beams, columns, etc.; ii) damage characterization, that aims to provide accuracy information about the damages and its effects on HC, and iii) non-destructive experimental testing, that can be used to collect additional/specific data on the structural components of the church.

All information should be organized and directed towards the implementation of the HC numerical modeling, if necessary. Sometimes due to absence of adequate information the construction of a numerical model is not possible, and the technical team should be following for structural assessment based on the information collected during the historic analysis, technical inspections and structural characterization steps. Often, it is the moment when some hypothesis on the structural behavior of the components under analysis is assumed.

In fact, the numerical modeling can contribute for optimization of the structural assessment and forecasts about the structural safety, especially due to the fact that through numerical modeling the most fragile zones and the most concentrated loading zones can be identified, being such essential for optimization of the SHM system and sensing cost reduction. So, numerical model construction should be performed always when requested by the technical team.

After the decision of constructing a numerical model, the next step forward is the structural assessment. Structural characterization comprises the step where all the experimental data, carried out on the previous steps are confronted with the information collected during the historic analysis and technical inspection and the facts concerning the structural systems of the HC is stated. As form to provide accurate information on physic-mechanical parameters, the Elastic modulus and compressive strength are essential parameters. Indeed, all information collected in this level can be used to design

the retrofitting proceedings as to evaluate the retrofitting measures adopted. According to assessment platform presented in Figure 89, it is during the structural assessment that the decision concerning the retrofitting measures and the retrofitting proposal is provided.

Following the flowchart present in Figure 89, the next step is the safety assessment, that in the present work it is constituted by Reliability Analysis Based on localized VIbration Measurements, so called RABVIM. The adoption of the present methodology for safety analysis has as main aim to offer an objective response to the owners about the structural risk of the HC under environmental excitation.

The employment of probabilistic methods for structural safety assessment of HC can be a relevant tool for support of the management of the structural integrity, structural safety and adoption of retrofitting measures. These methodologies can be interesting since the constructions performance is associated to a large number of uncertainties that cannot be easily modeled by deterministic methods, making the probabilistic methodologies a necessary resource for safety analysis, and the most adequate for random variables processing [182, 183].

However, the probabilistic methods are limited, in the RABVIM case these limitations are characterized by the local where the accelerometers are placed, environmental excitation and the failure limit criterion adopted.

Usually, the set of variables involved in reliability analysis are represented by *R* and *E*, where *R* represents the safety variable group for the analyzed scenario and *E* represents the variable group which affects negatively the structural safety. Then the structural probability of failure, *Pf*, can be written as shown by Expression 11, where, the limit failure condition can be represented by $g\ (R, E) \leq 0$.

$$Pf = \mathcal{P}\{\ g\ (R, E) \leq 0\} = \ \mathcal{P}\ \{r(R) \leq e(E)\} \qquad \text{(Expression 11)}$$

Thus, in view of Expression 11, the failure probability, *Pf*, can also be rewritten according to Expression 12, where fx represents the probability density function of X, and X represents all random variables from the problem in study, in the case of the RABVIM, the relative displacements collected by the accelerometers, in mm.

$$Pf = \ \int_{g(X)\leq 0} f\text{x}\ (x)\ dx \qquad \text{(Expression 12)}$$

From the failure probability, *Pf*, the reliability index β can be estimated through Expression 13, where Φ^{-1} is the inverse of the standard normal distribution function.

$$\beta = -\Phi^{-1}(Pf) \quad \text{(Expression 13)}$$

Considering the case analysis in which the set of variables are known for a determined time, and the maximum and minimum values of the probabilistic curves need to be predicted, it is common to resort to the generalized extremes values distribution (GEV) [182]. Additionally, GEV can be applied when the number of data is sufficiently large and the frequency distribution curve is asymptotic. However, in order to consider the asymptotic types of curve that a data distribution can assume, one of the three forms of GEV should be adopted, namely: Gumbel distribution (Type I), Fréchet distribution (Type II) or Weibull distribution (Type III) [184].

In the case of the RABVIM, the failure principle adopted is that the failure occurs when a determined set of values exceeds the safety value *R*, thus the Gumbel distribution is the most indicated [182]. Indeed, Gumbel distribution is frequently applied to modelling environmental phenomena, as for example wind velocity [185]; additionally the Gumbel distribution has been recently used in SHM systems for service life prediction in different type of structures [8, 11, 13].

Specifically, the Gumbel distribution for maximum values can be defined by function *Fx(x)*, according to Expression 14, where α and *u* can be estimated from the data set analyzed, and x is the limit exceedance values in the distribution curve that will be analyzed.

$$Fx(x) = exp\left[-e^{-\alpha(x-u)}\right] \quad \text{(Expression 14)}$$

The α and u values can be obtained by Expressions 15 and 16, where the variance $\mathbb{V}(X)$ is a necessary value for determination of constant α, and $\mathbb{E}(X)$ is the average of *Fx(x)* function, for a given value of γ = 0.577. A most detailed reading on reliability analysis can be found in [185].

$$\mathbb{E}(X) = u + \frac{\gamma}{\alpha} \quad \text{(Expression 15)}$$

$$\mathbb{V}(X) = \frac{\pi^2}{6\alpha^2} \quad \text{(Expression 16)}$$

The base for RABVIM is to define a set of random variables of *Si*, and to define the values of *R* and *E*, that represents the safety limits. In fact, *Si* represents the values obtained by SHM system (random variables) and it is assumed that this value can vary in an open interval limited by *R*, that represents the safety limit value, and by *E*, that comprises the idealized value of safety (design value). It is necessary to highlight that the *R* value does not represent the collapse situation but a limit value for preventive measures adoption.

Actually, the β values can vary according with the risk condition stated by R. When β presents values nears of 0, it does mean that the failure condition stated by R is near to be achieved. The *R* index value can be stated taking into account the type of structure/element and failure parameter analyzed and through consult some standards as Eurocode 8 [187] and the Italian guidelines for evaluation and mitigation of the seismic risk of the cultural heritage buildings [5]. Nevertheless, the safety limited stated by *R* in the case of the present methodology, that considered the failure of stone masonries by displacements, was stated as 30 mm, based on exhaustive experimental studies performed on several types of Portuguese stone masonries developed by LESE/CONSTRUCT team (see [188]).

The RABVIM methodology proposed in this work is based on random values of displacements, from accelerations spectra collected during the vibrational ambient modal characterization or through the accelerometers of the SHM sensing system. Essentially, this method considers the displacements provoked by environmental excitation in a specific point of the construction assessed, and analyzes the probability of the risk condition be achieved.

This way, the RABVIM methodology can be summarized in follow eight steps, namely:

- selection of a data set;
- data processing;
- establishment of a *R* limit value, where the function $G(R) \leq 0$ represents failure condition;
- statistic treatment and histograms constructions;
- selection of an adequate probabilistic distribution curve;
- determination of the statistic variables ($\mathbb{E}, \mathbb{V}$, α e u);

- determination of failure probability Pf, taking in account the *R* limit value and,
- obtainment of the reliability index β.

Once that the value of β is known, the owners and the technical team have a quantitative answer on the safety condition of the HC assessed under a determined scenario. That value can be used to support future decisions about adoption of retrofitting measures and for comparison with different risk conditions. Also, with a large number of HC analyzed, the β value could be used as support about the priority of which HC should be firstly retrofitted.

In order to provide a better explanation on the applicability of RABVIM approach, a case study, namely, Santo António de Viana do Castelo Church, was carried out and will be detailed in the next sections following the methodology proposed steps.

Next, in the flowchart presented in Figure 89, after the safety assessment be carried out, is the assessment process finishing, however the necessity of continuing the monitoring of the HC needs to be decided by the owners and technical team based on the information collected during all the assessment process.

6.3. Santo António Church: case study

The Santo António Church is a baroque church built in XVIII century, and located in Viana do Castelo, Portugal. The church is a stone masonry structure and presents a rectangular geometry (from the top view), as shown by Figure 90.a, with 15.08 m of width, 42.74 m of length and 14.00 m of height, and a roof with two ends, and in its interior five chapels are distributed along of the longitudinal length. The main facade is composed by a symmetric distribution of decorative baroque elements and a bell-tower in the lateral. Through Figure 90.b a transversal section of the interior of the church is presented while by Figure 90.c the main façade is showed.

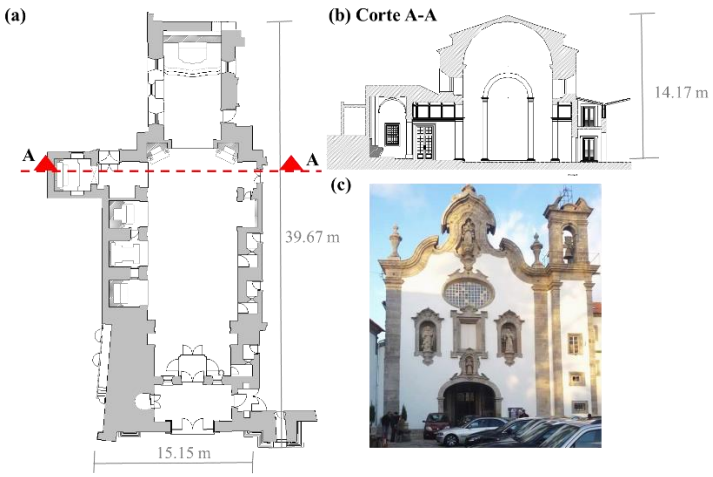

Figure 90. Santo António Church: (a) view in plant, (b) section AA and (c) main façade.

Essentially the church was built with irregular stone (Figure 91), and in the last two decades, some structural damages had been observed on Santo António Church, such as the displacements of the chapels' columns and cracks emergence, according to technical reports performed by Instituto da Construção – FEUP in the last years [36–40]. The Table 6 show in summarized form the contents of each report on Santo António de Viana's Church chronologically ordered.

By a visual inspection performed on Santo António's Church before the retrofitting measures it was possible to identify cracks on the columns bases concerning the compressive stress, and along the columns' body. Also, cracks on the Church's roof were observed, making evident the movements of the roof provoked by the columns displacement and rotation. A summary view of the main cracks observed at the Santo Antonio's Church are shown in Figure 92 and Figure 93. Without doubt, the damages observed constitute fundamental information for safety analysis and highlighting the necessity by retrofitting measures.

Table 6. Main contents of the technical reports performed on Santo António de Viana's Church.

Year	Authors	Reports contents
2002	Delgado, R.; Costa, A.; Rocha, P.; Delgado, P. and Oliveira, J.	In this report a visual inspection was carried out and cracks were identified as the main damages and geometrically located. Due to the high level of cracks observed on the church structure, especially on the chapels' columns base, the technical group recommend that a visual inspection in the foundations elements was carried out and also that were observed the cracks progression.
2003	Delgado, R.; Costa, A.; Rocha, P.; Delgado, P. and Oliveira, J.	The present technical report proposes some recommendations in order to provide most accurate informations about the structure: i) removal of the decorative elements from the Chapels; ii) new inspection; iii) implementation of a SHM system; iv) specific inspection on the foundation elements; v) to perform a geotechnical prospection. Now, as initial step for problem solving, in this reports the establishment of the main elements affected by damages was proposed.
2006	Delgado, R.; Costa, A.; Rocha, P.; Laranja M.; Delgado, P. and Oliveira, J.	In this document a retrofitting measure is proposed. Essentially, for solving the problems of crack emergence and progression it is proposed the execution of micro-columns in the base of the foundation elements.
2012	Costa, A.; Rocha, P. and Paupério, E.	Other inspection was carried out and the cracks problems aggravation was observed. Thus, it was recommended the construction of reinforcement bars for the structural displacements containment. It was highlighted that these recommendations didn't exclude the retrofitting measures recommended in 2012.
2013	Costa, A.; Rocha, P. and Paupério, E.	This reports provided information about the retrofitting measures carried out in 2012. The main reinforcement measures realized were: the strengthening of the walls and the columns by reinforcement rebars and the lateral confinement of the columns.
2015	Arêde, A.; Rocha, P.; Paupério, E. and Gomes, A.	This report provided information on the monitoring results. The Santo António's Church had a SHM system implemented in June of 2014, and since that, the structural displacements have been monitored.

Figure 91. Details of the chapel walls: (a) wall without mortar layer and (b) detail of the wall after the retrofitting.

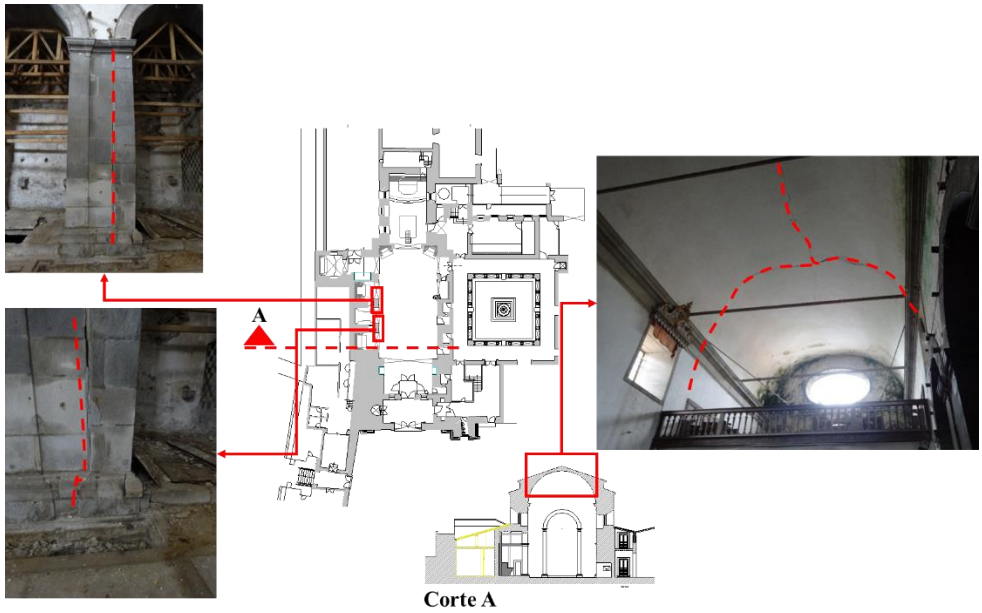

Figure 92. Main cracks observed on Santo António Church during the visual inspections.

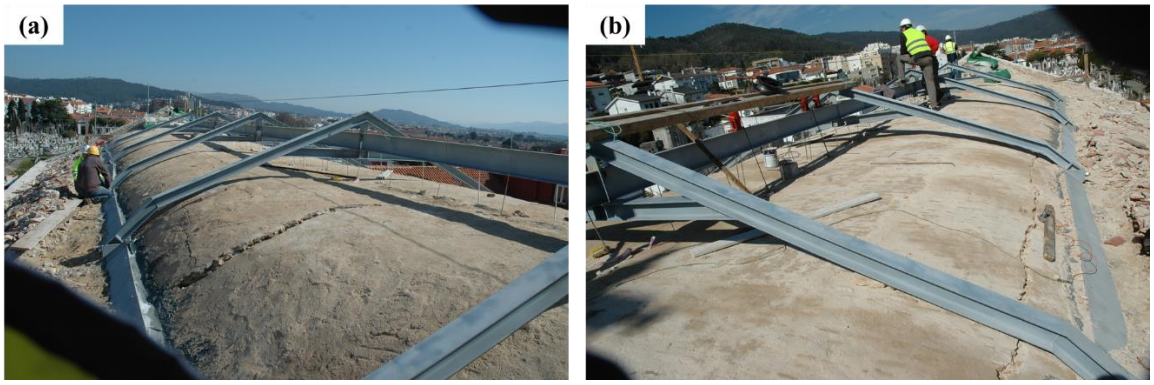

Figure 93. Superior view of the vaults with some cracks retrofitted through a steel structure.

6.4. Structural health monitoring of the Santo António Church retrofitting

This section is dedicated to description of the SHM system and the main results collected by Santo António Church monitoring. Essentially, the retrofitting measures included in the present work were performed focused on the columns of the church, and were divided in two phases:

- 1rst phase: retrofitting of the walls and columns using reinforcement rebars;
- 2nd phase: retrofitting of the lateral confinement of the columns.

All steps of the intervention were monitored and the results are described in the following sections.

Initially, the monitoring of the relative displacements of the structural elements located in the chapels area were recommend by the technical team in 2003 [27]. However, due to some restrictions the implementation of the SHM systems was only possible in June of 2014. Since then, the SHM system has been collecting data about the structural displacements 24 hours per day. The monitoring results presented in this work include measurements collected during the period from June 2014 to May 2015.

6.4.1. SHM system

The SHM system implement on Santo António de Viana do Castelo Church (see Figure 94) was composed by 14 sensors connected with an 8-channels NI-CFP-AI-100 module with 12 bits resolution and a real-time controller NI-CFP-2200 with a 400 MHz processor, 128 MB DRAM, both from *National Instruments*®. All the collected information is sent to a remote interface through a 3G modem.

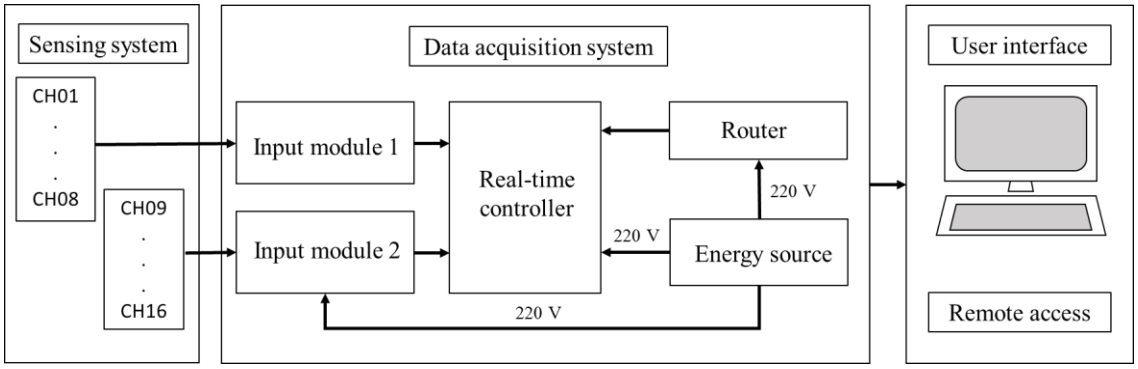

Figure 94. General setup of the SHM system implement on the Santo António de Viana Church.

In the sensing system, 5 crack progression sensors were assigned as F2, F3, F4, F5 and F6, also 3 displacement transductors, so-called L1, L2 and L3 were employed, as well 2 temperature sensors, namely T1 and T2 and 2 inclinometers, C1A and C1B were used.

6.4.2. Setups of monitoring

While the retrofitting was focused on the columns of the church, the SHM proceedings included the monitoring of the relative displacements at the columns and at chapels, as suggested in the technical report previously mentioned [190]. The monitored area can be seen in the Figure 95. The monitoring proceedings adopted in this work can be divided in three setups, that will be described below.

In the Setup 1 (Figure 96.a) the sensing system was installed on the arches A1, A2 and A3 and in the columns P1, P2 and P3. The main goal of this setup was to monitor the effect of the retrofitting measures on the relative displacements of the column P1, as suggested in [189] and showed in the (Figure 96). The sensors were installed in June 13, 2014, in the locations indicated in the Figure 96.a. The sensors F2, F4, F5 and F6 were installed in the interior of the chapels at 3.98 m, 3.98 m, 2.80 m and 3.17 m of height, respectively. The sensor F3 was destined to column P1 monitoring, thus it was placed in the front of column P1 at a height of 2.35 m. The sensors C1A, C1B and T1 were positioned between the base of arches A1 and A2 at 5.10 m and the temperature sensor T4 was positioned within the arch A2 at 3.32 m. Finally, the sensors L1, L2 and L3 were installed in the front of columns P1, P2 and P3, respectively, at 4.10 m of height. All sensors were connected to the data acquisition system, placed at the left of A1, by copper cables.

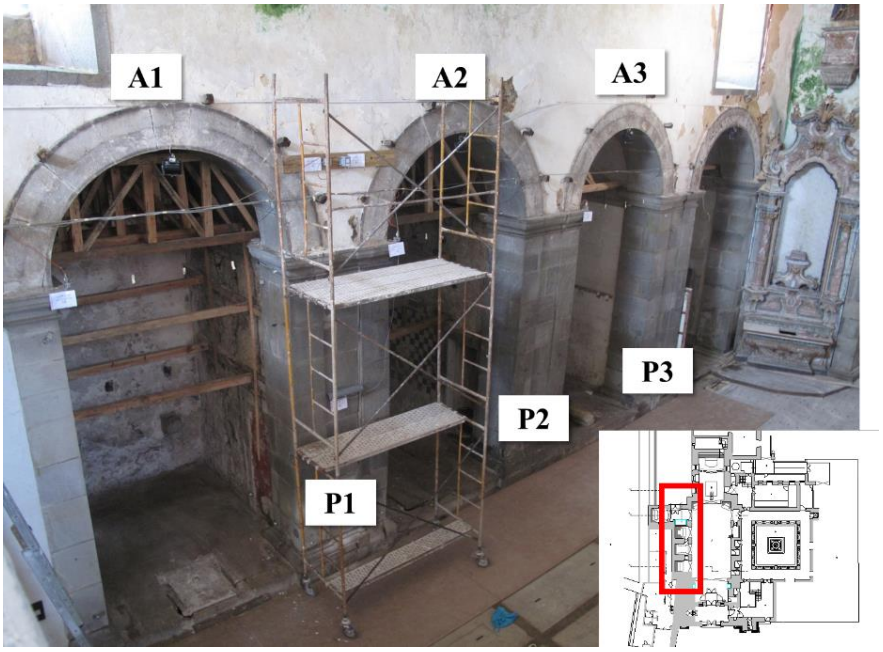

Figure 95. Columns 1, 2 and 3 and arches 1, 2 and 3.

The Setup 2 started in July 15, 2014 and was focused to monitoring of the influence of the retrofitting on the relative displacements of column P2. In this setup, the position of the sensor F2 was changed to the right side of the column P2. The sensors C1A, C1B and T1 were changed from its initial positioning to the front of P2 columns. The correspondent heights of all sensors were maintained according with Setup 1. The disposition of the sensors during the setup 2 can be seen through Figure 96.b.

Now, for the Setup 3 the sensors L1, T1, C1A and C1B were changed to column P3, while sensors L3, F3 were placed on column 2. The main aim of this step was monitoring, in special way, the relative displacements at the area of the chapel A3. The sensors F4, F2, F6 and F5 remained in the same places of the Setup 1. The disposition of the sensors during the setup 3 can be seen through Figure 96.c.

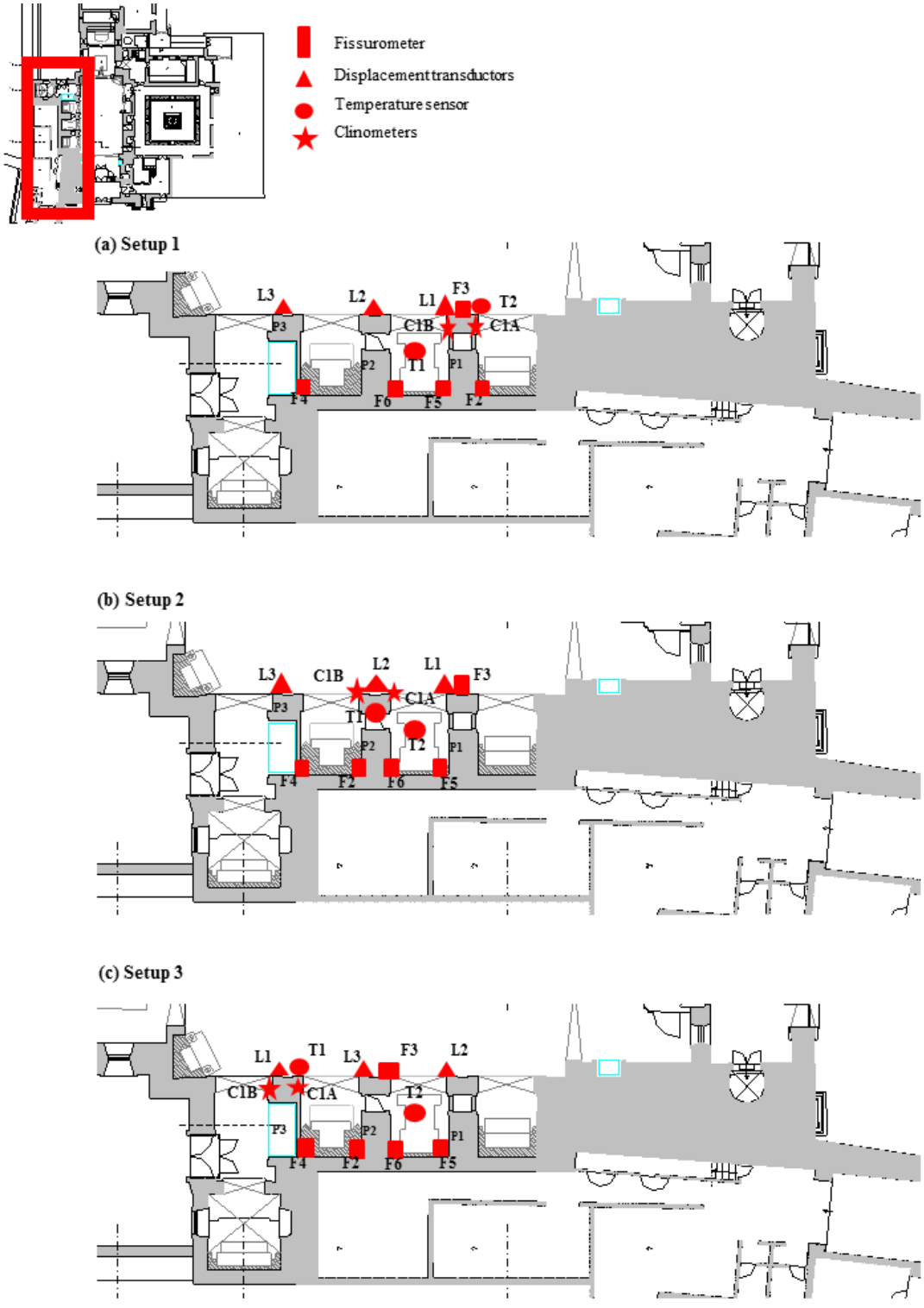

Figure 96. Monitoring steps of the Santo António de Viana Church, and correspondent sensors location.

6.4.3. Retrofitting monitoring of the Santo António Church

The monitoring results of all the sensors employed on the Santo António Church during the period from June 14th 2014 to May 03rd 2015 are showed in the figures below. The results are divided according to monitoring setups (1, 2 and 3) described in the previous section, although, during the periods from October 06th 2014 to November 12th 2014 and December 07th to February 06th 2015 a system failure does not allowed the data acquisition. Therefore, in these two periods the results were assigned as linear from the pre-failure to the post-failure.

The temperatures values collected by T1 and T2 sensors presented similar results (Figure 97). The maximum and minimum average temperature values observed in the monitored period were of 22ºC and 9ºC, respectively. During the setup 1, the results collected by C1A sensor (Figure 98.a) indicated rotation of the P1 column in the out of plane direction, with a maximum value of 2.7 mm/m. Also, the C1B sensor (Figure 98.b) measured movements of the P1 column in the plane direction, with a maximum value of 0.5 mm/m. After these two events, the retrofitting measures performed on the P1 column resulted in the return of the P1 column to its initial position, as can be seen through inclinations observed at the end of the setup 1 of the Figure 98.a and b).

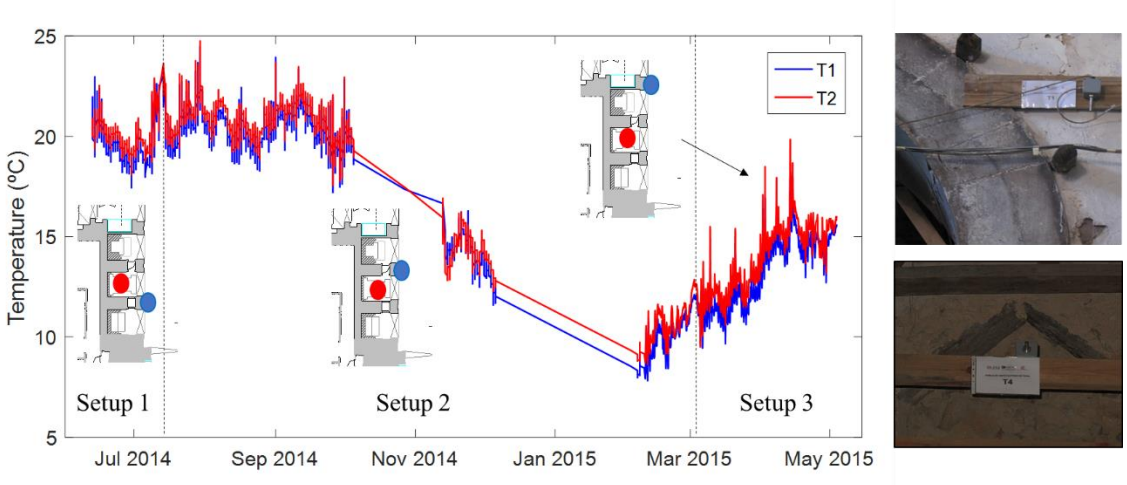

Figure 97. Time evolution of the temperatures collected by sensors T1 and T2.

During the setup 2 (Figure 98.a and b), the results of the sensors C1A and C1B demonstrated that till February 07th 2015 tenues rotations occurred in the P2 column, with maximum values of 2.0 mm/m and 1.0 mm/m, respectively. These movements can be understood as the effect of the foundation settlement attenuated by retrofitting measures performed on the column P1.

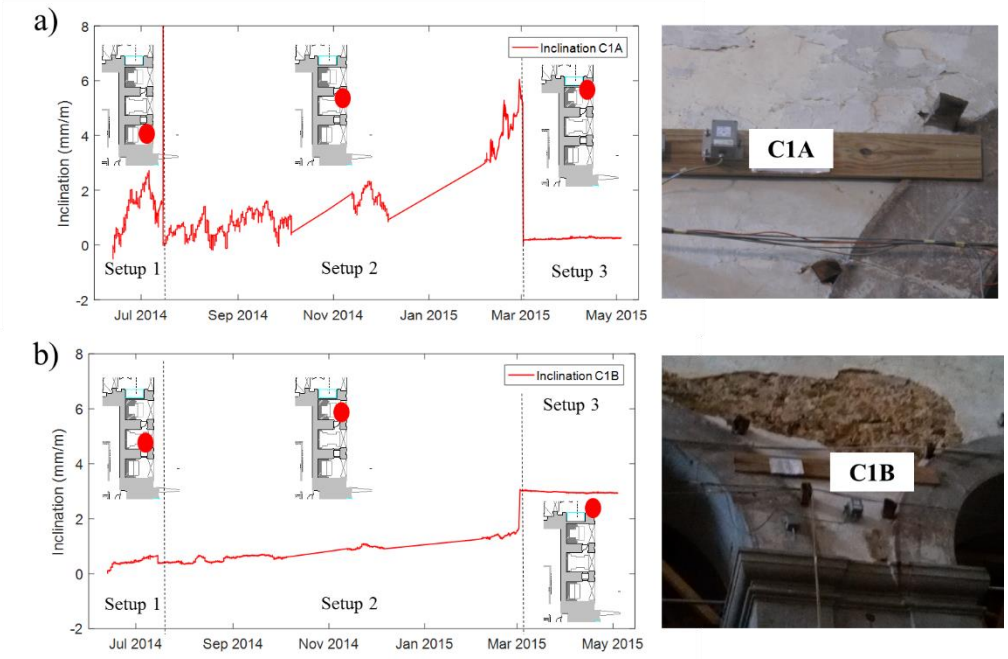

Figure 98. Time evolution of the inclination measured through (a) sensor C1A and (b)sensor C1B.

In the period from February 07th 2015 to March 02nd 2015 (Figure 98.a and b), the C1A and C1B sensors measured maximums rotation values of 5.5 mm/m and 3 mm/m in the column P2. These values are related with the retrofitting measures performed in the column P2 and in the roof (see Figure 93). After March 02nd 2015 (Figure 98.a and b), assigned as the final of the retrofitting measures on column P2 and in the roof, the sensors C1A and C1B were restarted, and no important rotation was noted since then.

During the first monitoring setup, the F2 and F3 (Figure 99.a and b) sensors measurements did not presented significant displacements. However, the measurements logged by sensors F4, F5 and F6 (Figure 100.a, b and c), presented displacements that can be related with the retrofitting measures performed on column P1. The maximums values observed at the sensors F4, F5 and F6 locations were 2.0 mm, 0.5 mm and 2.3 mm, respectively.

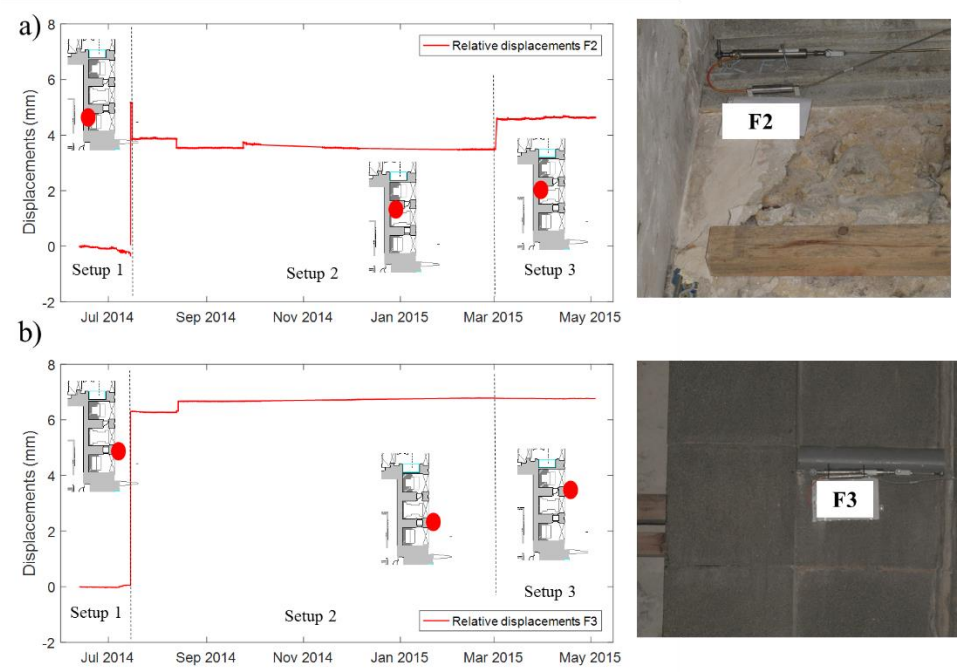

Figure 99. Time evolution of the relative displacements measured by sensors (a)F2 and (b)F3.

For setup 2, the sensors were not restarted. Therefore, the last recorded measurements were maintained as the initial point of setup 2. During this step, it was observed that the sensor F2 (Figure 99.a) measured displacements of 5 mm in the February 16th 2014, decreasing to 4 mm in February 18th 2014. In August 14th 2014, the displacement decreased again, to 3.7 mm, and in November 21th 2014 the displacement at the sensor F2 location increased to 3.8 mm. The displacements verified by the F3 sensor (Figure 99.b) presented two important progression points, namely, in February 16th 2014, with 6 mm and in August 14th 2014 with 7 mm displacements. After that, displacements at that location didn't presented any significant values, indicating the stabilization in the cracks progression.

The results collect by the F4 sensor (Figure 100.a) showed that during the Step 2 no significant displacement occurred. However, the results at the sensors F5 (Figure 100.b) and sensor F6 (Figure 100.c) locations showed that important displacements occurred in August 14th 2014 and in September 21th 2014.

The maximum displacements recorded in September 21th 2014 were of 1.0 mm to sensor F5 and -1.0 mm to sensor F6, respectively, and in August 14th 2014 the maximum

displacement variations observed were 0.1 mm and 3.0 mm, to the sensors F5 and F6 locations, respectively.

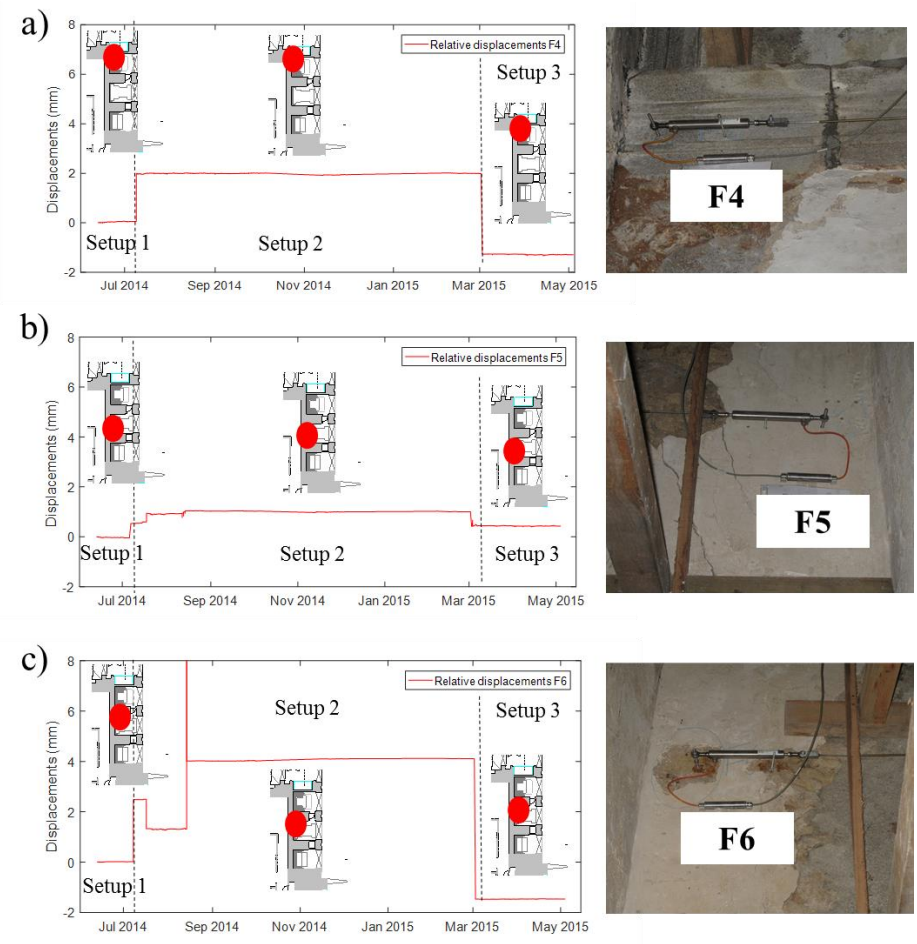

Figure 100. Time evolution of the relative displacements collected by sensors (a)F4, (b) F5 and (c)F6.

It was observed that the retrofitting measures performed during setup 3 were the ones with most impact on the recorded measurements in March 02nd 2015. However, after that date no significand change in the collected measurements were observed.

The data collected with sensors L1 (Figure 101.a), L2 (Figure 101.b) and L3 (Figure 101.c) does not presented substantial displacements during the setup 1 and 2. Some disturbs recorded through L1 and L2 are related with occurrences of human interference, and the ones by L3 are related with the occurrence of retrofitting measures.

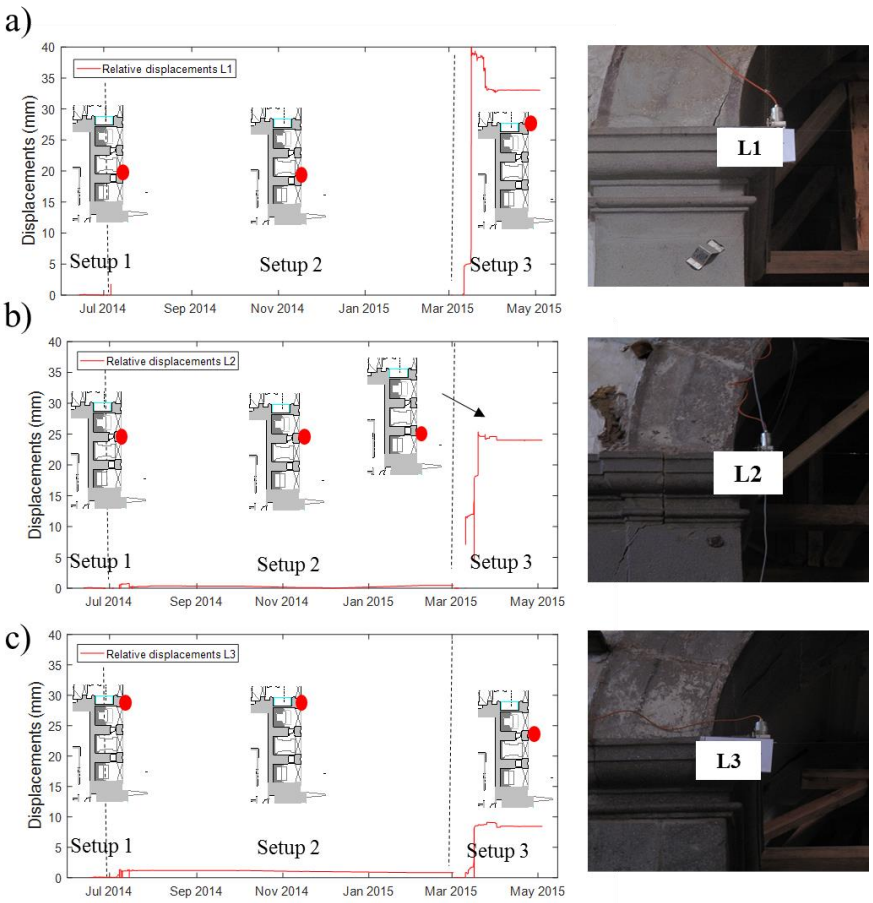

Figure 101. Time evolution of the relative displacements collected by sensors (a)L1, (b)L2 and (c)L3.

During setup 3, all sensors showed displacements related with the retrofitting measures performed in the P2 column and in the roof (Figure 101). The most critical situation of displacement during the structural intervention was acquired with sensor L1, namely 40.0 mm. At the same moment, sensors L2 and L3 logged displacement values of 26.0 mm and 9.5 mm, respectively.

6.5. Structural characterization of the Santo António de Viana Church

The experimental tests carried out on Santo Antonio de Viana Church after the conclusion of the retrofitting measures, will be presented in this section. The main objective of the tests was to characterize the current condition of the church, especially the columns, after the retrofitting process. Thus, the Pressuremeter tests were performed in the columns, as way of analyzing the physic-mechanic behavior of the columns and, then to characterize the global behavior of the church a modal characterization with recurrence to operational modal analysis was done.

The objective of this ambient vibration test is to identify the dynamic behavior of the church through the evaluation of its modal parameters (natural frequencies, modal shapes, damping ratios). Then, this information will be used on the structure assessment and modelling calibration by comparing the measured with the calculated dynamic characteristics. This allowed validating the adopted modelling strategy and proceeding with the structural behavior assessment and safety conditions.

All information concerning these two experimental proceedings are described below, as following.

6.5.1. Pressuremeter testing

The Pressuremeter testing is an *in situ* proceeding that aims to estimate the deformability properties of a solid body, commonly employed for mechanical characterization of soils and soft stones. The test consists in the introduction of a deformable (rubber) pressure probe inside a previously opened hole, afterwards pressure is applied on the walls surrounding the hole and the material deformation is measured by the changes in the volume readings. Figure 102 shows the locations where the tests were performed (P1 to P6), the Pressuremeter equipment and the process of holes opening.

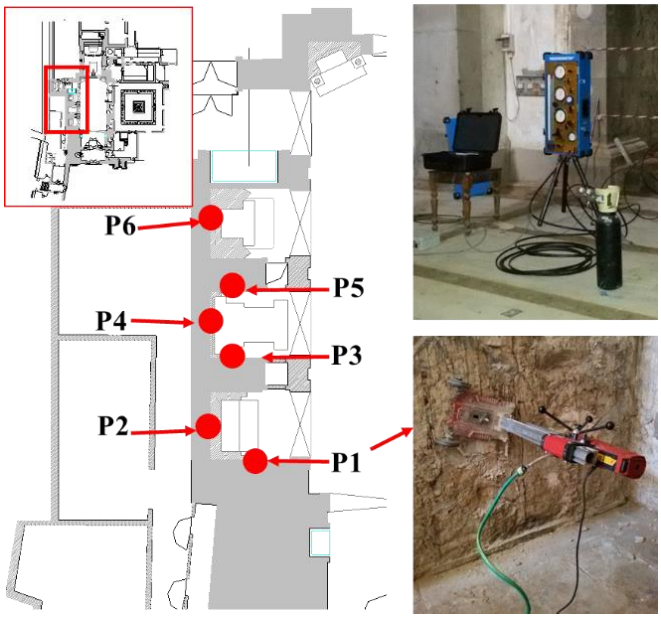

Figure 102. Experimental setup of the Pressuremeter testing and measurements location.

The Pressuremeter testing were performed according to [194]. Six circular openings with 66.00 mm of diameter and around 650.00 mm deep were made on the interior walls of A1, A2 and A3 arches, as showed in Figure 102. The Pressuremeter curves, relating the radial applied pressure with the volume variation of the surrounding probe area are showed in Figure 103.

From the analyses of the data in Figure 103, initially a gradual growing up to the (V_0, P_0) point is visible in each curve, which can be understood as the adaptation period of the probe along the opening. After that point, the behavior is linear, corresponding with the expected pseudo-elastic phase of the curve. In Figure 103.a, the probe data shows an abrupt volume variation, possibly due to any fast expansion of a fragile zone of the opening P1.

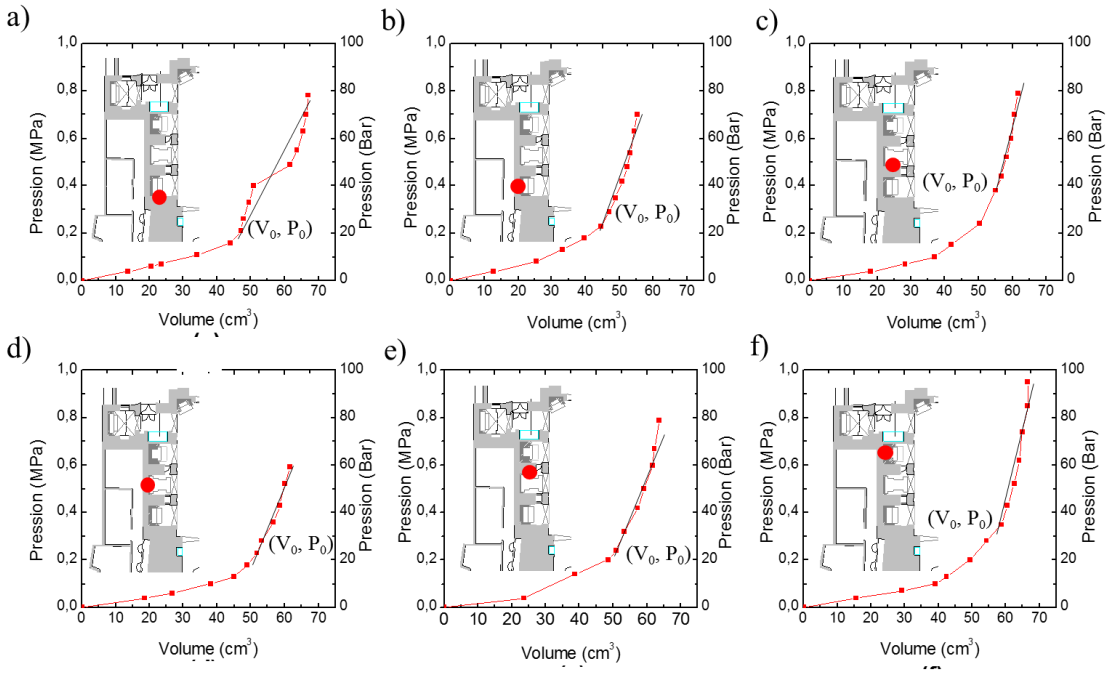

Figure 103. Experimental results of the Pressuremeter testing. a, b, c, d, e and f correspond to openings P1, P2, P3, P4, P5 and P6, respectively.

One of the difficulties in implementing this test technique, to the study of this type of material found in the walls of the church, is concerned with its higher strength (more similar to a rock than a granular material). The Pressuremeter curves obtained show this difficulty, by not presenting the typical shaped S curve, normal for these tests, indicating that the test has never reached pressures capable of yielding the material and well below

the proximity of plastic deformation. Therefore, it is impossible to derive shear strength parameters, and the results only gave an estimative for the deformability parameters of the material.

Based on the Pressuremeter curves, it was possible to obtain the deformability parameters, trough the Pressuremeter deformation modulus (G_{PMT}) and the Pressuremeter (or Ménard) modulus (E_{PMT}). For the G_{PMT} and E_{PMT} calculation, an empirical method was used, based on the expression proposed by Lamé (1952) for a variation of volume in a cavity. These parameters are calculated using the average values on the pseudo-elastic phase of the Pressuremeter curves was considered, along with a Poisson coefficient of 0.20.

The estimated values for the deformability modulus, as well as the mean values and respective variation ranges for the Pressuremeter modulus for each test are presented in Table 7. The deformability modulus (E) can be estimated by dividing the Pressuremeter modulus by a coefficient whose values can be found in [195].

Table 7. Average values of the GPMT and EPMT obtained from the Pressuremeter tests.

Test	Diameter (mm)/length(mm)	G_{PMT} (MPA)	E_{PMT} (MPA)	E_{PMT} (Min-Max)
P1	66.00/650.00	30.89	82.17	13.03 - 247.83
P2	66.00/650.00	26.01	69.18	15.47 - 128.08
P3	66.00/650.00	31.39	83.51	16.51 - 142.31
P4	66.00/650.00	37.09	98.65	16.83 - 256.16
P5	66.00/650.00	34.2	90.96	16.74 - 199.23
P6	66.00/650.00	29.22	77.74	20.78 - 170.77

In Figure 104 are presented the same Pressuremeter curves displayed in Figure 103, but relating the applied pressure with the cavity deformation, in mm, of each bore-hole test. The realized Pressuremeter tests can be organized, according to Figure 95, in different zones of test application, namely: Zone A1(P1 and P2), Zone A2 (P3, P4 and P5) and Zone A3(P6). From the Table 7 values, the E_{PMT} varies from 69.18 MPa to 98.65 MPa. Considering only the P1, P3 and P5 columns, the E_{PMT} ranges from 82.17 MPa to 90.96 MPa.

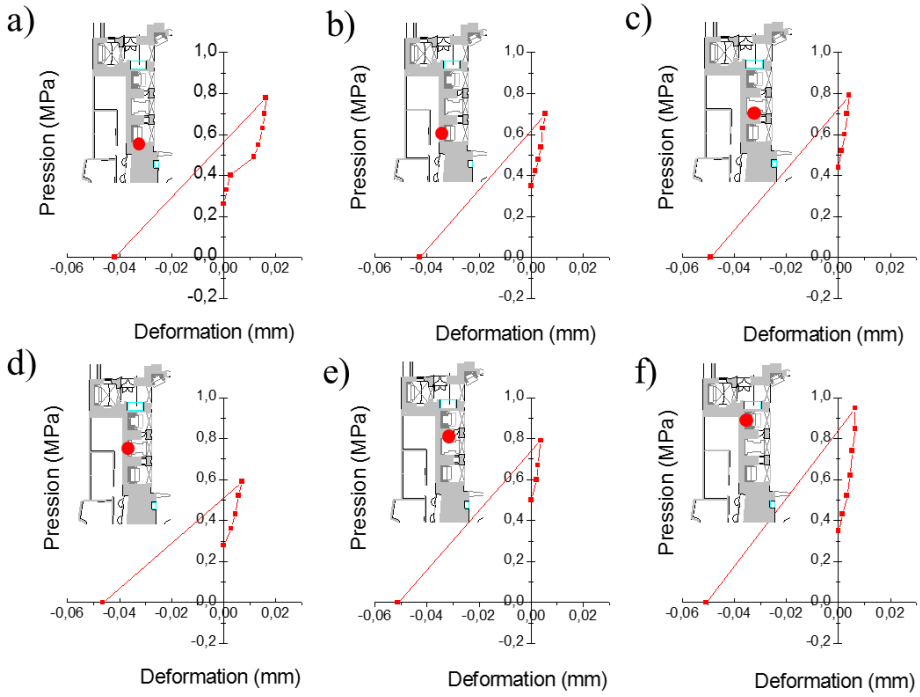

Figure 104. Pressure curves versus deformation, measured during the Pressuremeter testing, where (a), (b), (c), (d), (e) and (f) correspond to P1, P2, P3 P4, P5 and P6 positions, respectively.

6.5.2. Operational modal characterization

Operational Modal Analysis is based on the measurement of structural modal responses only by action of ambient and operational forces. This method is usually employed for modal characterization of large constructions, as bridges, towers, offshore structures and buildings, considering that the environmental and operational forces (random forces) are sufficient for the structural excitation [93].

Essentially, the modal parameters collected in field measurements are commonly used for calibrating numerical models, and one of the primary data analyses methods applied is the Fast Fourier Transform (FFT). The FFT can be understood as a Fourier series which the periodic signal is the sum of an infinite number of harmonic signals, or in another words, using the FFT function the time domain signals recorded in field can be resolved in terms of its frequency components [43, 44], and can be obtained by the Expression 14:

$$F(x) = a_0 + \sum_{n=1}^{\infty} \left(a_n \cos\frac{n\pi x}{L} + b_n \sin\frac{n\pi x}{L} \right) \qquad \text{(Expression 14)}$$

Where, *F(x)* is the FFT function, *L* is the interval analyzed (in this ranging $-L \leq x \leq L$) and *a* and *b* are coefficients according to interval *L*. However, in OMA the most common and easy way of to analyze the data is through Enhance Frequency Domain Decomposition (EFDD). Which can be understood as an extension of the Frequency Domain Decomposition (FDD) and is based on the power spectral density (PSD) function by processing the Inverse Discrete Fourier Transform (IDFT). In EFDD the natural frequencies are obtained by identification of the number of zero-crossings, as function of time, and the damping is obtained by the logarithmic decrement [198]. In addition, the peak-picking is the simplest and common method employed for identification of the frequency of vibrations in OMA, basically due to the fact that this method consists in the identification of the peaks of the frequency spectrum obtained by the processed PSD data.

The relation between the random excitation forces *F(t)* and the spectral responses *X(t)* can be described in the frequency domain through the Frequency Response Function (FRF), *H(w)*, according to Expression 15, where $S_{FF}(w)$ and $S_{XX}(w)$ are the PSD matrices of the random excitation forces and spectral response, and *T* indicated conjugate and transpose operation [199].

$$S_{XX}(w) = H(w)S_{FF}(w)H^T(w) \qquad \text{(Expression 15)}$$

However, the FRF can be also described in partial fraction, as pole/residue, as suggested by [200] and presented by Expression 16, where N is the number of modes, *i* is the index of mode, A_i and λ_i are residue and pole, respectively, when $A_i=\gamma_i\phi_i\phi_i^*$ and $\lambda_i = \zeta_i w_i + jw_i\sqrt{1-\zeta_i^2}$, noting that ζ_i represents the modal damping ratio, and γ_i and ϕ_i are the scaling factor and modal shape vector, respectively. So, this is a modal decomposition of the spectral matrix and the expressions 14 and 15 can be directly related, under the hypothesis of independent white noise input.

$$H(w) = \sum_{i=1}^{N}\left(\frac{A_i}{jw-\lambda_i} + \frac{A_i^*}{jw-\lambda_i^*}\right) = \sum_{i=1}^{N}\left(\frac{\gamma_i\phi_i\phi_i^*}{jw-\lambda_i} + \frac{\gamma_i^*\phi_i^*\phi_i^{*T}}{jw-\lambda_i^*}\right) \qquad \text{(Expression 16)}$$

For operational modal characterization of the Santo Antonio Church, 16 uniaxial accelerometers with dynamic range of ±0.5 g and average sensibility of 9.8 V/g were

used. The general view of the experimental setup and the accelerometers orientation is presented in the Figure 105.

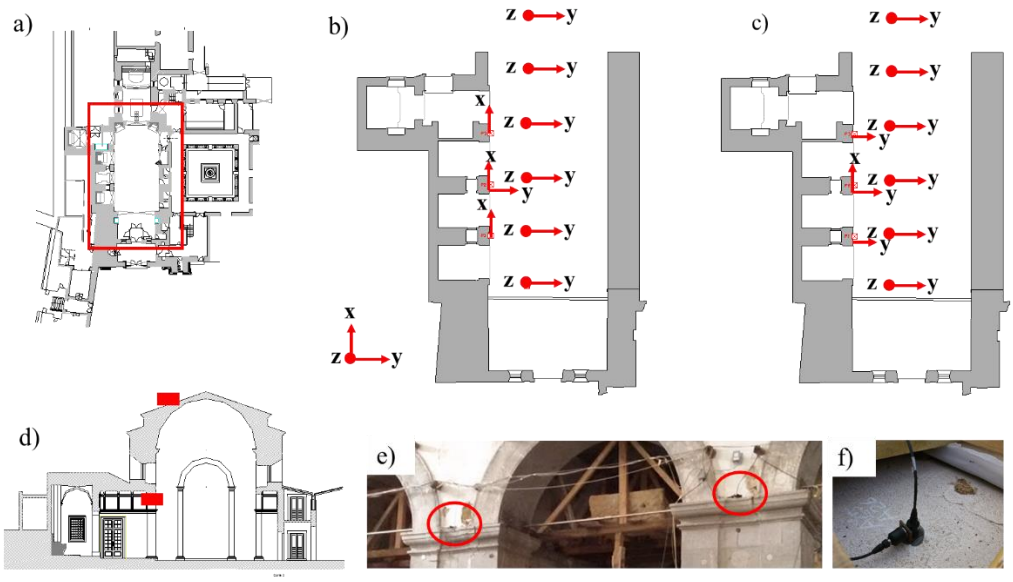

Figure 105. Experimental setup of the ambient vibrational characterization of the Santo Antonio's Church, where (a) testing area, (b) and (c) are trial 1 and 2 respectively, (d) transversal detail of the accelerometer positioning and (e) and (f) are details of the of the accelerometers placed on the columns and roof.

The accelerometers were positioned in the top of the columns and in the roof (Figure 105.d), as can be seen in the detailed Figure 105.e and f. Two different experimental approaches were performed, schematized in Figure 105.b and c. In the first trial (Figure 105.b), 6 points of measurement, spaced 4.00 m each other along the longitudinal direction of the roof where chosen. Each one with 2 accelerometers acquiring data in the Z and Y directions, and 4 accelerometers positioned on the top of the columns 1, 2 and 3 logging acceleration data in the X direction. Another accelerometer was placed on column 2 to collect data in the Y direction. For the second trial (Figure 105.c), 3 points in the roof are moved next to the border, and the direction of the accelerometers placed on the top of the columns 1 and 3 were changed from the X to the Y direction, relatively to the first trial setup.

Each data acquisition was performed during 10 minutes through a *Labview*® software application (see Figure 106) developed by the *CONSTRUCT*-LESE team, with an acquisition rate of 2048 Hz, and the results were processed by EFDD. For the acquisition

system was used a laptop PC, a NI-cDAQ 9172 acquisition system with NI 9234 modules from National Instruments®.

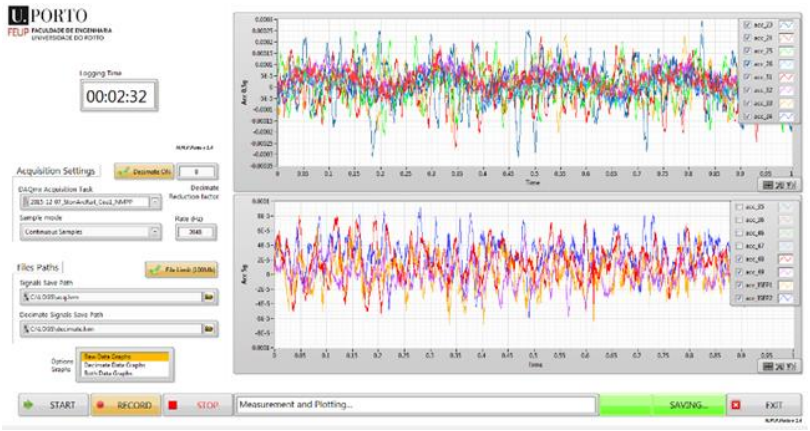

Figure 106. Visual aspect of the Labview® data acquisition system implemented, during the first trial.

The acceleration responses obtained were processed through EFDD method implemented on ARTEMIS [201] and the geometry of the sub-structure used as an input in the software is presented in Figure 107. This sub-structure consists in the dome roof and the 3 piers of the church. The points 2, 6, and 10, in Artemis input geometry, are interpolated nodes. Figure 108 presents the curves of the average normalized singular values of the spectral density matrices, containing the values of the accelerations measured in the two trials (setups), and where the peaks corresponding to 6 vibration modes of the church can be identified.

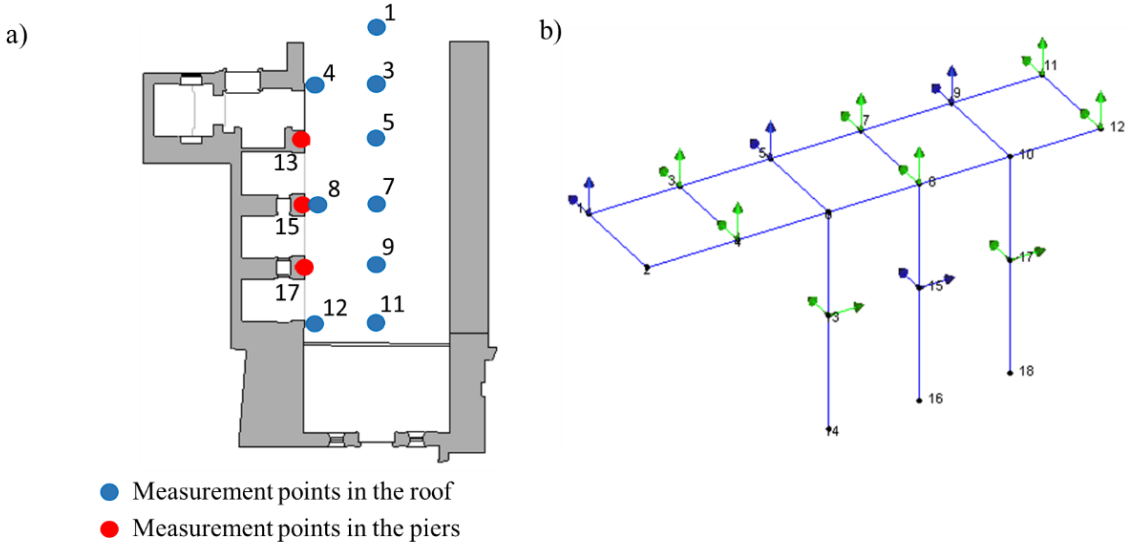

Figure 107. a) test setup and measurement points and b) corresponding geometry in Artemis.

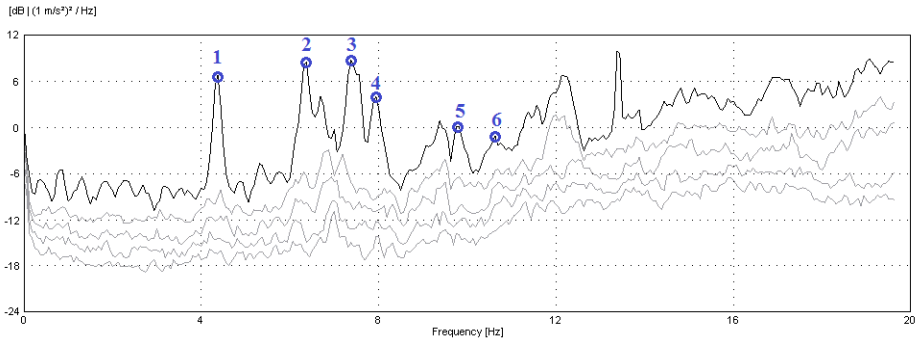

Figure 108. Enhance Frequency Domain Decomposition of the measured acceleration data collected by vibrational ambient characterization.

Figure 109, illustrates, in top or side view and in perspective, the identified modal configurations with an indication of the average values of frequencies (f) and damping coefficients (ζ).

The first vibration mode found has the frequency of 4.35 Hz and corresponds to a transversal mode of the sub-structure analyzed. The second mode found with a frequency of 6.36 Hz is the pure vertical bending mode of the dome roof. The third mode, with a frequency of 7.48 Hz is also a vertical bending mode but associated with some torsion. The fourth vibration mode found with a frequency of 7.93Hz is the second vertical bending mode of the dome roof. The fifth vibration mode found with a frequency of 9.85Hz is a torsional mode. The sixth mode found appeared to be a transversal mode with some torsion. The average values of the damping coefficients are between 0.40 and 2.03%.

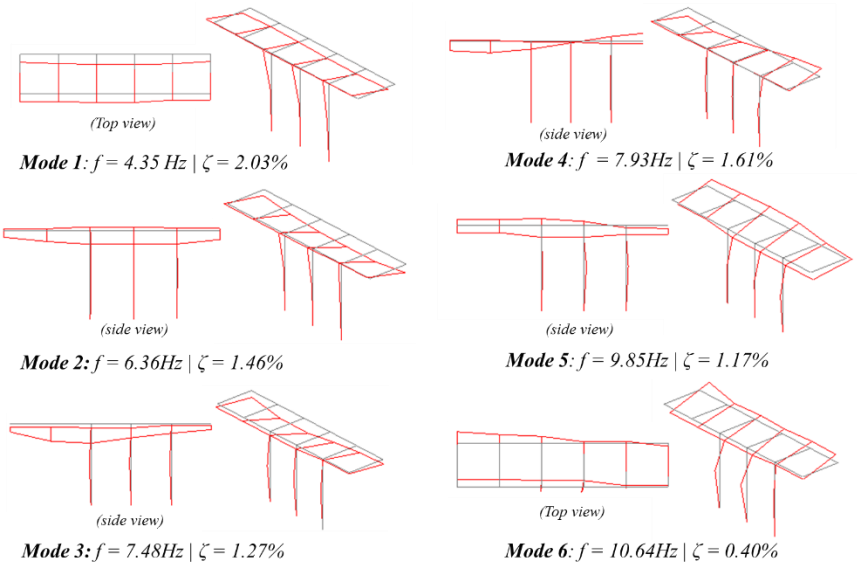

Figure 109. First six modal shapes of the Santo António Church.

6.6. Reliability analysis of the Santo António Church

As referred previously, the reliability analysis aims to provide objective response on structural safety. This way, the acceleration data of the first trial (Figure 110) were analyzed, and due to its amplitudes, the accelerations measured by accelerometers ACC01 and ACC16 are obviously candidates to the reliability analysis. In fact, this method is based on obtaining the displacements on two different directions from the acceleration data, through Expression 17, where s(t) is the displacement and a(t) represents the acceleration, booth in function of the time.

$$s(t) = \iint a(t)\, dt \qquad \text{(Expression 17)}$$

The relative displacements obtained by ACC01 and ACC16 correspond to the displacements on the X and Y directions, respectively. The histograms presented in Figure 111, for the X and Y directions, refer to the maximum displacements obtained on the first trial. For the Y direction, the Church's roof is more sensitive to environmental excitation than for the direction X, the maximum estimated displacements were 6.49×10^{-3} mm and 20.61×10^{-3} mm, in the X and Y directions, respectively.

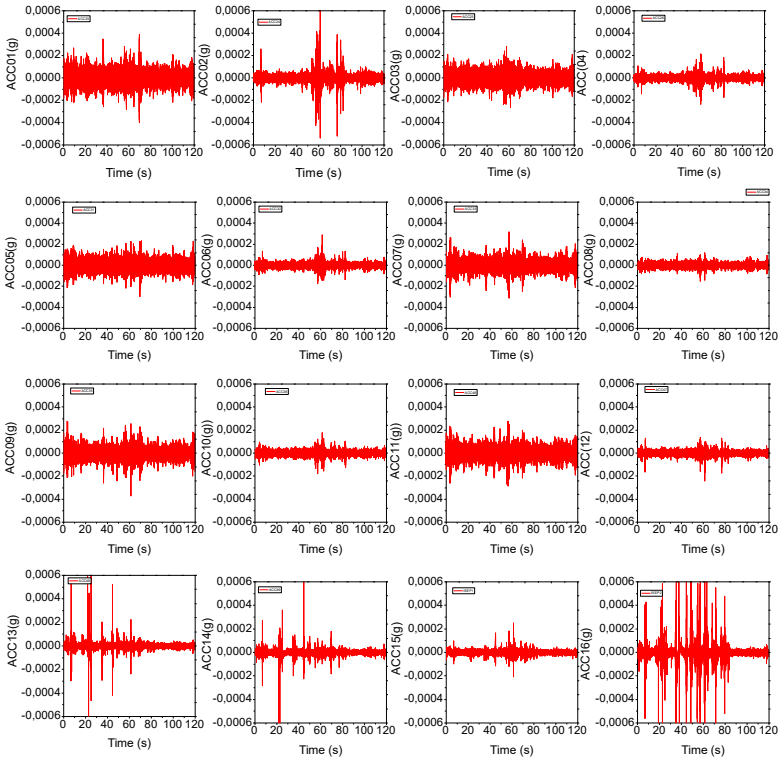

Figure 110. Acceleration data measured during the first trial.

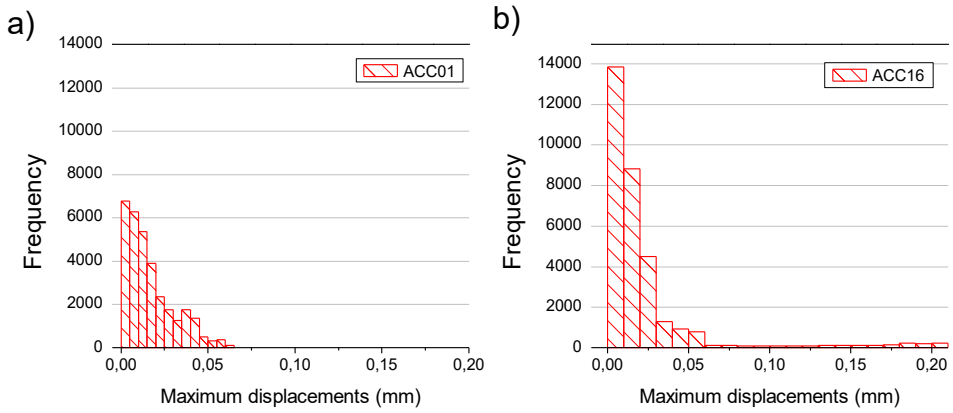

Figure 111. Maximum displacement histograms, on the X and Y directions for a) and b), respectively.

Sometimes due to the environmental excitation the initial condition of the motion does not correspond with "zero displacement" of the assessed structure. In this case, a fixed reference point need to be adopted and the acceleration records normalized before the double integration.

The GEV (Generalized Extremes Values) approach was used to estimate the frequency distribution of the maximum relative displacement values of the Santo Antonio Church roof, specifically through Gumbel distribution.

Once the values of average, μ, and standard deviation, δ, in the X and Y directions are calculated, the values of α and u are calculated based in the Expressions 15) and 16 and then the Expression 14 is employed, aiming to define of the probabilistic function *Fx(x)*. α and u can be estimated from the analyzed data set, and *x* is the limit exceedance values in the distribution curve that to be analyzed.

In fact, α and u values can be attained by expressions 15 and 16, where the variance $\mathbb{V}(X)$ is a required value for the determination of the α constant, and $\mathbb{E}(X)$ is the average of *Fx(x)* function.

Finally, the failure probability *Pf* was evaluated and the values of reliability index β were found using Expression 13. From the failure probability, *Pf*, the reliability index, β, can be estimated, considering Φ^{-1} as the inverse of the standard normal distribution function. In this analysis, the *R* (safety coefficient) was adopted as 30 mm, and considering the low displacements obtained during the experimental tests the displacements were enlarged 100 times for this analysis could be performed for demonstration of the proposed methodology.
Additionally, through Expressions 17 and 18, a predictive study about the reliability index evolution to the future, was performed employing the GEV.

$$\varepsilon_x(T) = \lambda - n\,.\ln\left[-\ln(1-\tfrac{1}{T})\right] \qquad \text{(Expression 17)}$$

where ε_x is the extreme value of a random variable, λ and *n* are constants to be determined according to data measured by statistic or graphic methods, and *T* is the return period. The ratio between of the GEV data in the future, ζ, is:

$$\zeta(s, t = T) = \frac{\varepsilon_x(T)}{\max(\varepsilon_1, \varepsilon_2, \varepsilon_3 \ldots \varepsilon_k)} \qquad \text{(Expression 18)}$$

For conservative considerations when the ζ value is lower than 1., it should be assigned as 1.

In this predictive reliability analysis, it was estimated that the annual number of times that the roof of Santo Antonio's Church is submitted to similar accelerations is 8736 (24 times per day). For the next *t* years it will be *T* = 8736 X *t*. The prediction was carried out to the following 5, 10, 15, 20, 25, 50 and 100 years.

After the predicted 5 years, up to the next 100 years, the β curves show a low and gradual decrement. All the predicted values of reliability for the next 100 years can be observed in Figure 112.

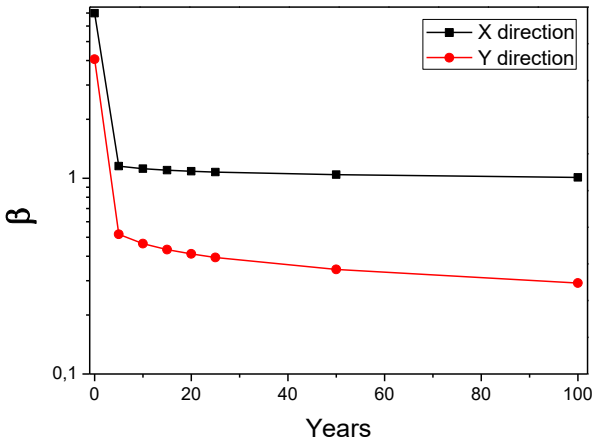

Figure 112. Reliability indexes of the Santo Antonio's Church from current state till next 100 years.

The initial β values, found for the X and Y directions, were 6.97 and 4.05, respectively. Considering the safety conditions previously stated in Section 6.2.4. the Santo Antonio's Church does not present risk (even with the displacements values considered in this reliability analysis enlarged 100 times), and can be classified in the safety condition II. As expected, direction Y is more sensitive to environmental excitation than X direction, therefore the β estimated to the Y direction are lower than the reliability values obtained on the X direction. Considering the β values in X direction, the variation ranges from 6.97 to 1.01 along the prediction time interval. In the Y direction, the β values ranges from 4.05 to 0.291.

6.7. Final comments

This work presented the strategies employed for the SHM strategy of a retrofitting process performed on the Santo Antonio Church, as well as describing the procedures followed for the modal characterization through OMA. In order to complement the structural

information collected by modal characterization, Pressuremeter testing was performed in the columns of the church, providing reliable data on its mechanic properties. Additionally, a new approach for HC assessment based on vibrational measurements, so-called RABVIM was proposed.

Concerning to SHM, the data collected, allowed the observation of the relative displacements and inclination during the retrofitting of the Santo Antonio Church, and to characterize the movements of the structural elements under monitoring. It was noted that the soil settlement was attenuated by retrofitting performed on the columns and that the roof retrofitting affected the displacements along of the longitudinal section of the columns. Moreover, it can be noted, through the monitoring results, the stabilization of the relative displacements on the monitored points after the Santo Antonio Church retrofitting.

The operational modal characterization allowed the identification of the six first natural frequencies and to characterize its respective modal shapes, as well as to provide useful data for the reliability assessment here presented. The first natural frequency of the Santo Antonio Church was identified as 4.35 Hz, and the mode characterized by transversal distortion. Essentially, the complexity and variability of the structural components of HC request a case-by-case approach for dynamic characterization and SHM, this way the present work also had contributed for the knowledge enlargement through description of the strategies employed for modal identification and SHM of the Santo Antonio Church.

Through Pressuremeter testing, it was possible to assess the mechanical properties of the Santo Antonio's Church after the retrofitting measures, and to estimate the Pressuremeter (or Ménard) modulus (E_{PMT}) for each column. Through the analysis of the pressure curves versus deformation it was possible to observe that E_{PMT} varies from 69.18 MPa to 98.65 MPa. However, analyzing only the P1, P3 and P5 columns, the E_{PMT} ranges from 82.17 MPa to 90.96MPa.

The use of the RABVIM revealed itself as an interesting technique for HC assessment, promoting an objective answer, in terms of β index, to the owners on the current structural safety. The case study carried out on Santo Antonio de Viana's Church provide an example on the applicability of the proposed methodology. Taking into account the large

number of uncertainties present in a structural system of the HC, the RABVIM should be adapted according to the necessities and risk scenarios of each case under study. Additionally, the safety assessment method here demonstrated can be an alternative and useful tool to support a real-time safety analysis of HC.

7

Conclusions and future work

Characterizing and monitoring heritage constructions constitute a new challenge opportunity for advances on civil engineering field. Therefore, this Thesis main contributions are supporting tools for the characterization and SHM of HC, namely through: 1) the development of new optical devices to be employed in SHM systems and 2) development of methodologies and strategies for the SHM of HC, with recurrence to case studies.

The literature review demonstrates that, since 1993, the main advances on the field of SHM occurred on the sensors developments area and strategies for employment of modal responses on SHM of large-scale structures (bridges, towers, offshore platforms, i.e.), as well shown the imminent necessity for the implementation of methodologies able to provide objective response to owners on the structural safety state and necessities.

Through the analyses of different SHM case studies reported in the literature, a method for classification of SHM platforms was developed and presented in this work (an extension of the method developed by Rytter), aiming to provide a most objective orientation to owners and technical team during the SHM system design.

Currently, approximately half of all innovation related with SHM field is dedicated to the new sensors development, which highlights the necessity of further advances on the other fields of SHM. Moreover, no SHM system or platforms is specifically addressed to HC assessment, making it a great opportunity for the development of studies and innovation on SHM. In fact, the literature review also demonstrates the existence of a lack of

knowledge on SHM dedicated to HC, making the implementation of studies related with it, a current necessity to be mitigated by technic-scientific community.

Due to the HC's structural variability and complex performance, there are many interesting cases to be considered on SHM development, imposing the necessity of flexible, non-intrusive and open SHM systems and platforms. The implementation of tools for the safety maintenance support, in real time, can be an effective way to avoid dramatic losses, especially for monuments and constructions with touristic activities.

Concerning the new optical sensors implemented during this Thesis, two prototypes of groundwater level monitoring sensors based on FBG were described, as well the relative displacement optical sensor devoted to bond-slip monitoring of old RC structures. The groundwater monitoring sensors are characterized by the present of grooves made along of the optical fiber length, with depth of 0.50 mm (sensor S050) and 0.25 mm (sensor S025) and experimentally tested. Both level sensors presented suitable performance for measurement of variations on water level, with an adequate sensitivity, demonstrating their applicability for *in situ* monitoring for water level monitoring. Nevertheless, the sensor S025 presented better performance than S050.

Regarding the relative displacement optical sensors, three prototypes for bond-slip monitoring of old RC structures were developed and experimentally tested. The results demonstrate that all the three implemented optical sensors were able to characterize the bond-slip displacements in the samples tested, as well to perform measures with high level of sensibility to micro-displacements. The experimental work also demonstrates the difference between the positioning of the sensors along of the rebar length and the relative displacements recorded, allowing the characterization of the pull-out displacement gradient along of the reinforcing bar.

The strategy for the bond-slip monitoring presented in this Thesis can be applied on existing RC structures, as a non-intrusive method without the necessity of removing samples from the structure. Furthermore, it is also possible to connect this monitoring system to the internet for long-term remote monitoring.

The strategy for the ambient vibration characterization of the Nossa Senhora das Dores Church, an heritage construction located in Sobral, Brazil, demonstrated that OMA can be a useful methodology to collect updating and supporting numerical analysis information. OMA allows the data acquisition on the current dynamic structural response of the HC, its safety analysis, as well as acting as a supporting tool to support the degradation monitoring and assessment of the church along time.

Finite element analysis guided the experimental setup design, nonetheless, OMA allowed the identification of the first five fundamental frequencies of the church, namely: 2.391 Hz, 2.880 Hz, 3.125 Hz, 3.466 Hz and 4.541 Hz, and the determination of its respective modal shapes. Considering the natural frequencies information collected by OMA, the numerical model built in 3D finite element was updated and the first twenty modal shapes were extracted, which allowed to recognize that modal displacements in the transversal axis represent a larger percentage of effective modal mass for modal shapes than in the longitudinal axis. Additionally, the results of the linear static analysis carried out allowed to build the graphical representation of the Von-Mises stresses and normal stresses (in the vertical axis) distribution on the Nossa Senhora das Dores Church. Subsequently, the dynamic characterization performed on the Church, represent a real contribution for the knowledge on the structural behavior of Brazilian heritage constructions, once the strategy employed demonstrates its ability to collect reliable support information for the maintenance decision.

The SHM of Foz Côa Church, located in Foz Côa, Portugal, allowed to study the environmental effects influence, namely temperature and relative humidity, on the structural displacements. Also, the relation between the thermal effects and the structural displacements was establish, allowing to estimate the structural movements provoked by thermal ambient cycles. Similarly, the removal of the thermal effect, as well the study of the combined temperature-relative humidity effect, allowed to conclude that the movements observed on the elements monitored are not related with structural issues. Moreover, the data collected along 1-year of monitoring allowed to collect accurate and reliable data on the relative displacements on stone structures provoked by environmental actions, suitable to support an adequate interpretation of the SHM results.

Following, the strategies employed for SHM retrofitting process, performed on the Santo Antonio Church, located in Viana do Castelo, Portugal, as well as the procedures description for the modal characterization through OMA were presented in this Thesis. Also, a Pressuremeter testing was performed in order to characterize the mechanical properties of the columns, and the results discussed. Furthermore, a new approach for HC assessment based on vibrational measurements, so-called RABVIM was proposed.

The SHM of the Santo António Church, allowed the observation of the relative displacements and inclination during the retrofitting process, and to characterize the movements of the structural elements under monitoring. From the results, it was noticed that the soil settlement was attenuated by the retrofitting performed on the columns, and that the roof retrofitting affected the displacements along of the longitudinal section of the columns. Moreover, based on the data collected by the SHM, a stabilization of the relative displacements of the structural elements monitored was noticed.

The operational modal characterization of the Santo António Church allowed the identification of the six first natural frequencies, and to characterize its respective modal shapes, providing useful data for the reliability assessment. The first natural frequency of the Santo Antonio Church was identified as 4.35 Hz, and the its mode shape characterized by transversal distortion. From the Pressuremeter testing, it was possible to characterize the mechanical properties of the Santo Antonio Church elements, after the retrofitting measures, and to estimate the Pressuremeter (or Ménard) modulus (E_{PMT}) for each column, as well to observe that E_{PMT} varies from 69.18 MPa to the maximum value of 98.65 MPa.

The use of the reliability methodology proposed in this Thesis, designated as RABVIM, revealed itself as an interesting technique for HC assessment, providing an objective answer, in terms of β index, to support the owners during the structural safety assessment. The Santo Antonio de Viana Church case study, provided a demonstration of applicability of the proposed methodology. Considering the uncertainties present in a HC structural system, the RABVIM should be adapted according to the particular necessities and risk scenarios of each case under study. Furthermore, the safety assessment method, demonstrated here, can be an alternative and useful tool to support a real-time safety analysis of HC.

The tools developed and presented in this Thesis contributed significantly for the broadening and dissemination of knowledge on the SHM field dedicated to HC, particularly to sensorial system advances and to the implementation of strategies and methodologies for safety assessment. Also, the experimental results found in this work are useful information for better understanding the structural behavior of HC.

In summary, this work also contributes for innovation in the HC assessment process, and for risk minimization. The employment of new SHM systems provide a non-destructive and non-intrusive assessment methodology as well, it can also be used for early structural damage detection. Moreover, the possibility of remote access to structural data collected by the sensing system can minimize the time needed to the assessment process, and to enable the structural safety management of a large number of buildings from a single place.

Throughout this work, several issues on SHM were discussed. Particularly, different aspects of the SHM, from the design phase to the data processing, recurring to real case studies. These aspects, and the main difficulties found during the development of this work, are disused next, as well as a synthesis of the main advances for the SHM field.

Typically, a SHM process can be divided into the following steps:

- *design*, where the main objectives of the system and its response level should be defined;
- *data collect*, where the system must be recording the data for further processing;
- *data processing and diagnosis*, where the data acquisition over the time needs to be processed and the structural state estimated.

Indeed, the data collecting is related with the time needed to characterize a damage situation, varying between short and long-term monitoring. In general, short-term monitoring is employed when the main aim of the monitoring system is to analyse retrofitting or maintenance measures on structural behavior, or when a few months of monitoring are requested, as for instance, the case of Santo António Church. On the other hand, long-term monitoring is commonly employed when a damage progression, or a long-term effect should be monitored, and years of monitoring are requested, as the case study of the Foz Côa Church. The longer the SHM is working, more storage capacity will

be request, and more complex and slower the data processing will be. In truth, with advances on computational tools, specifically the development of tools of real-time data processing, the data collecting and data processing steps tends to become a unique step, allowing the user not only to see the data collected in real time but also to check its real-time impact on the structural behavior.

To design a SHM system for HC monitoring can be a complex task, specifically because the large variety of damage scenarios and their origin that need to be identified. Regarding HC, commonly, the existing structure information is obtained from several sources, requesting a considerable time to its systematization. For instance, in the case of São Lourenço Church, at least six months were needed to collect sufficient data for a comprehensive view on its structural situation. An integrated platform, combining information from historic registers, architectural data, structural retrofits, maintenance measures, history of damage observations and progress, and changes in the structural system, can be a great opportunity for further developments on the HC information systematization, with impact on the assessment process optimization.

After a comprehensive review on the HC evolution, a visual inspection should be carried out, in order to check the information previously collected and to analyze the current condition of the building. The structural history evolution is important to understand the structural system components and to define the first hypothesis on its behavior. Afterwards, the damage mapping can suggest further evidences on the damage mechanisms and how they can affect the structural safety, and the damage characteristics are essential to the design of the sensorial system.

Considering the case study of the São Lourenço Church, the identification of cracks, relative displacements and rotations on structural components, defined the sensors to be used, such as linear differential variable transformers (LVDT's), FBG displacement sensors and inclination sensors. Nonetheless, the sensors positioning was selected according with the damages characteristics found along the church. Crossing information contributes for the optimization of the sensorial system, avoiding the employment of inappropriate sensors to structural behavior understanding. In fact, at this point, it's also important the definition of the SHM system response level. According to the SHM

platforms classification methodology, proposed in this Thesis, the response level can vary from Level 1 to Level 5.

After the sensorial system definition, the architecture of the SHM system should be defined, corresponding to the method that the several system components will communicate between them. Based on the IC-FEUP experience, around fifteen years ago, all monitoring system components were connect using cables, and the data storage capability was limited to the available memories cards. The sensorial systems presented a simple configuration, and the employment of different sort of sensors in the same system was not usual. However, while the data communication was advancing, new technologies, such as wireless systems are being more used.

Perhaps, the SHM design should be considered as the most import stage. Especially because all following steps and further data analysis will be based on its ability to collect reliable data. Notably, this step goes till the installation of the SHM system on the structural elements, that must also take into account the importance of the low visual impact demands of the heritage constructions, especially the ones open to public visits. In general, the procedures followed during the design step vary according with several factors, such as the construction typology and technical team experience. However, efforts focused on the definition of common good practices and standardization of the SHM of HC have been noticed in the last ten years, as can be cited the Bulletin number 11 of the *Associación Latinoamericana de Control de Calidad, Patología y Recuperación de la Construción* – ALCONPAT.

Within the next step is the data collecting process, comprising the time period in which the SHM system is recording data. The costs associated with this step are deeply related with the quantity of measured data, data acquisition frequency and the time duration of the monitoring, as expected, long-term monitoring will request a higher storage capacity of the system. Concerning the cost of a SHM system, for instance, the system employed in the case study of Foz Côa Church (which included: with 2 data acquisition systems, 2 temperature sensors, 2 relative humidity sensors, 3 LVDT's, 1 inclinometer, 1 potentiometer) during 2 years of monitoring, the data collection represent around 46% of the total costs, while the monitoring system can represent 56% of the remaining costs. Moreover, although the current cases of SHM of HC reported in the support literature are

addressed predominantly to examples where the damage situations is known, the employment of sensorial systems to deal with the damage emergence will be the next step. The use of nanotechnologies and sensors integrated with the construction or repairing materials (smart materials) with remote communication capabilities, will be each more used. Even if the data collecting can be considered as an autonomous step, without human intervention (on the autonomous systems), eventual technical interventions may be required, in order to check the system conditions.

The data processing comprises the treatment and analysis of the recorded data in order to obtain information on structural behavior of the HC. In general, the data are individually processed and then, globally analyzed, and essentially, this step need to be in line with the response level requested. Several data processing methods can be employed, from the ones focused on data reduction (such as filtering, averaging, …), to the ones to remove an affect, such as the thermal. In this work, for instance, all the data of the monitoring cases was reduced, and in the case of the Foz Côa Church, the effect of the temperature was removed in order to understand if the existing displacements were related with structural issues. Moreover, the Santo António Church case study allowed the employment of a probabilistic analysis, since the main goal of this work was to state an objective answer on the structural safety condition.

Based on above mentioned, SHM represents an interesting and useful tool for collecting reliable data, allowing the characterization and structural assessment of HC. The high cost of its implementation is still a negative argument for SHM large employment on HC, nevertheless the advances on sensors, data acquisition and transmission devices are evolving and contributing for this issue mitigation. Non-destructive assessment, long-term characterization, possibility of real time and remote assessment can be listed as the main advances provided by the SHM implementation.

Finally, during this Thesis development relevant necessities and opportunities for advances on SHM of HC were identified, among them, the main suggestions for further work on this topic are:

- the development and implementation of methodologies and tools focused to HC for optimization and systematization of the all available information, comprising architectural, structural and retrofit history information, as well as to allow the

introduction of inspection reports carried out and the interaction with the users/owners;

- the development of integration methodologies aiming to correlate SHM and virtual information models;
- implementation of new case studies on SHM, comprising different HC typologies, especially focused on structural behavior characterization and damage assessment;
- advancing on strategies for monitoring of HC and it data processing, focusing the safety maintenance;
- the standardization of the HC monitoring procedures and the implementation of methodologies for safety assessment;
- the development and implementation of new sensors for structural monitoring applications, especially optical fiber sensors;

References

[1] P. B. Lourenço, "The ICOMOS methodology for conservation of cultural heritage buildings : concepts , research and application to case studies," in *Proceedings of the International Conference on Preservation, Maintenance and Rehabilitation of Historic Buildings and Structures*, 2014, 1st ed., p. 12.

[2] G. Brandonisio, G. Lucibello, E. Mele, and A. De Luca, "Damage and performance evaluation of masonry churches in the 2009 L'Aquila earthquake," *Eng. Fail. Anal.*, vol. 34, pp. 693–714, 2013.

[3] D. Silveira, H. Varum, and A. Costa, "Rehabilitation of an important cultural and architectural heritage : the traditional adobe constructions in Aveiro district," *WIT Transit. Ecol. Environ.*, vol. 102, pp. 705–714, 2007.

[4] CIB, *Guide for the Structural Rehabilitation of Heritage Buildings*, 1st ed. Rotterdam: CIB, 2010.

[5] P. del C. dei Ministri, *Linee guida per la valutazione e la riduzione del rischio sismico del patrimonio culturale con riferimento alle Norme Tecniche per le Costruzioni di cui al decreto del Ministero delle Infrastrutture e dei trasporti del 14 gennaio 2008 (09/02/2011)*, vol. 1, no. c. Italy, 2011, pp. 1–83.

[6] E. Mesquita, E. Paupério, A. Arêde, and H. Varum, "Tehnical Report N 11 - Characterization, evaluation and structural recovery of historic buildings," Mérida, 2015.

[7] J. P. Lynch and K. J. Loh, "A summary review of wireless sensors and sensor networks for structural health monitoring," *Shock Vib. Dig.*, vol. 38, no. 2, pp. 91–130, 2006.

[8] A. De Stefano, E. Matta, and P. Clemente, "Structural health monitoring of historical heritage in Italy: some relevant experiences," *J. Civ. Struct. Heal. Monit.*, vol. 6, no. 1, pp. 83–106, 2016.

[9] G. Boscato, A. Dal Cin, S. Ientile, and S. Russo, "Optimized procedures and strategies for the dynamic monitoring of historical structures," *J. Civ. Struct. Heal. Monit.*, vol. 6, no. 2, pp. 265–289, 2016.

[10] F. Potenza, F. Federici, M. Lepidi, V. Gattulli, F. Graziosi, and A. Colarieti, "Long-term structural monitoring of the damaged Basilica S. Maria di Collemaggio through a low-cost wireless sensor network," *J. Civ. Struct. Heal. Monit.*, vol. 5, no. 5, pp. 655–676, 2015.

[11] V. Gattulli, M. Lepidi, and F. Potenza, "Dynamic testing and health monitoring of historic and modern civil structures in Italy," vol. 3, no. 1, pp. 71–90, 2016.

[12] P. Antunes, "Sensores ópticos para monitorização dinâmica de estruturas," Universidade de Aveiro, 2011.

[13] X. W. Ye, Y. H. Su, and J. P. Han, "Structural Health Monitoring of Civil

Infrastructure Using Optical Fiber Sensing Technology: A Comprehensive Review.," *ScientificWorldJournal.*, vol. 2014, p. 652329, Jan. 2014.

[14] A. Barrias, J. R. Casas, and S. Villalba, "A Review of Distributed Optical Fiber Sensors for Civil Engineering Applications," *Sensors*, vol. 16, no. 748, pp. 1–35, 2016.

[15] H. F. Lima, R. D. S. Vicente, R. N. Nogueira, I. Abe, P. S. D. B. Andre, C. Fernandes, H. Rodrigues, H. Varum, H. J. Kalinowski, A. Costa, and J. D. L. Pinto, "Structural Health Monitoring of the Church of Santa Casa da Misericórdia of Aveiro Using FBG Sensors," *IEEE Sens. J.*, vol. 8, no. 7, pp. 1236–1242, 2008.

[16] K. Mehta, "Greening of the Concrete Industry for Sustainable Development," *Concr. Int.*, vol. 24, no. 7, pp. 23–28, 2002.

[17] Euroconstruct, "77th Euroconstruct Summary Report," Oslo, 2014.

[18] K. Mehta and P. J. M. Monteiro, *Concreto: microestrutura, propriedades e materiais.*, 3 ed. São Paulo: Pini, 2008.

[19] G. Milani, "Lesson learned after the Emilia-Romagna, Italy, 20-29 May 2012 earthquakes: A limit analysis insight on three masonry churches," *Eng. Fail. Anal.*, vol. 34, pp. 761–778, 2013.

[20] B. Zhu and D. M. Frangopol, "Incorporation of structural health monitoring data on load effects in the reliability and redundancy assessment of ship cross-sections using Bayesian updating," *Struct. Heal. Monit.*, vol. 12, no. 4, pp. 377–392, Jul. 2013.

[21] P. Omenzetter, J. M. W. Brownjohn, and P. Moyo, "Identification of unusual events in multi-channel bridge monitoring data," *Mech. Syst. Signal Process.*, vol. 18, no. 2, pp. 409–430, Mar. 2004.

[22] N. M. Okasha and D. M. Frangopol, "Computational platform for the integrated life-cycle management of highway bridges," *Eng. Struct.*, vol. 33, no. 7, pp. 2145–2153, Jul. 2011.

[23] N. De Battista, J. M. W. Brownjohn, H. P. Tan, and K. Koo, "Measuring and modelling the thermal performance of the Tamar Suspension Bridge using a wireless sensor network," *Struct. Infrastruct. Eng.*, vol. 11, no. 2, pp. 176–193, 2014.

[24] N. Wu, C. Liu, Y. Guo, and J. Zhang, "On-Board Computing for Structural Health Monitoring with Smart Wireless Sensors by Modal Identification Using Hilbert-Huang Transform," *Math. Probl. Eng.*, vol. 2013, pp. 1–9, 2013.

[25] S. Jang, B. F. Spencer Jr, and S.-H. Sim, "A decentralized receptance-based damage detection strategy for wireless smart sensors," *Smart Mater. Struct.*, vol. 21, no. 5, p. 055017, May 2012.

[26] T. S. . Fu, "Smart buildins: synergy in structural control, structural health monitoring and environmental systems," University of Southern California, 2009.

[27] Munich RE, “Natural Catastrophes 2011. Analyses, assessments, positions.,” *Top. Geo*, 2012.

[28] I. Schumacher and E. Strobl, “Economic development and losses due to natural disasters: The role of hazard exposure,” *Ecol. Econ.*, vol. 72, pp. 97–105, Dec. 2011.

[29] Z. Zhengtang, “Natural Catastrophe Risk, Insurance and Economic Development,” *Energy Procedia*, vol. 5, pp. 2340–2345, Jan. 2011.

[30] Munich RE, “TOPICS GEO: Natural catastrophes 2015,” Munich, 2016.

[31] E. Skoufias, “Economic Crises and Natural Disasters: Coping Strategies and Policy Implications,” *World Dev.*, vol. 31, no. 7, pp. 1087–1102, Jul. 2003.

[32] United Nations, “The future we want,” Rio de Janeiro, 2012.

[33] P. Helene, “A nova NB 1/2003 (NBR 6118) e a vida útil das estruturas de concreto,” in *Anais do 52º Congresso Brasileiro do Concreto*, 2010, vol. 2003, no. Nbr 6118, p. 31.

[34] X. Shi, N. Xie, K. Fortune, and J. Gong, “Durability of steel reinforced concrete in chloride environments: An overview,” *Constr. Build. Mater.*, vol. 30, pp. 125–138, May 2012.

[35] K. Kovler and N. Roussel, “Properties of fresh and hardened concrete,” *Cem. Concr. Res.*, vol. 41, no. 7, pp. 775–792, Jul. 2011.

[36] V. C. D. O. Pereira, E. C. B. Monteiro, and K. D. S. Almeida, “Influence of cement type in reinforcement corrosion of mortars under action of chlorides,” *Constr. Build. Mater.*, vol. 40, pp. 710–718, Mar. 2013.

[37] K. Yoda and A. Shintani, “Building application of recycled aggregate concrete for upper-ground structural elements,” *Constr. Build. Mater.*, vol. 67, pp. 379–385, Sep. 2014.

[38] F. Schmidt, M. Rheinfurth, R. Protz, P. Horst, G. Busse, M. Gude, and W. Hufenbach, “Monitoring of multiaxial fatigue damage evolution in impacted composite tubes using non-destructive evaluation,” *Compos. Part A Appl. Sci. Manuf.*, vol. 43, no. 3, pp. 537–546, Mar. 2012.

[39] M. Faifer, L. Ferrara, R. Ottoboni, and S. Toscani, “Low frequency electrical and magnetic methods for non-destructive analysis of fiber dispersion in fiber reinforced cementitious composites: an overview.,” *Sensors (Basel).*, vol. 13, no. 1, pp. 1300–18, 2013.

[40] C. Rainieri, G. Fabbrocino, and G. M. Verderame, “Non-destructive characterization and dynamic identification of a modern heritage building for serviceability seismic analyses,” *NDT E Int.*, vol. 60, pp. 17–31, Dec. 2013.

[41] W. S. de Assis, “Sistemas computacionais de apoio à monitoração de estruturas de engenharia civil,” Universidade de São Paulo, 2007.

[42] Y. Xia, P. Zhang, Y. Ni, and H. Zhu, “Deformation monitoring of a super-tall structure using real-time strain data,” *Eng. Struct.*, vol. 67, pp. 29–38, May 2014.

[43] D. E. Adams, *Health Monitoring of Structural Materials and Components: Methods with Applications*, 1st ed. Hoboken, 2007.

[44] H. Sohn, C. R. Farrar, F. M. Hemez, D. D. Shunk, D. W. Stinemates, B. R. Nadler, and J. J. Czarnecki, "A review of structural health monitoring literature: 1996-2001," Los Alamos National Laboratory, Los Angeles, 2004.

[45] J. M. W. Brownjohn, "Structural health monitoring of civil infrastructure.," *Philos. Trans. A. Math. Phys. Eng. Sci.*, vol. 365, no. 1851, pp. 589–622, Feb. 2007.

[46] S. W. Doebling, C. R. Farrar, and M. B. Prime, "A summary review of vibration-based damage identification methods," Los Alamos, NM, 1997.

[47] J. M. Lifshitz and A. Rotem, "Determination of Reinforcement Unbonding of Composites by a Vibration Technique," *J. Compos. Mater.*, vol. 3, pp. 412–423, 1969.

[48] A. Rytter, "Vibrational based inspection of civil engineering structures," University of Aalborg, 1993.

[49] H. Sohn, "Effects of environmental and operational variability on structural health monitoring.," *Philos. Trans. A. Math. Phys. Eng. Sci.*, vol. 365, no. 1851, pp. 539–60, Feb. 2007.

[50] R. Jacques, T. Clarke, S. Morikawa, and T. Strohaecker, "Monitoring the structural integrity of a flexible riser during dynamic loading with a combination of non-destructive testing methods," *NDT E Int.*, vol. 43, no. 6, pp. 501–506, Sep. 2010.

[51] E. H. . Clayton, "Frequency correlation-based structural health monitoring with smart wireless sensors," *Master's Tesis Civ. Enginieering Washingt. Univ.*, vol. 1, p. 111, 2006.

[52] M. Kianian, a. a. Golafshani, and E. Ghodrati, "Damage detection of offshore jacket structures using frequency domain selective measurements," *J. Mar. Sci. Appl.*, vol. 12, no. 2, pp. 193–199, May 2013.

[53] G.-R. Gillich and Z.-I. Praisach, "Modal identification and damage detection in beam-like structures using the power spectrum and time–frequency analysis," *Signal Processing*, vol. 96, pp. 29–44, Mar. 2014.

[54] S. W. Doebling, C. R. Farrar, M. B. Prime, and D. W. Shevitz, *Damage identification and health monitoring of structural and mechanical systems from changes in their vibration characteristics: A literature review*, 1 ed. Los Alamos, NM: Los Alamos, 1996.

[55] K. Worden, C. R. Farrar, G. Manson, and G. Park, "The fundamental axioms of structural health monitoring," *Proc. R. Soc. A Math. Phys. Eng. Sci.*, vol. 463, no. 2082, pp. 1639–1664, Jun. 2007.

[56] C. R. Farrar and K. Worden, "An introduction to structural health monitoring.," *Philos. Trans. A. Math. Phys. Eng. Sci.*, vol. 365, no. 1851, pp. 303–15, Feb. 2007.

[57] H. Wenzel, *Health monitoring of bridges*, 1st ed. Chichester, UK: John Wiley & Sons, 2008.

[58] C. Rodrigues, C. Félix, A. Lage, and J. Figueiras, "Development of a long-term

monitoring system based on FBG sensors applied to concrete bridges," *Eng. Struct.*, vol. 32, no. 8, pp. 1993–2002, 2010.

[59] A. Mita, H. Sato, and H. Kameda, "Platform for structural health monitoring of buildings utilizing smart sensors and advanced diagnosis tools," *Struct. Control Heal. Monit.*, vol. 17, no. 7, pp. 795–807, Nov. 2010.

[60] O. Antón, R. Hidalgo, R. Rivera, and F. G. Tomasel, "Simple swept-sine analyzer for excitation and measurement of dynamic response in ocean structures," *Ocean Eng.*, vol. 29, no. 10, pp. 1209–1217, Aug. 2002.

[61] P. Antunes, J. Dias, T. Paixão, E. Mesquita, H. Varum, and P. André, "Liquid level gauge based in plastic optical fiber," *Measurement*, no. January, 2015.

[62] P. Antunes, H. Rodrigues, R. Travanca, L. Ferreira, H. Varum, and P. André, "Structural health monitoring of different geometry structures with optical fiber sensors," *Photonic Sensors*, vol. 2, no. 4, pp. 357–365, Oct. 2012.

[63] W. Carlos, D. S. Barbosa, E. Jaricuna, P. De Albuquerque, S. Soares, D. A. Melo, and Y. Nagato, "Theoretical and Experimental Study of Punching Strength of Flat Slabs with Reentrant," pp. 1–16, 2008.

[64] S.-H. Sim, J. F. Carbonell-Márquez, B. F. Spencer, and H. Jo, "Decentralized random decrement technique for efficient data aggregation and system identification in wireless smart sensor networks," *Probabilistic Eng. Mech.*, vol. 26, no. 1, pp. 81–91, Jan. 2011.

[65] S. G. Trost, K. L. Mciver, and R. R. Pate, "Conducting accelerometer-based activity assessments in field-based research," *Med. Sci. Sport. Exerc.*, vol. 3711, pp. 531–543, 2005.

[66] J. Wu, S. Yuan, S. Ji, G. Zhou, Y. Wang, and Z. Wang, "Multi-agent system design and evaluation for collaborative wireless sensor network in large structure health monitoring," *Expert Syst. Appl.*, vol. 37, no. 3, pp. 2028–2036, Mar. 2010.

[67] P. Antunes, H. Lima, H. Varum, and P. André, "Optical fiber sensors for static and dynamic health monitoring of civil engineering infrastructures: Abode wall case study," *Measurement*, vol. 45, no. 7, pp. 1695–1705, 2012.

[68] WIPO, "World Intellectual Property Organization," 2014. [Online]. Available: http://www.wipo.int/portal/en/index.html. [Accessed: 14-Feb-2014].

[69] C. G. Chiorean, "A computer method for nonlinear inelastic analysis of 3D composite steel–concrete frame structures," *Eng. Struct.*, vol. 57, pp. 125–152, Dec. 2013.

[70] W. D. Nothwang, S. G. Hirsch, J. D. Demaree, C. W. Hubbard, M. W. Cole, B. Lin, and V. Giurgiutiu, "Direct Integration of Thin Film Piezoelectric Sensors With Structural Materials for Structural Health Monitoring," *Integr. Ferroelectr.*, vol. 83, no. 1, pp. 139–148, Nov. 2006.

[71] EPO, "European Patent Office," 2014. [Online]. Available: http://www.epo.org/. [Accessed: 15-Feb-2014].

[72] USPTO, "United States Patent and Trademark Office," 2014. [Online]. Available: http://www.uspto.gov/. [Accessed: 20-Feb-2014].

[73] McKeown Berin, "System, device and associated methods for monitoring a physical condition or operating performance of a structure," 20130132032, 2013.
[74] G. S. B., "Software to facilitate design, data flow and decision support in structural health monitoring systems," 20120123981, 2012.
[75] S. Xiaodan, "Integral and local information fusing method of structure health diagnosis," CN102034021, 2011.
[76] D. Mathaeus, R. Ciprian, T. N. Cihan, and N. Claus, "Scalable and extensible framework for storing and analyzing sensor data," US20110035187, 2011.
[77] I. Jeong-Beom, "Virtual time reversal acoustics for structural health monitoring," 20090083004, 2009.
[78] I. Jeong-Beom, "Method and apparatus for modeling responses for a material to various inputs," US20090048721, 2009.
[79] K. G. Peter, "System and method for optical sensor interrogation," 20070223003, 2007.
[80] L. Zhou, G. Yan, L. Wang, and J. Ou, "Review of Benchmark Studies and Guidelines for Structural Health Monitoring," *Adv. Struct. Eng.*, vol. 16, no. 7, pp. 1187–1206, Jul. 2013.
[81] E. A. Johnson, H. F. Lam, L. S. Katafygiotis, and J. L. Beck, "Phase I IASC-ASCE Structural Health Monitoring Benchmark Problem Using Simulated Data," *J. Eng. Mech.*, vol. 130, no. 1, pp. 3–15, 2004.
[82] ISIS Canada, *Guidelines for Structural Health Monitoring*, 1st ed. Winnipeg: ISIS Canada, 2001.
[83] K. Bergmeister, "Monitoring and Safety Evaluation of Existing Concrete Structures "," Switzerland, 2002.
[84] A. E. Aktan, F. N. Catbas, K. A. Grimmelsman, and M. Pervizpour, "Development of a model health monitoring guide for major bridges," Philadelphia, 2002.
[85] ISO, *Mechanical vibration - Evaluation of measurement results from dynamic tests and investigations on bridges*. Switzerland: ISO, 2004, p. 26.
[86] W. Rucker, F. Hille, and R. Rohrmann, "Guideline for structural health monitoring," Berlin, 2006.
[87] P. W. Rücker, D. F. Hille, and D. R. Rohrmann, "Guideline for assessment of existing structures," Berlin, 2006.
[88] W. Daum, "Guidelines for Structural Health Monitoring," in *Handbook of Technical Diagnostics*, Springer, 2013, pp. 539–541.
[89] J. M. Nichols, "Structural health monitoring of offshore structures using ambient excitation," *Appl. Ocean Res.*, vol. 25, no. 3, pp. 101–114, Jun. 2003.
[90] S. Minakuchi and N. Takeda, "Recent advancement in optical fiber sensing for aerospace composite structures," *Photonic Sensors*, vol. 3, no. 4, pp. 345–354, Oct. 2013.
[91] X. Lin, L. Ren, Y. Xu, N. Chen, H. Ju, J. Liang, Z. He, E. Qu, B. Hu, and Y. Li, "Low-Cost Multipoint Liquid-Level Sensor With Plastic Optical Fiber," *IEEE*

Photonics Technol. Lett., vol. 26, no. 16, pp. 1613–1616, Aug. 2014.

[92] J. M. W. Brownjohn, F. Magalhaes, E. Caetano, and A. Cunha, "Ambient vibration re-testing and operational modal analysis of the Humber Bridge," *Eng. Struct.*, vol. 32, no. 8, pp. 2003–2018, Aug. 2010.

[93] F. Magalhães, a. Cunha, and E. Caetano, "Vibration based structural health monitoring of an arch bridge: From automated OMA to damage detection," *Mech. Syst. Signal Process.*, vol. 28, pp. 212–228, 2012.

[94] N. Martins, E. Caetano, S. Diord, F. Magalhães, and Á. Cunha, "Dynamic monitoring of a stadium suspension roof: Wind and temperature influence on modal parameters and structural response," *Eng. Struct.*, vol. 59, pp. 80–94, 2014.

[95] P. Razi, R. a. Esmaeel, and F. Taheri, "Improvement of a vibration-based damage detection approach for health monitoring of bolted flange joints in pipelines," *Struct. Heal. Monit.*, vol. 12, no. 3, pp. 207–224, Mar. 2013.

[96] R. P. Bandara, T. H. Chan, and D. P. Thambiratnam, "Structural damage detection method using frequency response functions," *Struct. Heal. Monit.*, vol. 13, no. 4, pp. 418–429, Feb. 2014.

[97] Z. Nie, H. Hao, and H. Ma, "Using vibration phase space topology changes for structural damage detection," *Struct. Heal. Monit.*, vol. 11, no. 5, pp. 538–557, May 2012.

[98] A. Naghashpour and S. Van Hoa, "A technique for real-time detecting, locating, and quantifying damage in large polymer composite structures made of carbon fibers and carbon nanotube networks," *Struct. Heal. Monit.*, vol. 14, no. 1, pp. 35–45, Sep. 2014.

[99] A. D'Alessandro, F. Ubertini, A. L. Materazzi, S. Laflamme, and M. Porfiri, "Electromechanical modelling of a new class of nanocomposite cement-based sensors for structural health monitoring," *Struct. Heal. Monit.*, vol. 14, no. 2, pp. 137–147, Mar. 2015.

[100] D. Hosser, C. Klinzmann, and R. Schnetgöke, "A framework for reliability-based system assessment based on structural health monitoring," *Struct. Infrastruct. Eng.*, vol. 4, no. 4, pp. 271–285, Aug. 2008.

[101] T. Yi, H. Li, and M. Gu, "Full-scale measurements of dynamic response of suspension bridge subjected to environmental loads using GPS technology," *Sci. China Technol. Sci.*, vol. 53, no. 2, pp. 469–479, Feb. 2010.

[102] W. Zhang, J. Gao, B. Shi, H. Cui, and H. Zhu, "Health monitoring of rehabilitated concrete bridges using distributed optical fiber sensing," *Comput. Civ. Infrastruct. Eng.*, vol. 21, pp. 411–424, 2006.

[103] Y. Q. Ni and K. Y. Wong, "Integrating Bridge Structural Health Monitoring and Condition-Based Maintenance Management," in *Civil Structural Health Monitoring Workshop (CSHM-4)*, 2012.

[104] T. Guo, A. Li, and H. Wang, "Influence of ambient temperature on the fatigue damage of welded bridge decks," *Int. J. Fatigue*, vol. 30, no. 6, pp. 1092–1102, Jun. 2008.

[105] A. Tavares, A. Costa, and H. Varum, *Manual de manutenção de edifícios em adobe*, 1st ed., vol. 24, no. 4. Aveiro: PUBLINDÚSTRIA, 2014.

[106] D. Abruzzese, M. Angelaccio, R. Giuliano, L. Miccoli, and A. Vari, "Monitoring and vibration risk assessment in cultural heritage via Wireless Sensors Network," *2009 2nd Conf. Hum. Syst. Interact.*, pp. 568–573, May 2009.

[107] L. Bencini, G. Collodi, D. Di Palma, G. Manes, and A. Manes, "An Embedded Wireless Sensor Network System for Cultural Heritage Monitoring," *2010 Fourth Int. Conf. Sens. Technol. Appl.*, pp. 185–190, Jul. 2010.

[108] D. Balsamo, G. Paci, L. Benini, and B. Davide, "Long term, low cost, passive environmental monitoring of heritage buildings for energy efficiency retrofitting," *2013 IEEE Work. Environ. Energy Struct. Monit. Syst.*, pp. 1–6, Sep. 2013.

[109] A. Costa, A. Arêde, E. Paupério, and X. Romão, *Reabilitação estrutural: casos práticos de intervenção em estruturas patrimoniais*, 1st ed. Porto: Universidade do Porto, 2014.

[110] R. Kostecki, H. Ebendorff-Heidepriem, S. C. Warren-Smith, G. McAdam, C. Davis, and T. M. Monro, "Optical Fibres for Distributed Corrosion Sensing - Architecture and Characterisation," *Key Eng. Mater.*, vol. 558, pp. 522–533, Jun. 2013.

[111] P. Antunes, H. Varum, and P. André, "Uniaxial fiber Bragg grating accelerometer system with temperature and cross axis insensitivity," *Measurement*, vol. 44, no. 1, pp. 55–59, Jan. 2011.

[112] D. C. Betz, G. Thursby, B. Culshaw, and W. J. Staszewski, "Structural Damage Location with Fiber Bragg Grating Rosettes and Lamb Waves," *Struct. Heal. Monit.*, vol. 6, no. 4, pp. 299–308, Dec. 2007.

[113] N. Kurata, B. F. Spencer, and M. Ruiz-Sandoval, "Risk monitoring of buildings with wireless sensor networks," *Struct. Control Heal. Monit.*, vol. 12, no. 3–4, pp. 315–327, Jul. 2005.

[114] C. Barbosa, N. Costa, L. a Ferreira, F. M. Araújo, H. Varum, A. Costa, C. Fernandes, and H. Rodrigues, "Weldable fibre Bragg grating sensors for steel bridge monitoring," *Meas. Sci. Technol.*, vol. 19, no. 12, p. 125305, Dec. 2008.

[115] D. Isidori, "A low-cost structural health monitoring system for residential buildings: experimental tests on a scale model," Università Politecnica Delle Marche, 2013.

[116] L.-J. Wu, F. Casciati, and S. Casciati, "Dynamic testing of a laboratory model via vision-based sensing," *Eng. Struct.*, vol. 60, pp. 113–125, 2014.

[117] P. S. André, H. Varum, P. Antunes, L. Ferreira, and M. G. Sousa, "Monitoring of the concrete curing process using plastic optical fibers," *Measurement*, vol. 45, no. 3, pp. 556–560, Apr. 2012.

[118] D. S. Li, L. Ren, H. N. Li, and G. B. Song, "Structural Health Monitoring of a Tall Building during Construction with Fiber Bragg Grating Sensors," vol. 2012, 2012.

[119] M. S. Laing, D. S. Homa, R. M. Harman, and C. H. LAMBERT, "Optical fiber sensor and method for adhering an optical fiber to a substrate." Google Patents, 2013.

[120] P. Antunes, A. M. Rocha, H. Lima, H. Varum, and P. S. André, "Thin bonding wires temperature measurement using optical fiber sensors," *Measurement*, vol. 44, no. 3, pp. 554–558, Mar. 2011.

[121] L. F. Ferreira, P. Antunes, F. Domingues, P. a. Silva, and P. S. André, "Monitoring of sea bed level changes in near shore regions using fiber optic sensors," *Measurement*, vol. 45, no. 6, pp. 1527–1533, Jul. 2012.

[122] G. Peng, J. He, S. Yang, and W. Zhou, "Application of the fiber-optic distributed temperature sensing for monitoring the liquid level of producing oil wells," *Measurement*, vol. 58, pp. 130–137, Dec. 2014.

[123] R. J. Bartlett, R. Philip-Chandy, P. Eldridge, D. F. Merchant, R. Morgan, and P. J. Scully, "Plastic optical fibre sensors and devices," *Trans. Inst. Meas. Control*, vol. 22, no. 5, pp. 431–457, 2000.

[124] M. Lomer, J. Arrue, C. Jauregui, P. Aiestaran, J. Zubia, and J. M. López-Higuera, "Lateral polishing of bends in plastic optical fibres applied to a multipoint liquid-level measurement sensor," *Sensors Actuators, A Phys.*, vol. 137, no. 1, pp. 68–73, 2007.

[125] H. Golnabi and P. Azimi, "Design and performance of a plastic optical fiber leakage sensor," *Opt. Laser Technol.*, vol. 39, no. 7, pp. 1346–1350, 2007.

[126] L. Lee, "Optica al Fibe er Sen tion In nk for Water r Imm ersion n Dete ection," *IEEE Photonics Technol. Lett.*, no. Ispacs, pp. 880–882, 2012.

[127] S. Sharifpour-Boushehri, S. M. Hosseini-Golgoo, and M.-H. Sheikhi, "A low cost and reliable fiber optic ethanol sensor based on nano-sized SnO2," *Opt. Fiber Technol.*, 2015.

[128] I. H. Justnes, "Low water permeability through hydrophobicity," Oslo, 2008.

[129] ICOMOS, *Madrid Letter's - International scientific committee on twentieth century heritage*. Madrid, 2011, p. 7.

[130] Z. Dahou, Z. Mehdi Sbartaï, A. Castel, and F. Ghomari, "Artificial neural network model for steel–concrete bond prediction," *Eng. Struct.*, vol. 31, no. 8, pp. 1724–1733, Aug. 2009.

[131] A. Daoud, O. Maurel, and C. Laborderie, "2D mesoscopic modelling of bar–concrete bond," *Eng. Struct.*, vol. 49, pp. 696–706, Apr. 2013.

[132] B. V Silva, M. P. Barbosa, L. C. P. Silva Filho, and M. S. Lorrain, "Experimental investigation on the use of steel-concrete bond tests for estimating axial compressive strength of concrete: Part 1," *Ibracon Struct. Mater. J.*, vol. 6, no. 5, pp. 715–725, 2013.

[133] *NP EN 12390-3: Ensaios do betão endurecido - Parte 3: Resistência à compressão dos provetes de ensaio*. Caparica, Portugal, 2003, p. 21.

[134] A. Torre-Casanova, L. Jason, L. Davenne, and X. Pinelli, "Confinement effects on the steel–concrete bond strength and pull-out failure," *Eng. Fract. Mech.*, vol.

97, pp. 92–104, Jan. 2013.

[135] RILEM, "Essais portant sur l'adherénce es armatures du béton - Essai par traction," *Mater. Struct.*, vol. 3, no. 3, pp. 175–178, 1970.

[136] J. Ožbolt, F. Oršanić, and G. Balabanić, "Modeling pull-out resistance of corroded reinforcement in concrete: Coupled three-dimensional finite element model," *Cem. Concr. Compos.*, vol. 46, pp. 41–55, Feb. 2014.

[137] B. Wang, J. G. Teng, L. De Lorenzis, L.-M. Zhou, J. Ou, W. Jin, and K. T. Lau, "Strain monitoring of RC members strengthened with smart NSM FRP bars," *Constr. Build. Mater.*, vol. 23, no. 4, pp. 1698–1711, 2009.

[138] M. A. Davis, D. G. Bellemoreb, and A. D. Kersey, "Distributed Fiber Bragg Grating Strain Sensing in Reinforced Concrete Structural Components," *Cem. Concr. Compos.*, vol. 19, pp. 45–57, 1997.

[139] F. Qin, Q. Kong, M. Li, Y. L. Mo, G. Song, and F. Fan, "Bond slip detection of steel plate and concrete beams using smart aggregates," *Smart Mater. Struct.*, vol. 24, no. 11, p. 115039, 2015.

[140] Q. I. U. Ye, W. Quan-bao, C. Ji-an, and W. Yue-ying, "Review on Composite Structural Health Monitoring Based on Fiber Bragg Grating Sensing Principle," vol. 18, no. 2, pp. 129–139, 2013.

[141] P. F. D. Antunes, H. F. T. Lima, N. J. Alberto, H. Rodrigues, P. M. F. Pinto, J. D. Pinto, R. N. Nogueira, H. Varum, a G. Costa, and P. S. Andre, "Optical Fiber Accelerometer System for Structural Dynamic Monitoring," *IEEE Sens. J.*, vol. 9, no. 11, pp. 1347–1354, 2009.

[142] P. Antunes, C. A. Marques, H. Varum, and P. S. André, "Biaxial Optical Accelerometer and High-Angle Inclinometer With Temperature and Cross-Axis Insensitivity," *IEEE Sens. J.*, vol. 12, no. 7, pp. 2399–2406, 2012.

[143] European Standard, *EN 10080: Steel for the reinforcement of concrete - Weldable reinforcing steel - General*. EN, 2005.

[144] P. Antunes, H. Lima, J. Monteiro, and P. André, "Elastic constant measurement for standard and photosensitive single mode optical fibres," *Microw. Opt. Technol. Lett.*, vol. 54, no. 12, pp. 2781–2784, 2012.

[145] M. Rafiee Fanood and F. M. Saradj, "Learning from the Past and Planning for the Future: Conditions and Proposals for Stone Conservation of the Mausoleum of Cyrus the Great in the World Heritage Site of Pasargadae," *Int. J. Archit. Herit.*, vol. 7, no. 4, pp. 434–460, 2013.

[146] R. Ceravolo, G. Pistone, L. Zanotti Fragonara, S. Massetto, and G. Abbiati, "Vibration-based monitoring and diagnosis of cultural heritage: a methodological discussion in three examples," *Int. J. Archit. Herit.*, no. June 2015, p. 150527102237009, 2014.

[147] A. Costa, R. Delgado, A. Arêde, J. Guedes, N. Vila-Pouca, X. Romão, and E. Paupério, "Intervenção no património - A experiência do Núcleo de Reabilitação IC-FEUP," in *Património Intervenção*, 1st ed., A. Costa, A. Arêde, D. Ferreira, E. Paupério, J. Guedes, P. Silva, and X. Romão, Eds. Porto: FEUP, 2013, p. 378.

[148] E. Paupério, "Relatório das atividades do Núcleo de Reabilitação do Instituto da Construção," Porto, 2017.

[149] D. Zonta, H. Wu, M. Pozzi, P. Zanon, M. Ceriotti, L. Mottola, G. P. Picco, A. L. Murphy, S. Guna, and M. Corrà, "Wireless sensor networks for permanent health monitoring of historic buildings," *Smart Struct. Syst.*, vol. 6, no. 5–6, pp. 595–618, 2010.

[150] D. Abruzzese, M. Angelaccio, B. Buttarazzi, R. Giuliano, L. Miccoli, and A. Vari, "Long life monitoring of historical monuments via wireless sensors network," *Proc. 2009 6th Int. Symp. Wirel. Commun. Syst. ISWCS'09*, pp. 570–574, 2009.

[151] M. Betti, G. Bartoli, and M. Orlando, "Evaluation study on structural fault of a Renaissance Italian palace," *Eng. Struct.*, vol. 32, no. 7, pp. 1801–1813, 2010.

[152] E. Mesquita, P. Antunes, F. Coelho, P. André, A. Arêde, and H. Varum, "Global overview on advances in structural health monitoring platforms," *J. Civ. Struct. Heal. Monit.*, vol. 6, no. 3, pp. 461–475, Jul. 2016.

[153] P. Antunes, J. Dias, T. Paixão, E. Mesquita, H. Varum, and P. André, "Liquid level gauge based in plastic optical fiber," *Measurement*, vol. 66, pp. 238–243, Apr. 2015.

[154] ICOMOS, *The Venice charter for the conservation and restoration of monuments and sites*. Venice, 1964, p. 5.

[155] H. Wenzel, *Health Monitoring of Bridges*, 1st ed. Vienna: John Wiley & Sons, Ltd, 2009.

[156] F. S. Martins, "O colégio de São Lourenço (1560-1774)," Universidade do Porto, 1986.

[157] P. Antunes, H. Varum, and P. Andréa, "Optical FBG Sensors for Static Structural Health Monitoring," *Procedia Eng.*, vol. 14, pp. 1564–1571, Jan. 2011.

[158] S. Beskhyroun, L. D. Wegner, and B. F. Sparling, "New methodology for the application of vibration-based damage detection techniques," *Struct. Control Heal. Monit.*, no. May 2011, p. n/a–n/a, 2011.

[159] C. Gentile and A. Saisi, "Ambient vibration testing of historic masonry towers for structural identification and damage assessment," *Constr. Build. Mater.*, vol. 21, no. 6, pp. 1311–1321, 2007.

[160] J. M. W. Brownjohn, "Ambient vibration studies for system identification of tall buildings," *Earthq. Eng. Struct. Dyn.*, vol. 32, no. 1, pp. 71–95, 2003.

[161] S. Hans, C. Boutin, E. Ibraim, and P. Roussillon, "In situ experiments and seismic analysis of existing buildings. Part I: Experimental investigations," *Earthq. Eng. Struct. Dyn.*, vol. 34, no. 12, pp. 1513–1529, 2005.

[162] S. S. Ivanovic, M. D. Trifunac, and M. I. Todorovska, "Ambient Vibration Tests of Structure-A Review," *J. Earthq. Tecknology*, vol. 37, no. 4, pp. 165–197, 2000.

[163] B. F. Spencer, M. E. Ruiz-Sandoval, and N. Kurata, "Smart sensing technology: Opportunities and challenges," *Struct. Control Heal. Monit.*, vol. 11, no. 4, pp. 349–368, 2004.

[164] C. Blasi and E. Coisson, "The effects of temperature on historical stone masonry structures," in *Structural Analysis of Historic Construction: Preserving Safety and Significance*, 1st ed., D'Ayala and Fodde, Eds. London: Taylor & Francis, 2008, pp. 1271–1276.

[165] ICOMOS, "Icomos Charter- Principles for the analysis , conservation and structural restoration of architectural heritage," in *International Council on Monuments and Sites*, 2003.

[166] J. P. Lynch, "A Summary Review of Wireless Sensors and Sensor Networks for Structural Health Monitoring," *Shock Vib. Dig.*, vol. 38, no. 2, pp. 91–128, Mar. 2006.

[167] E. Mesquita, P. Antunes, F. Coelho, P. André, A. Arêde, and H. Varum, "Global overview on advances in structural health monitoring platforms," *J. Civ. Struct. Heal. Monit.*, vol. 6, no. 3, pp. 461–475, Jul. 2016.

[168] J. M. Samuels, M. Reyer, S. Hurlebaus, S. H. Lucy, D. G. Woodcock, and J. M. Bracci, "Wireless sensor network to monitor an historic structure under rehabilitation," *J. Civ. Struct. Heal. Monit.*, vol. 1, no. 3–4, pp. 69–78, 2011.

[169] F. Federici, R. Alesii, A. Colarieti, M. Faccio, F. Graziosi, V. Gattulli, and F. Potenza, "Design of Wireless Sensor Nodes for Structural Health Monitoring Applications," *Procedia Eng.*, vol. 87, pp. 1298–1301, 2014.

[170] IHRU, "Vila Nova de Foz Côa." [Online]. Available: http://www.portaldahabitacao.pt/pt/ihru/. [Accessed: 22-Mar-2017].

[171] F. Parisi and N. Augenti, "Earthquake damages to cultural heritage constructions and simplified assessment of artworks," *Eng. Fail. Anal.*, vol. 34, pp. 735–760, 2013.

[172] European Commitee for Standardization, "Eurocode 8: Design of structures for earthquake resistance – Part 3: Assessment and retrofitting of buildings," Brussels, 2005.

[173] G. P. Cimellaro and A. De Stefano, "Ambient vibration tests of XV century Renaissance Palace after 2012 Emilia earthquake in Northern Italy," *Struct. Monit. Maint.*, vol. 1, no. 2, pp. 231–247, 2014.

[174] E. Mesquita, A. Arêde, E. Paupério, and N. Pinto, "SHM of heritage constructions through wireless sensor network : from design to the long-term monitoring," in *XVII International Conference on Structural Repair and Rehabilitation*, 2016, pp. 1–15.

[175] G. Comanducci, F. Ubertini, and A. L. Materazzi, "Structural health monitoring of suspension bridges with features affected by changing wind speed," *J. Wind Eng. Ind. Aerodyn.*, vol. 141, pp. 12–26, 2015.

[176] N. M. Okasha, D. M. Frangopol, and D. Saydam, "Reliability analysis and damage detection in high-speed naval craft based on structural health monitoring data," 2015.

[177] P. B. R. Dissanayake and P. A. K. Karunananda, "Reliability Index for Structural Health Monitoring of Aging Bridges," vol. 7, no. 2, pp. 175–183, 2015.

[178] E. Mesquita, P. Antunes, A. A. Henriques, A. Arêde, P. S. André, and H. Varum, "Structural reliability assessment based on optical monitoring system: case study," *IBRACON Struct. Mater. J.*, vol. 9, no. 2, pp. 297–305, 2016.

[179] D. Musiani, K. Lin, and T. S. Rosing, "Active Sensing Platform for Wireless Structural Health Monitoring," *2007 6th Int. Symp. Inf. Process. Sens. Networks*, pp. 390–399, 2007.

[180] D. Dan, T. Yang, and J. Gong, "Intelligent Platform for Model Updating in a Structural Health Monitoring System," *Math. Probl. Eng.*, vol. 2014, pp. 1–11, 2014.

[181] R. Vicente, "Estratégias e metodologias para intervenções de reabilitação urbana: avaliação da vulnerabilidade e do risco sísmico do edificado," University of Aveiro, 2008.

[182] C. Cremona, *Structural Performance: probabilistic-based assessment*, 1st ed. London: ISTE, 2011.

[183] P. B. R. Dissanayake and P. A. K. Karunananda, "Reliability Index for Structural Health Monitoring of Aging Bridges," *Structural Health Monitoring*, vol. 7. pp. 175–183, 2008.

[184] M. Liu, M. Asce, D. M. Frangopol, F. Asce, and S. Kim, "Bridge System Performance Assessment from Structural Health Monitoring : A Case Study," *J. Struct. Eng.*, vol. 135, no. June, pp. 733–742, 2009.

[185] A. Haldar and S. Mahadevan, *Probability, reliability and statistical methods in engineering desing*, 1st ed. New York: John Wiley & Sons, 2000.

[186] N. M. Okasha, D. M. Frangopol, D. Saydam, and L. W. Salvino, "Reliability analysis and damage detection in high-speed naval craft based on structural health monitoring data," *Struct. Heal. Monit.*, vol. 10, pp. 361–379, 2010.

[187] European Commitee for Standardization, *Eurocode 8: Design of structures for earthquake resistance - Part 1 : General rules, seismic actions and rules for buildings*, vol. 1, no. English. 2004, p. 231.

[188] C. Almeida, "Paredes de alvenaria do Porto: Tipificação e caracterização experimental," University of Porto, 2013.

[189] R. Delgado, A. Costa, P. Rocha, M. Laranjo, P. Delgado, and J. Oliveira, "Proposta de intervenção - Igreja de Santo António de Viana do Castelo," Porto, 2006.

[190] R. Delgado, A. Costa, P. Rocha, P. Delgado, and J. Oliveira, "Relatório de inspeção - Igreja de Santo António de Viana do Castelo," Porto, 2002.

[191] A. Costa, P. Rocha, and E. Paupério, "Implementação de Medidas de Consolidação e Reforço Estrutural da Igreja de Santo António de Viana do Castelo," Porto, 2013.

[192] A. Costa, P. Rocha, and E. Paupério, "Nota técnica intervenção de reforço igreja de santo antónio v," Porto, 2012.

[193] A. Arêde, E. Paupério, P. Rocha, and A. Gomes, *Igreja de Santo António de Viana - Relatório de monitorização*. Porto, 2015, p. 30.

[194] ISO, *Reconnaissance et essais géotechniques — Essais en place — Partie 4: Essai au pressiomètre Ménard*. France, 2012.
[195] J. Briaud, *The Pressuremeter*. Rotterdam: Trans Tech Publications, 1992.
[196] G. J. Yun, S.-G. Lee, J. Carletta, and T. Nagayama, "Decentralized damage identification using wavelet signal analysis embedded on wireless smart sensors," *Eng. Struct.*, vol. 33, no. 7, pp. 2162–2172, Jul. 2011.
[197] F. Magalhães, "Operational modal analysis for testing and monitoring of bridges and special structures," Faculty of Engineering of University of Porto, 2010.
[198] N. J. Jacobsen, P. Andersen, and R. Brincker, "Using Enhanced Frequency Domain Decomposition as a Robust Technique to Harmonic Excitation in Operational Modal Analysis," in *Proceedings of ISMA2006: International Conference on Noise & Vibration Engineering*, 2006, pp. 3129–3140.
[199] T. Le and Y. Tamura, "Modal Identification of ambient vibration structure using frequency domain decomposition and wavelet transform," in *Proceedings of the 7th Asia-Pacific conference on wind …*, 2009, no. 2001.
[200] R. Brincker and et al., "Modal identification of output-only systems using frequency domain decomposition," *Smart Mater. Struct.*, vol. 10, no. 3, p. 441, 2001.
[201] S. V. S. ApS, "ARTeMIS Extractor 5.3." Structure VibrationSolutions. A/S, Alborg, 2011.

Annex:

Scientific publications resulted from the work developed

Patent

1. Mesquita, E.; Antunes, P. ; André, P. ; Varum, H. . “Sensor baseado em fibra ótica para monitorização do nível de líquidos.” 2016, Portugal. Patente: Privilégio de Inovação. Register number: PT20161000039028, Institute: Instituto Nacional da Propriedade Industrial. Deposit date: 14/06/2016

Technical Reports

1. Mesquita, E.; Paupério, E.; Arêde, A.; Varum, H.; “Boletín Técnico nº 11: Caracterizacíon, evaluacíon y recuperacíon estructural de edifícios históricos.” In: Asociación Latinoamericana de Control de Calidad, Patología y Recuperación de la Construcción - ALCONPAT Int. 2015, Mérida. Acess: http://alconpat.org.br/wp-content/uploads/2012/09/B11-Caracteriza%C3%A7%C3%A3o-avalia%C3%A7%C3%A3o-e-recupera%C3%A7%C3%A3o-estrutural-de-constru%C3%A7%C3%B5es-hist%C3%B3ricas.pdf

Articles in international journals with referee

Published

1. Mesquita, E., Antunes, P., Coelho, F., André P., Arêde, A. and Varum, H. "Global overview on advances in structural health monitoring platforms". J Civil Struct Health Monit (2016) 6: 46, doi:10.1007/s13349-016-0184-5

2. Mesquita, E.; Antunes, P. ; Henriques, A. A. ; Arêde, A. ; André, P. ; Varum, H. . "Structural reliability assessment based on optical monitoring system: case study". Revista IBRACON de Estruturas e Materiais, v. 9, p. 297-305, 2016, doi:10.1590/S1983-41952016000200009

3. Mesquita, E.; Paixão, T.; Antunes, P. ; Coelho, F.; Ferreira, P.; André, P.; Varum, H. "Groundwater level monitoring using a plastic optical fiber". Sensors and Actuators. A, Physical, v. 240, p. 138-144, 2016, doi: dx.doi.org/10.1016/j.sna.2016.01.042

4. M. F. Domingues; M. F.; Paixão, T.; **Mesquita**, **E.**; Alberto, N.; Antunes, P.; Varum, H.; André, P. S.; "Pressure sensor based on micro-cavities developed by the catastrophic fuse effect." *IEEE Sensors* (2015), doi:10.1109/JSEN.2015.2446534

5. Antunes, P.; Dias, J.; Paixão, T.; **Mesquita, E.**; Varum, H.; André, P. S.; "Liquid level gauge based in plastic optical fiber". *Measurement* (2015), doi: http://dx.doi.org/10.1016/j.measurement.2015.01.030

Accepted for publication

1. Mesquita, E., Arêde, A., Silva, R., Rocha, P., Gomes, A., Pinto, N., Antunes, P. and Varum, H. "Structural health monitoring of the retrofitting process, characterization and reliability analysis of a stone heritage construction". J Civil Struct Health Monit (Submitted in May, 12, 2016; Revised in Jan, 25 of 2017; Accepted in Jun, 26 of 2017);

2. Mesquita, E., Brandão, F., Diógenes, A., Antunes, P., Varum, H. "Dynamic characterization of a heritage construction from 19th century". Revista IBRACON de Estruturas e Materiais, (Submitted in Aug, 04, 2016; Revised in Marc, 22 of 2017; Accepted in Jul, 05 of 2017);

Under submission

2. Mesquita, E., Brandão, F., Rodrigues, H., Deógenes, A., Cabral, A., Antunes, P., Arêde, A., and Varum, H. "Ambient vibrational characterization of the Nossa Senhora das Dores Church to support numerical modelling update". *Measurement* (Submitted in Feb, 14, 2017);

3. Mesquita, E., Arêde, A., Pinto, N., Antunes, P., Varum, H. "Long-term monitoring of a damaged historic structure using a wireless sensor network". *Measurement* (Submitted in Apr, 5, 2017);

Articles in conference proceedings

1. Mesquita, E.; Arêde, A.; Paupério, E.; Pinto, N.; Antunes, P.; Varum, H. "SHM of heritage constructions through wireless sensor network: from design to the long-term monitoring." In: XII International Conference on Building Pathology and Rehabilitation. Porto, 2016.

2. Mesquita, E.; Antunes, P.; Alberto, N.; Melo, J.; Marques, C.; André, P. S.; Varum, H; "Bond-slip Monitoring of RC through optical fiber sensor." In: XII International Conference on Building Pathology and Rehabilitation. Porto, 2016.

3. Alves, A. ; Santos, F. ; Brandão, F. ; Deógenes, A. ; **Mesquita, E**. ; Varum, H. "Estimativa do módulo de elasticidade global de uma edificação histórica de alvenaria de tijolos maciços pelo método ultrassônico." In: II Congresso Brasileiro de Patologia das Construções, 2016, Belém, 2016.

4. Cavalcante, A. ; Mota, L. ; Araújo, E. ; Deógenes, A. ; **Mesquita, E**. ; Varum, H. "Caracterização dos danos em construções históricas de alvenaria vernacular: casos de estudo." In: Congresso Brasileiro de Patologia das Construções, 2016, Belém. II Congresso Brasileiro de Patologia das Construções, 2016.

5. Mota, L. ; Cavalcante, A. ; Deógenes, A. ; **Mesquita, E.** ; Vicente, R. ; Varum, H. . Avaliação da vulnerabilidade sísmica à escala urbana: o centro histórico sobralense."

In: Congresso Brasileiro de Patologia das Construções, 2016, Belém. II Congresso Brasileiro de Patologia das Construções, 2016.

6. Brandão, F. ; Alves, A. ; Santos, F. ; Deógenes, A. ; **Mesquita, E**. ; Varum, H. "Caracterização dinâmica de um edifício histórico do século XIX construído de alvenaria de tijolos maciços." In: Congresso Brasileiro de Patologia das Construções, 2016, Belém, II Congresso Brasileiro de Patologia das Construções, 2016.

7. E. Mesquita, A. Henriques, P. Antunes, P. André, F. Coelho, A. Arêde, H. Varum. A monitorização como suporte à análise da confiabilidade estrutural: caso de estudo. IN: 57º CONGRESSO BRASILEIRO DO CONCRETO - ISSN: 2175-8182. Bonito, Brazil, October 2015.

8. E. Mesquita, T. Paixão, P. Antunes, P. Ferreira, F. Coelho, P. André, H. Varum. Sensors for groundwater level measurement based on plastic optical fibers for structural health monitoring. IN: 1st DOCTORAL CONGRESS IN ENGINEERING. Porto, Portugal, June 2015.